

Purine-Based Dual Inhibitors of CDK2 and CDK7

Elisa Meschini

**A Thesis Submitted to Newcastle University
for the Degree of Doctor of Philosophy**

June 2011

Declaration

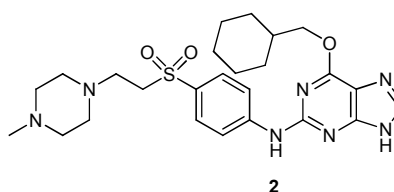
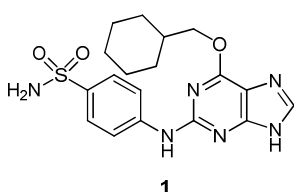
The work described in this thesis was carried out in the School of Chemistry, at Newcastle University, between November 2006 and July 2010. The work is original except where acknowledged by reference.

No other part of this work is being, or has been, submitted for a degree, diploma or any other qualification at any other university.

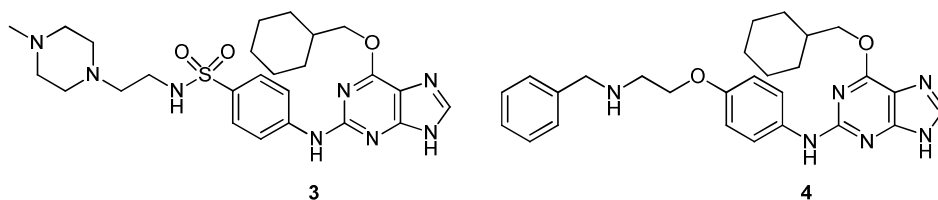
Abstract

Cyclin-Dependent Kinases (CDKs) play a fundamental role in eukaryotic cell cycle progression, particularly at cell cycle checkpoints, and are therefore important targets for anticancer drug discovery. Activation of CDK2 in complex with Cyclin A regulates entry into S phase of the eukaryotic cell cycle. CDK7, a dual-function enzyme, acts both as a CDK-Activating Kinase (CAK) and as a component of the general transcription factor TFIIH. However, experiments with MAT1-knockdown mice have shown that cell cycle arrest by CAK inhibition would not be detrimental for transcriptional activity in non-dividing cells, as CDK9 in complex with Cyclin T can perform transcriptional duties in the absence of TFIIH.

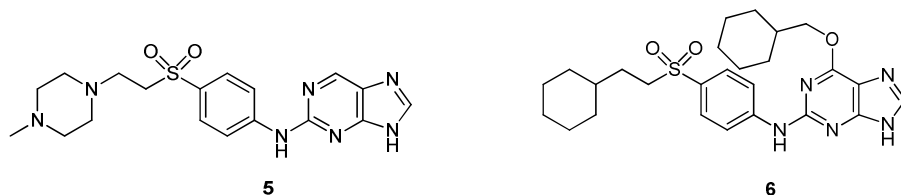
Previous studies have resulted in the identification of NU6102 (**1**, IC_{50} μ M = 0.005 (CDK2), 4.4 (CDK7)) as a potent and selective CDK2 inhibitor, and NU6247 (**2**, IC_{50} μ M = 0.12 (CDK2), 0.23 (CDK7)) as an equipotent CDK2/7 inhibitor. It was shown that the sulfonamide group of **1** confers potency and selectivity for CDK2, whereas the pendant piperazinyl substituent of **2** diminishes CDK2 activity whilst improving activity versus CDK7.



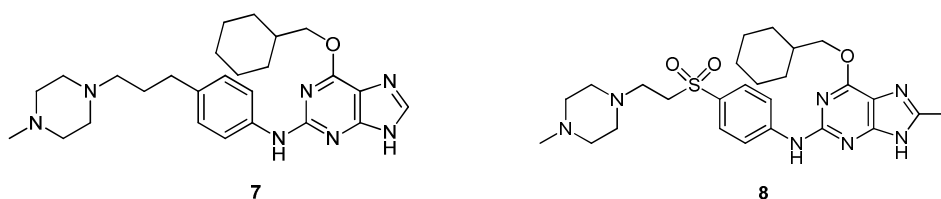
Accordingly, as part of the work described in the present thesis, sulfonamide **3** (IC_{50} μ M = 0.012 (CDK2), 0.67 (CDK7)) was synthesised and found to be a potent CDK2 inhibitor, but with some CDK7-inhibitory activity (IC_{50} μ M = 0.012 (CDK2), 0.67 (CDK7)). Further elaboration of the side-chain function has enabled the development of structure-activity relationships (SARs), and the identification of purines (e.g. **4**, IC_{50} μ M = 2.6 (CDK2), 0.56 (CDK7)) exhibiting some selectivity for CDK7, albeit with a loss of potency.



Subsequent SAR studies conducted on **2** have enabled the following observations to be made: firstly, the purine 6-cyclohexylmethoxy substituent is necessary for activity, with the corresponding 6-unsubstituted purine (**5**, IC_{50} μ M = 46.9 (CDK2), 20.8 (CDK7)) exhibiting a 100-fold loss of potency against both CDK2 and CDK7. A terminal basic group (e.g. piperazinyl in **2**) is required for activity, as replacement by a cyclohexyl substituent results in loss of activity against both kinases (**6**, 11% inhibition at 10 μ M (CDK2), 13% inhibition at 100 μ M (CDK7)).



The sulfone linker is not a prerequisite for CDK7 activity, with the simple alkylpiperazine derivative (**7**, IC_{50} μ M = 0.48 (CDK2), 0.51 (CDK7)) exhibiting comparable potency and selectivity. Finally, there appears to be some opportunity for expansion into the gatekeeper pocket of CDK7 by introducing small substituents at the purine C-8 position, with the potential for selectivity over CDK2 (**8**, 47% inhibition at 100 μ M (CDK2), IC_{50} = 5 μ M (CDK7)).



Isolation and biological evaluation of the vinyl sulfone **9**, an intermediate in the synthesis of **2**, indicated a time-dependent inhibition of CDK2, suggesting that **9** is an irreversible inhibitor of CDK2. This would be the first reported irreversible inhibitor of a cyclin-dependent kinase, and therefore the activity of the compound against CDK2 was investigated using protein crystallography and site-directed mutagenesis

techniques. From these studies, encouraging evidence has emerged that **9** acts as an irreversible inhibitor of CDK2, covalently binding to a lysine residue within the ATP-binding pocket.

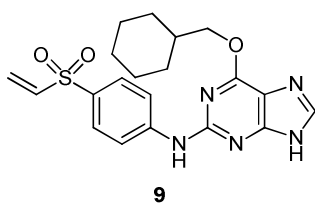


Table of Contents

<u>Declaration</u>	<u>2</u>
<u>Abstract</u>	<u>3</u>
<u>Table of Contents</u>	<u>6</u>
<u>Acknowledgements</u>	<u>10</u>
<u>Abbreviations</u>	<u>12</u>
<u>Chapter 1 – Kinases and Cancer</u>	
1.1 <u>Cancer: definition and hallmarks</u>	<u>17</u>
1.2 <u>Protein kinases</u>	<u>21</u>
1.3 <u>Kinase inhibitors as anticancer agents</u>	<u>26</u>
1.4 <u>ATP-competitive inhibition of protein kinases</u>	<u>29</u>
<u>Chapter 2 – Cyclin-Dependent Kinases</u>	
2.1 <u>The cell cycle</u>	<u>31</u>
2.2 <u>The Cyclin-Dependent Kinases (CDKs)</u>	<u>33</u>
2.2.1 <u>The role of the CDKs in regulating the cell cycle</u>	<u>37</u>
2.2.2 <u>'Non-cycling' CDKs</u>	<u>39</u>
2.3 <u>The regulation of CDK activity</u>	<u>40</u>
2.3.1 <u>Cyclin binding</u>	<u>41</u>
2.3.2 <u>T-loop phosphorylation</u>	<u>44</u>
2.3.3 <u>Endogenous CDK inhibition</u>	<u>45</u>

<u>2.3.3.1</u>	<u>The Cip/Kip family</u>	<u>46</u>
<u>2.3.3.2</u>	<u>The Ink4 family</u>	<u>48</u>
<u>2.3.4</u>	<u>CDK inhibitory phosphorylation</u>	<u>49</u>
<u>2.4</u>	<u>CDKs as anticancer targets</u>	<u>51</u>
<u>2.4.1</u>	<u>ATP-competitive inhibition</u>	<u>52</u>
<u>2.4.2</u>	<u>CDK inhibitors</u>	<u>53</u>
<u>2.5</u>	<u>CDK7</u>	<u>61</u>
<u>2.5.1</u>	<u>CDK7 activation</u>	<u>63</u>
<u>2.5.2</u>	<u>CDK7 as a CTDK</u>	<u>65</u>
<u>2.5.3</u>	<u>CDK7 as an anticancer drug target</u>	<u>67</u>
<u>2.5.4</u>	<u>Structural information on CDK7</u>	<u>71</u>
<u>2.5.5</u>	<u>ATP-competitive inhibition of CDK7</u>	<u>74</u>
<u>2.6</u>	<u>CDK redundancy and selectivity profile</u>	<u>76</u>

Chapter 3 – Project Background

<u>3.1</u>	<u>Purine-based inhibitors of CDKs</u>	<u>79</u>
<u>3.2</u>	<u>From NU2058 to NU6247</u>	<u>83</u>

Chapter 4 – Development of analogues of NU6247

<u>4.1</u>	<u>Hydrophobic analogues of NU6247</u>	<u>90</u>
<u>4.2.</u>	<u>Structural biology studies</u>	<u>96</u>
<u>4.3</u>	<u>Exploring the SARs for NU6247 analogues</u>	<u>104</u>
<u>4.4</u>	<u>Synthesis of NU6451 analogues</u>	<u>111</u>

Chapter 5 – Pharmacophore mapping and scaffold

hopping around NU6247

<u>5.1</u>	<u>Pharmacophore mapping around NU6247</u>	<u>121</u>
<u>5.1.1</u>	<u>Benzyl sulfone analogue</u>	<u>122</u>
<u>5.1.2</u>	<u>Removing the O⁶-substituent</u>	<u>124</u>
<u>5.1.3</u>	<u>Removing the terminal basic moiety</u>	<u>127</u>
<u>5.1.4</u>	<u>Identity of the linker</u>	<u>128</u>
<u>5.1.5</u>	<u>Introducing a substituent at the 8-position</u>	<u>129</u>
<u>5.2</u>	<u>Scaffold hopping from published CDK7 inhibitors</u>	<u>137</u>
<u>5.2.1</u>	<u>The Purvalanol A analogue of NU6247</u>	<u>137</u>
<u>5.2.2</u>	<u>The ‘Cyclacel’ analogue of NU6247</u>	<u>142</u>
<u>5.2.3</u>	<u>Replacement of the purine core pharmacophore by a pyrazolo-pyrimidine</u>	<u>147</u>

Chapter 6 – NU6300, an irreversible inhibitor of CDK2

<u>6.1</u>	<u>Irreversible enzyme inhibition</u>	<u>151</u>
<u>6.2</u>	<u>NU6300 as an irreversible inhibitor of CDK2</u>	<u>155</u>
<u>6.2.1</u>	<u>Surface Plasmon Resonance experiments</u>	<u>157</u>
<u>6.2.2</u>	<u>Band shift assays</u>	<u>159</u>
<u>6.2.3</u>	<u>Mass spectrometry experiments</u>	<u>161</u>
<u>6.3</u>	<u>CDK2 redundancy</u>	<u>166</u>

<u>Conclusions</u>	<u>168</u>
------------------------------------	----------------------------

Chapter 7 – Experimental

<u>7.1</u>	<u>Chemicals and solvents</u>	<u>170</u>
<u>7.2</u>	<u>Chromatography</u>	<u>170</u>
<u>7.3</u>	<u>Analytical techniques and instrumentation</u>	<u>171</u>
<u>7.4</u>	<u>Index of Compounds Synthesised</u>	<u>174</u>
<u>7.5</u>	<u>General Procedures</u>	<u>180</u>
<u>7.6</u>	<u>Experimental Procedures</u>	<u>184</u>
<u>7.7</u>	<u>Protein expression, kinase assays, MS and SPR</u>	<u>268</u>

<u>References</u>	<u>274</u>
--------------------------	------------

~~Table of Contents~~

Declaration	2
Abstract	3
Table of Contents	6
Acknowledgements	10
Abbreviations	12

~~Chapter 1 – Kinases and Cancer~~

1.1	Cancer: definition and hallmarks	17
1.2	Protein kinases	19
1.3	Kinase inhibitors as anticancer agents	24

1.4	ATP-competitive inhibition of protein kinases	27
-----	---	----

Chapter 2 – Cyclin-Dependent Kinases

2.1	The cell cycle	29
2.2	The Cyclin-Dependent Kinases (CDKs)	34
2.2.1	The role of the CDKs in regulating the cell cycle	35
2.2.2	'Non-cycling' CDKs	37
2.3	The regulation of CDK activity	38
2.3.1	Cyclin binding	39
2.3.2	T-loop phosphorylation	42
2.3.3	Endogenous CDK inhibition	43
2.3.3.1	The Cip/Kip family	44
2.3.3.2	The Ink4 family	46
2.3.4	CDK inhibitory phosphorylation	47
2.4	CDKs as anticancer targets	49
2.4.1	ATP-competitive inhibition	50
2.4.2	CDK inhibitors	51
2.5	CDK7	59
2.5.1	CDK7 activation	61
2.5.2	CDK7 as a CTDK	63
2.5.3	CDK7 as an anticancer drug target	65
2.5.4	Structural information on CDK7	69
2.5.5	ATP-competitive inhibition of CDK7	72
2.6	CDK redundancy and selectivity profile	74

Chapter 3—Project Background

3.1	Purine-based inhibitors of CDKs	77
3.2	From NU2058 to NU6247	84

Chapter 4—Development of analogues of NU6247

4.1	Hydrophobic analogues of NU6247	88
4.2	Structural biology studies	94
4.3	Exploring the SARs for NU6247 analogues	102
4.4	Synthesis of NU6451 analogues	109

Chapter 5 — Pharmacophore mapping and scaffold hopping around NU6247

5.1	Pharmacophore mapping around NU6247	119
5.1.1	Benzyl sulfone analogue	120
5.1.2	Removing the O ⁶ -substituent	122
5.1.3	Removing the terminal basic moiety	125
5.1.4	Identity of the linker	126
5.1.5	Introducing a substituent at the 8-position	127
5.2	Scaffold hopping from the literature	135
5.2.1	The Purvalanol A analogue of NU6247	135
5.2.2	The ‘Cyclacel’ analogue of NU6247	140
5.2.3	Replacement of the purine core pharmacophore by a pyrazolo-pyrimidine	145

Chapter 6—NU6300, an irreversible inhibitor of CDK2

6.1	Irreversible enzyme inhibition	149
6.2	NU6300 as an irreversible inhibitor of CDK2	153
6.3	CDK2 redundancy	164

Conclusions —166

Chapter 7—Experimental

7.1	Chemicals and solvents	168
7.2	Chromatography	168
7.3	Analytical techniques and instrumentation	169
7.4	Index of Compounds Synthesised	172
7.5	General Procedures	178
7.6	Experimental Procedures	182
7.7	Protein expression, kinase assays, MS and SPR	266

References 272

Acknowledgements

I should like to begin by thanking my supervisor, Prof. Roger Griffin, for the great opportunity he granted me by letting me join the Northern Institute for Cancer Research (NICR), and for his invaluable support and guidance throughout this PhD, which has been an incredible experience.

I would like to express my most sincere gratitude to Dr. Ian Hardcastle, Prof. Bernard Golding and Dr. Celine Cano for their continuing support, guidance and assistance over my four years at Newcastle University. I gratefully acknowledge all the members of the ADDI lab for their precious advice, encouragement and company, in particular Dr. Mangaleswaran Sivaprakasam, Dr. Benoit Carbain and Francesco Marchetti for their support with the CDK project.

Professor David 'Herbie' Newell, Dr Nicola Curtin, Professor Hilary Calvert and members of the NICR are gratefully acknowledged for their assistance with the biological aspects of my research. Thanks to Lan-Zhen Wang for performing the biological evaluation of the inhibitors that I have produced.

Special thanks to Professor Jane Endicott and Professor Martin Noble, for granting me the incredible opportunity of working in their laboratories at Oxford University between February and June 2010, and for providing me with help and guidance while I learned to perform molecular biology studies on my inhibitors. I gratefully acknowledge Elizabeth Anscombe for her assistance with the project and Dr. Ed Lowe, Dr. Nick Brown and Dr. David Staunton for allowing my experience at Oxford to be pleasurable and deeply instructive at the same time.

I thank our technicians, Dr. Karen Haggerty and Carlo Bawn, for the analytical work and the maintenance of the LCMS, HPLC and NMR [instruments](#). Thanks to all the members of the university staff who have provided the necessary technical support for my research, in particular John Marshall from the glassware workshop.

I would like to express my kind affection toward all members of the ADDI lab with whom I have had the pleasure and honour of working, including Dr. Eric Valeur, Dr. Celine Roche, Sara Payne, Christopher Coxon, Christopher Wong, Anna Watson, Dr. Barry Dodd, Dr. Kate Clapham, Dr. Tim Blackburn, Charlotte Revill, Ruth Taylor, Tommy Rennison, Stephanie Myers, Christopher Matheson, Dr. Jennyfer Goujon,

Dr. Andrey Zaytsev, Lauren Barrett, Sarah Cully, David Turner, Dr. Betty Cottyn and Dr. Sandrine Vidot.

Finally, I would like to gratefully acknowledge Cancer Research UK for providing me with generous funding to carry out my research.

I would like to conclude by dedicating this work to my friends and family for their unconditional love and support, as a sign of thankfulness for getting through these years with me and for standing by me during this challenging experience.

Abbreviations

A

AcOH	Acetic Acid
ADP	Adenosine Diphosphate
Ala	Alanine
AMP	Adenosine Monophosphate
anh.	Anhydrous
aq.	Aqueous
Ar	Aromatic Group
Arg	Arginine
Asp	Aspartic Acid
atm	Atmosphere
ATP	Adenosine Triphosphate

B

Bn	Benzyl
br	broad (NMR)
n-BuOH	n-Butanol
t-Bu	tert-Butyl
t-BuOH	tert-Butanol

C

°C	Degrees Celsius
CDK	Cyclin-Dependent Kinase
<i>m</i> CPBA	<i>meta</i> -Chloroperbenzoic Acid
conc.	Concentrated
CTDK	Carboxy-terminal domain kinase
Cy	cyclohexyl

D

d	Doublet (NMR)
DABCO	1,4-Diazabicyclo[2.2.2]octane
DEAD	Diethyl azodicarboxylate
DIBAL	Diisobutylaluminum Hydride
DIEA	<i>N,N</i> -Diisopropylethylamine
DMAP	<i>N,N</i> -Dimethyl-4-aminopyridine
DME	1,2-Dimethoxyethane
DMF	<i>N,N</i> -Dimethylformamide
DMSO	Dimethyl Sulfoxide
DNA	Deoxyribonucleic Acid
D₂O	Deuterium Oxide
δ	Chemical Shift

E

EI	Electron Ionisation
ES	Electrospray
Et	Ethyl
Et₂O	Diethyl Ether
EtOAc	Ethyl Acetate
EtOH	Ethanol
equiv.	Molar Equivalents

G

g	Gram
Glu	Glutamic Acid
Gln	Glutamine
Gly	Glycine

H

h	Hour
¹ H	Proton

HCl	Hydrochloric Acid
His	Histidine
HPLC	High Performance Liquid Chromatography
Hz	Hertz
I	
IC ₅₀	Drug concentration required for 50% enzyme inhibition
Ile	Isoleucine
IR	Infrared
iPrOH	Isopropanol
K	
kDa	KiloDalton
K _i	Inhibition Constant
J	
<i>J</i>	Coupling Constant
L	
λ _{max}	Wavelength of Maximum Absorbance
LCMS	Liquid Chromatography Mass Spectrometry
Leu	Leucine
LHMDS	Lithium Hexamethyldisilazane
Lys	Lysine
M	
M	Molar
M ⁺	Molecular Ion
m	Multiplet (NMR)
Me	Methyl
MeCN	Acetonitrile
MeOH	Methanol

Met	Methionine
MHz	MegaHertz
mL	Millilitre
min	Minutes
mmol	Millimolar
m.p.	Melting Point
MS	Mass Spectrometry
<i>m/z</i>	Mass to Charge Ratio

N

NBS	<i>N</i> -Bromosuccinimide
<i>n</i>-BuLi	<i>n</i>-Butyllithium
NEt₃	Triethylamine
NICR	Northern Institute for Cancer Research
nM	Nanomolar
NMR	Nuclear Magnetic Resonance
Nu	Nucleophile

P

Pd(PPh₃)₄	Tetrakis(triphenylphosphine) Palladium(0)
Petrol	Petroleum Ether (40-60 °C)
Ph	Phenyl
Phe	Phenylalanine
POCl₃	Phosphorous oxychloride
P₂O₅	Phosphorous Pentoxide
PPh₃	Triphenylphosphine
ppm	parts per million
Pro	Proline

Q

q	Quartet (NMR)
---	---------------

R

R	Alkyl Group
Rb	Retinoblastoma
r.t.	room temperature
R _T	Retention Time

S

s	Singlet (NMR)
Ser	Serine
SAR	Structure-Activity Relationship
S _N Ar	Nucleophilic Aromatic Substitution
SPR	Surface Plasmon Resonance
Sulfanilyl	4-Aminobenzenesulfonyl

T

t	Triplet (NMR)
TFA	Trifluoroacetic Acid
TFE	2,2,2-Trifluoroethanol
THF	Tetrahydrofuran
Thr	Threonine
TLC	Thin Layer Chromatography
TMS	Tetramethylsilane
Trp	Tryptophan
Tyr	Tyrosine

U

UV	Ultra-Violet
----	--------------

V

Val	Valine
-----	--------

Chapter 1 - Kinases and Cancer

1.1 Cancer: definition and hallmarks

The term “cancer” is used to describe a disease in which loss of regulation in cellular processes results in uncontrolled proliferation of cells and, subsequently, in the generation of a malignant tumour. Cancer cells have defects in regulatory circuits that govern normal proliferation and homeostasis. ¹

To date, more than 100 types of cancer have been described, subtypes of which can arise within certain specific organs. Hanahan and Weinberg ¹ have suggested that this wide variety of cancer phenomenology is a manifestation of six essential alterations in cell physiology:

- **Self-sufficiency in growth signals**

Normal cell proliferation depends upon correct communication with the external environment through the exchange of signalling molecules (growth factors). Tumour cells ~~are~~ do not divide according to external growth factor signalling. Acquired genetic mutations result in the cell bypassing growth factor pathways, which leads to unregulated growth, either by internal production of growth factors or by responding to levels of external signals usually not sufficient to induce proliferation in normal cells.

- **Insensitivity to anti-growth signals**

In normal tissue, the stability of the cell population (homeostasis) is maintained by a number of signals and processes inhibiting cell proliferation and differentiation (e.g. contact with neighbouring cells inhibits cell growth). Cancer cells survive and replicate by not responding to anti-growth signals, as acquired mutations interfere with, or allow, the cell to bypass the inhibitory pathways.

- **Evasion of apoptosis**

In normal tissues, the stability of the cell population is maintained through a process of programmed cell death, or apoptosis. In response to DNA damage, or any other sign of abnormality within a cell, sensors monitoring the cellular environment regulate the action of apoptotic effectors, resulting in cell death. Loss of apoptotic regulators through mutation leads to evasion of apoptosis in cancer cells. This mechanism is thought to be a critical survival factor for the majority of tumours.

- **Limitless replicative potential**

After every round of DNA replication, chromosomal ends (telomeres) are shortened. This constitutes an effective method by which normal cells are able to 'keep count' of their doublings, and results in the cell entering senescence after a finite number of replications. Tumour cell populations acquire unlimited replicative potential by maintenance of telomere length, either by overexpressing telomerase or by recombination processes, effectively gaining "immortality".

- **Angiogenesis**

In normal tissues, continued cell function is dependent on the availability of oxygen and nutrients through the capillary beds. The vascular architecture is more or less constant in adults, and angiogenesis, the ability to induce the growth of new blood vessels, is transitory and carefully regulated. Cancer cells have acquired the capability to override angiogenesis inhibitors and activate the angiogenetic switch to supply the resources necessary for tumour survival and expansion.

- **Tissue invasion and metastasis**

Normal cells maintain their location in the body and generally do not migrate. Cancer cells spread from the primary tumour site through the body to colonise distant tissues to form metastases. Up to 90% of cancer deaths are due to metastatic disease. Several classes of proteins involved in the tethering of cells to their surrounding tissues are altered in cancer cells. Cell-cell adhesion

and cell-to-environment interactions are subverted so that the metastatic cell acquires the ability to colonise distant territories where nutrients and space are more abundant.

These six capabilities that a cancerous cell acquires are found to be common in most, if not all, types of tumours.

In a recent revisitation of their earlier 2000 work,² Hanahan and Weinberg expanded upon these six established characteristics and recognised two additional emerging hallmarks of cancer, as well as two enabling characteristics that allow a cell to become physiologically altered in this manner.

- The first emerging hallmark is the **reprogramming of the cell's energy metabolism**.

Chronic and uncontrolled cell proliferation in cancer involves not only deregulated control of cell proliferation but also corresponding adjustments of energy metabolism in order to fuel cell growth and division. Cancer cells can reprogram their glucose metabolism, and therefore their energy production, by limiting their energy metabolism largely to glycolysis. This has been shown to be associated with activated oncogenes and mutated tumour suppressor genes, resulting in the onset of malignancy.

- The second emerging hallmark is the **evasion of immune destruction**.

Normal cells and tissue are constantly monitored by the immune system, and this immune surveillance is responsible for recognising and eliminating a vast proportion of incipient cancer cells and nascent tumours. Solid tumours that do reach a malignant stage have either managed to avoid detection by the immune system, or to limit the extent of the immunological response, thereby evading eradication.

Acquisition of the above eight fundamental hallmarks of cancer (two of which are in the course of being validated and therefore remain deemed "emerging") appears to be enabled by two fundamental characteristics of cancerous cells:

Formatted: Font: Bold

Formatted: List Paragraph, Bulleted + Level: 1 + Aligned at: 0.63 cm + Tab after: 1.27 cm + Indent at: 1.27 cm, Don't adjust space between Latin and Asian text, Don't adjust space between Asian text and numbers

Formatted: Font: (Default) Arial, 12 pt, English (United Kingdom)

Formatted: Font: (Default) Arial, 12 pt, English (United Kingdom)

Formatted

Formatted: Font: (Default) Arial, 12 pt, English (United Kingdom)

Formatted

Formatted: Font: (Default) Arial, 12 pt, English (United Kingdom)

Formatted

Formatted: English (United Kingdom)

Formatted: List Paragraph, Don't adjust space between Latin and Asian text, Don't adjust space between Asian text and numbers

Formatted

Formatted: List Paragraph, Bulleted + Level: 1 + Aligned at: 0.63 cm + Tab after: 1.27 cm + Indent at: 1.27 cm, Don't adjust space between Latin and Asian text, Don't adjust space between Asian text and numbers

Formatted: Font: Bold

Formatted

Formatted: Don't adjust space between Latin and Asian text, Don't adjust space between Asian text and numbers

- The first enabling characteristic is the instability of the genome.

The ability of the genome maintenance system to detect and correct defects in the DNA ensures that mutation rates remain low during each cell generation. In the course of acquiring the mutant genes needed to initiate tumorigenesis, cancer cells are able to increase the rate of mutation through increased sensitivity to mutagenic agents, a breakdown in ordinary DNA repair pathways, or both.

Formatted: Font: Bold

Formatted: List Paragraph, Bulleted + Level: 1 + Aligned at: 0.63 cm + Indent at: 1.27 cm, Don't adjust space between Latin and Asian text, Don't adjust space between Asian text and numbers

- The second enabling characteristic is tumour-promoting inflammation.

Virtually every neoplastic lesion contains immune cells present at densities ranging from subtle infiltration to gross inflammation. Such tumour-associated inflammatory response has the effect of enhancing tumorigenesis and progression, contributing to multiple hallmark capabilities by supplying growth factors, survival factors, angiogenic factors etc. Additionally, inflammatory cells can release reactive chemical species, such as oxygen radicals, that are actively mutagenic and contribute the genetic evolution towards a heightened state of malignancy.

Formatted: List Paragraph, Don't adjust space between Latin and Asian text, Don't adjust space between Asian text and numbers

Formatted: List Paragraph, Bulleted + Level: 1 + Aligned at: 0.63 cm + Indent at: 1.27 cm, Don't adjust space between Latin and Asian text, Don't adjust space between Asian text and numbers

Formatted: Font: Bold

-Despite the apparent simplicity of this description, cancer is an extremely complex disease and, as such, has so far presented an immense challenge to the development of effective treatments. After the human genome was elucidated,³ genomics has offered an additional tool aiding the comprehension of cancer from a molecular point of view. **Oncogenes** (genes whose *activation* cause cancer) and **tumour suppressor genes** (genes whose *inactivation* cause cancer) were discovered and found to be mutated in tumours, although depending on the specific type of tumour, mutations can occur at different stages of its development. Cancer genomics contributes to defining molecular targets for tumour specific effects and constitutes an important tool for the design of new molecular therapies.^{4 5} Relevant studies have focused on the tumour suppressor genes p53 and retinoblastoma (Rb), which are found mutated in over a half of all cancers cases, as they play key roles in inhibiting carcinogenesis. The most common mutations within these cancer-related genes are found within the protein kinase domain.⁶

Formatted: Font:

Formatted: Don't adjust space between Latin and Asian text, Don't adjust space between Asian text and numbers

Protein kinases play a leading role in the control of cellular biology and in signal transduction pathways, and it is therefore of little surprise that they would be universally recognised as targets of primary interest for anticancer drug discovery.

1.2 Protein Kinases

Ever since the discovery more than 50 years ago that reversible phosphorylation regulates the activity of glycogen phosphorylase,⁷ there has been intense interest in the role of protein phosphorylation in regulating protein function.

The protein kinase family is the largest functional family of enzymes encoded by the human genome.⁸ The completion of the human genome sequence has allowed the identification of 518 kinases, constituting approximately 1.7% of all human genes.⁸

To compare related kinases in human organisms and to gain insights into kinase function and evolution, all kinases are divided into nine broad groups, comprising 134 families and 196 subfamilies, classified with regard to the sequence alignment of their catalytic domains which all relate to the same superfamily containing a eukaryotic protein kinase (ePK) domain. A family of 13 atypical protein kinases (aPK) were also identified.

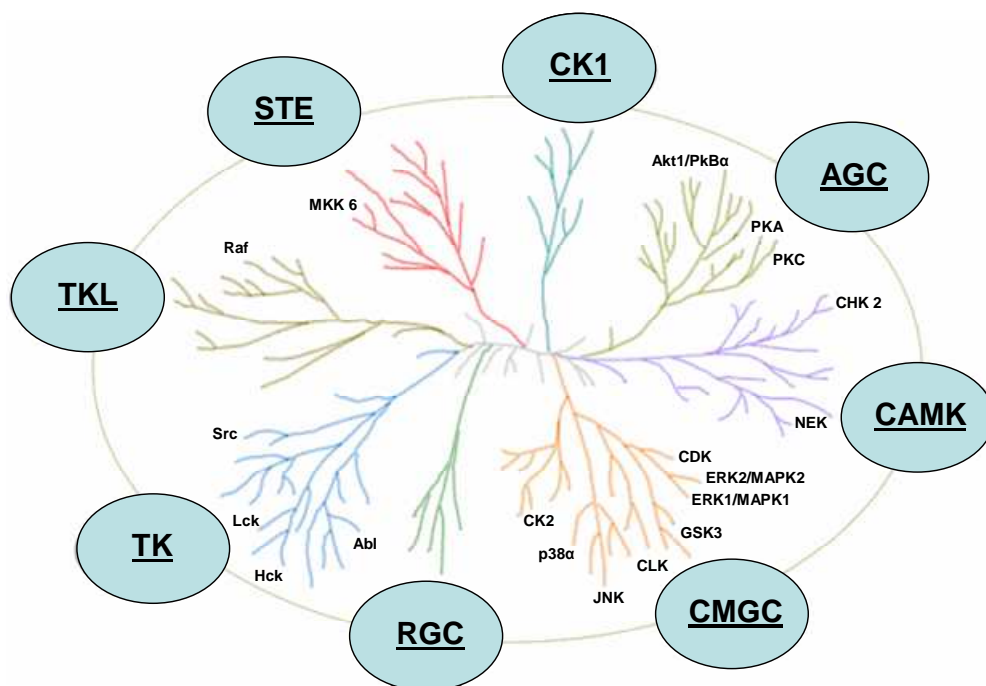


Figure 1

Phylogenetic tree representing the main protein kinase families ⁸

The reaction of ATP, which contains a somewhat activated linkage between the β - and γ -phosphate groups, with an alcohol or phenol will produce very little phosphate ester, as the reaction is kinetically very slow and also rather disfavoured in an aqueous medium, where the water itself is a competing nucleophile. Therefore, for the reaction to be useful, it must be catalysed. ⁹ Protein kinases are ATP-dependent phosphotransferases that deliver a single phosphate group from the γ position of ATP to a hydroxyl group of a tyrosine, serine or threonine residue belonging to a specific protein substrate. ¹⁰

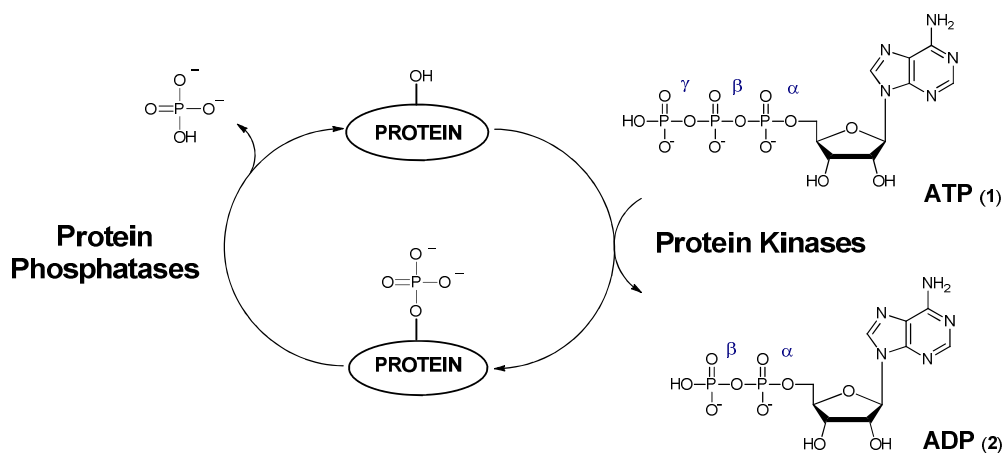


Figure 2

The protein phosphorylation cycle

The phosphoryl transfer reaction is facilitated by the presence of a divalent metal ion (usually Mg^{++}) which assists in the ATP binding, and the phosphorylation reaction taking place in the active site of the protein kinase is a complex process which involves structural changes. Protein phosphatases remove the phosphate, thereby creating a “molecular switch”,¹¹ which enables the control and mediation of most of the signal transduction processes in eukaryotic cells. Protein kinases also control many other cellular processes, including transcription, cell cycle progression, cytoskeletal rearrangement and cell movement, apoptosis and differentiation. Metabolic activities involving carbohydrate and lipid metabolism, neurotransmitter biosynthesis and organelle trafficking are also organised by the combined action of kinases and phosphatases.^{7 12} Phosphorylation is one of the most important post-translational modifications that a protein can undergo, and it has a profound impact at both the molecular and the cellular level.

Sequence comparisons of members of the protein kinase family reveal that the [catalytic domains, normally ranging from 200-250 amino acids](#), often share a conserved [region of approximately 200-250 amino acids sequences alternating](#)

regions of high and low conservation. ~~This is~~ the catalytic core domain ~~that constitutes~~ contains the ATP-binding site and confers kinase activity to the protein.¹³

Protein kinase structures share a characteristic fold, which comprises an N-terminal lobe of mostly β -sheets, with one α -helix known as the C-helix, and a second C-terminal lobe, constituted largely of α -helices. The catalytic site hosts the ATP-binding domain, which resides at the interface of the two lobes, in the so-called hinge region, allowing a prompt opening or closure of the ATP-binding cleft in response to kinase activation or inactivation (**Figure 3**).

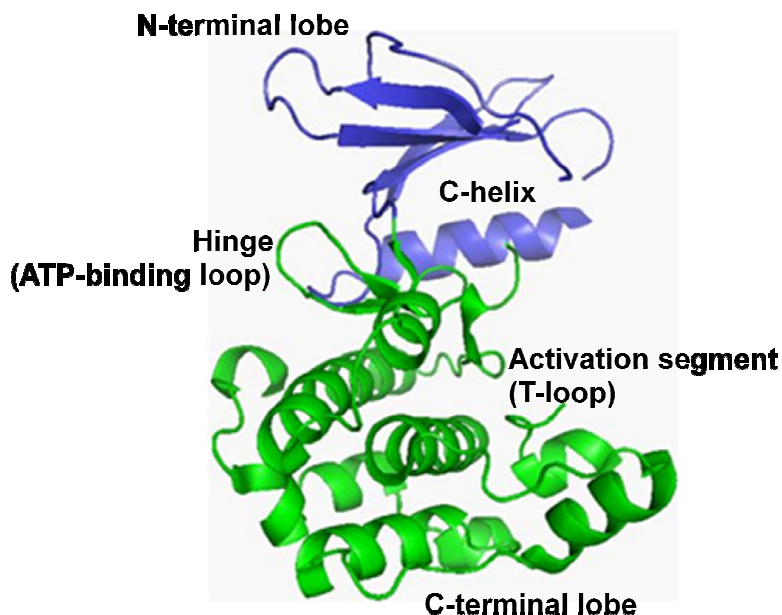


Figure 3

Crystal structure of a typical protein kinase (AMPK α 2 kinase domain)¹⁴

As kinase-signalling cascades were further investigated, it was discovered that kinase activation requires phosphorylation by another kinase, usually on a threonine (e.g. Thr 160 in CDK2) or a tyrosine residue, positioned in a conserved region in the C-terminal lobe. This is termed the activation segment or 'T-loop'.

Nearly all protein kinases thus far characterised with regard to substrate specificity fall within one of two broad classes, **serine/threonine-specific** and **tyrosine-specific**. There is a third and less common class, called the **dual-function kinases**, which phosphorylate all three amino acids.

Although classified so broadly, protein kinases have an extremely high specificity towards their chosen substrate. The specificity is primarily due to the variations in the local sequence of amino acids either side of the phosphorylation site. These highly characteristic amino acidic residues provide significant interactions between the enzyme and the substrate, thereby directing the phosphoryl transfer. Additional assistance may also be provided by interactions of the substrate with functionalities remote from the active site. Many examples exist of long-distance recognition assessed even at a 40 Å distance from the phosphorylation site,¹⁰ demonstrating that although protein kinases share a highly conserved ATP-binding site, they are absolutely specific to the substrate assigned to them.

This specific reversible phosphorylation of protein substrates in the cell is among the most important post-translational modifications to occur, and it is the principal method by which cellular control and adaptation is achieved. Today, it is difficult to discuss any biochemical event in the living cell that is not affected directly or indirectly by protein phosphorylation. Protein activation leads to the amplification of cellular signalling (**Figure 4**) and aids the regulation of virtually all cellular processes such as metabolism, growth and proliferation.¹⁵ Protein kinases therefore play a crucial role in signal transduction pathways.

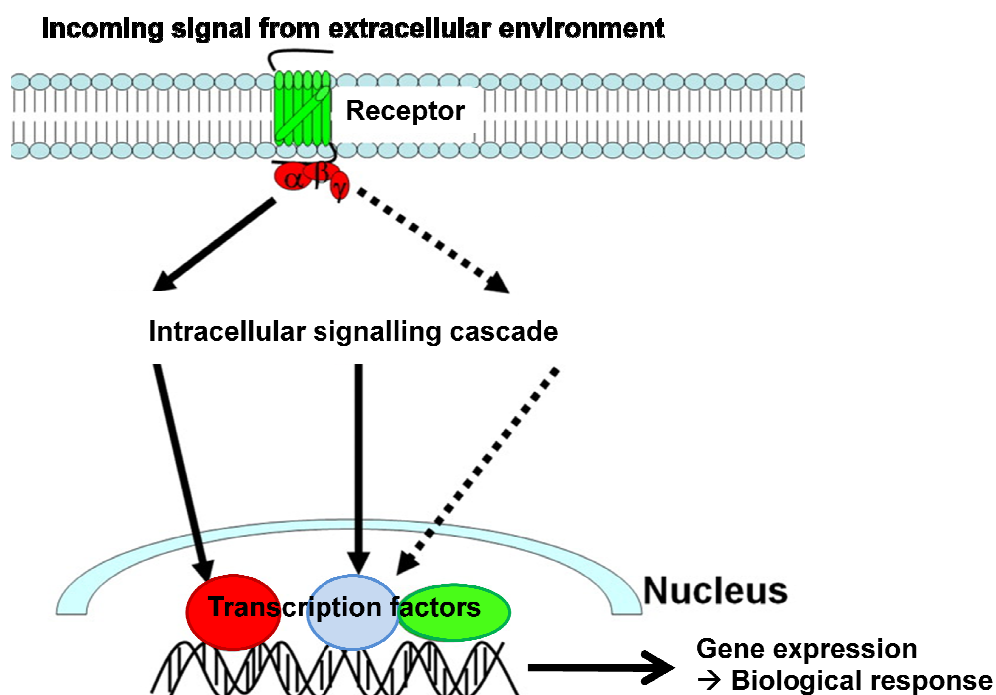


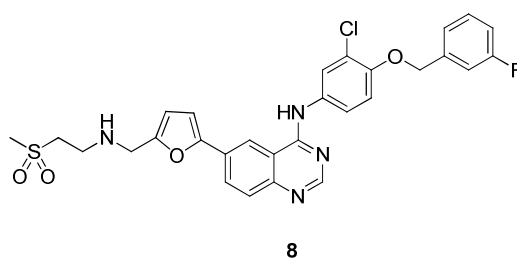
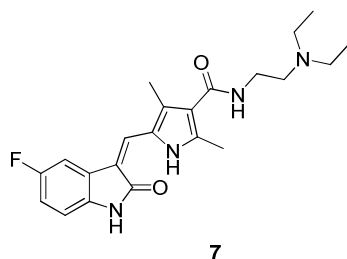
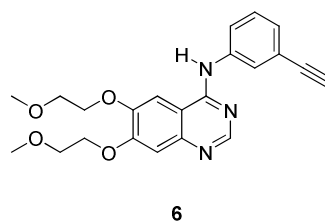
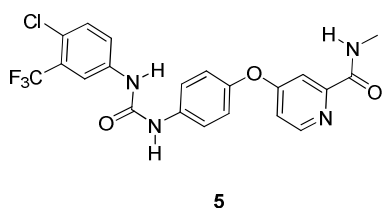
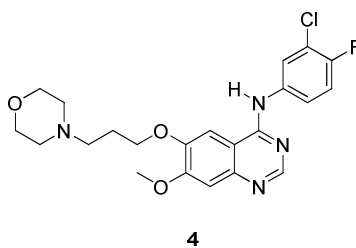
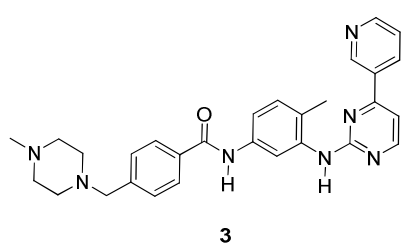
Figure 4

Schematic representation of a signal transduction pathway.

1.3 Kinase inhibitors as anticancer agents

Kinase activity is of primary importance in a wide range of vital cellular processes.¹⁶ The biological significance of protein kinases as key regulators of all aspects of neoplasia, including proliferation, angiogenesis and invasion, has increased considerably in recent years. The fact that kinases share a common catalytic mechanism, many aspects of structural similarity, and sequence homology within the catalytic domain were initially a cause of concern that the pursuit of kinase inhibitors may not be an ideal strategy for anticancer drug discovery. Moreover, considering the high intracellular concentrations of ATP, the fact that most of these kinase

inhibitors were intended to be ATP-competitive increased the degree of uncertainty regarding this therapeutic approach.¹⁶ However, the marketing of imatinib (**3**), gefitinib (**4**), sorafenib (**5**), erlotinib (**6**), sunitinib (**7**) and lapatinib (**8**) in the last decade has dispelled these concerns, and established the value and efficacy of kinase inhibitors as anticancer agents.



Imatinib (**3**, *Glivec*/ST1571) received Food and Drug Administration (FDA) * approval in 2001. It was developed by Novartis in one of the first successful examples of a rational drug design approach. Imatinib is the first member of a new class of agents that are intended to specifically inhibit a certain enzyme that is characteristic of a

* The **Food and Drug Administration (FDA or USFDA)**, an agency of the United States Department of Health and Human Services, is responsible for the regulation and supervision of food safety, tobacco products, dietary supplements, prescription and over-the-counter pharmaceutical drugs, vaccines, biopharmaceuticals, blood transfusions, medical devices, electromagnetic radiation emitting devices (ERED), veterinary products and cosmetics.

particular cancer cell (Bcr-Abl tyrosine kinase), rather than non-specifically inhibiting and killing all rapidly dividing cells, and served as a model for other targeted therapy modalities. This drug is mainly used in the treatment of chronic myeloid leukaemia (CML), but its applications were extended to the treatment of gastrointestinal stromal tumours (GISTs), after the observation that **3** also inhibited the c-Kit receptor tyrosine kinase. This observation emphasises that complete kinase selectivity is not necessarily a crucial factor for the clinical success of protein kinase inhibitors.¹⁷

Sunitinib (**7**, *Sutent*/SU11248) is a multi-targeted receptor tyrosine kinase (RTK) inhibitor, which was approved in 2006 for the treatment of renal cell carcinoma (RCC) and Imatinib-resistant GISTs. It was the first anticancer drug simultaneously approved for two different indications, and has now become the standard treatment for both of these cancers.¹⁸

Gefitinib (**4**, *Iressa*/ZD1839), Erlotinib (**6**, *Tarceva*/OSI-774) and Lapatinib (**8**, *Tykerb*/GW572016) are small molecule kinase inhibitors based upon the 4-anilinoquinazoline scaffold. Gefitinib was the first drug to selectively target the epidermal growth factor receptor (EGFR) tyrosine kinase, which is highly expressed and occasionally mutated in various forms of cancer.¹⁹ Gefitinib was approved in 2004 for the treatment of advanced non-small cell lung cancer (NSCLC). However, later studies revealed that efficacy seems to rely on the dependence of the cancer upon particular molecular abnormalities.^{20 21}

Sorafenib (**5**, *Nexavar*/BAY43-9006) targets the Raf/Mek/Erk signalling pathway. Raf and Mek are members of the mitogen-activated protein (MAP) kinase family, while Erk is an extracellular signal-regulated kinase. The drug was originally identified as an ATP-competitive inhibitor of b-Raf and approved for the treatment of RCC in 2005. Subsequent studies revealed its activity against platelet-derived growth factor (PDGF), VEGF and c-Kit kinases, which play a role in both tumour angiogenesis and tumour cell proliferation. These investigations resulted in approval of Sorafenib for the treatment of hepatocellular carcinoma (HC), which is the most common form of liver cancer. Sorafenib thus represents an example of a multiple kinase inhibitor.²²

1.4 ATP-competitive inhibition of protein kinases

Kinase inhibition can be approached in several possible ways. Firstly, it is possible to interfere with the factors that regulate the translation of a kinase; secondly, substrate binding may be inhibited by targeting the substrate specific binding site; thirdly, the activity of a kinase may be ablated by interfering with the factors that regulate its activation. The fourth approach is, of course, to target the ATP-binding site of the kinase. ATP-competitive inhibition is the mechanism by which the vast majority of kinase inhibitors prepared to date are thought to function.¹⁶

Although ATP-competitive kinase inhibitors exhibit a wide spectrum of chemical diversity, for the most part they all interact with the kinase in a broadly similar fashion, *via* key hydrogen bonding interactions with the hinge region of the ATP-binding domain.^{23 24} Determination of the crystal structure of ATP-kinase complexes reveals two important hydrogen bond interactions between ATP and the backbone amino acid residues of the active site cleft. Thus, N¹ of the adenine acts as a hydrogen-bond acceptor from an amide proton of the protein backbone, whilst the 6-amino group donates a hydrogen bond to the oxygen of a backbone carbonyl group. This doublet of hydrogen bonds anchors the adenine to the hinge region, allowing the ribose to point towards and interact with a highly hydrophobic region of the ATP-binding domain.^{25 26}

Structural studies on protein kinases in complex with ATP have further revealed that there are regions within, or close to, the binding cleft that ATP does not fully occupy, such as the gatekeeper and specificity pocket (**Figure 5**).²⁷ The gatekeeper region is a lipophilic pocket located furthest away from the entrance to the ATP-binding cleft, in the direction of N⁷ and C⁶ of the adenine. The size of the pocket is determined by the bulk of the amino acid sidechains surrounding this region. The specificity pocket is a cleft that opens to solvent, characterised by lipophilic surfaces above and below the adenine heterocycle surface and providing for additional interactions with potential inhibitors. The name arises from the poor homology observed among the different families of protein kinases, and this cavity has been

exploited to introduce water-solubilising groups on inhibitors, as it faces the exterior of the ATP-domain and does not hinder binding of the inhibitor to the kinase.²⁸

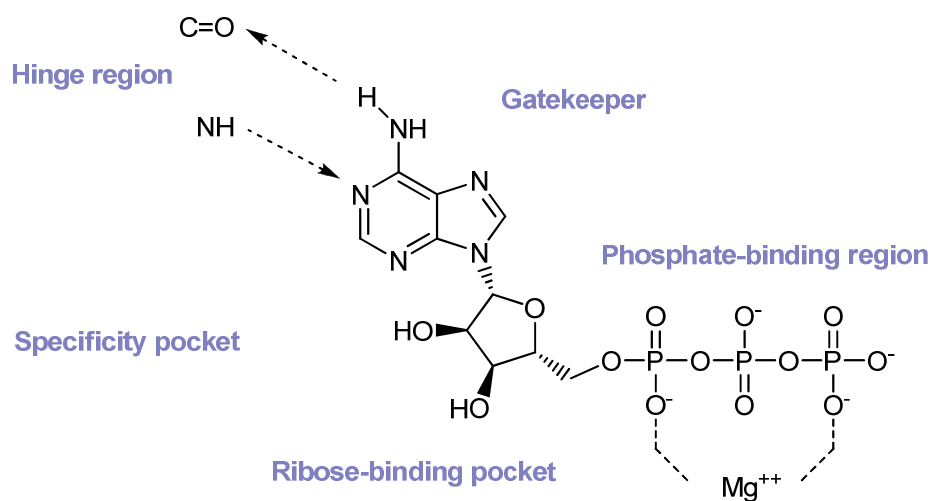


Figure 5

Schematic representation of the regions into which the ATP-binding site of most kinases is usually divided.²⁷

These pockets are usually poorly occupied by ATP, and show structural diversity between members of the kinase family, thereby providing opportunities for the design of selective ATP-competitive inhibitors.²⁸

Chapter 2 – Cyclin-Dependent Kinases (CDKs)

2.1 The cell cycle

The cell is the structural and functional unit of all living organisms, containing all components necessary for the continuation and expression of life. The continued integrity of every life form relies on the ability of its component cells to transfer faithfully their genetic material. Cells proliferate through a complex process, known as the cell cycle, which consists of a series of checkpoints and regulatory mechanisms to ensure that the DNA is correctly replicated and equally distributed between the two daughter cells (**Figure 6**).²⁹

The cell cycle is divided into four phases: **S phase** (DNA replication), **M phase** (mitosis) and two **gap phases** (G_1 and G_2) that separate the M and S phases. The sequence G_1 -S- G_2 is sometimes collectively referred to as interphase.

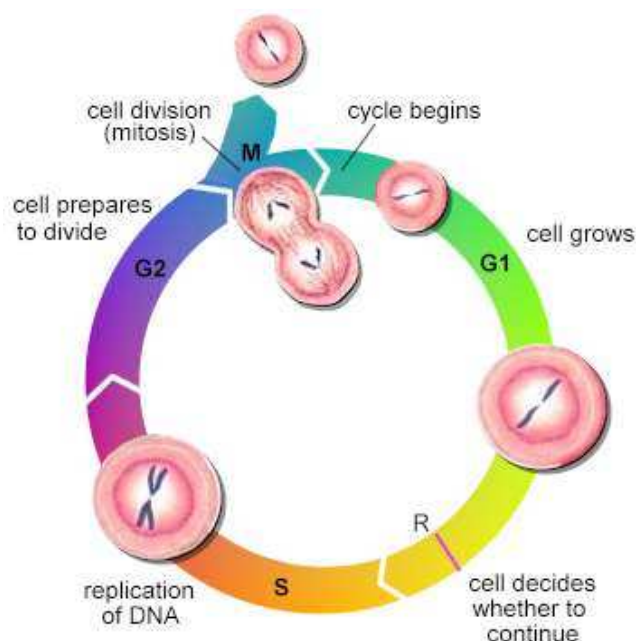


Figure 6

The cell cycle.³⁰

The M phase is itself composed of two tightly coupled processes: **mitosis**, where the cell's chromosomes are divided between the two daughter cells (**Figure 7**), and **cytokinesis**, where the cell's cytoplasm physically divides.

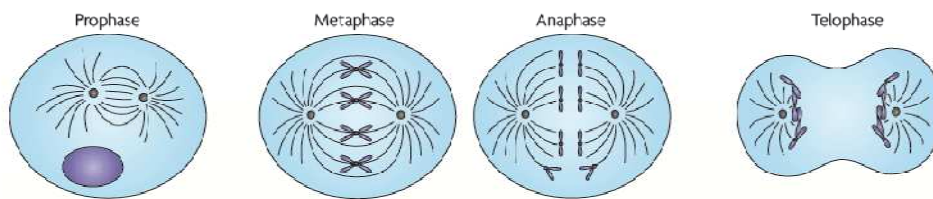


Figure 7

The progression of mitosis through four phases. ³¹

The cell cycle is a very delicate process occurring in an extremely complex environment. The gap phases are necessary for the cell to correctly decipher and interpret the vast array of information and signalling that regulate the mechanisms of DNA repair and replication, and the preparation for cell division. ³²

During G_1 phase, for instance, growth factors (mitogens) must be available for the cell to correctly enter S phase. If that is not the case, at the restriction point ³³ (R in **Figure 6**) the cell enters a phase called G_0 and is described as being **quiescent**. Despite being termed 'the quiescent phase', G_0 is an active phase in that cellular functions and cell growth occur. Cell growth (the increase in cell size and protein mass) is a term that is frequently confused with cell proliferation. However, in certain biological systems – such as oocytes, neurons and muscle cells, where cell growth might exist without cell division, and in fertilised eggs, where cell division might occur without cell growth – these processes function in an independent, or even complementary, fashion. In most cells, cell division without concurrent cell growth would generate smaller daughter cells, which would affect their viability. ³⁴ Once mitogens become available, the cell can pass the restriction point and correctly complete the cell cycle. It is to be noted that the restriction point constitutes a critical stage for the cell: once it has made the decision to progress past this stage, it is

irreversibly committed to entering DNA synthesis and completing the cycle. Cells that have entered the G_0 phase permanently, due to age, extensive DNA damage or other irreversible problems are said to be **senescent**. Some cell types in mature organisms, such as parenchymal cells of the liver and kidney, enter the G_0 phase semi-permanently and can only be induced to begin dividing again under very specific circumstances;³⁵ other types, such as epithelial cells, continue to divide throughout an organism's life and are never known to enter the G_0 phase at all.

Although the various stages of interphase are not usually morphologically distinguishable, each phase of the cell cycle has a distinct set of specialised biochemical processes that prepare the cell for initiation of the cell division. The term **post-mitotic** is sometimes used to refer to both quiescent and senescent cells. Nonproliferative cells in multicellular eukaryotes generally enter the quiescent G_0 state from G_1 and may remain quiescent for long periods of time, possibly indefinitely (as is often the case for neurons). This is very common for cells that are fully differentiated. Cellular senescence is a state that occurs in response to DNA damage or degradation that would make a cell's progeny non-viable; it is often a biochemical alternative to programmed cell death (apoptosis).³⁶

2.2 The Cyclin-Dependent Kinases (CDKs)

The cell cycle is a unidirectional process, where progression from one phase to the next can be initiated only after passage through specific control mechanisms – checkpoints. Each separate transition cannot take place without verifying the correct completion of the previous one, the two often being linked via regulatory loops.^{33 37} Cancer cells often show alterations in the signal transduction pathways that lead to proliferation in response to external signals. Indeed, many growth factors and their receptors, as well as their membrane, cytoplasmic and nuclear downstream effectors have been identified as oncogenes or tumour-suppressor genes. Other genes mutated in cancer include those that inactivate apoptotic pathways, induce genomic instability and promote angiogenesis. Tumour-associated mutations in many of these molecules result in the alteration of the basic regulatory mechanisms that control the mammalian cell cycle.³⁴

Instrumental to the regulation of these checkpoints are the cyclin-dependent kinases (CDKs), which facilitate critical cell cycle transitions. CDK inhibitors are therefore recognised to have potential therapeutic effect in the treatment of proliferative diseases.^{38 39}

The cyclin-dependent kinases (CDKs) are members of the serine-threonine protein kinase family and are key components in maintaining the systematic progression of cells in the cell cycle. The hallmark of cyclin-dependent kinases is that they are inactive in their monomeric form and require association with a specific cyclin partner for activation (**Figure 8**).⁴⁰ Also necessary for CDK activation is phosphorylation on a specific activation site (T-loop). This phosphorylation is carried out by the CDK-Activating Kinase (CAK), itself a member of the CDK family, the details of which will be discussed later in this chapter. Since the discovery of the *cdc2* protein (also known as CDK1) in the fission yeast *Schizosaccharomyces pombe*, a further 10 CDK family members (CDK2 – CDK11) have been identified along with 25 proteins with homology in the cyclin box, found as a result of the sequencing of the human genome.⁴¹

Each CDK shares 40-75% sequence homology and all are of similar size, between 30-40 kDa. CDKs are identified by a unique sequence of their amino acid code, the PSTAIRE motif (single letter amino acid code), corresponding to an α -helix in the active site that plays an important role in cyclin binding and phosphate transfer. Elucidation of the X-ray crystal structure of the CDK2/Cyclin A complex revealed the common kinase motif of a small N-terminal lobe consisting predominantly of β -sheets, and a larger C-terminal lobe formed largely from α -helices.⁴²

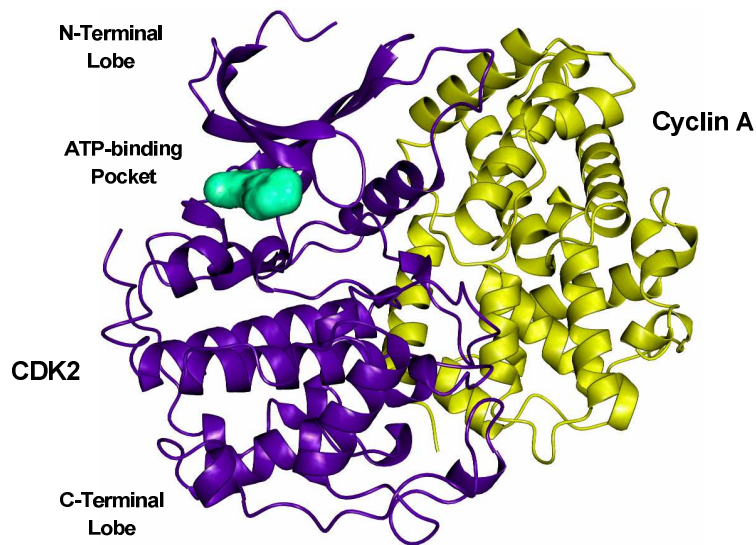


Figure 8

ATP bound within phosphorylated (T160P) CDK2/Cyclin A.⁴³

Although 11 CDKs have been identified to date, only 8 are believed to play integral roles in regulating cell cycle progression (**Figure 9**).⁴⁰

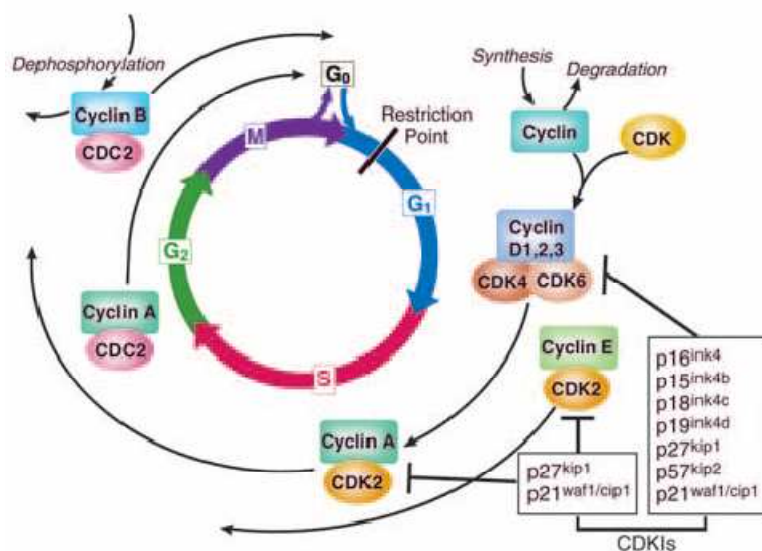


Figure 9

Regulation of the cell cycle by CDK/Cyclin complexes.⁴⁰

CDK	Cyclin partner	Related phase of the cell cycle / Other functions
CDK1	A, B	G ₂ , G ₂ /M, M. Also active in nervous system and RNA transcription.
CDK2	A, B, E	G ₁ , G ₁ /S, M. Also active for apoptosis and in RNA transcription.
CDK3	C, E	G ₀ /G ₁ , G ₁
CDK4	D	G ₁
CDK5	p25, p35, p29, p39	Active for apoptosis and in nervous system
CDK6	D	G ₁
CDK7	H	Active as a CAK and in RNA transcription.
CDK8	C	Active in RNA transcription
CDK9	T, K	Active for apoptosis and in RNA transcription
CDK10	Unknown	G ₂ /M
CDK11	L	M. Also active for apoptosis and in RNA transcription.

Table 1

The known CDKs, their cyclin partners and their roles in cellular biology. ⁴⁴

The cellular levels of CDKs remain relatively constant throughout the cell cycle, and their ability to regulate the cell cycle relies primarily on the oscillatory expression of their activating cyclin partners. The sequential fluctuation in cellular levels of a particular cyclin dictates the activation of the partner CDK, allowing the timely phosphorylation of the relevant protein target.⁴⁵ The name 'cyclin' accounts for this peculiar cyclic pattern. Cyclins vary considerably in size (30-80 kDa) but show structural similarities in certain specific regions, particularly within a 100 amino acid sequence, known as the cyclin box, which is the domain used to bind and activate CDKs.⁴⁶

2.2.1 The role of CDKs in regulating the cell cycle

CDKs coordinate the cell cycle by acting as molecular on/off switches in response to raised and lowered cyclin levels, T-loop phosphorylation, and the expression of endogenous CDK inhibitors (CKIs). When one CDK is activated ('on'), the cell can progress through the transition that the particular CDK/Cyclin complex controls. Alternatively, when the activity of that kinase is inhibited ('off'), cell cycle progression is halted.

In the early stages of G₁ phase, CDK4 and 6, in complex with D-type Cyclins (D₁/D₂/D₃), participate in the phosphorylation of the retinoblastoma protein pRb.⁴⁷ pRb is the product of the retinoblastoma tumour suppressor gene and is an important mediator of cell cycle progression, primarily influencing the transition from G₁ to S. pRb represses DNA transcription by binding to and inactivating specific members of the E2F family of proteins that act as transcription factors. Phosphorylation of pRb inactivates it and releases the transcription factors, thus permitting correct entry into S phase (**Figure 10**). CDK2 in complex with Cyclin E also plays a role in phosphorylation of pRb. The activity of these CDKs accompanies the cells all through G₁ and into S phase.⁴⁸ Upon entry into S phase, Cyclin A is expressed and binds to CDK1, activating the kinase. As a consequence, the cell passes smoothly from S into G₂ phase, and E2Fs are deactivated following CDK2/A-mediated phosphorylation, since transcriptional activity on their behalf is no longer needed. On completion of DNA synthesis and replication, and prior to the transition

from G₂ to M, CDK1 is expressed and activated for the purpose of monitoring pre-M checkpoints before the initiation of cell division.⁴⁹

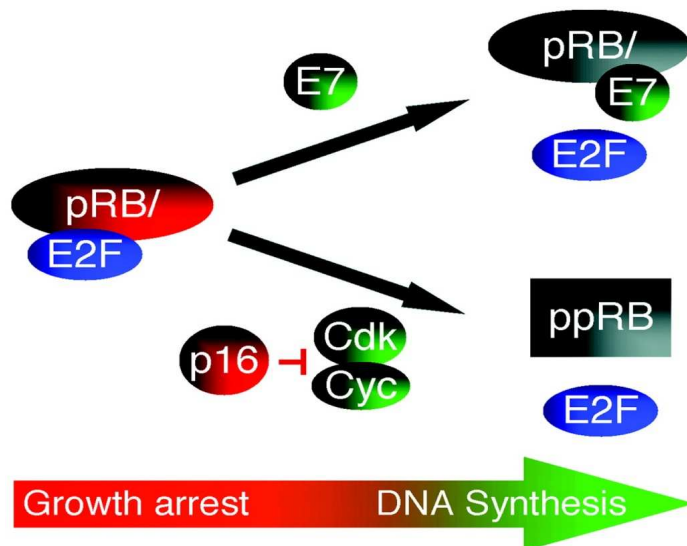


Figure 10

The retinoblastoma tumour suppressor pathway contains multiple oncogenes (green) and tumour suppressors (red).⁵⁰

Oncogenic processes exert their greatest effect by targeting particular regulators of the G₁ phase progression.⁵¹ G₁ progression normally relies on stimulation by mitogens and can be blocked by antiproliferative factors. As already explained above, it is during G₁ that cells face the decision as to whether to proceed with the cell cycle or enter a quiescent phase. Cancer cells are not controlled at this crucial point and remain permanently in the cell cycle; all processes that may lead to permanent exit from the cell cycle are also subverted.

As CDKs (CDK2, 3, 4 and 6 in complex with Cyclin A, D and E) are the key agents in controlling passage through the restriction point and entry into S phase, any malfunctioning or loss of control in their regulation directly causes uncontrolled cell proliferation, which may result in the development of cancer.

2.2.2 'Non-Cycling' CDKs

Members of the CDK family that are not involved directly in cell cycle regulation are described as '*non-cycling CDKs*' and fulfil secondary or peripheral roles in controlling the cell cycle progression.^{44, 52-53} A number of CDKs, including some that are also involved in the cell cycle, have been observed to target additional biological substrates whose functions are unrelated to the cell cycle, such as neurotransmission, transcription, differentiation and apoptosis (**Table 2**).

CDK	Cyclin Partner	Function
CDK1	A,B	Nervous system, apoptosis
CDK2	A, B, E	Centrosome duplication, apoptosis
CDK4	D	Nervous system, apoptosis, cell differentiation
CDK5	p25, p35, p29, p39	Neuronal functions, nervous system, apoptosis
CDK6	D	Nervous system, apoptosis, cell differentiation
CDK7	H	CAK (CDK-Activating Kinase), transcription
CDK8	C	Transcription
CDK9	T, K	Transcription, apoptosis, cell differentiation
CDK11	L	Transcription, apoptosis, nervous system

Table 2

Activities of 'non-cycling' CDKs.⁵³

One of the most widely researched non-cycling CDK is CDK5, which is expressed in post-mitotic cells of the central nervous system and is recognised to play numerous key functions during neuronal differentiation and migration.⁵⁴⁻⁵⁵ Unlike other CDKs,

CDK5 does not require CAK-mediated T-loop phosphorylation prior to activation, but is instead dependent on binding to cyclin-related proteins (e.g. p25, p35, p29 and p39).⁵⁶ CDK5 activity is deregulated in the pathogenesis of various neurodegenerative diseases, including Alzheimer's.⁵² CDK5 has therefore become an interesting target in the development of treatments for such diseases.⁵⁷

As is evident from **Table 2**, involvement in RNA transcriptional activity is common within the CDK family. Transcription requires phosphorylation of the carboxy-terminal domain (CTD) of RNA polymerase II (RNA Pol II), a large subunit required for the elongation process. CTD phosphorylation by different kinases, including some CDKs, may control several key transcriptional events.⁵² CDK9/Cyclin T and K complexes are components of the basal transcription elongation factor P-TEFb, which also phosphorylates the CTD on the largest subunit (RBB1) of RNA Pol II, thus promoting transcriptional elongation. CDK9 is also required for the kinase-dependent HIV-1 Tat transactivation. The Tat-associated kinase (TAK) complex can bind to the human immunodeficiency virus (HIV) Tat1 and Tat2 components, which are important regulators of gene expression.⁵⁸ CDK11 is also believed to be very important in regulating RNA processing and transcription, in association with cyclin L.⁵² Unlike CDK9, which has a positive effect on the transcriptional cycle, CDK8/Cyclin C and CDK1/Cyclin B suppress mRNA production during mitosis.^{59 60} As shown in **Table 2**, CDK7/Cyclin H, apart from having CAK activity, is also active in transcription. The details of the activity of this enzyme will be discussed in greater detail later in this chapter.

2.3 The regulation of CDK activity

Although CDKs are regulated by several different processes (phosphorylation, tight-binding inhibitors, regulated assembly of holoenzymes and ubiquitin-mediated proteolysis of cyclins and CDK inhibitors), all processes implicated in CDK regulation are observed to induce extensive conformational changes, especially in the shape of the catalytic cleft.⁶¹ Of the four main CDKs involved in the cell cycle (CDK1, 2, 4, and 6), only the crystal structures of CDK2 and 6 have been reported to date, even though the amino acid sequences of the other members have been determined.

CDK2/Cyclin A and CDK4/Cyclin D complexes are often used as prototypes for the major classes of regulatory pathways that control CDK activity.⁶²

2.3.1 Cyclin binding

Although monomeric CDK2 will bind ATP, the residues within the ATP-binding site are incorrectly positioned to align the triphosphate moiety of ATP for catalysis, conferring a poor catalytic ability to the monomeric unit, which is regarded as almost completely inactive.⁴⁵ Kinetic studies have shown that cyclin binding increases the affinity of CDK2 for ATP by 3-fold and decreases its release from the active site by up to 5-fold.⁴⁵

Structural studies may provide an explanation as to why the monomeric form of CDK2 is inactive. Firstly, the T-loop which is the site for the activating phosphorylation of a CDK is situated, in the case of CDK2, in very close proximity to the substrate binding unit and actually occludes the close approach of peptide substrates to the catalytic site. Secondly, several catalytic residues are misaligned with respect to their positions in the active enzyme.

Upon Cyclin A binding, which occurs spontaneously even *in vitro*, residues Asp145, Glu51 and Lys33 are altered in their positions and thereby succeed in orienting the ATP for catalysis. Moreover, the T-loop undergoes a large conformational change that displaces it from the vicinity of the substrate-binding cleft.^{26, 63}

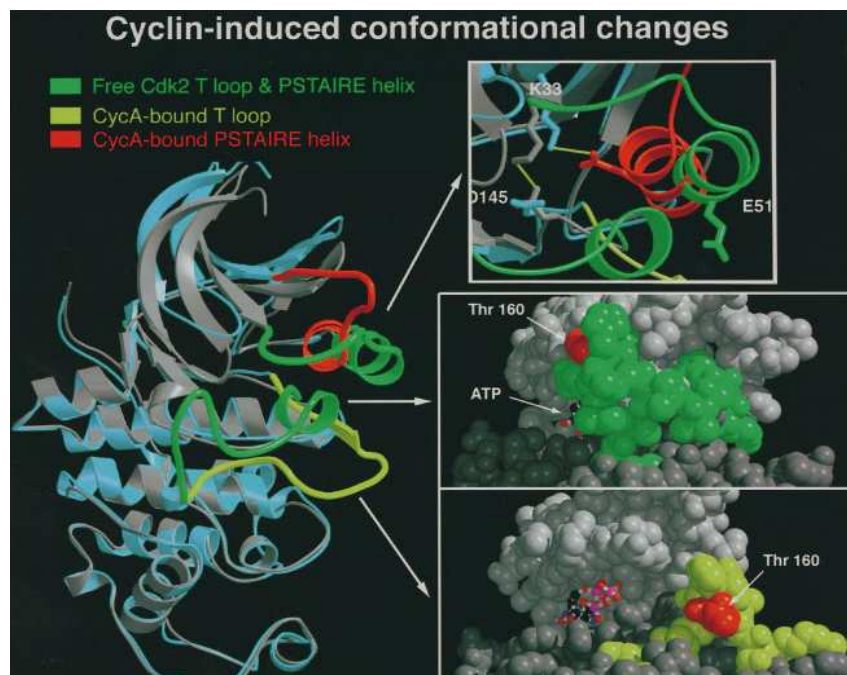


Figure 11

The structural change in CDK2 following Cyclin A binding. ^{56, 64}

Upon cyclin binding to CDK2, a continuous protein-protein interface is formed, as Cyclin A approaches the kinase subunit at one side of the catalytic cleft, interacting with both the N- and C-terminal lobes (see **Figure 7** in **Chapter 1**). Thus, Cyclin A promotes CDK2 activation by inducing radical conformational changes, as illustrated in **Figure 12**, which compares the conformation of CDK2 in the monomeric and cyclin-associated forms. ⁶² The PSTAIRE helix is reoriented toward the catalytic cleft *via* a rotation of 90°, bringing the catalytic residue Glu51 inside the ATP-binding pocket. This residue, together with Lys33, Asp145 and a magnesium ion, coordinates the γ -phosphate group and correctly orients it for catalysis. As a result of the binding of Cyclin A, the T-loop structure and position are altered as well. The activation segment is repositioned, clearing the entrance of the catalytic cleft, which is blocked in the monomeric form. In addition, these changes also expose the key phosphorylation site on the T-loop (Thr160), allowing for full activation of the kinase.

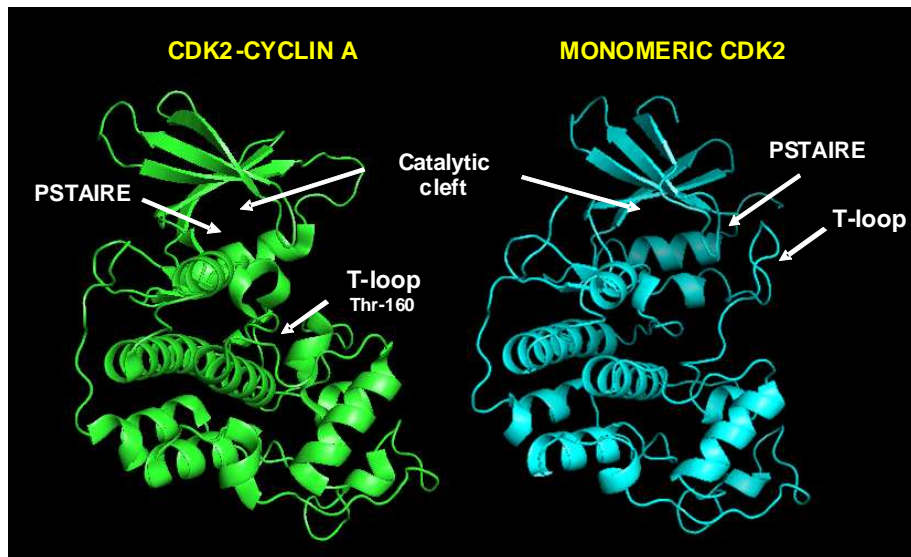


Figure 12

Structural alterations in monomeric CDK2 (right) following Cyclin A binding (left).⁶²

The mechanism of activation of the CDK4/Cyclin D complex is more complicated, and regulated by the stability of both CDK4 and Cyclin D subunits and by their assembly. Newly synthesised CDK4 appears to be intrinsically unstable and assembles into a high molecular weight complex containing a variety of other proteins (Hsp90, p50/Cdc37). This chaperone complex is thought to stabilise and/or help fold CDK4, and this appears to be required for productive interaction with Cyclin D.⁶⁵ Once CDK4 is properly stabilised, it is released from the chaperone complex and is free to interact with Cyclin D, although it appears that free CDK4 and Cyclin D associate very poorly in the absence of an assembly factor. Like CDK2, CDK4 then requires phosphorylation in the T-loop for maximal activity.⁶⁶

The regulation of CDK activity by cyclin binding implies, as a consequence, that the timing of CDK activation can be controlled by the expression of a particular cyclin subunit.⁶⁵ Cyclin association also plays a role in CDK substrate selectivity. These two aspects are linked together and provide the basis for kinase selectivity.

2.3.2 T-loop phosphorylation

After CDK2/Cyclin A binding has occurred, CAK phosphorylates the complex on Thr160 (Thr161 in CDK1),⁶⁷ and in this way a complete activation of the cyclin-dependent kinase is achieved. T-loop phosphorylation induces conformational changes of its own (**Figure 13**), as the phosphate group interacts with three separate arginine side-chains (**Figure 14**), each coming from a different part of the structure: Arg50, from the C-helix PSTAIRE motif within the N-terminal domain, Arg126, which is adjacent to the catalytic Asp145 in the C-terminal lobe, and finally Arg150, which is located at the beginning of the activation segment.

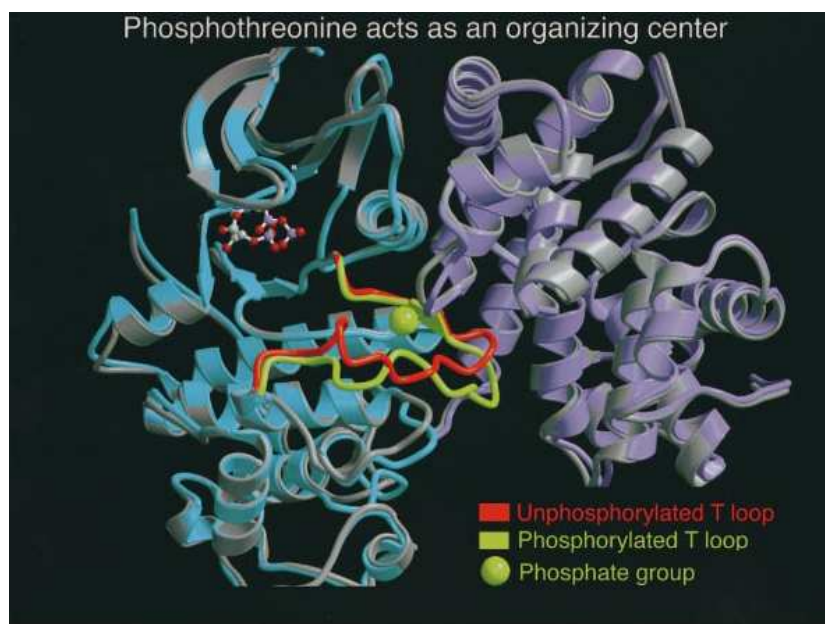


Figure 13

The structural change in CDK2 following T-loop phosphorylation.⁵⁶

The arginine residues, once positioned, participate in hydrogen bonding interactions with other CDK and cyclin residues, resulting in complete reorganisation of the substrate-binding site.²⁵

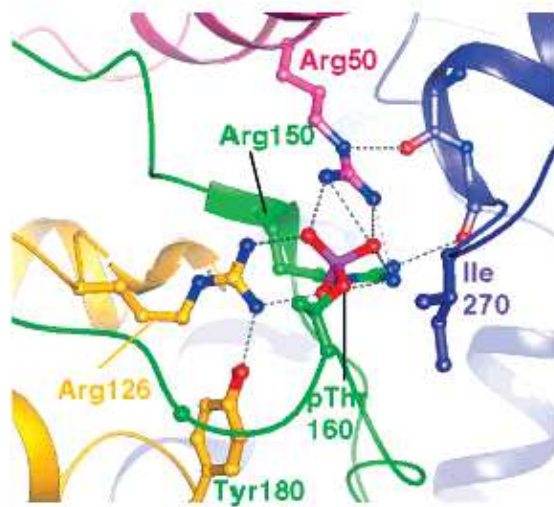


Figure 14

Phosphate binding site of CDK2.²⁵

2.3.3 Endogenous CDK inhibition

The third component of endogenous CDK regulation is the transcription and expression of endogenous CDK inhibitors (CDKIs). There are two main families of CDKIs, Cip/Kip and Ink4, classified according to their structure and CDK targets.⁶⁸ CDKIs orchestrate and integrate various signalling pathways and regulatory mechanisms, complementing CDK activity in controlling cell cycle progression. Inhibitors, including p16^{Ink4a}, p27^{Cip2}, p15^{Ink4b}, and p21^{Cip1}, are induced by cellular events such as senescence, contact inhibition, extracellular anti-mitogenic factors (e.g. transforming growth factor beta, TGF- β), and cell cycle checkpoints (e.g. p53), respectively.⁶¹ These CDK regulators are frequently altered in cancer, as a further proof of the vital role they play in controlling cell proliferation.^{69 70} Members of the Cip family target the active CDK/Cyclin complex, while the INK4 family binds and inhibits monomeric CDKs, preventing cyclin association and therefore activation. The Ink4 inhibitors act specifically on CDKs involved in the G₁ phase, whereas the Cip inhibitors have a broader CDK preference.⁷¹

2.3.3.1 The Cip/Kip Family

Members of the Cip/Kip family bind to cyclin and CDK substrates *via* conserved motifs found within their N-terminal domains.⁶⁸ Cip/Kip CDKIs inhibit cyclin D-, cyclin E- and cyclin A-dependent kinases, affecting G₁, G₁/S and G₂ control mechanisms in the cell cycle. This family includes proteins such as p21, p27 and p57/KIP2, which contain a characteristic sequence of 65 amino acids at their N-terminal domain, an important site in recognising and binding to CDK complexes.⁷² X-ray crystallography studies have identified three different ways of binding of p27 to the CDK2/Cyclin A complex, thus accounting for potential multiple inhibition mechanisms.⁷³

A rigid coil from the N-terminus of p27 has been observed to interact with a conserved hydrophobic groove on Cyclin A. This weakens the heterodimeric complex and results in a loss of CDK activity (**Figure 15**).⁷³

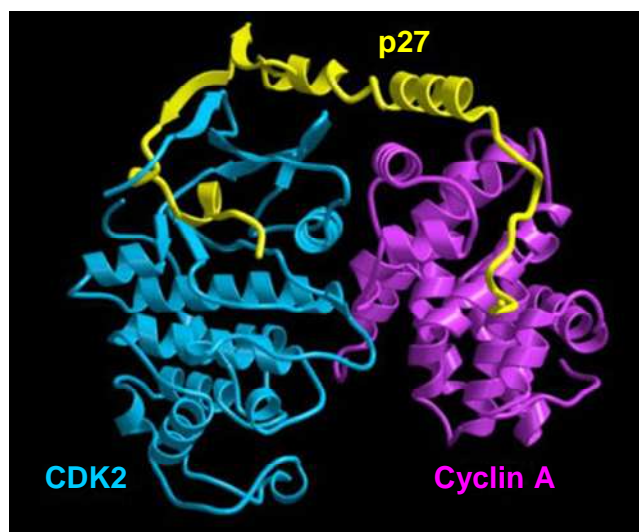


Figure 15

p27 binds to the CDK2/A complex.⁷¹

The protein p27 can also induce rearrangements of the N-terminal domain of CDK2. Upon p27 binding, the catalytic cleft is reshaped, abolishing enzyme activity as a result of the glycine-rich loop no longer interacting with the ATP ribose. p27 co-folds

into a new structure with CDK2, inserting some of its own β -strands into the N-terminal domain, and forming a new mixed hydrophobic core (**Figure 16**).

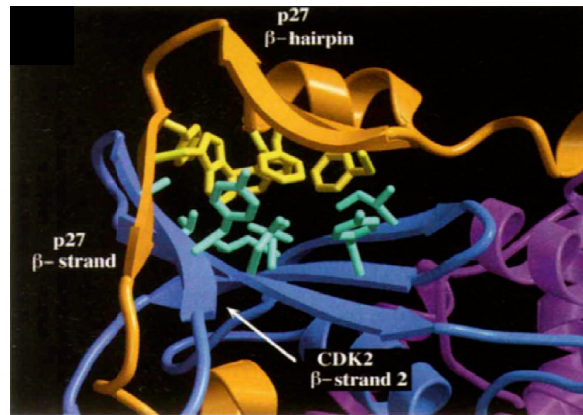


Figure 16

p27 inserts into the CDK2/A N-terminal domain.⁶⁴

Finally, p27 inhibits the activity of CDK2/Cyclin A by the insertion of a small 3_{10} -helix within the catalytic cleft of CDK2, mimicking both the Van der Waals contacts of the adenine ring of ATP and its hydrogen bond interactions *via* the highly conserved Tyr88 residue.⁶¹

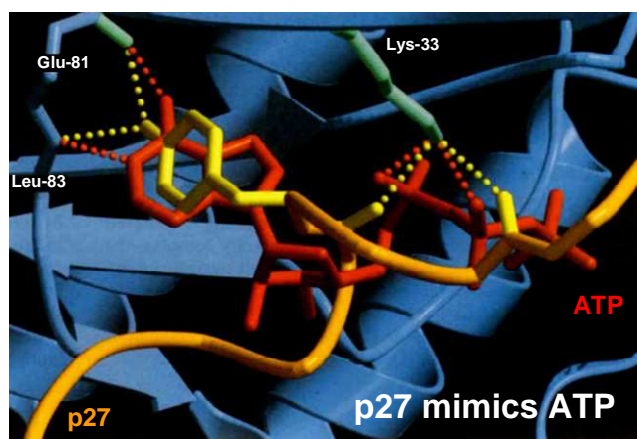


Figure 17

p27 mimics ATP binding within the CDK2/A catalytic cleft.⁶⁴

p21 binds to the CDK2/Cyclin A complex *via* its N-terminal domain in a similar fashion to p27. The expression of this gene is tightly controlled by the tumor suppressor protein p53, through which this protein mediates the p53-dependent cell cycle G₁ arrest in response to a variety of stress stimuli. In addition to growth arrest, p21 can mediate cellular senescence.⁷⁴ The third member of the Cip/Kip family is p57. p57 and p27 are thought to operate together to control cell cycle exit and differentiation.⁷⁵

2.3.3.2 The Ink4 Family

Members of the Ink4 family, which include the p15, p16, p18 and p19 proteins, bind only to CDK4 and CDK6, specifically inhibiting their catalytic subunits.⁷¹ Ink4 inhibitors bind adjacent to the catalytic cleft of CDK4/6, on the opposite side of the Cyclin D binding site, and interact with both the N and C lobes to form a continuous interface (**Figure 18**). Ink4 family members inhibit the formation of CDK4/6/Cyclin complexes in an allosteric manner, causing a propagation of structural changes that alter the conformation of the cyclin-binding site of CDK4/6.⁶¹

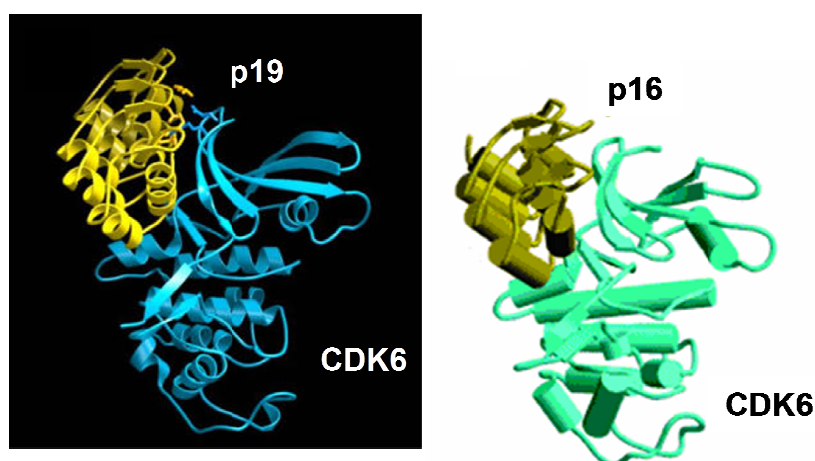


Figure 18

p16 (right) and p19 (left) bound to CDK6.⁷¹

p16 binds to CDK4/6, causing the N and C lobes to rotate by approximately 15° on a vertical axis. This leads to a misalignment between the N and C lobes and the PSTAIRE helix, which prevents cyclin binding, as shown in **Figure 19**.

Both p16 and the cyclin need to interact with each CDK lobe to exploit their function, but it appears that they require them in different relative orientations. This new positioning of the N lobe in the p16 complex has been observed to be incompatible with cyclin binding, resulting in an inactive conformation. p16 seems to have a higher affinity toward the CDK target than the cyclin partner, as it has been reported to bind preferentially in *in vivo* studies.⁷¹

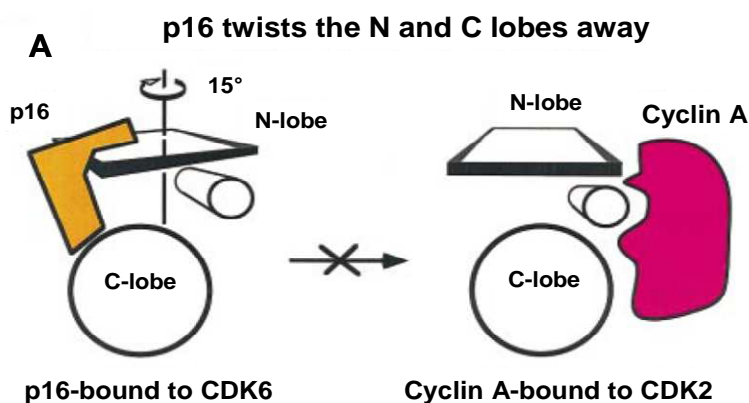


Figure 19

p16 binding causes a misalignment between the N and C-lobes of CDK6, resulting in impeded cyclin binding.⁶¹

2.3.4 CDK-Inhibitory Phosphorylation

Another mechanism by which CDK/Cyclin complexes may be inactivated is by dephosphorylation of threonine and tyrosine residues, *e.g.* Thr14 and Tyr15 in CDK1 and CDK2. In monomeric CDK2, these residues are located within the ATP-binding site, under the T-loop, and are inaccessible to solvent. They become accessible for dephosphorylation only after cyclin binding and subsequent repositioning of the T-loop.⁷⁶

The onset of mitosis is mediated by the regulatory activity of the CDK1/Cyclin B complex, which is tightly regulated by its phosphorylation status, both by an activating phosphorylation by CAK (Thr161) and inhibitory phosphorylations at Thr14 and Thr15 residues by protein kinases Wee1 and Myt1. During the G₂ phase of the cell cycle, cdc25, a protein phosphatase, dephosphorylates both residues on CDK1. This initiates the activation of CDK1/Cyclin B, which results in the onset of mitosis.⁷⁷⁻

78

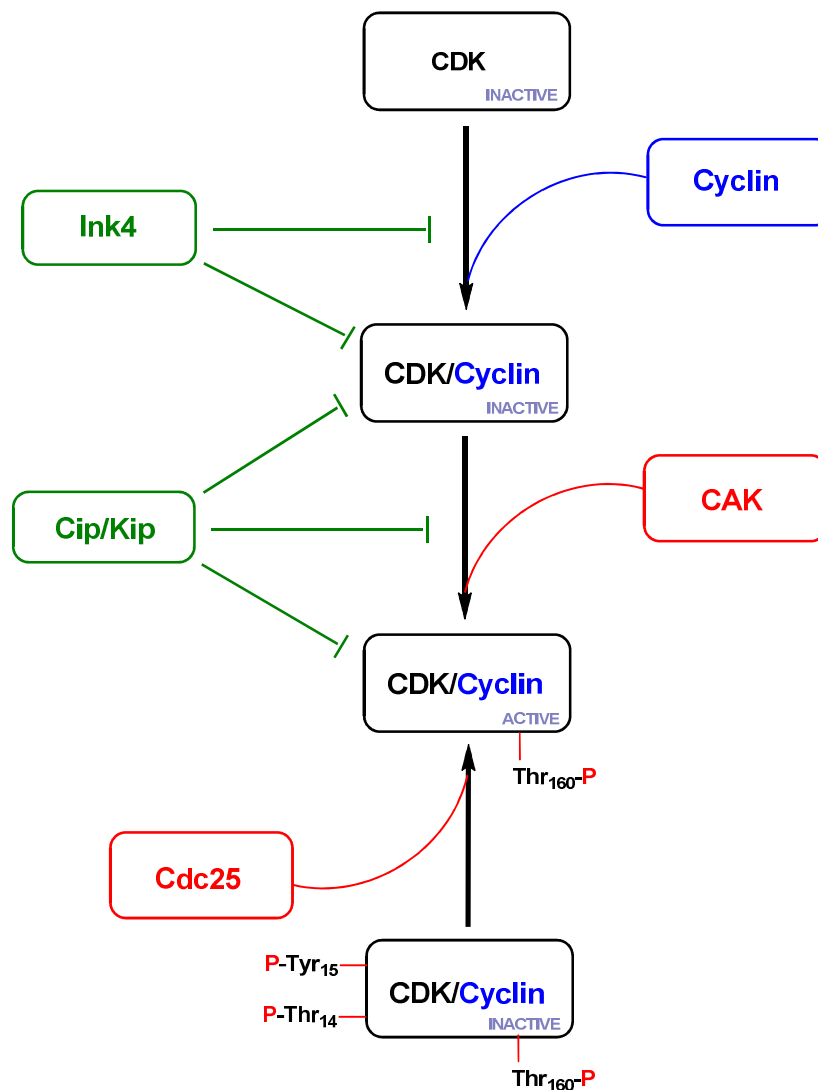


Figure 20

A summary of regulatory activation mechanisms of CDKs. ^{61, 79}

In summary, in order to guide the passage of cells through the cell cycle, CDKs undergo a number of regulatory processes, which are summarised in **Figure 20**. Faulty execution of these mechanisms can potentially lead to uncontrolled proliferation and the development of cancer.

2.4 CDKs as anticancer Targets

Phosphorylation and subsequent inactivation of Rb by CDKs is a key step in the regulation of cell cycle progression, promoting or inhibiting protein biosynthesis (*i.e.* G₁/S transition).³² CDKs play a pivotal role in the control of cell cycle checkpoints (*e.g.* G₂/M via p53), effectively protecting the integrity of the genome. A direct link has been established between the molecular pathology of cancer and a number of CDK-related cellular aberrations, such as cyclin overexpression (especially D-type cyclins), amplification and mutation of CDKs (CDK2 and 4), direct (p16) and indirect (p53) loss of endogenous CDK inhibition, and alterations in the levels of CDK-specific substrates (Rb loss or mutation).³⁷ The rationale for the development of synthetic CDK inhibitors relies on the assumption that these compounds might be able to counteract these effects, by reinstating the proliferative controls in transformed cells. Restoring cell cycle checkpoints may also induce apoptosis selectively in tumours, owing to high levels of constitutive DNA damage and genomic instability.⁸⁰

Due to the multi-functional nature of CDKs, and their aberrant activity in a range of disease states, a large number of structurally diverse CDK inhibitors have been reported. Although their primary intended use is for treating cancer, CDK inhibitors have been shown to have potential for counteracting several diverse diseases, including neurodegenerative disorders (*e.g.* Alzheimer's disease), cardiovascular disorders (*e.g.* atherosclerosis), and infections (*e.g.* HIV and malaria).^{37, 52, 81}

2.4.1 ATP-Competitive Inhibition

Despite the existence of several possible approaches to kinase inhibition (outlined in **Chapter 1**), the vast majority of CDK inhibitors reported to date are ATP-competitive. Although exhibiting a wide spectrum of chemical diversity, for the most part they all exploit the two key hydrogen bonding interactions with the hinge region of the active site described in **Chapter 1**.²⁴

Elucidation of the X-ray crystal structure of the CDK2/Cyclin A/ATP complex reveals two important hydrogen bonds between ATP and backbone amino acid residues of the active site cleft. N¹ of the purine accepts a hydrogen bond from the backbone NH of Leu83, while the N⁶-amino group donates a hydrogen bond to the backbone carbonyl of Glu81 (**Figure 21**).²⁶ There are additional hydrophobic and Van der Waals interactions between ATP and CDK2, most notably the hydrophobic pocket within which the ribose moiety of ATP resides. At least one of these interactions is replicated with most ATP-competitive CDK2 inhibitors, most frequently the hydrogen bonds with Leu83.

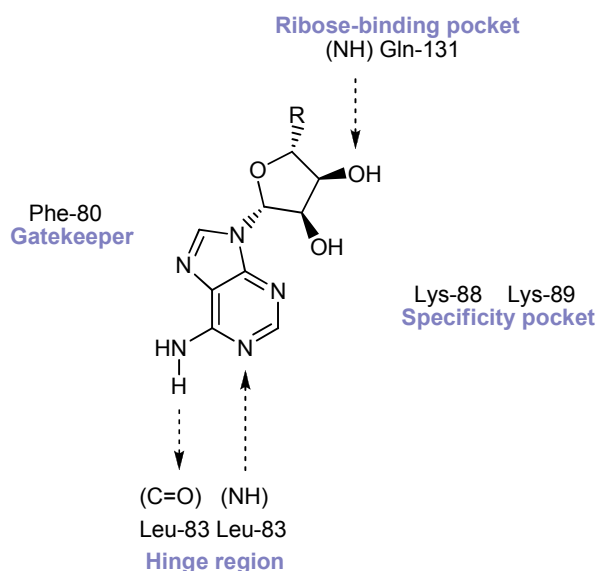


Figure 21

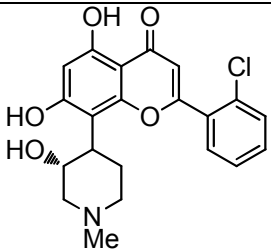
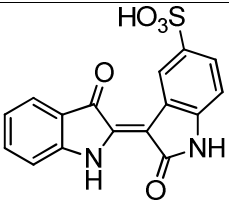
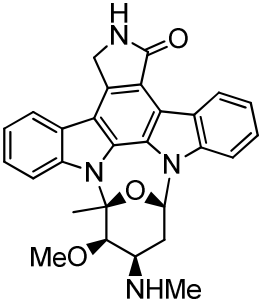
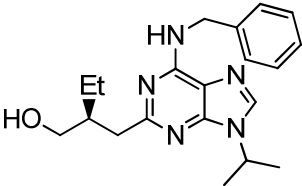
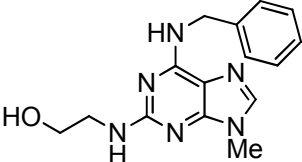
Hydrogen bonding interactions between ATP and CDK2.

2.4.2 CDK inhibitors

During recent years, many novel and potent ATP-competitive CDK inhibitors have been developed, providing an extensive array of structurally diverse pharmacophores. Consequently, a variety of compounds have progressed to clinical and late preclinical evaluation, supplying a wealth of information as to the validity of CDKs as 'druggable' targets.⁸²

Elucidation of the interactions between inhibitors and the CDK ATP-binding site has been facilitated by crystallographic studies. Similar to ATP, most of these inhibitors interact with CDKs through a donor-acceptor motif. This in turn has led to the design and development of new classes of inhibitors with modifications that target specific residues on the protein to improve potency. Recently, this effort has been directed at achieving selectivity toward one particular kinase or kinase subtype. Several classes of inhibitors have been successfully modified to improve the potency of CDK inhibition, and a number of inhibitors have shown moderate to significant subtype selectivity.^{26, 83}

The literature contains a number of interesting CDK inhibitors, some of which have been acquired from natural sources and some of which, like *R*-roscovitrine, have reached clinical trials.^{52, 84-86} Examples are included in **Table 3**.

	CDK inhibitory activity (IC ₅₀)			
	CDK1/B	CDK2/A	CDK5/p25	CDK4/D
 <p>Flavopiridol (9)</p>	0.4 μM	0.1 μM	N. A.	0.4 μM
 <p>Indirubin (10)</p>	40 nM	22 nM	40 nM	0.2 μM
 <p>Staurosporine (11)</p>	6 nM	7 nM	N. A.	<10 μM
 <p>R-roscovitine (12)</p>	0.45 μM	0.7 μM	0.16 μM	>100 μM
 <p>Olomoucine (13)</p>	7 μM	7 μM	3 μM	>1000 μM

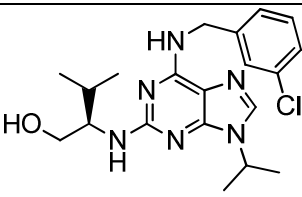
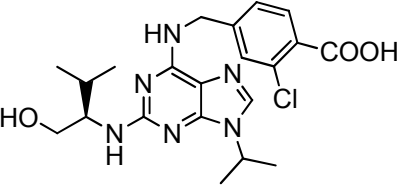
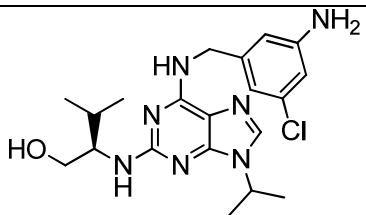
	CDK inhibitory activity (IC ₅₀)			
	CDK1/B	CDK2/A	CDK5/p25	CDK4/D
 Purvalanol A (14)	35 nM	70 nM	75 nM	0.85 μM
 Purvalanol B (15)	6 nM	6 nM	6 nM	>10 μM
 Aminopurvalanol (16)	33 nM	33 nM	20 nM	N. A.

Table 3

Literature CDK inhibitors and their IC₅₀ values.

Flavopiridol (**9**) is a synthetic flavonoid analog of a natural alkaloid extracted from the stem bark of the Indian plant *Dysoxylum binectariferum*, and shows activity as a rather promiscuous CDK inhibitor. Indirubin (**10**) is a minor constituent of a Chinese prescription (Danggui Longhui Wan, a preparation comprising some 11 herbal medicines) that is traditionally used to treat certain types of leukaemia. The microbial alkaloid staurosporine (**11**) is a very potent but also very unspecific CDK inhibitor, which exhibits too high a level of toxicity to be used in therapy. The family of purvalanols, of which purvalanol A (**14**), B (**15**) and aminopurvalanol (**16**) are prominent members, has been found to include many potent CDK inhibitors. Variations on the main purine scaffold have been explored⁸⁴ to yield a set of very potent but also nonspecific small-molecule CDK inhibitors.

R-roscovetine (**12**) was developed through a series of structure-based SAR studies from 6-dimethylaminopurine and is currently undergoing phase II clinical trials.¹⁹

The purine scaffold shared by roscovetine, olomoucine (**13**) and the purvalanols has been one of the most frequently used during the search for bioactive compounds, given the extensive natural abundance of purines in living organisms. Guanine and adenine, two of the most common purines, are essential components of nucleic acids, cofactors and a whole range of signalling molecules that modulate protein functions. Purine-based CDK inhibitors are benchmark ATP-mimetics.

More recent work has shifted the attention from the purine core pharmacophore to alternative scaffolds, among which one of the most popular is the pyrimidine moiety.

Pyrimidines provide a very effective scaffold for the development of CDK inhibitors.⁸⁷⁻

⁸⁹ Among the best pyrimidine- and pyridopyrimidine-based CDK inhibitors in terms of potency are 2-anilino-4-pyrrol-3-ylpyrimidines⁸⁹ (e.g. **17**), pyrido-2,3-pyrimidin-7-ones⁸⁷ (e.g. **18**) and 2-anilino-4-thiazolylpyrimidines⁸⁸ (e.g. **19**). Examples of these compounds and their activity are shown in **Table 4**.

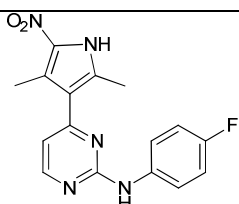
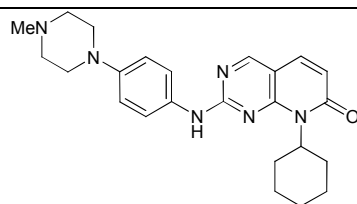
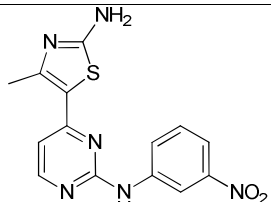
	CDK inhibitory activity (IC ₅₀)			
	CDK1/B	CDK2/A	CDK5/p25	CDK4/D
 17	N. A.	0.03 μ M	N. A.	0.12 μ M
 18	79 nM	15 nM	N. A.	4 nM
 19	80 \pm 40 nM	2 \pm 0.6 nM	4 \pm 3 nM	53 \pm 5 nM

Table 4

Pyrimidine-based CDK inhibitors and their IC₅₀ values.

In all cases, lead compounds were identified using virtual screening methods and then used as starting points for the generation of libraries of compounds, the most potent of which would be evaluated against different members of the CDK family to establish a selectivity profile.⁸⁷⁻⁸⁹

The pyrimidine scaffold proved suitable for the synthesis of a set of CDK4-selective inhibitors.⁹⁰⁻⁹⁴ The pyrido-2,3-pyrimidin-7-one scaffold, previously mentioned as a source of potent but unspecific CDK inhibitors, was more extensively investigated by Van der Wel and co-workers⁹²⁻⁹³ leading to the discovery of compounds **20** and **21** in **Table 5**, which show a good degree of selectivity towards CDK4.

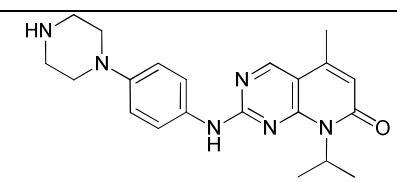
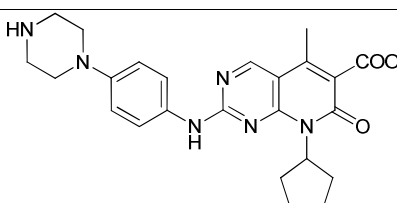
	CDK inhibitory activity (IC ₅₀)		
	CDK1/B	CDK2/A	CDK4/D
 <p>20</p>	>5 μ M	>5 μ M	0.265 μ M
 <p>21</p>	N. A.	>5 μ M	6 nM

Table 5

Pyrimidine-based CDK4-selective inhibitors and their IC₅₀ values

The pyrimidine scaffold is not the only one on which good CDK4-selective inhibitors have recently been based; other examples include indolo-6,7-pyrrolo-3,4-carbazoles^{90, 94} (e.g. **22-26**) and 5-pyrimidinyl-2-aminothiazoles⁹¹ (e.g. **27, 28**). Examples are shown in **Table 6**.

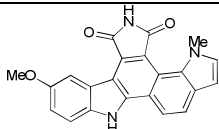
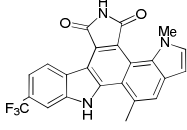
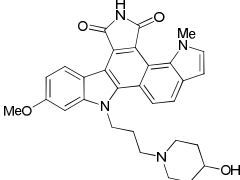
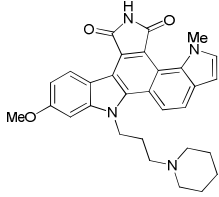
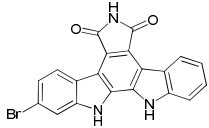
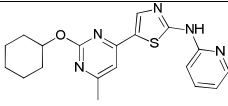
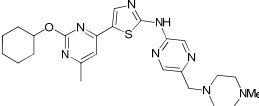
	CDK inhibitory activity (IC ₅₀)					
	CDK1/B	CDK2/A	CDK4/D	CDK5/p25	CDK6/D	CDK9/T
 22	N. A.	>2 μ M	40 nM	N. A.	N. A.	N. A.
 23	N. A.	>2 μ M	25 nM	N. A.	N. A.	N. A.
 24	N. A.	2.1 μ M	4 nM	N. A.	N. A.	N. A.
 25	N. A.	1.1 μ M	11 nM	N. A.	N. A.	N. A.
 26	2.1 μ M	0.5 μ M	76 nM	N. A.	N. A.	N. A.
 27	>10 μ M	>10 μ M	34 nM	>10 μ M	>10 μ M	>10 μ M
 28	0.6 μ M	1.7 μ M	9.2 nM	3 μ M	7.8 μ M	2.5 μ M

Table 6

Other notable CDK4-selective inhibitors and their IC₅₀ values

Within the Northern Institute for Cancer Research (NICR) at Newcastle the investigation of both purine and pyrimidine scaffolds has led to the discovery of potent and selective CDK1 and CDK2 inhibitors^{95-96, 55} (**Table 7**).

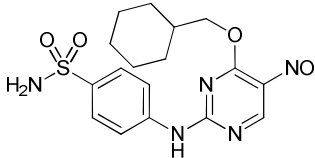
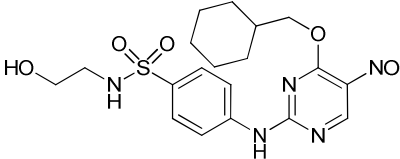
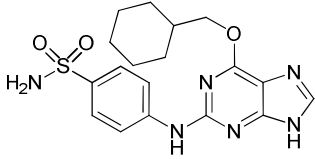
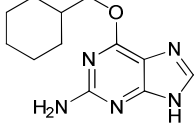
	CDK inhibitory activity (IC ₅₀)			
	CDK1/B	CDK2/A	CDK4/D	CDK9/T
 <p>29</p>	100 ± 10 nM	1 ± 0.3 nM	1.5 ± 0.5 μM	0.74 ± 0.1 μM
 <p>30</p>	56 ± 20 nM	0.7 ± 0.1 nM	1.5 ± 0.5 μM	2.63 ± 0.2 μM
 <p>31</p>	9.5 ± 1.3 nM	5.4 ± 1 nM	N. A.	N. A.
 <p>32</p>	7 ± 1 μM	17 ± 2 μM	N. A.	N. A.

Table 7

Purine- and pyrimidine-based CDK1/2 selective inhibitors at Newcastle and their IC₅₀ values, or percentages of inhibition at a specified concentration.

Some of the many CDK inhibitors that have been described to date⁵² are active at low nanomolar concentrations. Despite the fact that they show a wide range of chemical diversities, there are some common properties that they appear to share:

they are normally small molecules with a molecular weight no higher than 600, and they are flat and hydrophobic heterocycles; they are ATP-competitive and bind to the target kinase by hydrophobic interactions and hydrogen bonds (they are reversible ligands); and finally, they bind to more or less always the same hydrogen bond donors and acceptors on the carbonyl and amino side chain of the target enzyme. As can be seen in **Tables 3-7**, most inhibitors are not selective for any specific CDK (**Table 3**), while groups of them show selectivity towards CDK1 and 2 or CDK4 and 6 (**Tables 4-7**). To date, CDK1, 2, 4 and 6 have been the most explored targets for anticancer drug development based on CDK inhibition, although CDK7, 8 and 9 have also been investigated more recently.⁹⁷⁻⁹⁸

2.5 CDK7

Two non-overlapping sets of CDKs have been defined in metazoans: CDK1, 2, 4 and 6 are solely dedicated to cell cycle control, whereas CDK8 and 9 are primarily devoted to transcriptional activity.⁹⁹

One CDK, however, is less readily classified. CDK7 acts both as a CDK-Activating Kinase (CAK), phosphorylating other cell cycle CDKs within their activation segment (T-loop), and as a component of the general transcription factor TFIIH, whose function is to phosphorylate the C-terminal domain (CTD) of the largest subunit of Pol II.⁹⁹

Ever since it was first understood that there existed a CAK whose role was to phosphorylate and activate CDK1 and 2, much interest was raised with regard to the structure and properties of such an enzyme. After the CAK was isolated and purified, it came as a surprising discovery that its catalytic subunit was structurally related to that of the other CDKs. It also appeared to be bound to a cyclin partner, which was subsequently named Cyclin H. At that point, the CAK was decreed a member of the CDK family and renamed CDK7.¹⁰⁰

CDK7 does not exclusively bind to Cyclin H, but it also interacts, in near-stoichiometric amounts, with another protein. This protein has been isolated from humans, mice and starfish and structural studies have revealed that it contains an amino-terminally located putative zinc-binding domain conforming to a typical Ring-Finger motif (**Figure 22**).¹⁰¹

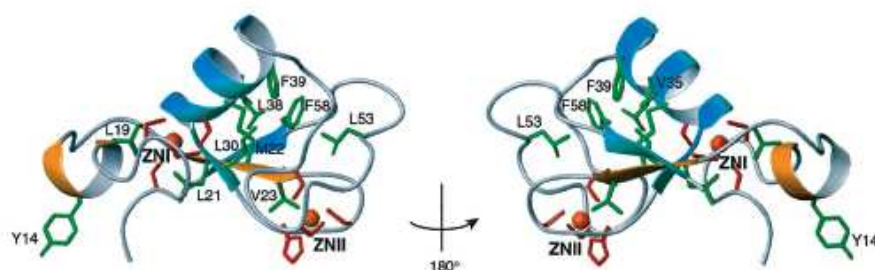


Figure 22

The three-dimensional structure of the human MAT1 Ring-Finger domain in the presence of Zn(I) (left) and Zn(II) (right).¹⁰¹

With regard to the functions of ring-finger motifs there is still much to be unveiled, but it appears likely, in this case at least, that this protein acts as an assembly factor, promoting a stable interaction between CDK7 and Cyclin H. Accordingly, the protein was named MAT1 (Mènage-à-trois). *In vivo*, MAT1 forms a trimeric complex with CDK7 and Cyclin H under most conditions, and it has not yet been observed in complex with any other CDK or protein. It appears, so far, to be completely specific towards CDK7. It may be assumed, even if there is no conclusive proof of this to date, that it has a role in modulating CAK activity.

Structural studies have been carried out to investigate the characteristics of the interaction between CDK7 and MAT1, and it has been revealed that CAK activity is triggered by interaction of the CDK7/Cyclin H complex with the hydrophobic C-terminal domain of MAT1. The ring-finger motif of MAT1 has a crucial role in basal transcription complex activity and, consequently, in the CTD phosphorylation process.¹⁰² It has also been suggested that MAT1 plays an important part in directing CDK7 substrate preferences: the addition of the MAT1 subunit to recombinant CDK7-Cyclin H switches its substrate specificity to favour Pol II over

CDK2.¹⁰³ Whether this is connected to the stimulatory function of MAT1 towards CDK7 itself or to its structure remains to be established.

The role of CDK7 both as a CAK and as a component of a transcription factor has been the subject of discussion. *In vitro* studies demonstrate that the CDK7/Cyclin H/MAT1 trimeric complex phosphorylates CDK2 at Thr160 in the activation loop, but evidence arguing against CDK7 being the physiological CAK for CDK2, or at least the only one, raises from two main observations. Firstly, a temperature sensitive mutation in the *drosophila* CDK7 homologue causes ovarian cells to arrest in mitosis, and also causes CDK1 to exhibit deficiency of T-loop phosphorylation, but this is not the case with CDK2. Secondly, the budding yeast ortholog of CDK7, Kin28, is very similar to CDK7 in being part of the general transcription factor TFIIH, but does not possess any CAK activity, either *in vitro* or *in vivo*.¹⁰⁴

It had been suggested that another cell cycle-related kinase, p42, might serve as a CAK towards CDK2 when CDK7 is unavailable,¹⁰⁵ but more recent studies presented evidence arguing against a role for p42 as a CAK for CDK2.¹⁰⁶ It was demonstrated that monomeric p42 does not possess any CAK activity against CDK2, and the only circumstance in which it can actually show such activity is when CDK7 is also present.

It was therefore concluded that CDK7 acts as a CAK, and genetics also provided conclusive proof that CDK7 is a CAK *in vivo*: by mutating the *Dmcdk7* gene responsible for the coding of CDK7, CDK7 activity was abated in *Drosophila melanogaster*.¹⁰⁷ As a result, CDK7 mutant embryos appeared to be deficient in physiological CAK activity. CDK phosphorylation and activation was absent, and therefore CDK activity stopped. This demonstrates that CDK7 is essential for *in vivo* CAK activity. CDK7 plays a dual role in metazoans but two proteins, Kin28 and Cak1, fulfil the two functions separately in budding yeast.¹⁰⁸

2.5.1 CDK7 activation

Like other CDK family members, the T-loop of CDK7 contains a site (Thr170) which is phosphorylated *in vivo*. Phosphorylation on this site favours Cyclin H binding, but it would appear that the MAT1-mediated stabilisation of the CDK7/Cyclin H complex is

independent of the Thr170 residue being phosphorylated.¹⁰⁰ These results permit some highly significant conclusions. MAT1 is able to bypass the requirement for T-loop phosphorylation, showing that the CDK7/Cyclin H complex can form by two distinct mechanisms. It is not clear which of the two mechanisms is favoured *in vivo*, or even whether there is a preferred mechanism at all, but the unique interaction that the CDK7/Cyclin H complex forms with MAT1 may provide one solution to a fundamental problem: kinase cascades operating through T-loop phosphorylation do not extend indefinitely. One protein is needed to begin the cascade and to act as an upstream regulator of CDK activity.³⁴

Regarding the mechanisms of activation of the complex CDK7/Cyclin H/MAT1 there is still much to be unveiled. As a cyclin-dependent kinase, CDK7 requires binding to a cyclin partner, Cyclin H (**Figure 23**).

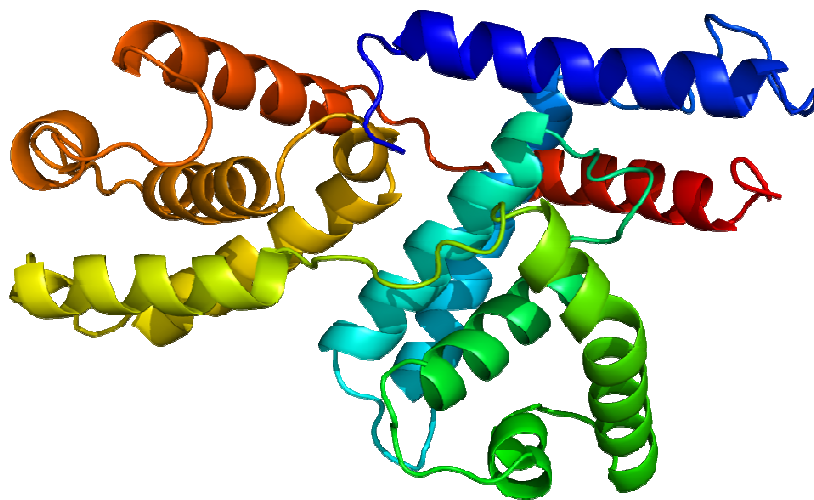


Figure 23

Crystal structure of Cyclin H.¹⁰⁹

Human Cyclin H is a protein comprising 323 amino acids and has a molecular weight of 38 KDa. It was recently shown that Cyclin H binds to the growth suppressor protein p53,¹¹⁰ and this leads to a down-regulation of CDK7 kinase activity both *in vitro* and *in vivo*. p53 is a growth suppressor and one of the regulators of cell cycle

progression, because it indirectly regulates kinase activity by transactivating inhibitor molecules for these enzymes. Cyclin H also possesses several potential phosphorylation sites, and this makes the protein a potential target for regulation by phosphorylation and dephosphorylation. It was recently shown ¹¹¹ that the CDK8/Cyclin C complex phosphorylates Cyclin H, thereby inhibiting the formation of the CDK7/H complex. Cyclin H is also a substrate for another kinase, namely protein kinase CK2. Protein kinase CK2 is a holoenzyme composed of two regulatory β -subunits and two catalytic subunits (α - and α' -). CK2 phosphorylates Cyclin H on Thr315 (while CDK8/Cyclin C phosphorylates Ser304), thereby inhibiting its ability to bind correctly to CDK7. ¹¹²

2.5.2 CDK7 as a CTDK

The cloning of the largest subunit of RNA polymerase II (Pol II) from mouse and *Saccharomyces cerevisiae* in 1985 ¹¹³⁻¹¹⁴ revealed a remarkable and highly conserved domain known as the Pol II Carboxy-terminal Domain (CTD). The CTD is structurally very simple, consisting mainly of repeats of the 7-amino acid sequence Tyr-Ser-Pro-Thr-Ser-Pro-Ser (52 repeats in mouse and human; 27 repeats in budding yeast; 45 repeats in *Drosophila*).



Figure 24

Structure of RNA Pol II from *Saccharomyces cerevisiae*. ¹¹⁵

In contrast to this structural simplicity, the functions of the CTD are many and varied.¹¹⁶ The CTD is involved in all major steps of mRNA formation and performs important regulatory roles. It has been found to be phosphorylated, and phosphorylation levels vary during the transcription cycle, suggesting that a regulatory switch *via* an activating phosphorylation process/deactivating dephosphorylation process is in action. The natural question followed as to which kinase was responsible for this particular phosphorylation, and that activity was found to reside in the TFIIH transcription factor. TFIIH was found to consist in mammals of ten subunits (schematically represented in **Figure 25**), 7 of which (XPD, XPB, p62, p52, p44, p34 and TTDA) form the core complex. The CDK activating kinase-subcomplex (CDK7, MAT1, and cyclin H) is linked to the core via the XPD protein. Two of the subunits, ERCC2/XPD and ERCC3/XPB, have helicase and ATPase activities and help create the transcription bubble.¹¹⁷

Phosphorylation of the CTD regulates protein-protein interactions between the CTD itself and the CTD-binding proteins, and these interactions have effects on transcription, initiation and elongation of RNA, leading to the processing and production of full-length mRNA.

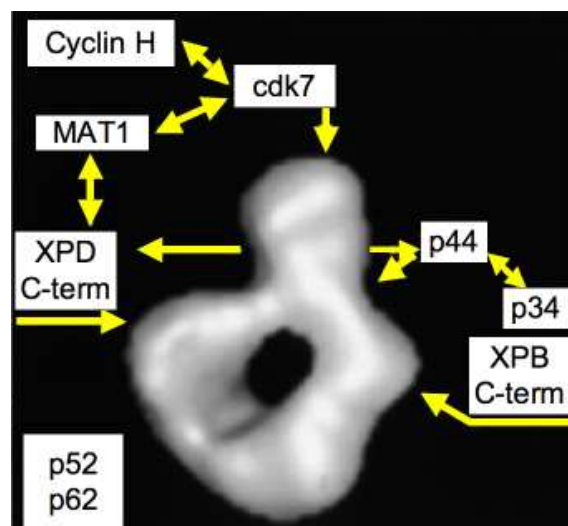


Figure 25

The TFIIH transcription factor.¹¹⁸

It is not clear how many CTDs exist in nature, and what actually directs the substrate specificity of the CTDs towards the different phosphorylation sites present on the CTD. It appears that serine residues 2 and 5 from the repeated sequence above are the favourite sites for phosphorylation over, for example, Thr4 and Ser7, but the reason for this is still unknown and the relative ratio of phosphorylation of these two favourite residues is also unknown. Also, the CTD is known to undergo other particular modifications at the hands of different enzymes, for example glycosylation. The relationships between these other modifications and phosphorylation have still not been satisfactorily explained.¹¹⁹

Another interesting point to be discussed regards the nature of the CTD kinases currently known and the way in which they are regulated. The majority of those that have been described to date are CDKs. During the progression of the cell cycle, CDKs are regulated by cyclin binding, which oscillates accordingly to the level of activity required as the phases of the cell cycle succeed one another. Cyclin binding is required for activity towards the CTD as well, but the levels of the cyclins involved in CTD phosphorylation processes do not vary.¹²⁰ Another mechanism shared between the cell cycle CDKs and the CTDs is phosphorylation within the T-loop. In CDK7 this mechanism cooperates with MAT1 binding and it has been demonstrated that when these two processes occur together, the CDK7/Cyclin H/MAT1 complex is highly stabilised and stimulated to act towards the CTD (while activity towards CDK2 and other fellow kinases is not greatly affected).¹²¹ The substrate-specific increase in activity caused by T-loop phosphorylation is entirely due to accelerated enzyme turnover. In other words, upon T-loop phosphorylation catalytic efficiency specific to the Tyr-Ser-Pro-Thr-Ser-Pro-Ser target sequence of the CTD is ~25-fold increased ($k_{\text{cat}} = 0.22 \rightarrow 3.69 \text{ s}^{-1}$). Thr170 phosphorylation is therefore a key step in regulating the rate of CTD phosphorylation by TFIIH during transcription.¹²¹

2.5.3 CDK7 as an anticancer drug target

As a demonstrated crucial agent in the regulation of the activity of the CDKs throughout the cell cycle, CDK7 would be an interesting and important target for anticancer drug development. Therefore, much interest has recently been raised

towards this enzyme and its properties both in a normal and in a cancerous cell environment.

Surveys of cell and tissue specificity, subcellular localisation and protein abundance of human CDK7 in a wide range of normal and cancer cell types, both in cellular and tissue cultures, led to the following observations: ¹²²

- CDK7 is ubiquitously expressed in all cell types examined;
- It is located exclusively in the nucleus;
- Its abundance is constant throughout the cell cycle;
- It is moderately elevated in tumour cells when compared to normal cell counterparts;
- It is clearly detectable even in quiescent cells.

The protein partners that bind to CDK7, namely Cyclin H and MAT1, do not appreciably oscillate during the cell cycle. Cyclin H is also overexpressed in cancer cells as demonstrated by immunohistochemical studies on endometrial cancerous tissues. ¹²³

This experimental evidence is accounted for by the apparently universal role of CDK7 in performing the activating T-loop phosphorylation of CDKs operating during the G₁, S, G₂ and M phases of the cell cycle. In particular the ubiquitous expression of CDK7 in all cell types, the location in nucleus and the constant levels throughout the cell cycle are all consistent with a very broad function towards a wide range of other enzymes (the cell cycle CDKs). ^{104, 124}

The presence of CDK7 in quiescent cells agrees with the fact that CDK7 is, as discussed above, not only a CAK, but also a CTDK and is required not only for cell cycle regulation (which does not take place in quiescent cells) but also for transcriptional duties.

Any consideration of CDK7 as a potential drug target must take into account its dual functions in cell cycle control and transcription. Inhibiting an enzyme that has a role in such a wide range of cellular activities, with the purpose of abating the growth of tumour cells, might prove prohibitively toxic to normal cells. However, it is possible to re-evaluate these assessments in the light of some recent encouraging evidence. ⁹⁹

Firstly, it is possible to separate the two functions of CDK7 (the TFIIH-correlated transcriptional activity and the CAK activity) by specific mutations that selectively impair only one process^{103, 121, 125-129} in two ways: by changing requirements for cell division and transcription at different times or by manipulating subunit composition and modification state of the CDK7 complex.^{103, 121, 128-129} The enzyme has two separate classes of substrates for its two activities (the downstream cell cycle regulating CDKs and the CTD) and it is now apparent that they are recognised in different modes, and presumably even by different surfaces of the CDK7/Cyclin H/MAT1 complex. Selective inhibition of CAK or CTDK activity now seems at least possible.

Secondly, not all transcription by Pol II depends on the catalytic activity of CDK7. If it were demonstrated in mammals (as already is the case in yeast) that CDK7 activity preferentially affects transcripts needed by dividing cells, inhibition of CDK7 could simultaneously deprive tumour cells of the CAK activity they require and crucially limit the synthesis of mRNA needed for other steps in cell division, without shutting down transcription globally in nondividing cells.¹³⁰⁻¹³¹

Whether or not CDK7 inhibition could cause toxicity in relation to its role in transcription is still controversial, but encouraging evidence is accumulating that a selective CAK inhibition that would not be too detrimental to transcriptional activity is achievable. For example, using CDK7 temperature sensitive mutants in *C. elegans* embryonic blastomeres it was shown that loss of CAK function of CDK7 (and *not* loss of CTDK activity) caused cell cycle block. Defects were observed in both interphase and mitosis. In mice, MAT1 disruption severely affected mitosis but no decrease in transcription was observed.¹³² Given that in *Drosophila* the complex CDK9/Cyclin T phosphorylates the CTD and regulates the elongation phase of transcription, it has been suggested that CDK9 might be able to compensate partially for CDK7 when the latter is absent.^{125, 133-135}

Information on CDK7 inhibitors is limited. Inhibitors known to date include flavopiridol (**9**), purvalanol A (**14**), (*R*)-roscovitine (**12**) and, more recently, the compounds shown in **Figure 25**.^{88, 91, 55} Purvalanol A (**14**) was tested at Newcastle for activity against CDK7 and was found to be a ~100 nM inhibitor (unpublished results). Referring back to **Table 3** the values show that the potency of **14** is higher against

CDK1 and 2 than CDK7, and the same holds generally true for the CDK7-inhibitory activity of most of the other literature compounds included in **Table 3** and in **Figure 26**.

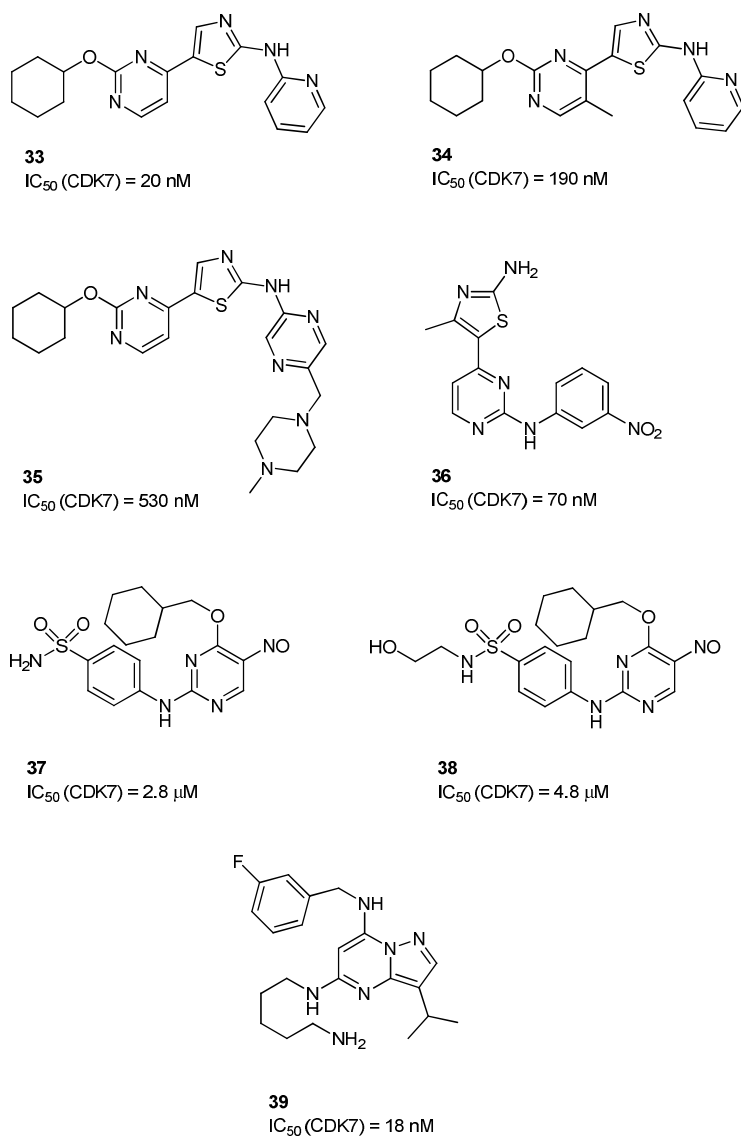
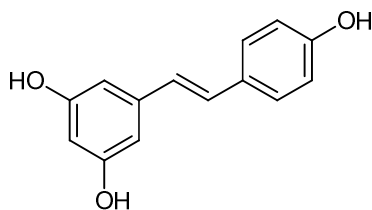


Figure 26

Known CDK7 inhibitors

It has been shown that resveratrol (**40**) can induce G₂ arrest in cancer cell lines by preventing phosphorylation of CDK1 at its Thr161 residue.¹³⁶



Resveratrol (**40**)

CDK1 is a key mediator of the transition from the G₂ to the M phase in eukaryotic cells. It is associated with a cyclin partner, Cyclin B, but it is also necessary for the kinase to be phosphorylated at Thr161 to be completely active, and this phosphorylation is carried out by CDK7. Selected cell extracts exposed to 100 μ M resveratrol do not show phosphorylation of p34 at the relevant site because of CDK7 inactivation.¹³⁶

In vitro, however, resveratrol is a poor CDK7 inhibitor, and so are flavopiridol and R-roscovitine. The development of potent and selective CDK7 inhibitors would therefore provide new perspectives to the development of cancer treatments.

To date, the only existing selective CDK7 inhibitor is BS-181 (**39**), developed and patented jointly by Emory University and Imperial College, London.¹³⁷ With a 40-fold selectivity over CDK2, it is the only CDK7-selective compound within the reported series. This compound will be discussed in more detail in **Chapter 5**.

2.5.4 Structural information on CDK7

The crystal structure of human CDK7 in complex with ATP at 3 Å resolution was recently determined by Professor L. N. Johnson and colleagues at the University of Oxford.¹³⁸

Figure 27

The structure of monomeric CDK7 bound to ATP. ¹³⁸

CDK7 has a molecular weight of 39,141 KDa when monophosphorylated at Thr170 (an additional phosphorylation at Ser164 is observed in 30% of the cases).

The structure exhibits a typical kinase fold comprising the N-terminal lobe (residues 13-96), which is constituted mostly by β -sheets with the presence of one α -helix, and a C-terminal lobe (residues 97-311), which on the contrary shows a majority of α -helices. ATP is bound between the two domains.

In the absence of the cyclin partner, the two structures of inactive CDK7 and CDK2 are quite similar (**Figure 28**). Differences may be noted between the inactive (monomeric) and active (cyclin-associated) form of CDK7 in terms of three-dimensional conformation, leading to stabilising interactions between amino acids that are necessary for correct ATP binding.

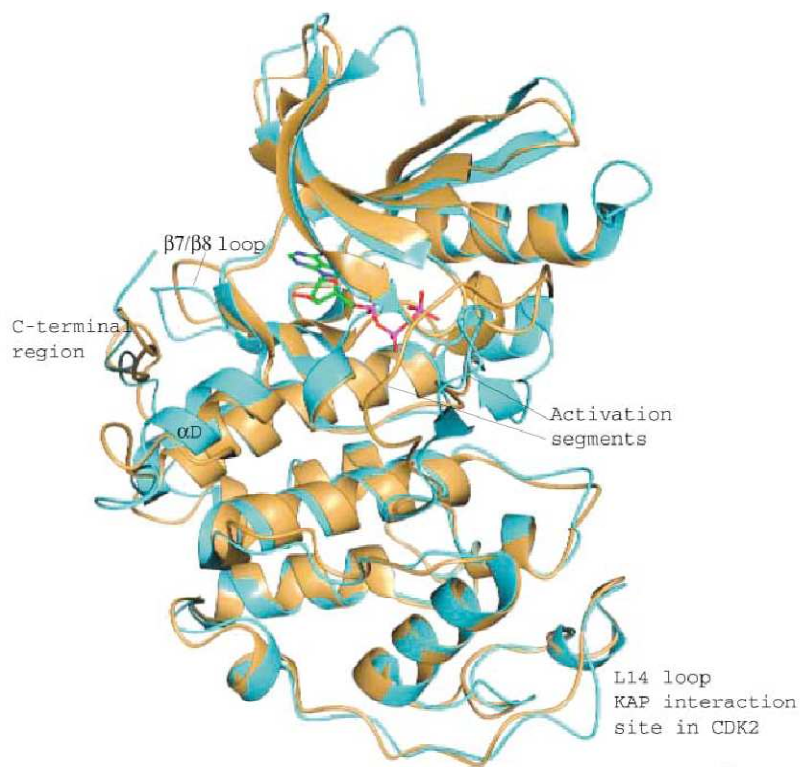


Figure 28

Overlay of monomeric CDK2 (blue) and CDK7 (yellow).¹³⁸

CDK7 has a 44% sequence identity with CDK2. Major changes are observed in three regions:¹³⁸

- The activation segment (residues 155-174);
- The region where the sections α D, β 7/ β 38 loop and the C-terminal domain (residues 101-112, 146-149 and 297-311) come together;
- Part of the recognition site for the Kinase-Associated Phosphatase (KAP), the enzyme that dephosphorylates CDK7 (residues 247-251).

Over all, the number of Van der Waals contacts made between ATP and CDK7 and between ATP and CDK2 are quite similar, even though a number of the residues

involved are different (**Figure 29**). The major differences between the CDK7 and CDK2 ATP-binding sites occur at the CDK2 Lys89 pocket ('hydrophobic pocket'). This pocket lies at the bottom of the ATP-binding site, opposite to the sequence of Phe23, Ala24 and Lys41 that constitutes the site for the hydrogen bonding of the three γ -phosphate oxygens of ATP.

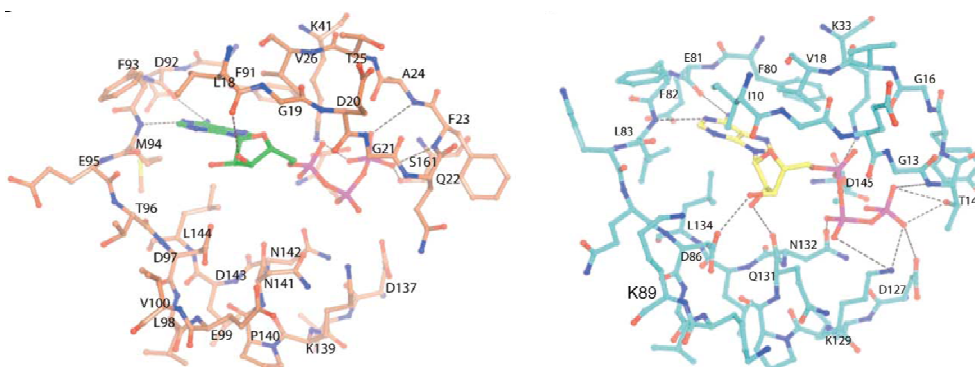


Figure 29

ATP-binding pocket of CDK7 (left) and CDK2 (right).¹³⁸

In this hydrophobic pocket, some amino acids that are found in CDK2 are different in CDK7. For example, Gln85 is replaced by Thr96, a proline residue is found at position 310 (which is absent in CDK2), and the residue corresponding to Lys89 in CDK2 is replaced by Val100 in CDK7.

2.5.5 ATP-competitive inhibition of CDK7

Elucidation of the X-ray crystal structure of CDK7 bound to ATP reveals the following interactions that are made between ATP and the backbone amino acid residues of its specific binding site (**Figure 30**):¹³⁸

- The adenine makes two hydrogen bonds to the backbone chain of the region containing Phe93 and Met94;
- The ribose is close to the pocket where Leu18, Gly19 and Asp20 are, and hydrogen-bonds to the carbonyl oxygen of Leu18 by means of one of its two hydroxyls;

- The γ -phosphate oxygens hydrogen-bond to the main chain nitrogens of Phe23, Ala24, Lys41 and Ser161.

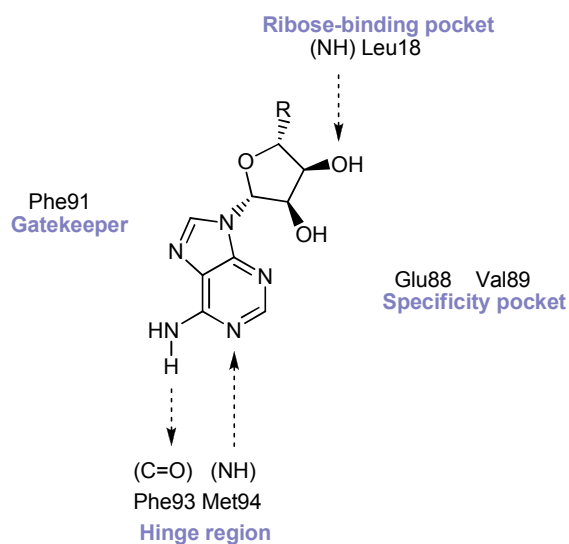


Figure 30

Schematic representation of the interactions made by ATP in the CDK7 active site.

The specificity pocket within the CDK7 active site has a much greater hydrophobic character than is the case for CDK2, and this pocket may be targeted with inhibitors that could form stable hydrophobic interactions that would not be possible with CDK2, thereby achieving selectivity (see **Chapter 4**).

2.6 CDK Redundancy and Selectivity Profile of inhibitors

The pursuit of drugs that inhibit CDKs has been an intense area of research for several years and significant clinical progress has been made. Combinations of CDK inhibitors with cytotoxic drugs have also shown promise in a number of tumour models.⁴⁴ Newer CDK inhibitors were designed to exhibit decreased toxicity and more selective activity. However, the development of CDK inhibitors has been hindered by uncertainties as to the optimal selectivity profile.¹³⁹

Research was focused initially on CDK2/Cyclin A as a therapeutic target. However, recent reports have questioned the validity of CDK2 as a target for the reinstatement of cell-cycle checkpoints in cancer.¹⁴⁰⁻¹⁴² It is becoming evident that the pharmacological effects of most CDK inhibitors do not emanate from CDK2 inhibition, and that effects on CDK-mediated RNA Pol II CTD phosphorylation are important for the observed antiproliferative effects of, for example, flavopiridol (**9**) and (*R*)-roscovitine (**12**) through inhibition of CDK7, 8 or 9.

The apparent redundancy of CDK2 in normal proliferating cells does not necessarily mean that CDK2 is not a valid target in anticancer drug design.¹⁴³ The expression of catalytically inactive CDK2 in cells results in cell cycle arrest and more closely resembles the pharmacological inhibition of CDK2 than the genetic knockout of CDK2.¹⁴⁴ Additionally, research on the inhibition of CDK2, combined with the disruption of DNA synthesis and replication, where a p53-induced response toward apoptosis is triggered, provides evidence in favour of CDK2 as a viable cellular target for cancer therapy.¹⁴⁵ The initial response to DNA damage in the cell is regulated by a family of protein kinases related to phosphatidylinositol 3-kinase (PI3K). Following DNA damage, members of this family, namely ATM and ATR, phosphorylate p53 modulating both cell cycle progression and apoptosis. Consequently, sustained CDK2 inhibition and the resulting disruption to DNA synthesis leads to amplification of ATM and ATR activity and, ultimately, p53-induced apoptosis.

The high homology of the ATP-binding sites of CDK1, CDK2 and CDK9, has led to the assumption that it will be difficult to develop truly CDK-selective inhibitors.³⁷ Optimal selectivity profiles for a particular cancer, such as pan-CDK inhibition versus CDK1/2, 4/6 or 7/9 specificity may represent a possible solution. However, little progress has been made to date in this direction, the notable exception being the highly CDK4/6-selective compound **21**.⁴⁴

A recent report detailing the kinase selectivity of 20 inhibitors, including imatinib (**3**), against a panel of 119 protein kinases, stated that selectivity varied widely and did not significantly correlate with chemical structure or the nature of the intended target.¹⁴⁶ These observations further emphasised the difficulty of achieving complete kinase selectivity, but also suggested that this is not necessarily the most important factor in developing a successful drug candidate. Highly selective inhibitors of specific CDKs may be preferable to reduce toxicity, but selectivity may also diminish anticancer efficacy due to the inherent functional redundancy observed for this family of kinases. Thus, absolute selectivity might not be the best approach to treat such a complex disease as cancer, where multiple pathways are deregulated. A broader-spectrum compound that inhibits CDK1, CDK2, CDK4 and CDK6 at low nanomolar concentrations may therefore be optimal.¹⁴⁷ The recent observation that selectively inhibiting CDK2 in certain tumour cell lines is not sufficient for antitumour activity would support this view,¹⁴² as would the demonstration that the CDK2 knockout mouse shows no major abnormalities and, in particular, no effects on proliferation.

¹⁴¹

As the CTD kinase associated with the general transcription factor TFIIF, CDK7 has long been suspected of playing an indispensable catalytic role in transcription. The belief that CDK7 is globally required for transcription by Pol II *in vivo* is based largely on hybridisation studies in budding yeast, in which the large majority of Pol II transcripts are repressed upon thermal inactivation of a temperature-sensitive Kin28.¹⁴⁸ Exceptions to this behaviour (e.g. promoters refractory to inactivation of the TFIIF-associated kinase) exist in budding yeast¹⁴⁹⁻¹⁵⁰ and in *Drosophila*.¹³⁵ These exceptions might reflect compensation by other CTD kinases, such as the recently identified ortholog of metazoan CDK9.¹⁵¹⁻¹⁵² Synthetic genetic interactions between

orthologs of CDK7 and CDK9 in both budding and fission yeast indicate a degree of functional overlap.¹⁵³ This feature among the CDKs that phosphorylate the Pol II CTD to influence transcription is still hypothetical, but would be reminiscent of the apparent redundancy among the cyclins and CDKs that control cell-cycle progression.

Interestingly, the essential role of CDK1/Cyclin B1 as the M phase-promoting factor appears to have survived unchallenged to date. Expression of CDK1 in proliferating cells has been observed to cause an arrest in the G₂/M transition. Furthermore, a recent study demonstrated that selective cyclin B1 depletion inhibits proliferation and induces apoptosis in tumour cells, whereas normal cells are essentially unaffected.⁴⁴ As cyclin B is frequently overexpressed, selective CDK1 inhibition may be an attractive therapeutic strategy. However, it remains unclear at this stage whether pharmacological CDK1 inhibition in tumour cells can result in the same effect as cyclin B1 depletion. At present, no truly selective ATP-competitive CDK1 inhibitor has been developed.

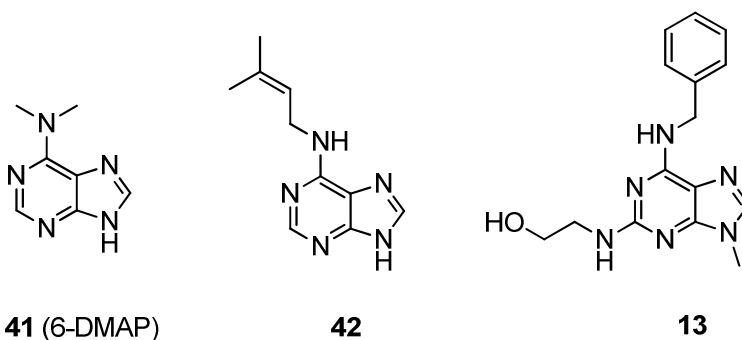
Another approach, which is currently being investigated, involves the development of non ATP-competitive inhibitors. Targeting allosteric sites can potentially provide an increased selectivity for individual kinases. In particular, CDKs offer an interesting starting point for the design of corresponding inhibitors because of their complex network of mechanisms of regulation.¹⁴⁷

Chapter 3 – Project background

3.1 Purine-based inhibitors of CDKs

In the search for structures that closely reproduce the interactions made by ATP within the ATP-binding site, purines were early candidates as inhibitors of CDKs.

The first purine compound to be identified as a CDK inhibitor was 6-dimethylaminopurine or 6-DMAP (**41**). Originally designed to inhibit protein biosynthesis as a puromycin analogue, 6-DMAP inhibited mitosis in sea urchin oocytes without blocking protein synthesis. The mechanism of action of 6-DMAP was finally elucidated when it was demonstrated that this compound inhibited the recently discovered histone H1 kinase, or CDK1/Cyclin B, with an IC_{50} of 120 μ M.¹⁵⁴



Further screening experiments using a newly established *in vitro* kinase assay led to the identification of additional purine CDK inhibitors, including isopentenyladenine (**42**, IC_{50} = 55 μ M) and olomoucine (**13**, IC_{50} = 7 μ M).¹⁵⁵ Olomoucine was found to be selective for the CDK family with the exception of ERK2, a member of the MAP kinase family; this purine inhibits CDK2/Cyclin E and CDK7/Cyclin H with an IC_{50} of 0.94 and 0.6 μ M, respectively.¹⁵⁶

X-ray crystal structure analysis of **13** bound to CDK2 showed the adenine group adopting a different binding orientation from that of ATP (**Figure 31**).

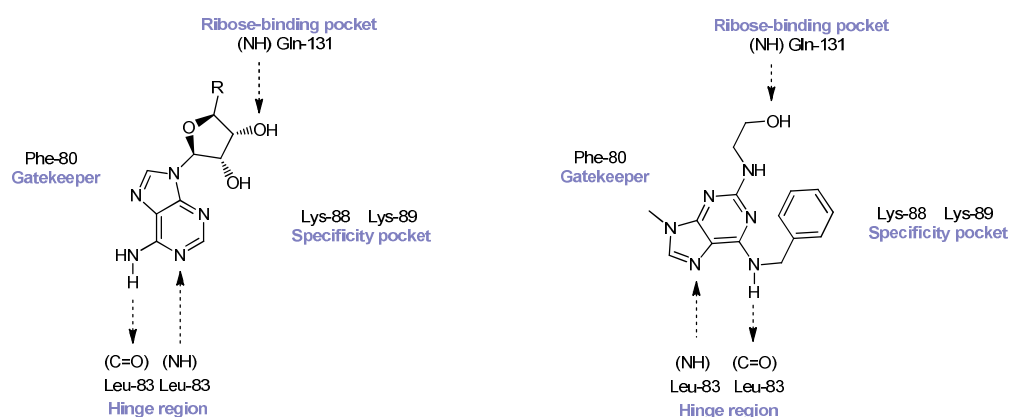
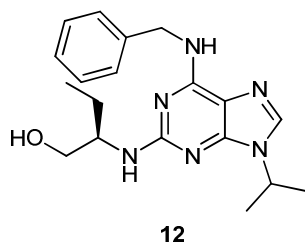


Figure 31

ATP (left) and Olomoucine (right) bound to CDK2/A.

The N⁷ of olomoucine accepts a hydrogen bond from the NH group of Leu83, whilst the exocyclic NH₂ donates a hydrogen bond to the carbonyl of the same residue *via* the 6-amino group. In addition, a third hydrogen bond was identified between the hydroxyl group on the N⁶ substituent and the backbone carbonyl group of Gln131. The alternative binding mode of olomoucine projects the N⁶ substituent out of the conserved region in the binding pocket, allowing for interactions with the specificity surface of CDK2. The benzyl ring makes favourable Van der Waals interactions with residues Ile10, Phe82 and His84.¹⁵⁷ This avoids a steric clash between the benzyl group and the Phe80 sidechain.

From the early screening of purines as CDK inhibitors, 2,6,9-trisubstituted purines gave the best inhibitory results. (*R*)-roscovitine (**12**), a derivative of olomoucine, is an inhibitor of CDK2, CDK7 and CDK9 (IC₅₀ CDK2/Cyclin A = 2.2 μM; IC₅₀ CDK7/Cyclin H = 0.46 μM; IC₅₀ CDK9/Cyclin T1 = 0.78 μM).¹⁵⁶



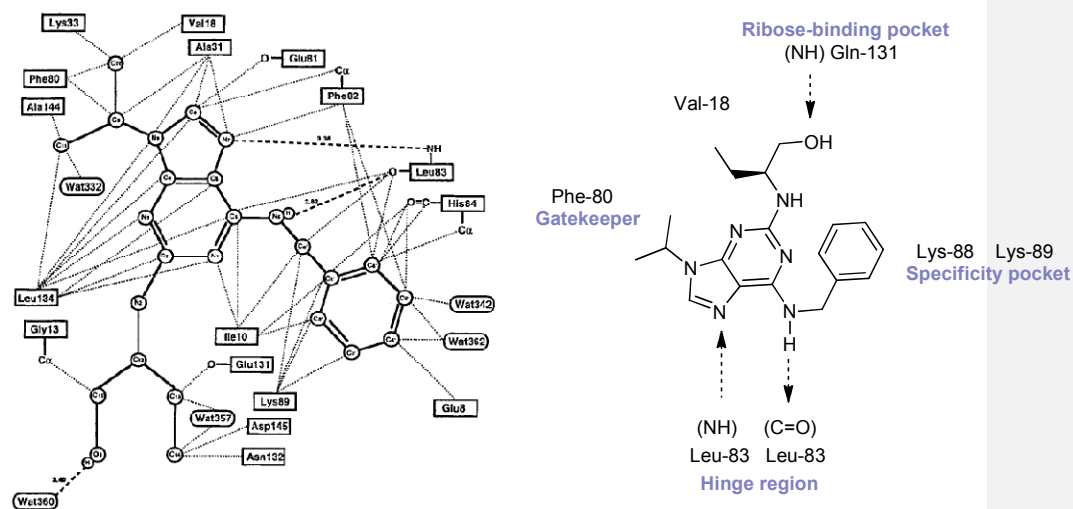


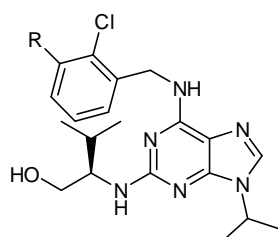
Figure 32

(*R*)-roscovitine bound to CDK2/A. ¹⁵⁸

(*R*)-roscovitine (**12**) binds to CDK2 in the same orientation as the parent olomoucine ¹⁵⁹ (**Figure 31**), and the N⁹-isopropyl group fits inside a small hydrophobic pocket formed by the side-chains of Ala31, Phe80, Leu134 and Ala144. The stereoisomer bearing a side-chain with an (*R*)-configuration is more active against CDK1/Cyclin B than the corresponding (*S*)-enantiomer ($IC_{50} = 0.95 \mu M$). This was also observed for analogues with different side-chains at the 2-position, with the (*R*)-isomer being more active than the (*S*)-isomer. Selective interaction of this side-chain with Val-18 in the ribose-binding pocket has been suggested as the reason for this difference in activity between the two enantiomers. ¹⁶⁰ Tested against a panel of 151 kinases, **12** exhibited good selectivity for the CDK family, with the only other significant target to be recognised being pyridoxal kinase, the enzyme responsible for phosphorylation and activation of vitamin B₆. ¹⁶¹ (*R*)-Roscovitine (**12**) can arrest cells in both the G₁ and G₂ phase of the cell cycle, depending on the cell line. Studies have also shown that treatment of colorectal cancer cells with **12** resulted in a decrease in pRb phosphorylation, indicative of direct CDK2 inhibition, while G₂/M checkpoint reactivation was attributed to inhibition of CDK1. ¹⁵⁵ (*R*)-Roscovitine also blocks the degradation of p53 through inhibition of MDM2 expression, arising from inhibition of

CDK7 and CDK9.¹⁴⁷ Upon successful completion of phase I clinical trials, **12** has undergone several phase II studies, including the treatment of haematological β -cell malignancies and breast cancer.^{44, 69, 162}

Another important class of purine-based CDK inhibitors that share a similar binding mode to olomoucine and (*R*)-roscovitine is the purvalanols. Identified in 1998¹⁵⁸ as a result of screening numerous 2,6,9-trisubstituted purines against CDK2, purvalanols A (**14**) and B (**15**) have IC₅₀ values of 4 and 6 nM against CDK1/Cyclin B, and 70 nM and 6 nM versus CDK2/Cyclin A, respectively.¹⁴⁷ Purvalanol A causes an arrest of the cell cycle of human fibroblasts in the G1/S and G2/M transitions, in line with the observed inhibition of CDK1 and CDK2. It also exhibits antiproliferative activity against different human tumour cell lines in contrast to purvalanol B, with average GI₅₀ values of 2 μ M. This is probably due to the higher membrane permeability of **14**, although **15** is more active against the isolated CDKs.³⁷



Purvalanol A (**14**) (R = H), Purvalanol B (**15**) (R = CO₂H)

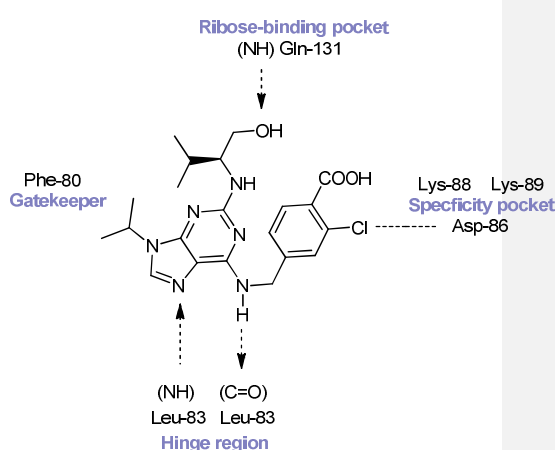
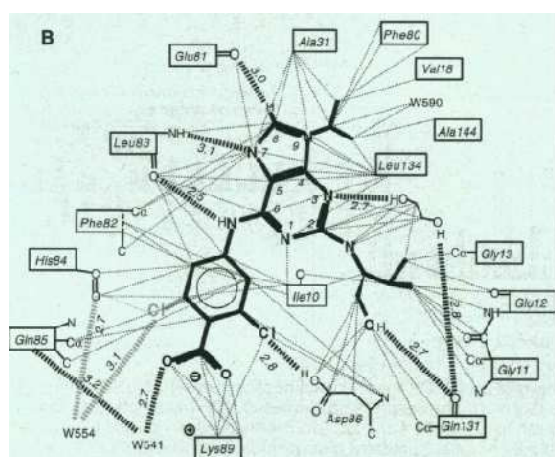


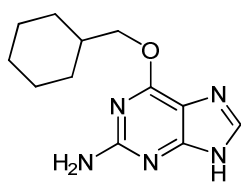
Figure 33

Purvalanol B bound to CDK2/A.¹⁵⁸

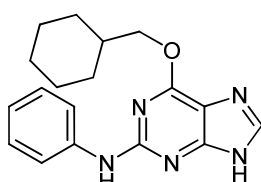
Crystallographic studies with CDK2 confirmed that the binding mode of the purvalanols mirrored that of other 2,6,9-trisubstituted purine inhibitors (**Figure 33**). In addition to the characteristic donor-acceptor motif with the backbone peptide, it has been argued that further stabilisation is gained from polar interactions between the chloro group and the side-chains of Asp86, whilst the (*R*)-isopropyl group is packed tightly to the backbone atoms of the glycine-rich loop (Val18).³⁷ When assessing the selectivity profile of the 2,6,9-trisubstituted purine derivatives the general trend was towards inhibition of CDK1, 2, 5, 7 and 9, rather than CDK4/6. MAP kinases ERK1 and ERK2 were also sensitive but none of the other kinases tested showed significant inhibition.¹⁵⁵

3.2 From NU2058 (32) to NU6247 (44)

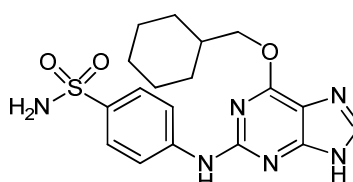
Previous work carried out at Newcastle University was focused on the synthesis and evaluation of *O*⁶-substituted guanine derivatives as potential inhibitors of the DNA-repair protein *O*⁶-alkylguanine-DNA-alkyltransferase (AGT).¹⁶³ *O*⁶-Cyclohexylmethylguanine (**32**, NU2058) emerged as inactive against AGT, but exhibited moderate inhibition of CDK1/Cyclin B and CDK2/Cyclin A, with IC₅₀ values of 26 ± 1 µM and 17 ± 3 µM, respectively.¹⁶⁴ This compound also shows selectivity over CDK4/Cyclin D (IC₅₀ > 100 µM).¹⁶⁵



NU2058 (32)



NU6094 (43)



NU6102 (31)

Elucidation of the crystal structure of **32** bound to CDK2/Cyclin A revealed a different binding orientation compared with the other known purine-based inhibitors, such as

olomoucine (**13**), (*R*)-roscovitine (**12**) and the purvalanols (**14** and **15**), indicating the formation of a unique triplet of hydrogen bonds within the hinge region. The N³ and 2-amino groups of **32** accept and donate hydrogen bonds with the carbonyl and amide groups of Leu83, respectively, whereas the 9-NH donates a hydrogen bond to the carbonyl group of Glu81 (**Figure 34**).¹⁶⁴

The O⁶-cyclohexylmethyl substituent of **32** makes significant hydrophobic interactions with various residues within the ribose-binding pocket, forming highly complementary packing against the glycine-rich loop.¹⁶⁵ In addition, Van der Waals interactions between the purine ring and the top and bottom of the ATP-binding cleft are observed, forming an edge-to-face aromatic-aromatic contact between the purine ring of **32** and Phe80.

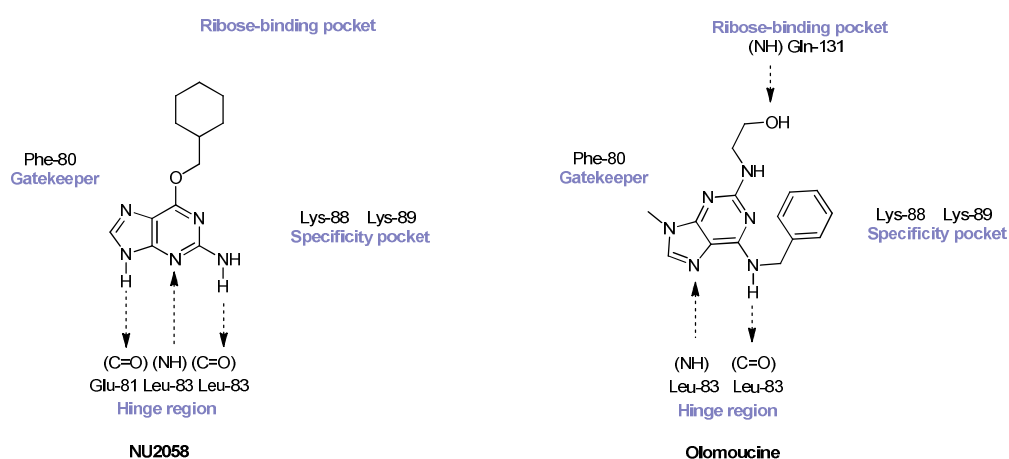
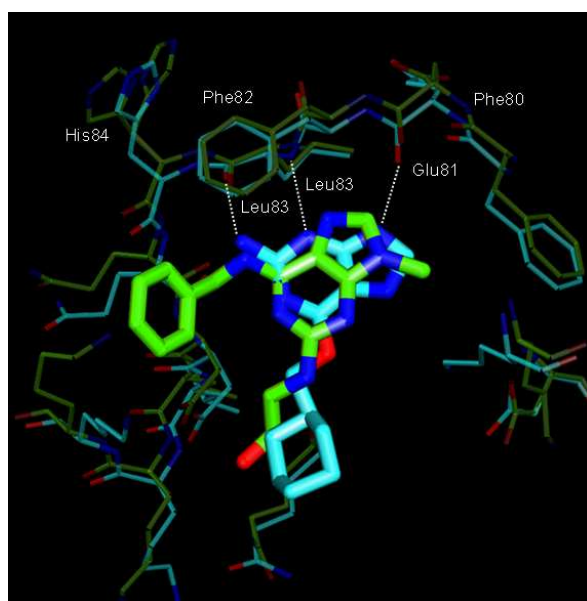


Figure 34

NU2058 (blue, left) and olomoucine (green, right) bound to CDK2/A. ¹⁶⁵

As previously described, the N⁶-benzyl group of olomoucine (**13**) projects out of the ATP-binding site of CDK2 and forms interactions with the specificity surface of the kinase. By comparing the binding modes of **32** and **13**, it was suggested that suitable aromatic substituents could be introduced at the N² position of **32**, thus packing

against the specificity surface occupied by the N⁶-benzyl group of olomoucine, with potential for improving both potency and selectivity.

Accordingly, the 2-anilino derivative **43** exhibited approximately a ten-fold increase in potency for CDK2 in comparison with its parent compound **32**, with IC₅₀ values of 10 μ M and 1.0 μ M *versus* CDK1/Cyclin B and CDK2/Cyclin A, respectively.⁴³ It was confirmed *via* a crystal structure determination that, as predicted, the aniline group at the 2-position projects out of the ATP-binding domain and packs against the kinase specificity surface, forming a π - π stacking interaction with the peptide backbone between Gln85 and Asp86. The planes of the purine and the aniline rings are separated by an interplanar angle of 50°, closely resembling the energetically favoured angle, estimated as approximately 48° (**Figure 35**).⁴³

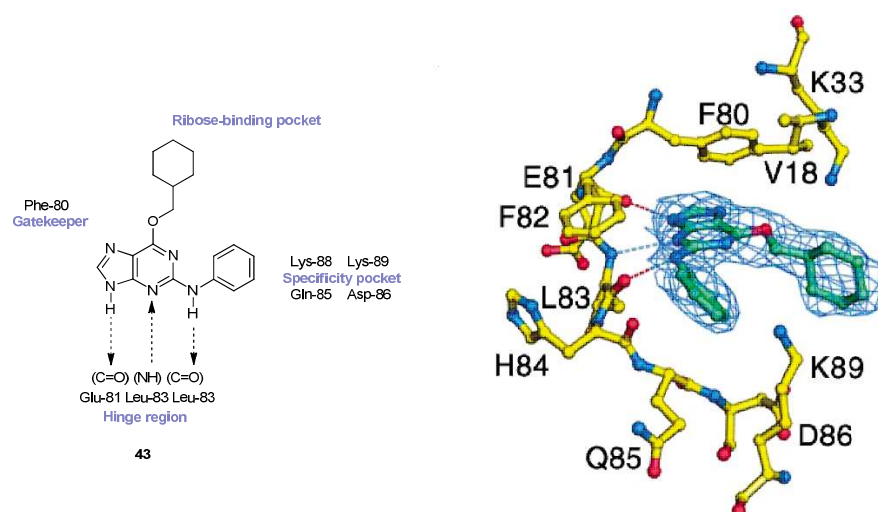


Figure 35

Purine **43** bound to CDK2/A.⁴³

In order to probe the specificity pocket further, a variety of functionalities were introduced at different positions on the aniline ring.⁹⁵ The sulfonamide derivative NU6102 (**31**) proved to be an extremely potent CDK2 inhibitor (IC₅₀ = 5 nM), as it makes two additional bonding interactions with the target kinase. One sulfonamide oxygen accepts a hydrogen bond from the backbone NH of Asp-86 ($r_{\text{NH-O}} = 3.1$ Å), while the sulfonamide NH₂ group donates a hydrogen bond to the side-chain carbonyl of Asp86 ($r_{\text{NH}_2\text{-O}} = 2.9$ Å) (**Figure 36**).

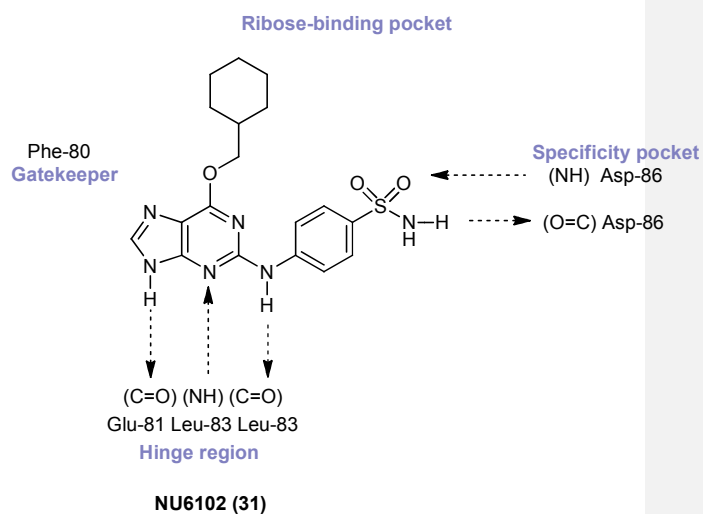
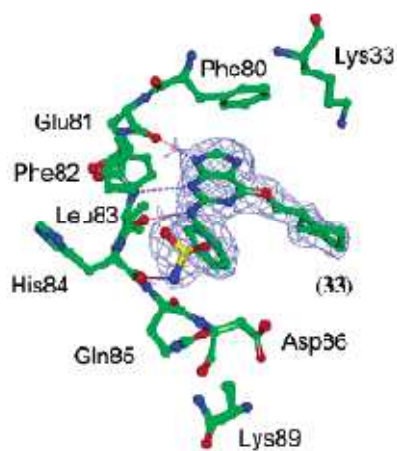
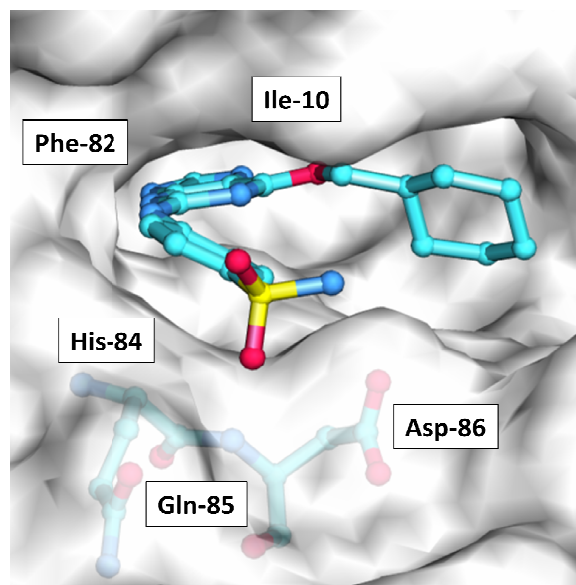


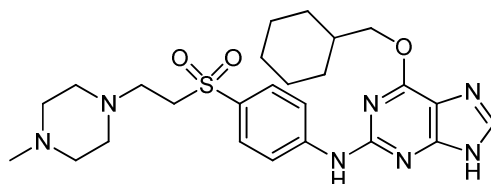
Figure 36

NU6102 (31) bound to CDK2/A ⁹⁵

Unfortunately, tumour cell growth inhibition for **31** was only observed in the 1-10 μ M concentration range, suggesting poor cellular uptake or failure to compete effectively

with high intracellular levels of ATP. Another increasingly plausible explanation has been suggested to be the redundancy of CDK2, as discussed in **Chapter 2**.

To address the issue of presumed poor cellular uptake of **31**, or the possibility that the arylsulfonamide moiety may be conferring affinity for other proteins, for example carbonic anhydrase, ¹⁶⁶ systematic replacement of the sulfonamide group with isosteric functionalities was undertaken. An ideal sulfonamide isostere, in this case, would be a group that retains the ability to form the key hydrogen bonds with Asp-86, recognised as important to attain CDK2 potency, whilst gaining favourable cellular properties and losing features of promiscuous affinity. An innovative approach was adopted to generate a library of compounds based on the sulfone moiety. ¹⁶⁷ The piperazin-1-ylethylsulfonyl compound NU6247 (**44**), whilst not one of the most potent compounds generated within this series (IC_{50} CDK2 = 120 nM), proved to be almost equipotent against CDK7 (IC_{50} = 230 nM), the first purine within this series to show activity against this member of the CDK family.



NU6247 (44)
 IC_{50} μ M = 0.12 (CDK2), 0.23 (CDK7)

Purine **44** was co-crystallised with CDK2 (**Figure 37**, right), showing that this compound binds in essentially the same orientation as **31** (left). The interaction of the sulfone moiety with the backbone amide NH of Asp-86 is retained, but the interaction with the backbone carbonyl of Asp-86 is lost and is not replaced by any meaningful interaction made by the terminal piperazine, which may account for the loss in potency.

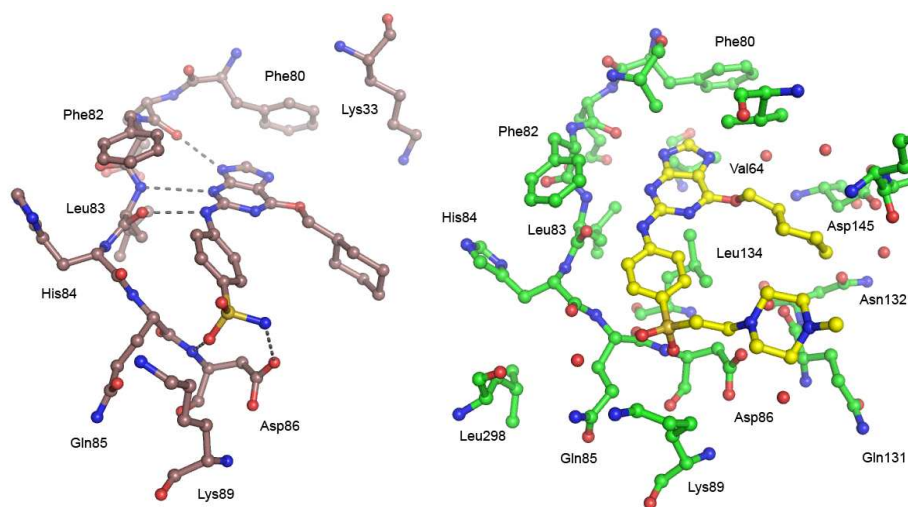


Figure 37

31 (left) and **44** (right) bound to CDK2/A. ⁹⁵

At the time that the sulfone series was developed, **44** was the most potent CDK7 inhibitor synthesised at Newcastle. The following chapters outline the work conducted since then, aimed at designing out CDK2 activity from this family of compounds while improving CDK7 activity.

Chapter 4 – Development of analogues of NU6247 (44)

4.1 Hydrophobic analogues of NU6247 (44)

As discussed at the end of **Chapter 2**, the recently elucidated crystal structure of CDK7 provides guidance towards designing potent and selective ATP-competitive inhibitors of CDK7. As mentioned in **Chapter 2**, the specificity surface of CDK7 exhibits some amino acid residues that have a hydrophobic character. These residues could, if appropriately targeted with specifically designed inhibitors, form productive interactions with CDK7 that would not be possible in CDK2, thereby providing selectivity. The bottom of the “hydrophobic pocket”²⁷ of CDK7 contains Thr96 and Val100 instead of Gln85 and Lys89 (the region in question also includes Asp97, Leu98 and Glu99; in the vicinity, residues Pro140, Asn141, Asn142, Asp143, Leu144 and Pro310 can also be found).

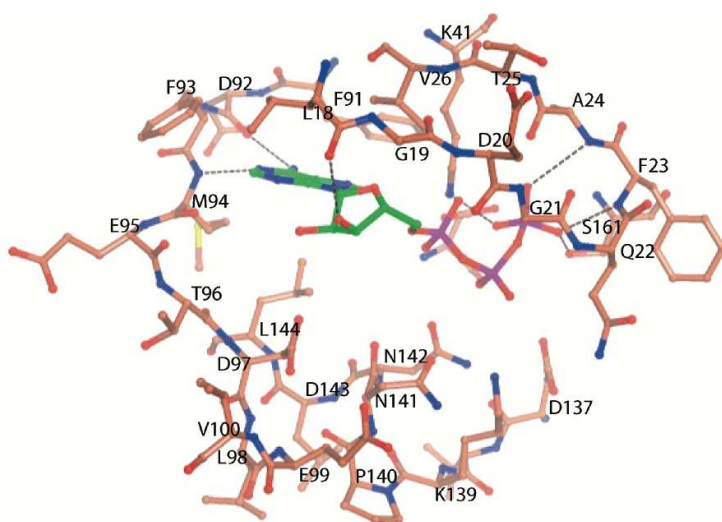
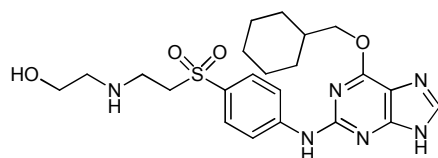


Figure 38

The ATP binding site of CDK7.¹³⁸

Following the identification of **44** as a nanomolar CDK7 inhibitor, a small group of similar purines containing the ethylsulfonyl moiety was tested against the same kinase (**Table 8**), establishing the role of **44** as a structural lead within this family.



45
IC₅₀ CDK2 = 0.047 μ M
IC₅₀ CDK7 = 100 μ M

Interestingly, the aminoethanol derivative **45** was 100-fold less potent than **44**. This suggested a different binding mode for the two compounds within the ATP binding pocket of CDK7, potentially providing a platform from which to develop potent and selective inhibitors of CDK7.

The activity shown by **44** against CDK7 was retained in all four compounds in **Table 8**. The presence of an alkyl substituent on the terminal piperazine nitrogen increased potency, with purines **47** and **48** being essentially equipotent and approximately 5-fold more potent than the parent unsubstituted piperazine (**46**). These compounds are also selective over CDK9, thus retaining the selectivity profile seen with NU6102 (**31**).

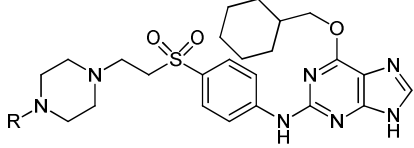
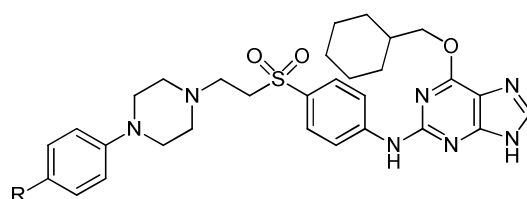
		IC ₅₀ (μM) or percentages of inhibition at 100 μM		
R	Code	CDK2	CDK7	CDK9
H	46	0.34	0.99	75
Me	44	0.12	0.23	100
Et	47	0.29	0.27	78
<i>i</i> Pr	48	0.34	0.48	46

Table 8

CDK2- and 7-inhibitory activity for compounds **44** and **46-48**

Compounds **46-48** lack selectivity for CDK7 over CDK2 but represent a good starting point for structural modifications targeting the “hydrophobic pocket” of CDK7.

With a view to synthesising derivatives of **44** that are more hydrophobic, compounds **49-52** were identified as initial targets.

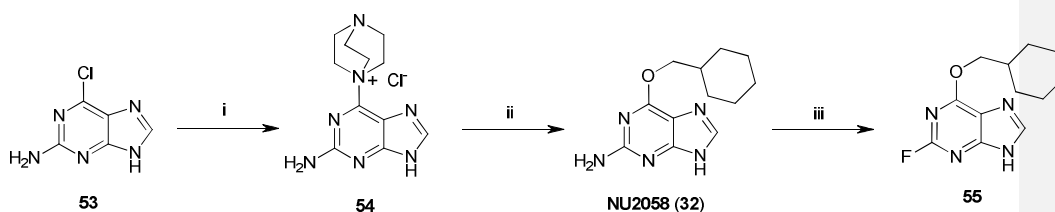


49, R = H
50, R = OMe
51, R = Cl
52, R = CF₃

The aim was to investigate the effect of having an aromatic substituent on the terminal piperazine nitrogen of **44**, and to explore the effect of an electron-donating

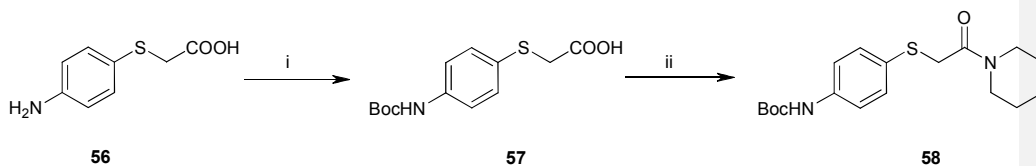
versus an electron-withdrawing substituent on the phenyl ring, with respect to the parent phenyl compound.

The route chosen to the desired synthetic targets was one previously developed at Newcastle.¹⁶⁸ Starting from commercially available 2-amino-6-chloropurine and 4-aminophenylthioacetic acid, the steps outlined in **Schemes 1-3** were carried out.



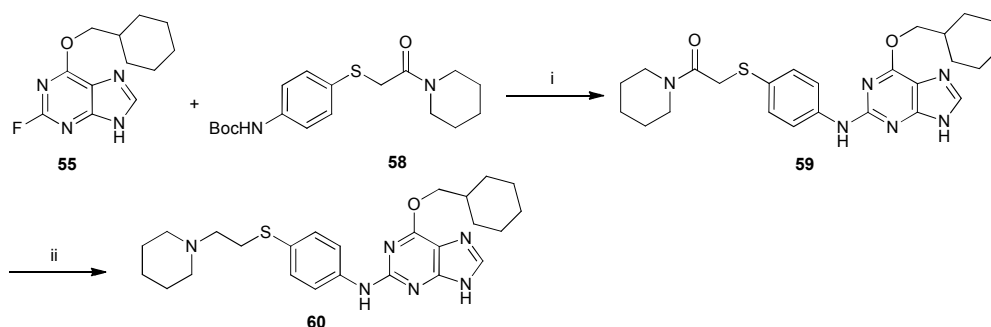
Scheme 1

Reagents and conditions (i) DABCO, DMSO, 25°C; (ii) Cyclohexylmethanol, NaH, DMSO, 25°C; (iii) HBF₄, NaNO₂, 0°C.



Scheme 2

Reagents and conditions (i) Boc₂O, TEA dioxane, H₂O, 25°C; (ii) SOCl₂, piperidine, DMF, THF, 25°C.

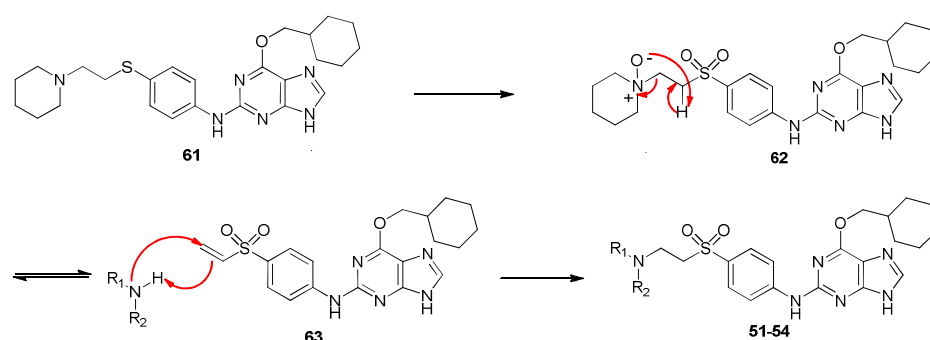


Scheme 3

Reagents and conditions (i) TFA, TFE, 25°C; (ii) Li AlH₄, THF, 25°C.

The two key precursors to the target structures are compounds **55** and **58**. The fluoropurine **55** was prepared from 2-amino-6-chloropurine *via* a three-step process involving nucleophilic substitution followed by a Balz-Schiemann reaction.¹⁶⁹ The commercially available 4-aminophenylthioacetic acid was Boc-protected and converted into the piperidine amide **58** *via* a Vilsmeier-Haack-like reaction,¹⁷⁰ employing thionyl chloride, piperidine and DMF.

In the presence of a catalytic amount of TFA the Boc protecting group was cleaved *in situ* from compound **58** and the desired compound **59** was obtained *via* an aromatic nucleophilic substitution on **55** with displacement of the fluoro substituent. The amide functionality of compound **59** was subsequently reduced, affording amine **60**. Oxidation followed by Cope-like elimination^{167, 171} and reaction with the appropriate amine, afforded the target compounds **49-52** according to the mechanism outlined in **Scheme 4**.



Scheme 4

The mechanism for the formation of compounds **49-52** from **60**.¹⁶⁷

The results shown in **Table 9** demonstrate that these compounds failed to afford the desired activity and selectivity towards CDK7. Potency drops dramatically as the steric bulk on the terminal basic nitrogen of the piperazine ring increases, as does selectivity, with compounds **49-52** all being approximately ten-fold selective for CDK2.

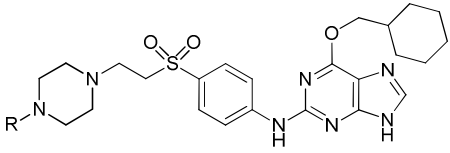
		IC ₅₀ μM	
R	Code	CDK2	CDK7
Me	44	0.12	0.23
<i>i</i> Pr	48	0.34	0.48
Ph	49	1.2	33
<i>p</i> -MeO-C ₄ H ₆	50	1.25	11.3
<i>p</i> -Cl-C ₄ H ₆	51	3.3	37
<i>p</i> -CF ₃ -C ₄ H ₆	52	3.5	26

Table 9

CDK2- and CDK7-inhibitory activity for compounds **44** and **48-52**.

Several explanations can be proposed for the bulky *N*-substituents in **49-52** failing to form the desired interactions within the 'hydrophobic pocket' of CDK7. The planarity of the aromatic rings may not confer the desired binding orientation, or the steric bulk may be excessive; the reversal of selectivity may indicate that the 'hydrophobic pocket' is not targeted at all, and that these purines bind in a different orientation.

The results indicated that it was necessary to select new and different targets to probe the ATP-binding site of CDK7, and gain new insight into how best to employ the available structural information to our advantage. In particular, structural biology studies carried out by collaborators at Oxford University focused on site-directed mutagenesis experiments with CDK2. These could aid the structure-based design of CDK7 inhibitors, and are therefore presented in the following section.

4.2 Structural biology studies

Although the crystal structure of CDK7 has been determined, efforts to solve a structure in complex with an inhibitor have been unsuccessful to date.

Taking advantage of the fact that the crystal structure of CDK2 has been solved in complex with a number of Newcastle inhibitors (see **Figure 37** in **Chapter 3** for the crystal structure of **31** and **44** bound to CDK2), colleagues at the University of Oxford have prepared a number of mutant versions of CDK2, where one or more amino acids within the ATP-binding site have been replaced with those found in CDK7. In one of these mutants, referred to as K88E K89V CDK2(7), Lys88 and Lys89 of CDK2 have been replaced by a glutamic acid and a valine, respectively. In another mutant, referred to as Hinge CDK2(7), Leu83, His84 and Glu85 have been substituted with a methionine, a glutamic acid and a threonine, respectively.

This approach has enabled the successful crystallisation of **44** in complex with CDK2(7) (**Figure 39**).

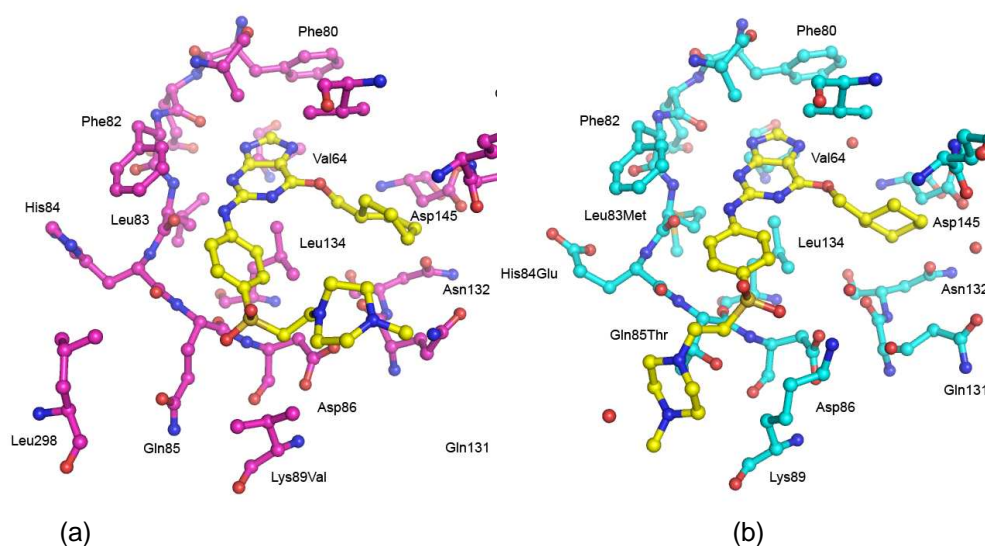


Figure 39

Crystal structures of CDK2(7) mutant kinases in complex with NU6247 (**44**, in yellow) (a) ATP-binding site of CDK2 where Lys88 and 89 have been replaced by a Glu and a Val. (b) ATP-binding site of CDK2 where Leu83, His84 and Glu85 have been replaced by a Met, a Glu and a Thr.

Inspection of the **44**-CDK2(7) complexes indicated the existence of two possible binding orientations of the sidechain of **44**, one of which is not seen with the wild-type enzyme. This revealed the presence of an additional binding pocket that may be amenable to probing with a suitably modified derivative of **44**.

Figure 40 shows a comparison between the molecular surfaces of the complexes of **44** with K88E K89V CDK2(7) (left) and Hinge CDK2(7) (right). The potential for the sidechain of **44** to orientate in two different directions on the specificity surface of the enzyme is particularly evident in the Hinge mutant (red arrows).

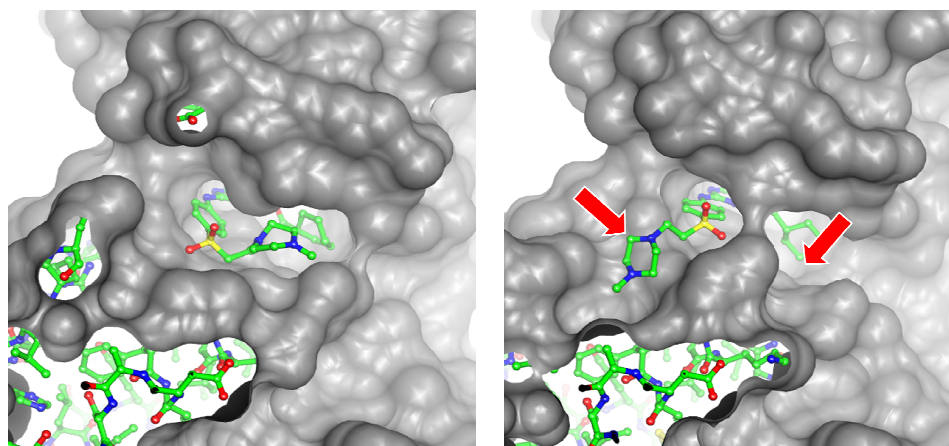
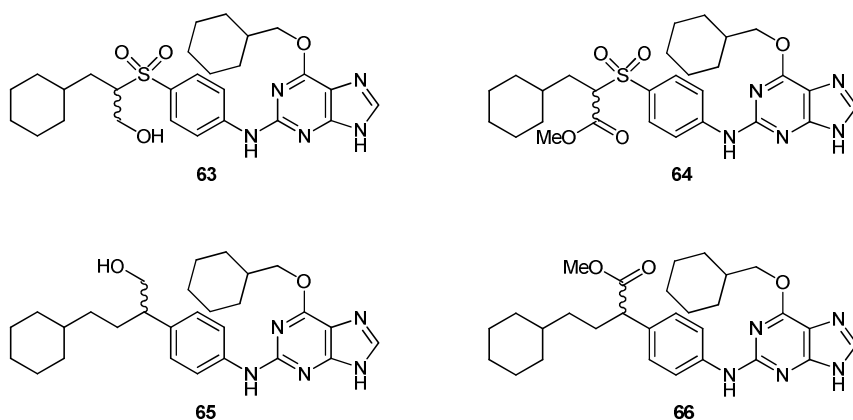


Figure 40

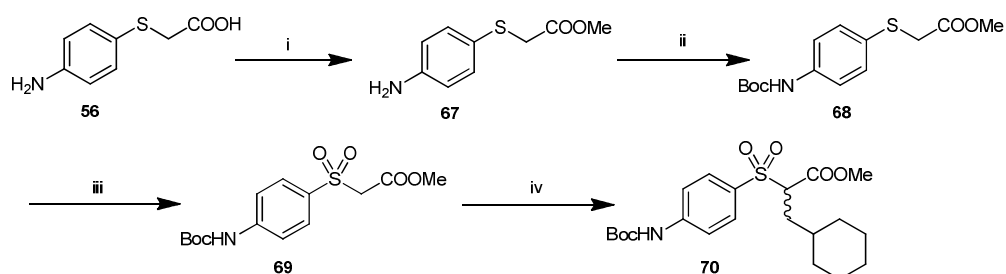
The molecular surface of K88E K89V CDK2(7) (left) and with Hinge CDK2(7) (right), in complex with NU6247 (**44**)

To explore the additional binding pocket, the following target compounds were proposed:



These purines are “bifurcated”, in that they possess a hydrophobic sidechain intended to target the pocket identifiable in **Figure 40**, while retaining a polar functionality (a hydroxyl group) meant to target the same surface area of CDK7 as the piperazine ring of **44**.

The synthesis of racemic targets **63** and **64** was undertaken starting from 4-(aminophenyl)thioacetic acid (**56**), and carried out following the steps outlined in **Schemes 5** and **6**.

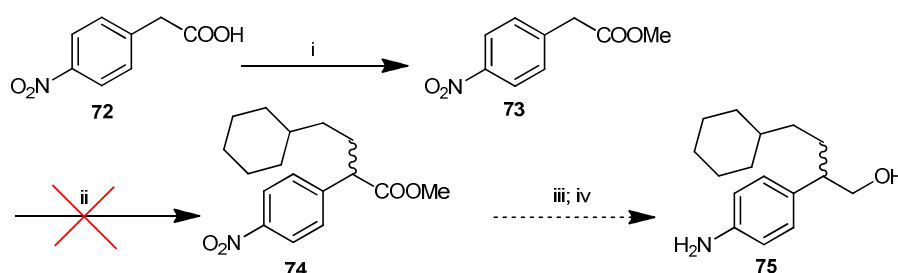


Scheme 5

Reagents and conditions: (i) SOCl_2 , MeOH, 3 h, RT; (ii) Boc_2O , TEA, THF/ H_2O , 12 h, $0\text{ }^\circ\text{C} \rightarrow \text{RT}$; (iii) mCPBA, CH_2Cl_2 , 12 h, RT; (iv) NaH, CyCH_2Br , DMF, 12 h, $0\text{ }^\circ\text{C}$.

Compound **56** was converted into the methyl ester **67** using SOCl_2 in methanol. The aniline moiety was then Boc-protected and mCPBA was used to convert the sulfide **68** into a sulfone (**69**). Reaction of the sulfone **69** with one equivalent of sodium

A synthetic scheme was proposed for the preparation of these compounds, starting from *p*-nitrophenylacetic acid (**72**), and including an LDA-mediated alkylation step for the introduction of the cyclohexylethyl residue. (**Scheme 7**).



Scheme 7

Reagents and conditions: (i) SOCl₂, MeOH, 3 h, RT; (ii) *n*BuLi, *i*Pr₂NH, CyCH₂CH₂Br, THF, 12 h, -78 °C; (iii) DIBAL-H, THF, 12 h, -78 °C; (iv) H₂/Pd/C, MeOH, 12 h, RT.

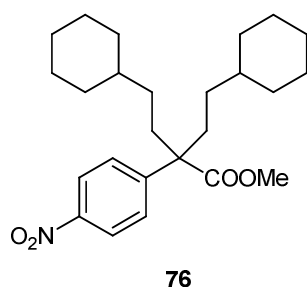
The esterification step proceeded quantitatively to furnish compound **73**, but the LDA-mediated alkylation reaction did not give a satisfactory result. The reaction was attempted using both commercial LDA and LDA generated *in situ* from *n*-butyl lithium and isopropylamine. Different ratios of LDA to cyclohexylethyl bromide were also employed, with the results shown in **Table 10**.

Number of equivalents		Result
LDA	CyCH ₂ CH ₂ Br	
3	3	Dialkylated product (78) isolated (quantitative)
3	1.5	Dialkylated product (78) isolated (~50% yield)
1.5	1.5	Complex reaction mixture – no major product identifiable

Table 10

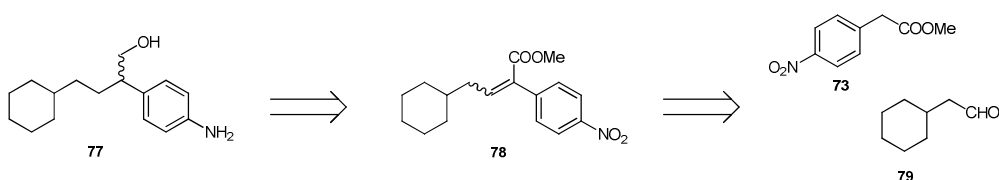
Conditions attempted for the alkylation of **73**

The use of an excess of base gave the dialkylated product **76**, which precipitated out of the reaction mixture as colourless crystals.



Attempts at performing the reaction of **73** with cyclohexylethyl bromide in the presence of near-stoichiometric amounts of base were not successful. The reaction mixture was very complex and no significant amount of the desired product **74** was detected by LCMS or NMR analysis. As a straightforward alkylation reaction did not give good results, a different synthetic strategy was devised.

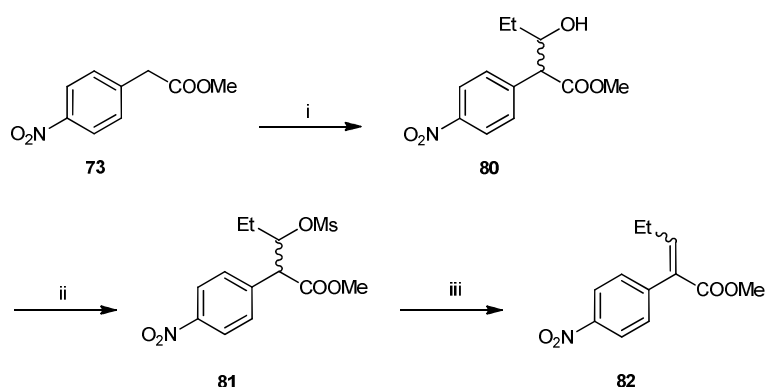
Target compound **65** can be disconnected in a manner that suggests the application of a Henry-like reaction. In a typical Henry reaction,¹⁷⁴ an anion derived from a nitroalkane reacts with an aldehyde to give a β -nitroalcohol.¹⁷⁵ In the present case, the *p*-nitro function facilitates the condensation by increasing the acidity of the methylene protons in compound **73**. (**Scheme 8**).



Scheme 8

Retrosynthetic Henry approach for the synthesis of aniline **77** as a precursor to targets **65** and **66**

This idea was initially explored with **73** using propanal as a model aldehyde. The reaction proceeded smoothly (3 h, RT) when propanal was used as a solvent with tetramethylguanidine (TMG) as a base,¹⁷⁶ but was considerably slower (12 h, with heating) when acetonitrile was used as a solvent and the aldehyde was present in a 3 molar excess. Microwave irradiation was used to accelerate the reaction (15 minutes, 120°C) and alcohol **82** was isolated, converted into the mesylate and underwent elimination as expected (**Scheme 9**).

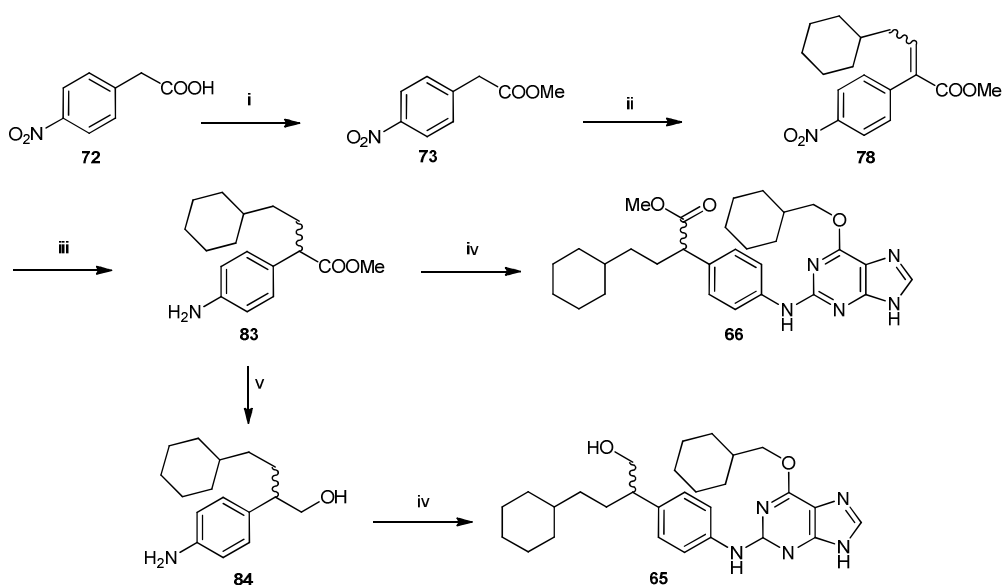


Scheme 9

Reagents and conditions: (i) Propanal, TMG (cat), CH₃CN, μ W, 15 min, 120 °C; (ii) MsCl, TEA, CH₂Cl₂, 12 h, RT; (iii) Toluene, 12 h, reflux.

Having established successful reaction conditions with the model reaction, 2-cyclohexylacetaldehyde (**79**), necessary for the synthesis of the target molecule, was prepared from commercially available 2-cyclohexylethanol. After attempting different oxidation methods for the conversion of 2-cyclohexylethanol to the corresponding aldehyde (Swern, Dess-Martin, TEMPO)¹⁷⁷ it was found that PCC oxidation¹⁷⁸ converted 2-cyclohexylethanol into 2-cyclohexylacetaldehyde (**79**) in quantitative yield with minimal purification.

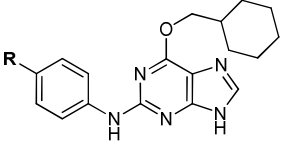
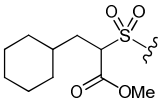
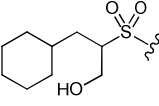
Condensation of **73** with a 12 molar excess of **79** (30 min, 120 °C, μ W) resulted in spontaneous elimination to give alkene **78**, without the need to isolate and mesylate the alcohol intermediate. The following steps (reduction of the double bond and of the nitro group of **78** to yield the saturated aniline **83**, reduction of the ester moiety of **77** to give the alcohol **84** and TFA/TFE coupling to **55**) as outlined in **Scheme 10** were successful, and provided both target purines **65** and **66** in a similar fashion to that described previously for **63** and **64**.



Scheme 10

Reagents and conditions: (i) SOCl_2 , MeOH, 3 h, RT; (ii) CyCH_2CHO , TMG (cat), CH_3CN , μW , 15 min, 120 °C; (iii) $\text{H}_2/\text{Pd/C}$, MeOH, 12 h, RT; (iv) **55**, TFA, TFE, 48 h, reflux; (v) DIBALH, THF, 12 h, -78 °C.

Target compounds **63-66** were submitted for biological testing, and the results are summarised in **Table 11**.

		IC₅₀ μM or percentage of inhibition at 10 μM	
R	Code	CDK2	CDK7
	64	46.9	19%
	63	1.2	33%

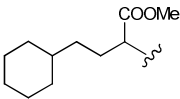
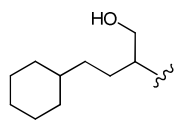
	66	43	13%
	65	3	4%

Table 11

IC₅₀ values, or percentages of inhibition at a given concentration, of compounds **64-67** against CDK2 and CDK7

The observed CDK-inhibitory activity of compounds **63-66** was much lower than predicted. In an attempt to understand the reason for this, compound **63** was submitted for co-crystallisation with [K88E K89V](#) CDK2(7). This was hoped to elucidate the binding mode of compound **63** within the ATP-binding site of CDK7. Although a crystal structure was obtained, this failed to provide any further insight into the binding mode of compound **63**. With the resolution at which the data were collected, the sidechain of compound **63** was not clearly visible in the ATP-binding site of CDK2(7). This indicates that, while the purine core pharmacophore was making the usual interactions with the hinge region, the hydrophobic sidechain failed to make any useful interactions with the specificity surface of the enzyme. This confirmed the observations already made with compounds **49-52**, and suggested that a highly hydrophobic sidechain for compounds of this family is not well tolerated within the CDK7 ATP-binding site.

4.3 Exploring SARs for analogues of NU6247 (44)

As the hydrophobic sidechains explored in the previous section failed to confer significant potency against CDK7, it was necessary to review existing data on CDK7 inhibition by purines, in order to obtain information on what might constitute a good sidechain for a purine-based CDK7 inhibitor.

Table 12 summarises purines that were previously tested against CDK7 at Newcastle and found to have IC₅₀ values of 500 nM or lower.

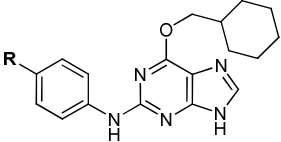
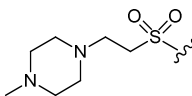
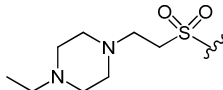
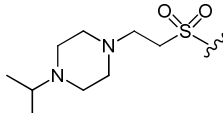
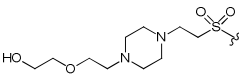
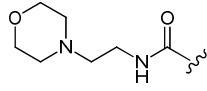
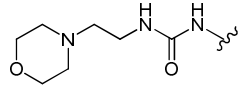
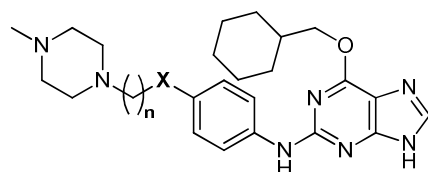
		CDK-inhibitory activity (IC ₅₀ μM)	
R	Code	CDK2	CDK7
	NU6247 (44)	0.12 ± 0.03	0.23
	47	0.29 ± 0.05	0.27 ± 0.01
	48	0.34	0.48
	85	0.31	0.44
	86	0.7 ± 0.1	0.38 ± 0.75
	87	1.1 ± 0.1	0.53

Table 12

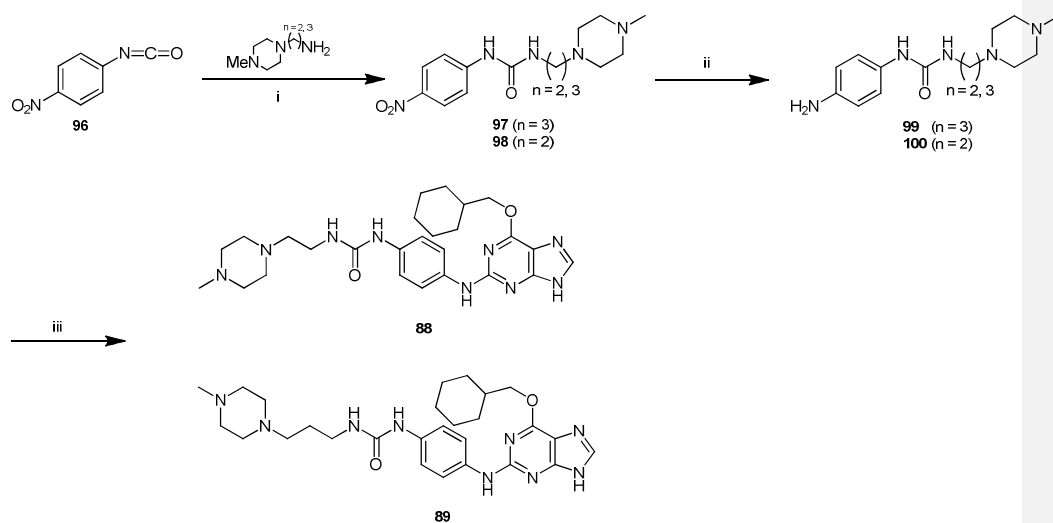
6-cyclohexylmethoxypurines with activity against CDK7 at IC₅₀ values lower than 0.5 μM

As it appears from **Table 12**, the best results for purines with sub-micromolar CDK7 activity are seen when a piperazine or morpholine ring is present at the purine 2-position. With this in mind, another small series of analogues of NU6247 (**44**) was synthesised, in which the piperazine ring was retained, but the linker between the 2-arylamino moiety and the pendant piperazine ring was varied. The chosen linkers included carboxamides, sulfonamides, ureas and phenylethers.



X = NHCONH, n = 2	88
X = NHCONH, n = 3	89
X = SO ₂ NH, n = 2	90
X = SO ₂ NH, n = 3	91
X = CONH, n = 2	92
X = CONH, n = 3	93
X = O, n = 2	94
X = O, n = 3	95

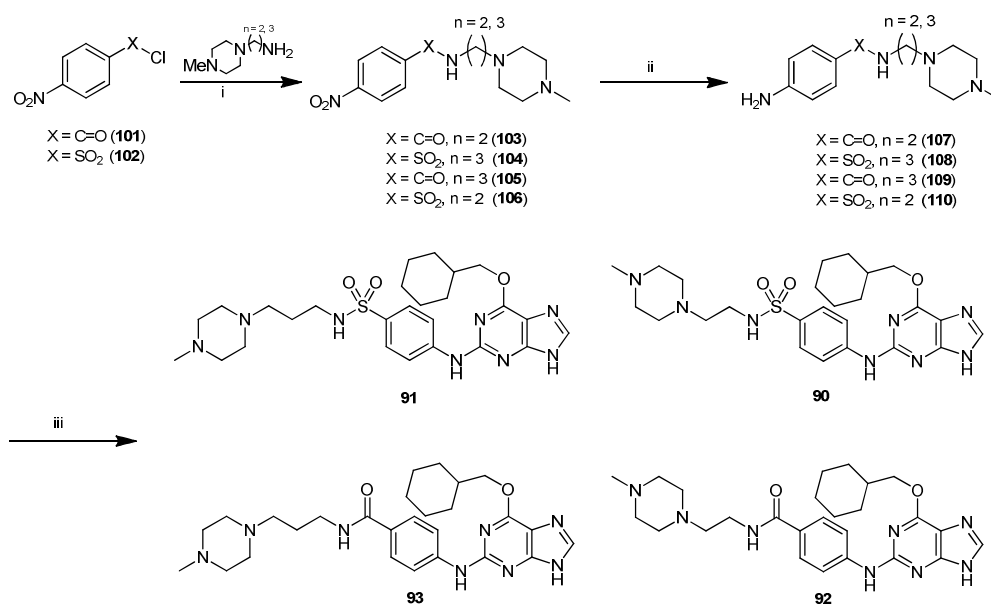
The urea moiety was first explored by a previous researcher when pursuing selective inhibitors of CDK1 (Andrew Henderson, unpublished results). The activity shown by purine **87** (see **Table 12**) against CDK7 (IC_{50} = 530 nM) justifies the interest in a urea analogue of NU6247 (**44**). The synthetic pathway for target compounds **88** and **89**, starting from commercially available *p*-nitrophenyl isocyanate (**96**), is shown in **Scheme 11**.



Scheme 11

Reagents and conditions: (i) THF, 3 h, RT; (ii) $\text{H}_2/\text{Pd/C}$, MeOH, 12 h, RT; (iii) **55**, TFA, TFE, 48 h, reflux.

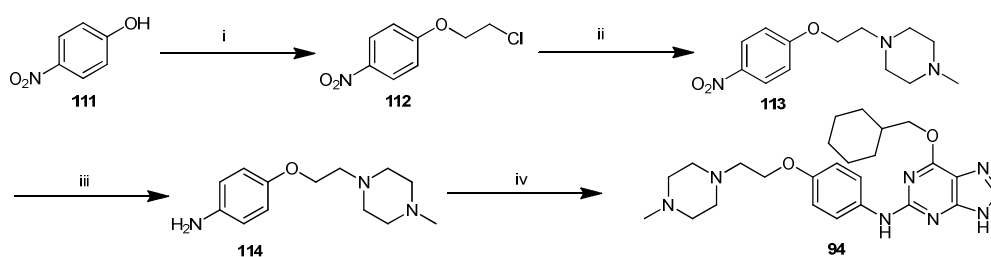
The synthesis of target compounds **90-93** (Scheme 12) was generally straightforward and started with the corresponding *p*-nitrobenzoyl (or benzenesulfonyl) chloride (**101**, **102** respectively), which were reacted with the appropriate amine under standard conditions.



Scheme 12

Reagents and conditions: (i) CH_2Cl_2 , K_2CO_3 , 4 h, RT; (ii) $\text{H}_2/\text{Pd/C}$, MeOH, 12 h, RT; (iii) **55**, TFA, TFE, 48 h, reflux.

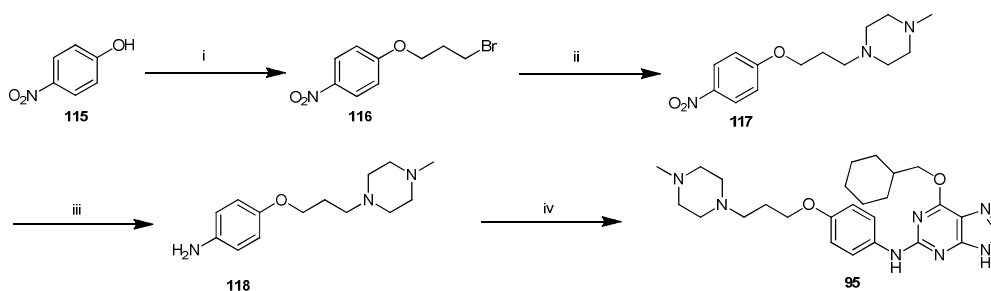
Targets **94** and **95** were synthesised according to a literature procedure suitable for the generation of a library of compounds having the general structure $\text{R}_2\text{N}-\text{CH}_2-\text{CH}_2-\text{O}-\text{Ar}$.¹⁷⁹ The protocol described in this paper was followed to synthesise **97**, a phenyl ether analogue of NU6247 (**44**). Reaction of *p*-nitrophenol (**111**) with 1,2-dichloroethane gave compound **112** which, in the presence of *N*-methylpiperazine, underwent substitution at the chloro group to yield intermediate **113**. Subsequent catalytic hydrogenation of **113** and **117** and coupling to purine **55** under previously described conditions completed the pathway (**Scheme 13**).



Scheme 13

Reagents and conditions: (i) 1,2-Dichloroethane, K_2CO_3 , CH_3CN , 48 h, reflux; (ii) N-Methylpiperazine, CH_3CN , μW , 30 min, 140 $^{\circ}C$; (iii) $H_2/Pd/C$, MeOH, 12 h, RT; (iv) **55**, TFA, TFE, 48 h, reflux.

Similar conditions were employed for the synthesis of compound **95** (Scheme 14).



Scheme 14

Reagents and conditions: (i) 1,3-Dibromopropane, K_2CO_3 , CH_3CN , 48 h, reflux; (ii) N-Methylpiperazine, CH_3CN , μW , 30 min, 140 $^{\circ}C$; (iii) $H_2/Pd/C$, MeOH, 12 h, RT; (iv) **55**, TFA, TFE, 48 h, reflux.

Table 13 summarises the results of the biological evaluation of compounds **88-95**.

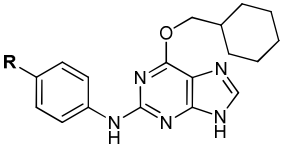
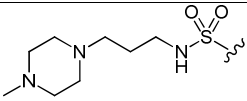
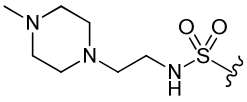
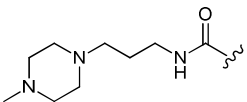
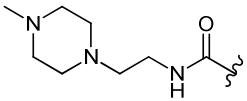
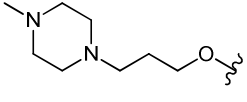
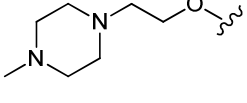
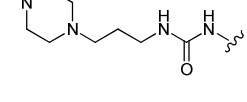
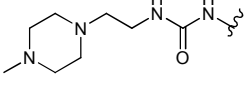
		CDK-inhibitory activity (IC ₅₀ μM)	
R	Code	CDK2	CDK7
	91	0.012	0.75
	90	0.027	0.67
	93	0.35	0.38
	92	0.38	0.23
	95	0.52	0.74
	94	0.63	0.37
	89	0.71	0.52
	88	0.64	0.52

Table 13

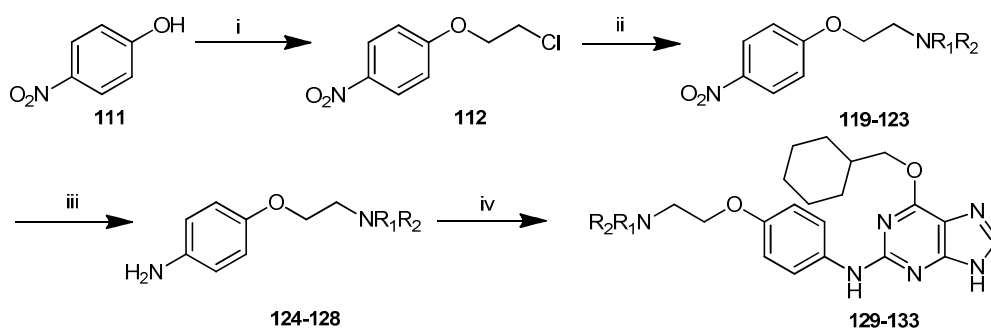
CDK-inhibitory activity for compounds **88-95**

These results showed that for analogues of NU6247 (**44**) where the purine scaffold and the piperazine side-chain are retained, and the sulfone linker and 2-carbon spacer are varied, CDK-inhibitory activity was essentially unaffected with only minor changes in the IC_{50} values, that range from 230 nM (**92**) to 740 nM (**95**). The sulfonamide linker (**90** and **91**) confers high potency and selectivity (~45-fold) for CDK2 over CDK7. This was in keeping with the selectivity profile exhibited by NU6102 (**31**), and the IC_{50} values for compounds **90** and **91** (670 and 750 nM respectively), showed that the introduction of the NU6247 sidechain does not appreciably increase selectivity for CDK7.

No compound in **Table 13** was highly selective for CDK7, although a 2-fold selectivity is observed for compound **94**. However, as no other compound to date exhibited selectivity for CDK7 over CDK2, further studies with **94** were undertaken. In an attempt to further improve activity and selectivity for CDK7, a small library of compounds was synthesised where the ether linker and terminal amine were varied in order to determine structure-activity relationships around the sidechain of **94**.

4.4 Synthesis of analogues of 94

Five analogues of purine **94** were synthesised in which the ether linker was maintained and the amine was varied (**Scheme 15**).



Scheme 15

Reagents and conditions: (i) 1,2-Dichloroethane, K_2CO_3 , CH_3CN , 48 h, reflux; (ii) R_1R_2NH , CH_3CN , 30 min, 140 °C, MW; (iii) $H_2/Pd/C$, MeOH, 24 h, RT; (iv) **55**, TFA, TFE, 48 h, reflux.

As described above, reaction of commercially available *p*-nitrophenol (**111**) with 1,2-dichloroethane gave **112**. The primary alkyl chloride underwent substitution by a range of amines (dimethylamine, pyrrolidine, piperidine, morpholine and benzylamine) and the products obtained (**119-123**) were hydrogenated to yield the corresponding anilines (**124-128**). These were reacted with fluoropurine **55** under TFA/TFE conditions to yield the final products **129-133**, which were tested for inhibitory activity against CDK2 and CDK7 (**Table 14**).

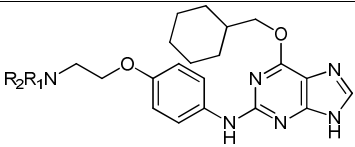
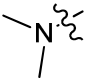
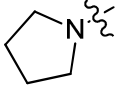
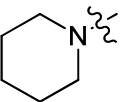
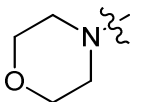
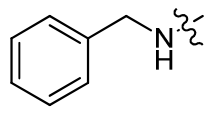
		CDK-inhibitory activity (IC ₅₀ μM)	
NR ₁ R ₂	Code	CDK2	CDK7
	129	0.85	0.42
	130	0.92	0.32
	131	0.96	0.27
	132	1.6	0.94
	133	2.6	0.56

Table 14

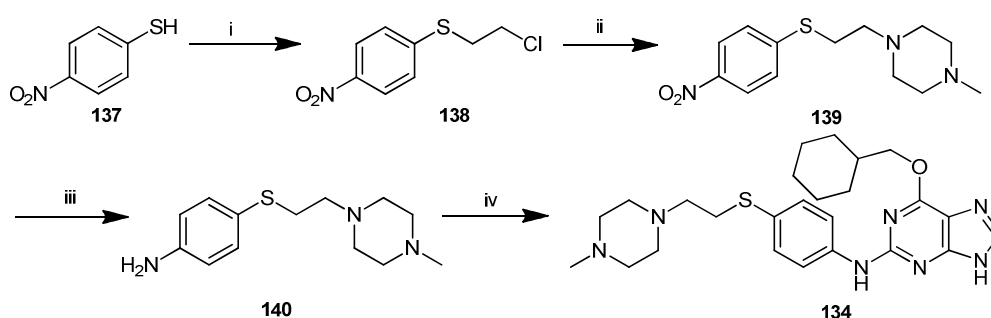
CDK-inhibitory activity for compounds **129-133**

As shown in **Table 14**, compounds **129-133** exhibited similar activity to **94** (IC_{50} (CDK2) = 630 nM, IC_{50} (CDK7) = 370 nM), with all of the compounds being approximately 2-fold selective for CDK7. The best results were obtained in the case of compounds **130** and **131** (3-fold selective). Interestingly, replacing the piperidine group by a morpholine (**132**) diminished activity compared with the parent compound (**94**).

For compound **133**, the introduction of a benzyl group decreased CDK2-inhibitory activity more than for CDK7, and the compound was some 4-fold selective for CDK7. A comparison of this result with those obtained for the *N*-arylpiperazines **49-52** discussed earlier suggests that conformational constraint to the side-chain might play a role in the activity of these particular inhibitors, and this will be discussed in more detail subsequently.

As a further modification of **94**, three compounds were synthesised where the terminal piperazine function was retained, but the ether linker was replaced by isosteres (thioether (**134**), amine (**135**) and methylene (**136**)).

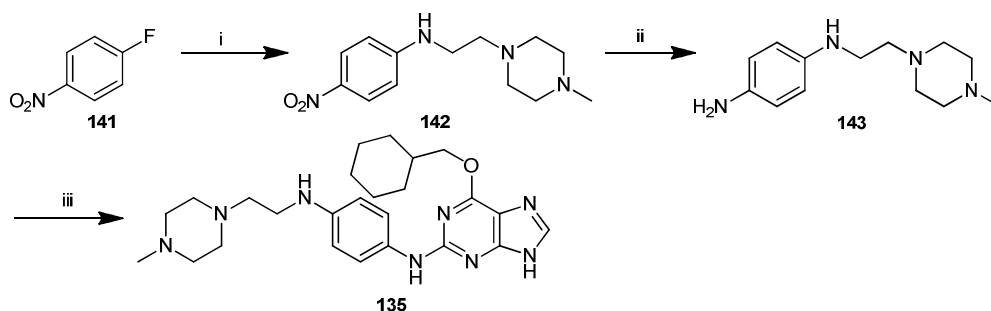
Thioether **134** was synthesised according to a procedure similar to that employed for the synthesis of **94** (**Scheme 16**). Thus, *p*-nitrothiophenol (**137**) was converted into **138** by reaction with 1,2-dichloroethane. The primary chloride **138** was then subjected to nucleophilic substitution by *N*-methylpiperazine yielding compound **139**, which was reduced to the aniline (**140**) and coupled with **55** to furnish the required purine **134**.



Scheme 16

Reagents and conditions: (i) 1,2-Dichloroethane, K_2CO_3 , CH_3CN , 48 h, reflux; (ii) *N*-methylpiperazine, CH_3CN , 30 min, 140 °C, MW; (iii) $H_2/Pd/C$, MeOH, 24 h, RT; (iv) **55**, TFA, TFE, 48 h, reflux.

The amine analogue **135** was synthesised from commercially available *p*-nitrofluorobenzene (**141**) following the steps outlined in **Scheme 17**. Compound **141** was reacted with 2-(4-methylpiperazin-1-yl)ethanamine, affording **142**, which was converted into the aniline **143** and then coupled to **55**, yielding compound **135**.



Scheme 17

Reagents and conditions: (i) 2-(4-methylpiperazin-1-yl)ethanamine, CH₃CN, 30 min, 140 °C, MW; (ii) H₂/Pd/C, MeOH, 24 h, RT; (iii) **55**, TFA, TFE, 48 h, reflux.

The analogue **136** was synthesised from commercially available 3-chloropropylbenzene (**144**) (**Scheme 18**). The first step entailed introduction of a nitro group at the 4-position of the aromatic ring, which was performed with a standard mixture of nitric acid and sulfuric acid (2:1)¹⁸⁰ and proceeded in 70% yield. The unwanted *ortho*-nitro isomer was separated from the desired product **145** by column chromatography. Compound **145** underwent substitution at the primary chloride to yield compound **146**, which was reduced to the aniline **147**. Final coupling with **55** afforded the target purine **136**.



Compounds **137-139** were tested for CDK-inhibitory activity and the results are shown in **Table 15**.

Table 15

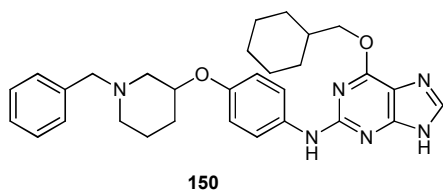
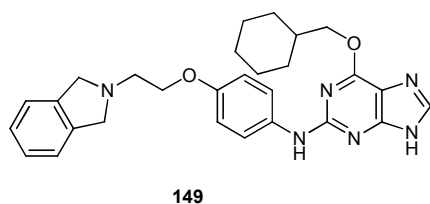
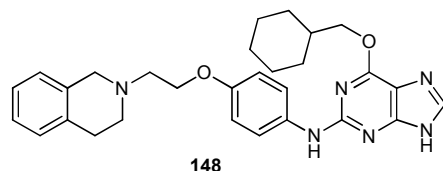
The activity of compounds **134-136** (**Table 15**) does not notably differ from that of the parent purine **94**, and the alternative linkers offer no evident advantage over the ether. The result for **136** suggests that no hydrogen bond acceptor (O, S) or donor (NH) function is needed at this position of the sidechain, and that activity depends on

the terminal basic centre(s), as exemplified by the cyclohexylethyl analogue **186** discussed in the next chapter.

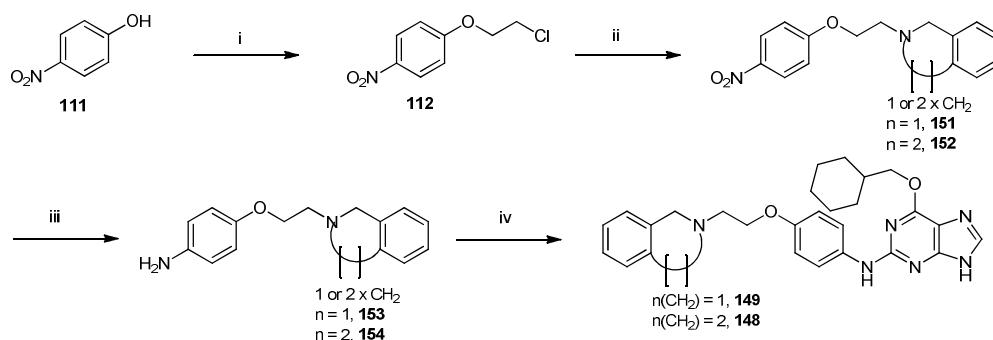
The results obtained for compound **133** posed an interesting question when compared with those of compounds **49-52**, described at the beginning of this chapter. The reduced activity of **49-52** with respect to the parent compound NU6247 (**44**) was ascribed to the relatively bulky sidechain. The sidechain of compound **133**, however, appears to match that of **49** in length, and yet **133** is 60-fold more potent than **49** against CDK7.

One possible explanation for this observation may reside in the rigidity and/or directionality of the sidechain of these compounds. Compound **49** incorporates a piperazine ring which adds an element of conformational constraint to the sidechain, and this may influence the direction in which the terminal aromatic ring is oriented within the ATP-binding domain of CDK7.

To test this hypothesis, conformationally constrained derivatives **148-150** were proposed as synthetic targets.



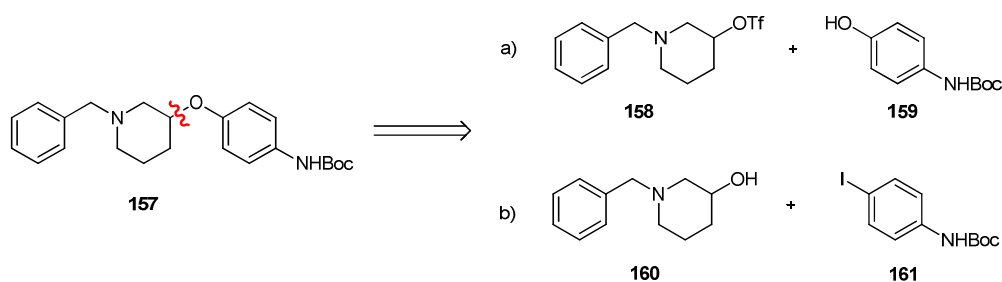
Compounds **148** and **149** were prepared according to a synthetic strategy analogous to that previously employed for the synthesis of the parent compound **94** (Scheme 19).



Scheme 19

Reagents and conditions: (i) 1,2-Dichloroethane, K_2CO_3 , CH_3CN , 48 h, reflux; (ii) 1,2,3,4-Tetrahydroisoquinoline or isoindoline, CH_3CN , 30 min, 140 °C, MW; (iii) $H_2/Pd/C$, MeOH, 24 h, RT; (iv) **55**, TFA, TFE, 48 h, reflux.

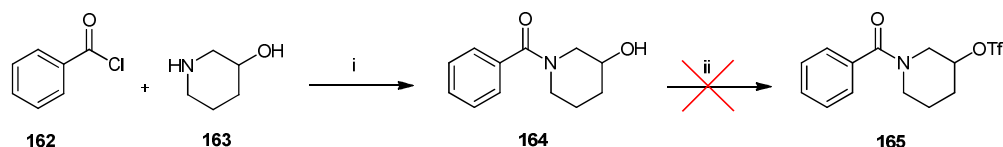
To approach **150** as a synthetic target, a retrosynthetic strategy involving the disconnection of the sidechain C-O bond was originally considered (Scheme 20).



Scheme 20

C-O bond disconnection approaches to compound **157**.^{181,182}

Strategy a) required the synthesis of secondary triflate **158**. This was undertaken starting from benzoyl chloride (**162**) and 3-hydroxypiperidine (**163**) which were reacted under standard conditions to generate amide **164**. Triflation of this precursor was subsequently attempted as a model reaction (**Scheme 21**).



Scheme 21

Reagents and conditions: (i) TEA, CH₂Cl₂, 10 min, 0 °C; (ii) See **Table 16**.

Triflating agent/conditions	Result
Tf ₂ O, TEA, CH ₂ Cl ₂ , 0 °C	Complex reaction mixture
N-phenyl bis-triflamide, K ₂ CO ₃ , THF, RT	
Tf ₂ O, TEA, CsCO ₃ , CH ₂ Cl ₂ , 0 °C	
Tf ₂ O, pyridine, CH ₂ Cl ₂ -20 °C	

Table 16

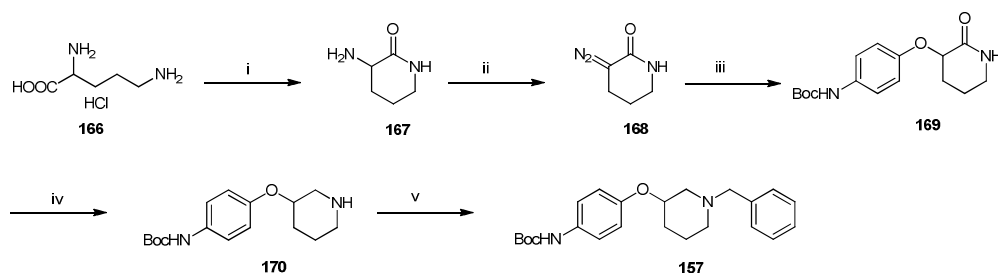
Attempted conditions for the generation of secondary triflate **165** in **Scheme 21**

Unfortunately, triflate **165** could not be synthesised and all attempts resulted in the isolation of complex fluorinated decomposition products (¹⁹F NMR evidence). ¹H NMR analysis of the crude reaction mixture showed evidence for possible elimination of the triflate to give an alkene derivative.

Approach b) involved a copper-catalysed coupling reaction between an unprotected secondary alcohol (**160**) and an aryl iodide (**161**). The reaction was attempted with **161** and **164** using copper iodide and tetramethylphenanthroline as catalysts, but no coupling was observed to take place, even after 24 h at 100 °C.

Following the failure of both strategies, an alternative synthetic scheme was devised where the 2-alkoxypiperidine moiety was synthesised from ornithine hydrochloride ¹⁸³ (**Scheme 22**). Ornithine hydrochloride (**166**) was cyclised to amide **167**.

Diazotisation of **167** with isoamyl nitrite afforded compound **168** which was coupled with **159** using rhodium acetate dimer as catalyst. The amide functionality of **169** was subsequently converted into an amine (**170**) which was coupled with benzaldehyde in the presence of phenylsilane and dibutyltin dichloride affording compound **157**.



Scheme 22

Reagents and conditions: (i) NaOH, alumina, H₂O/Toluene, reflux, Dean-Stark; (ii) isoamyl nitrite, AcOH, CHCl₃, reflux; (iii) *tert*-butyl (4-hydroxyphenyl)carbamate (**159**), [Rh(CH₃CO)₂]₂, THF, RT; (iv) LiAlH₄, THF, 0 °C to RT; (v) PhCHO, PhSiH₃, Bu₂SnCl₂, THF, 100 °C, MW.¹⁸⁴

Compound **157** was coupled to **55** under TFA/TFE conditions, yielding target compound **150** as a racemate. The results of the biological evaluation of compounds **148-150** are shown in **Table 17**.

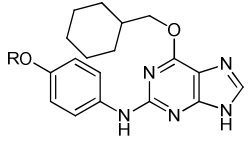
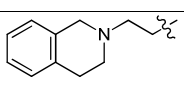
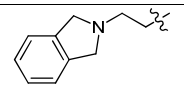
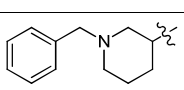
		CDK-inhibitory activity (IC ₅₀ μM)	
R	Code	CDK2	CDK7
	148	2.6	1.8
	149	1.3	1.5
	150	1.9	0.9

Table 17

CDK-inhibitory activity for compounds **148-150**

Conformationally constrained purines **148-150** exhibited IC_{50} values against both CDK2 and CDK7 intermediate between those obtained for compounds **49** and **133**. This indicates that conformational constraint in the sidechain does play a role in the binding mode of these molecules within the CDK2 and CDK7 active sites, but it appears that none of the ring systems employed in compounds **49**, **148-150** provides the optimal directionality, and the parent compound **133** remained the one with the best activity and selectivity for CDK7.

Chapter 5 – Pharmacophore mapping and scaffold hopping around NU6247 (44)

5.1 Pharmacophore mapping around NU6247 (44)

The results described in the previous chapter addressed the problem of determining SARs for CDK7 inhibition by modifying the sidechain of NU6247 (44). The compounds synthesised permitted a number of valuable observations to be made, but failed to identify a strong correlation between the nature of the sidechain moieties and CDK7 binding affinity.

In order to broaden the scope of the SARs around NU6247 (44), some analogues were synthesised where identifiable pharmacophores in NU6247 (44) (**Figure 40**) were systematically varied. It was hoped that these studies would result in the identification of the structural parameters necessary for CDK7-inhibitory activity.

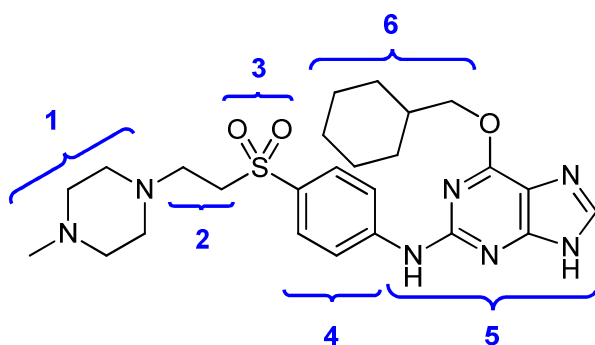


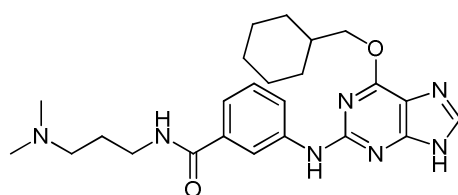
Figure 40

Pharmacophore mapping for NU6247 (44). 1, pendant basic functionality; 2, 2-carbon chain spacer; 3, sulfone linker; 4, aromatic ring; 5, purine core pharmacophore; 6, 6-cyclohexylmethoxy substituent.

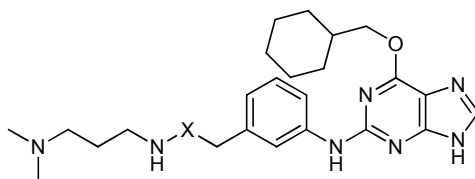
In the following section, the importance of each of the pharmacophores identified in **Figure 40** for CDK7-inhibitory activity is discussed.

5.1.1 Benzyl sulfone analogue of NU6247 (**44**)

As stated in the introductory paragraph of this chapter, the rationale for the development of a pharmacophore mapping profile around NU6247 (**44**) was to identify structural features that maintain or improve CDK7-inhibitory activity but diminish or abolish CDK2-inhibitory activity. For a small series of compounds previously synthesised within the research group, the following results were obtained:



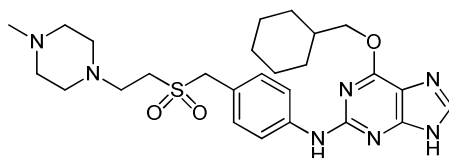
171, IC₅₀ CDK2 = 470 nM



172, X = SO₂, IC₅₀ CDK2 = 530 nM

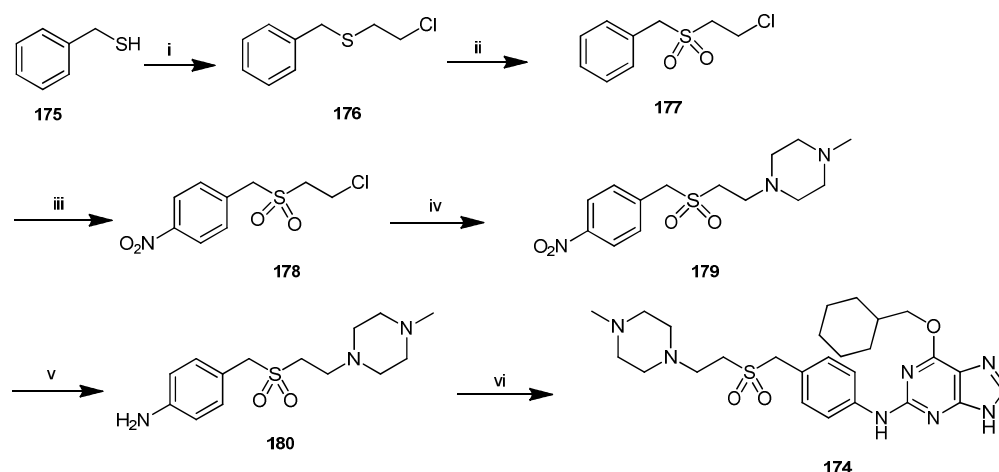
173, X = CO, IC₅₀ CDK2 = 1 μM.

Although the compounds were originally prepared as potential inhibitors of a different kinase, interestingly, the introduction of a CH₂ between the carbonyl (or sulfonyl) group and the aromatic ring reduced potency against CDK2 with respect to the parent compounds. As a result of these observations, it was reasoned that introducing an extra methylene between the aromatic ring and the sulfone moiety in NU6247 (**44**) may diminish potency against CDK2 but not against CDK7. Therefore, homologue **174** was synthesised.



174

Purine **174** was synthesised starting from benzyl mercaptan (**175**) according to the procedure outlined in **Scheme 23**.



Scheme 23

Reagents and conditions: (i) 1,2-Dichloroethane, K_2CO_3 , CH_3CN , 48 h, reflux; (ii) *m*CPBA, CH_2Cl_2 , 24 h, RT; (iii) HNO_3/H_2SO_4 , 3 h, 0 °C to RT; (iv) *N*-methylpiperazine, CH_3CN , 30 min, 140 °C, MW; (v) $H_2/Pd/C$, MeOH, 24 h, RT; (vi) **55**, TFA, TFE, 48 h, reflux.

Alkylation of **175** with 1,2-dichloroethane in the presence of potassium carbonate afforded compound **176**, which was oxidised to the corresponding sulfone with *m*CPBA. Nitration conditions analogous to those utilised for the preparation of **149** were employed to convert **177** into the nitro derivative **178**. Microwave-assisted nucleophilic substitution to yield compound **180**, reduction of the nitro functionality and coupling to **55** afforded the final compound (**174**).

Compound **174** was tested against CDK2 and CDK7 and the IC_{50} values were 400 nM and 800 nM, respectively. The selectivity profile was thus the same as for NU6247 (**44**) (2-fold selective for CDK2) although compound **174** was 4-fold less potent than **44**. This suggests that the binding mode within CDK2 and CDK7 of compound **174** is essentially the same as for **44**, and if introducing the extra CH_2 is responsible for decreased activity against CDK2, this modification has the same effect on CDK7.

5.1.2 Removing the O⁶-substituent from NU6247 (44)

Early structural biology studies with NU6102 (**31**) bound within the ATP-binding pocket of CDK2 showed that, in addition to the usual triplet of hydrogen bonds with the hinge region (Glu81, Leu83), hydrophobic interactions were made by the cyclohexyl ring with an apolar pocket in the glycine-rich loop (residues 9-19), especially with Gly11 and Val18.⁴³ This binding mode was found to be conserved among all the purine- and pyrimidine-based CDK2 inhibitors synthesised.

The co-crystal structure of CDK2 in complex with NU6247 (**44**) (see **Figure 35** in **Chapter 3**) showed a similar binding mode, with the cyclohexylmethyl group binding in the same pocket for both compounds within the ATP-binding site.

In the absence of a co-crystal structure of CDK7 with an inhibitor, in the early stages of this project it was assumed that NU6102 (**31**) (IC₅₀ CDK7 = 4.82 µM) and NU6247 (**44**) interacted with the ribose-binding pocket of CDK7 and CDK2 in a similar manner. The glycine loop of CDK7 shares a 66% sequence identity with CDK2, with 6 out of 9 residues being conserved, including the key residues Gly11, Gly13 and Val18.¹³⁸

Supporting evidence for the hypothesis that the cyclohexylmethyl group at the 6-position of the purine makes important interactions within the ribose-binding pocket of CDK7 was provided by **181** and **182**, two urea compounds synthesised within the research group and tested against CDK7. Urea **181** shows a selectivity profile not unlike **88** and **89**, but **182**, where the substituent at the 6-position of the purine has been removed, is more than 100-fold less active against CDK2 and CDK7. The results are summarised in **Table 18**.

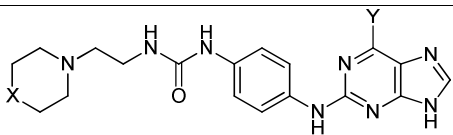
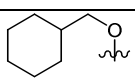
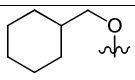
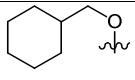
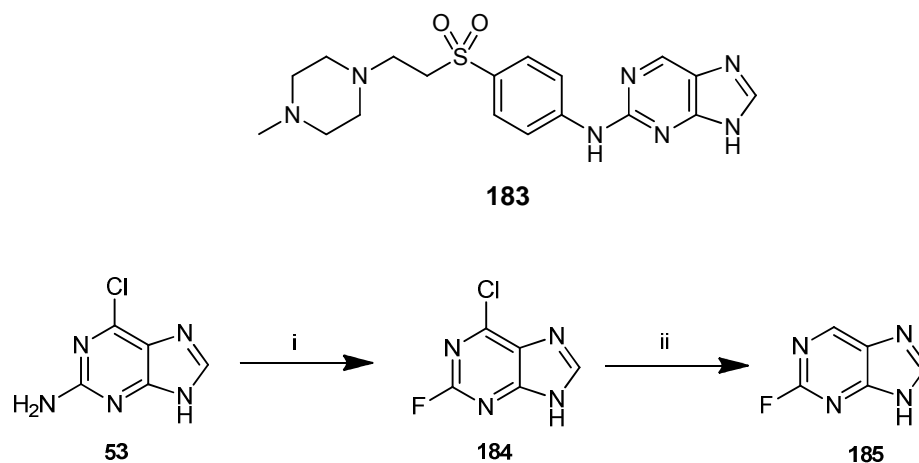
			CDK-inhibitory activity (IC ₅₀ μM or percentage of inhibition at 100 μM)	
X	Y	Code	CDK2	CDK7
NMe		89	0.64	0.52
O		88	0.71	0.52
CH ₂		181	0.86	0.45
CH ₂	H	182	30%	64.6

Table 18

CDK-inhibitory activity for compounds **88**, **89**, **181** and **182**

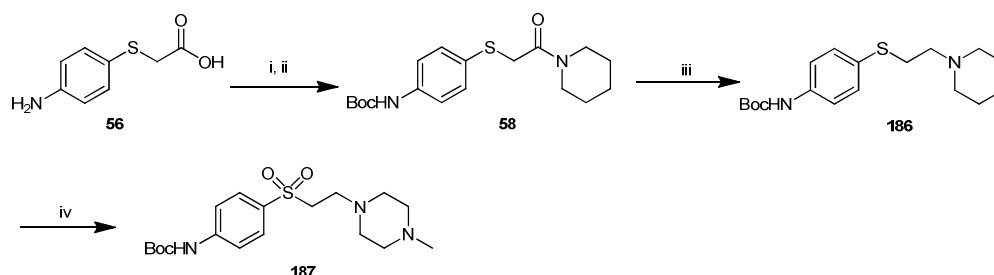
Definitive evidence of the importance of the O⁶-cyclohexylmethyl substituent in NU6247 (**44**) and related CDK7 inhibitors could potentially be provided by the 6-unsubstituted analogue (**183**), which was therefore identified as a target molecule.



Scheme 24

Reagents and conditions: (i) HBF₄, NaNO₂, H₂O, 75 min, RT; (ii) HCOONH₄, Pd(OH)₂, MeOH, 3 h, reflux.

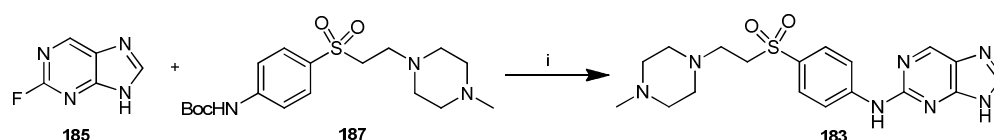
2-Amino-6-chloropurine (**53**) was converted into 2-fluoro-6-chloropurine (**184**) using standard Balz-Schiemann conditions.¹⁸⁵⁻¹⁸⁶ Removal of the 6-chloro substituent was achieved by Pd-catalysed hydrogenation, affording **185**, the 6-unsubstituted analogue of **55** (Scheme 24).



Scheme 25

Reagents and conditions: (i) Boc_2O , TEA, Dioxane/ H_2O , 24 h, RT; (ii) SOCl_2 , piperidine, THF, 24 h, RT; (iii) LiAlH_4 , THF, 24 h, 0 °C to RT; (iv) mCPBA, N-methylpiperazine, CH_2Cl_2 , 24 h, RT.

To achieve the synthesis of **183** from **185**, compound **187** was required. This arylsulfone was synthesised from commercially available 2-(4-aminophenylthio)acetic acid (**56**) using a synthetic sequence analogous to that employed for the synthesis of NU6247 (**44**) and analogues (Scheme 25, see Chapter 4).



Scheme 26

Reagents and conditions: (i) TFA, TFE, 24 h, reflux.

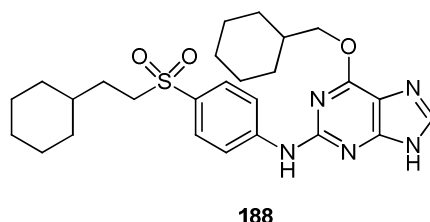
As a final step, **185** and **187** were mixed in TFE containing TFA, under which conditions the Boc group of **187** was removed and the aniline thus generated *in situ* reacted with **185** to afford the required purine derivative **183** (Scheme 26).

Compound **183** was tested against CDK2 and CDK7 and the IC₅₀ values were 46.9 μ M and 20.8 μ M, respectively. The values obtained showed a 400-fold decrease in potency against CDK2 and a 100-fold decrease in potency against CDK7 with respect to NU6247 (**44**). The effect of removing the C⁶-substituent appears to be more pronounced in the case of CDK2, but nonetheless this drastic modification is not tolerated by either CDK2 or CDK7.

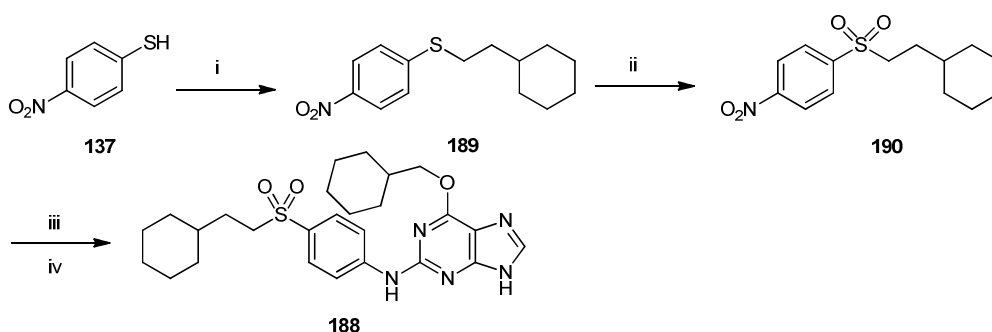
5.1.3 Removing the terminal basic moiety of NU6247 (**44**)

Another prominent functional group identified in **Figure 40** is the terminal piperazine ring. All CDK7 inhibitors synthesised to date contain a basic sidechain, which may be a desirable feature for providing water solubility. Lack of information on the binding interactions made by the basic moiety within CDK7, however, required further investigation into the usefulness of this group.

Compound **188**, including a sidechain the same size as NU6247 (**44**) but lacking the basic centres, was therefore identified as a synthetic target:



The synthesis of purine **188** is outlined in **Scheme 27**. *p*-Nitrobenzenethiol was heated in the presence of base and the resulting thiolate coupled *in situ* with cyclohexylethyl bromide. The sulfide moiety was oxidised to sulfone **190** using *m*CPBA, and the nitro moiety reduced to the aniline prior to coupling with **55** under TFA/TFE conditions.



Scheme 27

Reagents and conditions: (i) Cyclohexylethyl bromide, K_2CO_3 , CH_3CN , reflux; (ii) mCPBA, CH_2Cl_2 , RT; (iii) $H_2/Pd/C$, MeOH, RT; (iv) **55**, TFA, TFE, 24 h, reflux.

Compound **188** was tested for CDK2 and CDK7 activity and found to be essentially inactive (11% inhibition at 10 μM for CDK2 and 13% inhibition at the same concentration for CDK7). These results are in line with the values obtained for the 'bifurcated' analogues described in the previous chapter, with which compound **188** shares the essential properties of the sidechain. A pendant cyclohexyl ring is detrimental for CDK7-inhibitory activity and a terminal basic moiety is essential for the sidechain to interact effectively with the specificity pocket of the kinase.

5.1.4 Replacement of the sulfone linker of NU6247 (**44**)

Systematic replacement of the sulfone linker by a number of isosteres was carried out as part of the investigation of analogues of **94** discussed in **Chapter 4** (see **Tables 13** and **15**). In particular, the result obtained for compound **136** in **Table 15** demonstrated that the sulfone linker was not an essential pharmacophore of NU6247 (**44**) and that its removal and replacement by a CH_2 group was not detrimental to activity.

5.1.5 Introducing a substituent at the purine 8-position of NU6247 (44)

As discussed in **Chapter 3**, crystal structures of CDK2 in complex with purine-based inhibitors (NU6102 (**31**) and NU6247 (**44**), **Figure 36**, NU2058 (**32**), **Figure 35**)¹⁶⁴ indicated that the purine C⁸-position is directed towards the gatekeeper residue Phe80 within the ATP-binding domain.⁴³

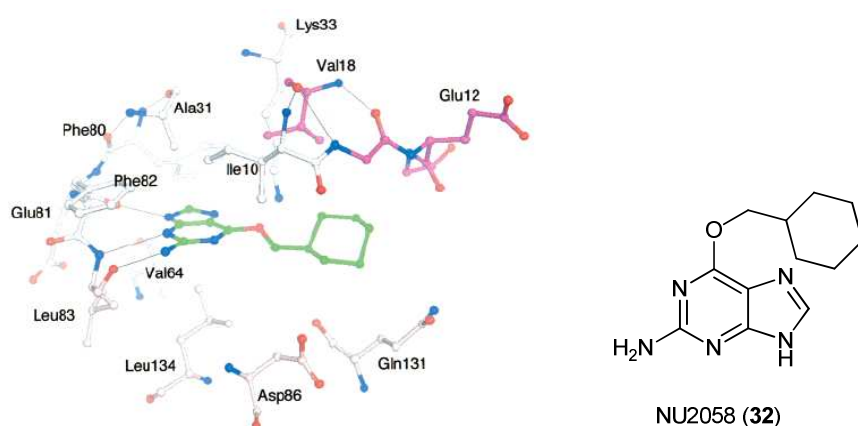


Figure 41

NU2058 (**32**) bound within the ATP binding pocket of CDK2.¹⁶⁴

It has been observed that C⁸-substituted purine-based CDK2 inhibitors tend to adopt a 'flipped' binding mode within the active site (**Figure 42**). In the 'normal' binding orientation seen in **Figure 41**, the isopropyl substituent of **191** would sterically clash with Phe80 and therefore the binding orientation is reversed, allowing for the expansion of the purine C⁸-substituent into the specificity pocket of the enzyme.

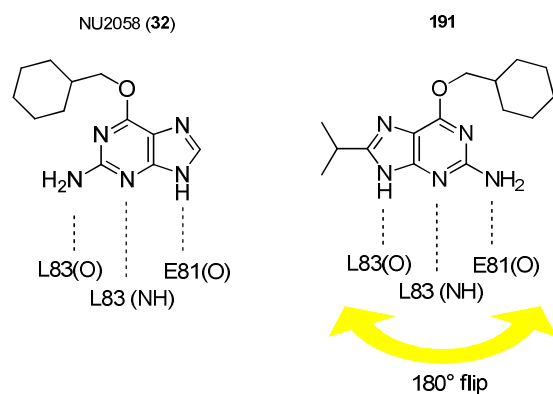


Figure 42

The binding mode of NU2058 (**32**) and of its C⁸-cyclopropyl derivative (**191**) within the ATP binding pocket of CDK2.

The data published regarding the crystal structure of CDK7 in complex with ATP ¹³⁸ show that the gatekeeping residue in CDK7 is also a phenylalanine (Phe91) (**Figure 43**).

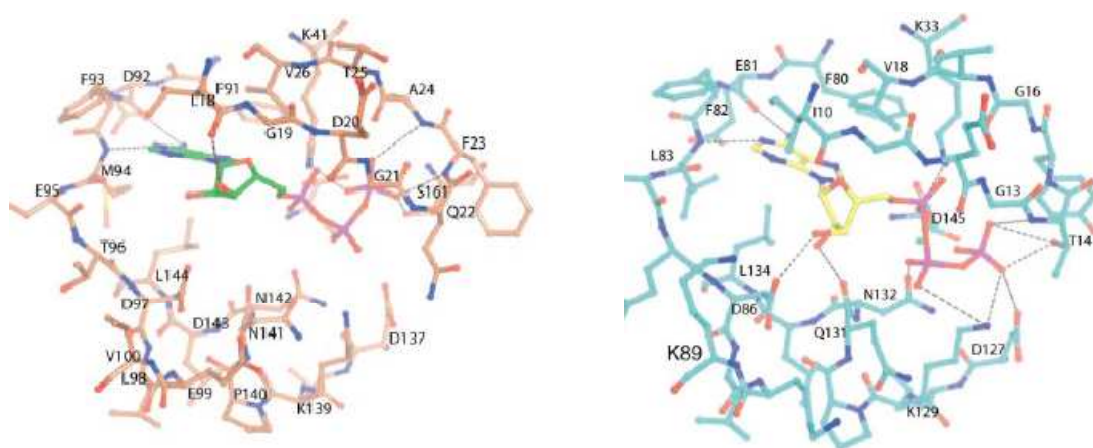
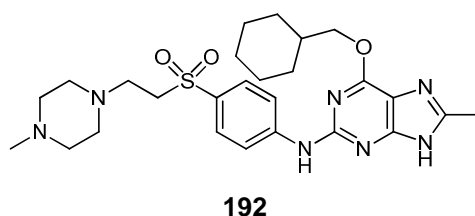


Figure 43

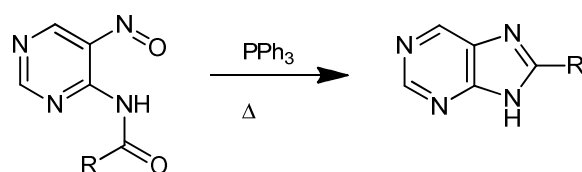
ATP bound within the active site of CDK7 (left) and CDK2 (right). ¹³⁸

To probe the area around Phe91 in CDK7 and to determine whether or not substitution at the C⁸-position of the purine would be tolerated in the case of CDK7 inhibitors, a C⁸-methylpurine analogue of NU6247 (**44**) was synthesised (**192**).



The initial choice of a methyl substituent for the C⁸-position was based on the assumption that a smaller group than isopropyl will not trigger flipping of the inhibitor with subsequent expulsion from the binding pocket. This is because it is expected that the side-chain of **44** will not be tolerated on account of its size should the inhibitor flip 180° within the pocket.

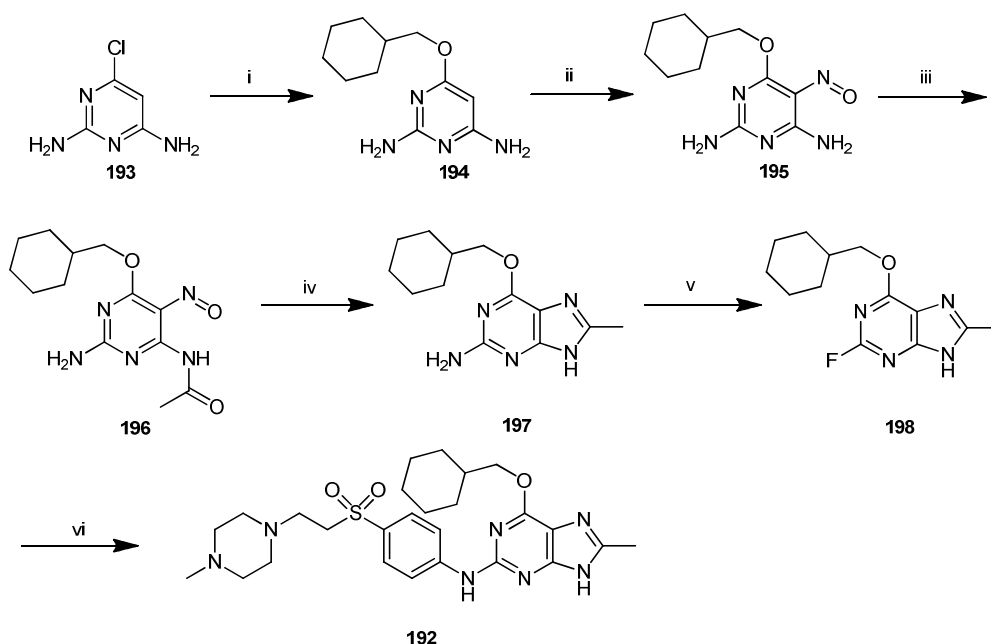
To approach **192** as a synthetic target, the Pfeleiderer variant of the Traube synthesis of purines was selected as the best strategy. The Traube synthesis of purines¹⁸⁷ is based on the cyclisation of 5,6-diaminopyrimidine to purine when reacted with formic acid. The Pfeleiderer variant of this synthesis¹⁸⁸⁻¹⁸⁹ employs 5-nitroso-6-acylaminopyrimidine, which is ring-closed *via* an intramolecular aza-Wittig reaction in the presence of triphenylphosphine. This approach allows the synthesis of purines with a wide variety of substituents at the C⁸-position depending on the starting acyl group introduced at the 6-amino position (**Scheme 28**).



Scheme 28

General cyclisation of 6-acylamino-5-nitrosopyrimidine into an 8-substituted purine.

Scheme 29 shows the synthetic route adopted to synthesise target compound **192** from 2,6-diamino-4-chloropyrimidine (**193**).



Scheme 29

Reagents and conditions: (i) Cyclohexylmethanol, Na, 3 h, 180 °C; (ii) NaNO₂, AcOH, 40 min, 80°C ; (iii) Ac₂O, 30 min, 80°C; (iv) PPh₃, *o*-xylene, 48 h, reflux; (v) HBF₄, LiBF₄, NaNO₂, H₂O, 0 °C to RT, 24 h; (vi) **187**, TFA, TFE, 48 h, reflux.

Pyrimidine **193** was reacted with sodium cyclohexylmethoxide in cyclohexylmethanol and converted into 2,6-dichloro-4-cyclohexylmethoxypyrimidine (**194**). Pyrimidine **194** was nitrosated at the 5-position and then selectively monoacetylated at the 6-amino group, affording 2-amino-6-cyclohexylmethoxy-5-nitrosopyrimidin-4-ylacetamide (**196**). This compound was heated at reflux in *o*-xylene in the presence of triphenylphosphine to generate 2-amino-6-cyclohexylmethoxy-8-methylpurine **197**, which was converted into the 2-fluoro derivative (**198**) and coupled with **187** to give the final compound **192**.

Purine **192** was submitted for biological evaluation against CDK2 and CDK7, and found to be a poor inhibitor of CDK2 (47% inhibition at 100 μM). Since no C⁸-substituted purine tested at Newcastle until this point had contained a sidechain at the 2-position of the purine, it may be reasonable to infer that the presence of such a sidechain is not compatible with the ‘flipped’ binding mode adopted by compound **191**. However, **192** was found to be a respectable inhibitor of CDK7, with an IC₅₀

value of 5.3 μM . This compound was further evaluated against other members of the CDK family (CDK1, 2, 4, 5, 9), and found to be essentially inactive against all except CDK7. Purine **192** was further evaluated for growth-inhibitory activity against an MCF-7 human breast adenocarcinoma cell line and found to have a GI_{50} value of approximately 10 μM (**Figure 44**).

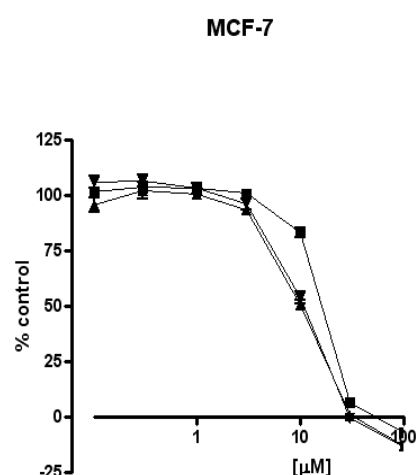
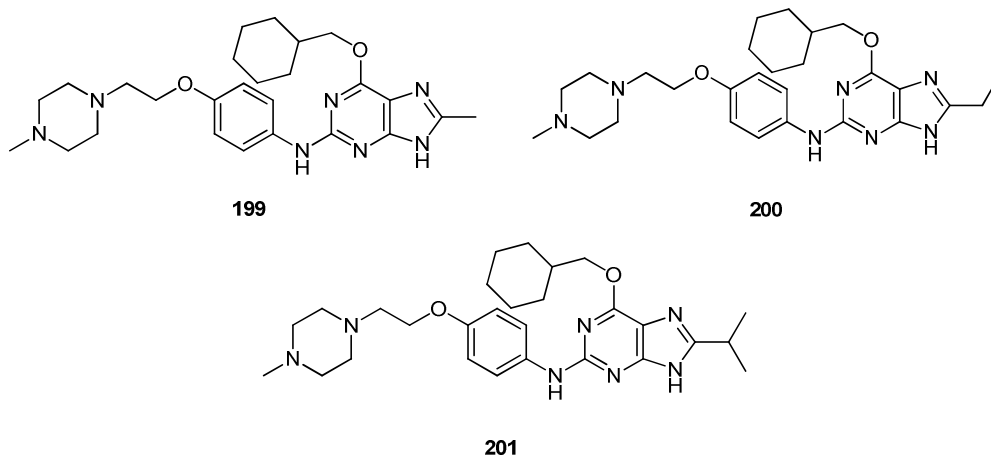


Figure 44

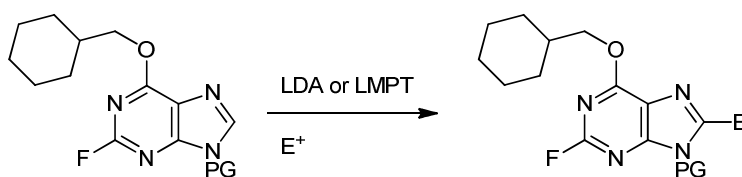
Growth inhibition of MCF-7 adenocarcinoma cell line by compound **192**.

While 10-fold less potent than the parent compound NU6247 (**44**), **192** is at least 20-fold more effective against CDK7 than CDK2 and such a difference in activity is most likely explained by a difference in the binding orientation within the active sites of the two enzymes. Without the aid of structural biology, this question may be addressed by the synthesis and biological evaluation of a small number of analogues of **195**, where either the sidechain or the C⁸-substituent of the purine are systematically modified. Compounds **199-201** were therefore identified as synthetic targets.



The sidechain at the 2-position of purines **199-201** was chosen for its ease of synthesis and has been a feature of a number of compounds since the identification of **94** as a 2-fold selective inhibitor of CDK7. The size of the substituent at the 8-position of the purine was increased from methyl (**199**) to ethyl (**200**) to isopropyl (**201**).

With a view to synthesising three closely related purine analogues, the strategy outlined in **Scheme 29**, successfully employed to synthesise **192**, was deemed inefficient. It was necessary to find a synthetic strategy for the preparation of compounds **199-201** *via* C⁸-alkylation of a common purine intermediate. Therefore an approach based on a metal-mediated C-C bond-forming reaction was investigated (**Scheme 30**).¹⁹⁰



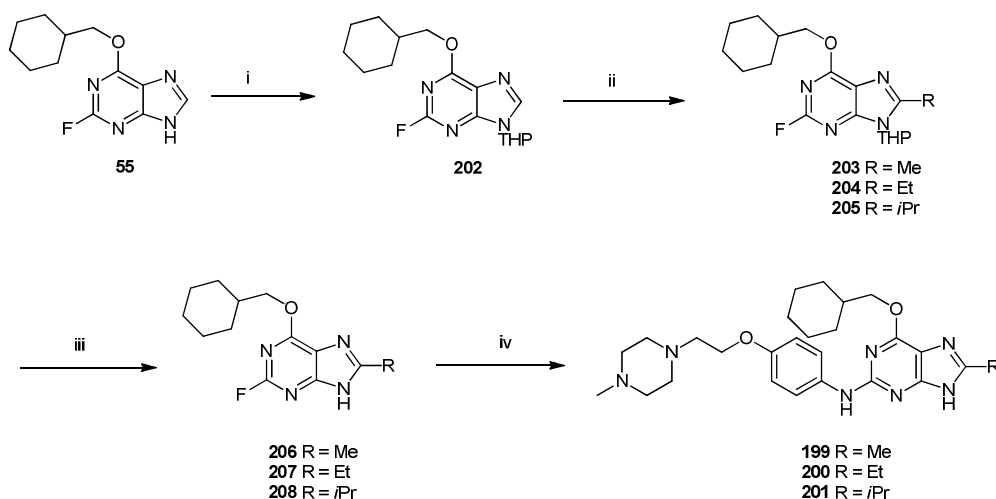
Scheme 30

Lithium-mediated C⁸-alkylation of a purine; E⁺ = electrophile.

Carbon substituents have been successfully introduced at the 2-, 6- and 8-position of a purine *via* metal-mediated reactions employing a number of conditions.¹⁹¹ In the

case of 6-halo-*N*⁶-protected purines, LDA- and LTMP-mediated lithiation occurs selectively at the 8-position over the 2-position when both are unsubstituted,¹⁹² and the lithiated product can subsequently react with electrophiles to generate a variety of 8-substituted purines. In the case of 8-methylation with methyl iodide in the presence of excess base, the methyl carbon at the 8-position is liable to further deprotonation and reacts with excess MeI to generate 8-ethyl- and 8-isopropylpurines.¹⁹³⁻¹⁹⁴

Taking all of the above into consideration, the synthetic approach outlined in **Scheme 31** was devised for the preparation of target compounds **198-201**.



Scheme 31

Reagents and conditions: (i) DHP, EtOH, 60 °C; (ii) *i*Pr₂EtN, *n*BuLi, MeI, -78 °C; (iii) TFA, *i*PrOH, H₂O, RT; (iv) **114**, TFA, TFE, 48 h, reflux.

The second step in **Scheme 31** was carried out initially with one equivalent each of LDA and MeI to obtain the 8-methyl purine **203**. Increasing the number of equivalents to two afforded the ethyl derivative **204** as the major product, while using three equivalents resulted in the isopropyl derivative **205** being the main product isolated. The three 2-fluoro-8-alkylpurines (**203-205**) thus generated were heated in aqueous isopropanol in the presence of TFA to remove the THP protecting group and then coupled to aniline **114** to generate the final target compounds **199-203**.

The results of the biological evaluation on compounds **192** and **199-201** against CDK2 and CDK7 are summarised in **Table 19**.

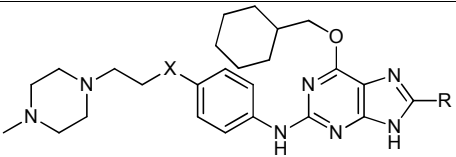
			IC ₅₀ μM or percentages of inhibition at 100 μM	
X	R	Code	CDK2	CDK7
SO ₂	Me	192	47%	5.3
O	Me	199	11.6	16.2
O	Et	200	45%	12.5
O	<i>i</i> Pr	201	41%	18.5

Table 19

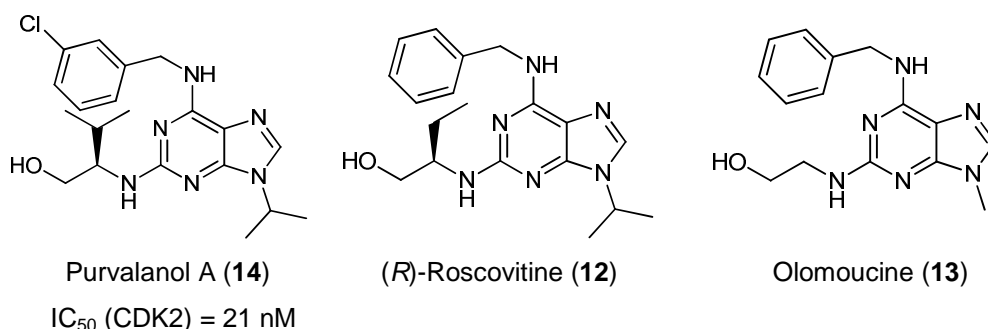
CDK-inhibitory activity for compounds **192**, **199-201**

With the exception of purine **199**, all compounds were essentially inactive against CDK2; compounds **199-201** were 2 to 3-fold less effective against CDK7 than **192**. These results were difficult to interpret: there is no apparent reason for compound **199** to be 3-fold less potent than **192** against CDK7 but 10-fold more potent against CDK2. The sidechain alone does not explain these results, as seen with NU6247 (**44**) and **94**. However, there clearly appears to be a difference in the binding mode of compounds **192** and **199-201** within the CDK2 and CDK7 active site, and it would seem that, unlike CDK2, the CDK7 ATP-binding site has the flexibility to accommodate substituents as large as isopropyl at the purine 8-position in the gatekeeper pocket.

5.2 Scaffold-hopping from ~~the literature~~published CDK7 inhibitors

5.2.1 The Purvalanol A analogue of NU6247

Purvalanol A (**14**) was identified by Gray *et al.* in 1998⁸⁵ as a result of screening numerous 2,6,9-trisubstituted purines against CDK2. The interest in the purine scaffold was motivated by olomoucine (**13**), which exhibits good selectivity for members of the CDK family over other kinases but only moderate inhibition ($IC_{50} = 7 \mu M$).^{53, 195-196} The binding mode of olomoucine within the ATP-binding site of CDK2 is rotated almost 160° relative to that of the aden osine ring of ATP. Thus, it seemed that the introduction of new substituents at the 2, 6, and 9 positions of the purine ring might lead to enhanced binding affinity and selectivity.⁸⁵



Crystal structure studies of **12** bound within the ATP-binding pocket of CDK2¹⁵⁹ showed hydrogen-bonding interactions of the purine with the same amino acids of the hinge region (Glu81, Leu83) as for the Newcastle inhibitors (e.g. **31**). However, the binding mode in this case is different, with the hydrogen atom at the 8-position of the purine **12** donating a hydrogen bond to Glu81, while Leu83 interacts with the purine N⁷ (*via* its backbone NH) and with the NH of the 6-anilino substituent (*via* its backbone carbonyl) (**Figure 45**).

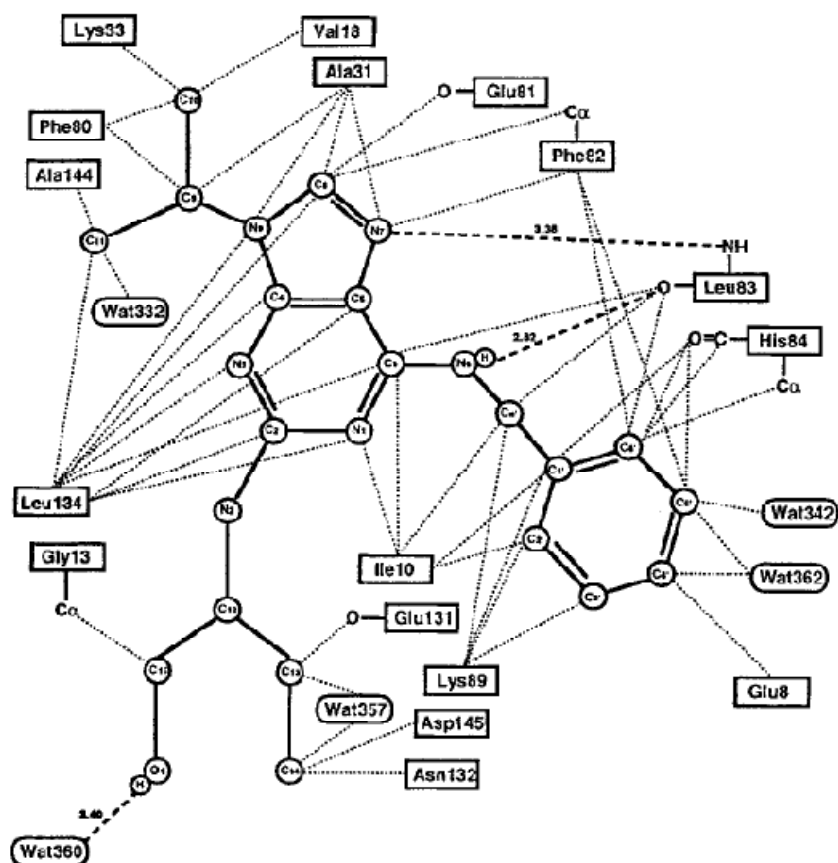


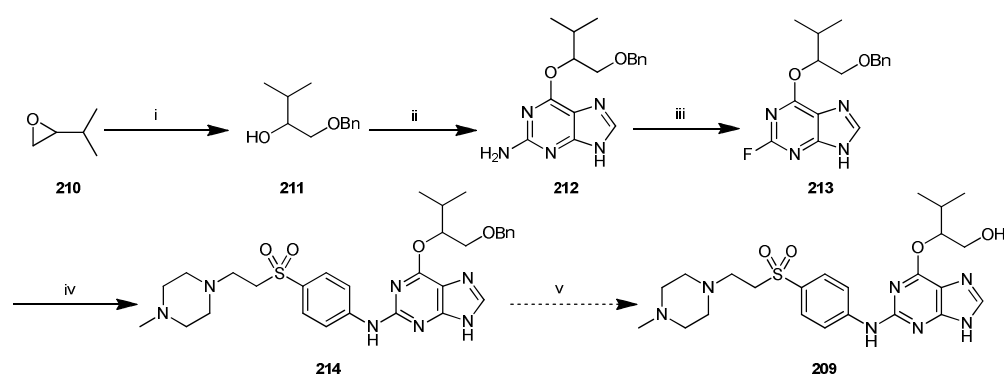
Figure 45

Schematic representation of (*R*)-roscovitine (**12**) bound within the CDK2 ATP-binding domain. ¹⁵⁸

As a result of this binding mode, the substituent at the 2-position of **12** binds into the ribose binding pocket, while the aniline substituent at the 6-position of the purine binds into the specificity pocket (Leu83-Asp86) with the terminal two carbons of the aromatic ring pointing out towards solvent. Analogous studies with **14** ⁸⁵ have shown similar results, and predictably, on account of the similar substitution pattern around the purine core pharmacophore, **14** binds to CDK2 in a similar orientation to the parent **12** (Figure 46).

To allow compound **209** to be prepared *via* the same synthetic approach already known to be suitable for the generation of 6-alkoxypurines,¹⁹⁷ 2-isopropyl-1,2-ethanediol was introduced at the purine 6-position instead of valinol. However, introducing an unsymmetrical diol at the 6-position of **209** posed problems of selectivity.

The route devised for the synthesis of **209** is shown in **Scheme 32**.



Scheme 32

Reagents and conditions: (i) BnOH, Na, 48 h, 180°C; (ii) **54**, NaH, DMSO, 48 h, RT; (iii) HBF₄, LiBF₄, NaNO₂, TFE/H₂O, 3 h, 0°C → RT; (iv) **187**, TFA, TFE, reflux, 48 h; (v) H₂/Pd/C, MeOH.

The ring opening of 2-isopropyloxirane (**210**)¹⁹⁸ proceeded smoothly to yield derivative **211**. This was reacted with 1-(2-amino-9H-purin-6-yl)-4-aza-1-azoniabicyclo[2.2.2]octane chloride (**54**) under previously developed conditions¹⁹⁹ to yield compound **212**.

Previously optimised conditions for the Balz-Schiemann reaction¹⁸⁵ proved unsuitable for the conversion of **212** into **213**, as **212** was not stable to the acidic reaction conditions and product **213** was isolated in extremely poor yields (<10%).

To render the reaction medium less acidic, an initial modification to the reaction conditions was to decrease the molar equivalents of HBF₄ used from 22 to 2. The remaining 20 equivalents of fluorinating agent reportedly required for the reaction to proceed were introduced by using lithium tetrafluoroborate. As a result, the approximate pH of the reaction mixture increased from 1 to 5.5, and under these conditions product **213** was isolated in 40% yield.

This yield was further improved by introducing TFE as a cosolvent after observing that **212** was poorly soluble in water. By performing the reaction in a 4:1 mixture of water and TFE, the yield was increased to 58%.

The studies performed towards optimisation of the third step in **Scheme 32** are summarised in **Table 20**. Yields are estimated from LCMS analysis of the crude reaction mixture.

HBF ₄	LiBF ₄	Solvent	Temp.	Time	Yield
22 eq	/	H ₂ O	0°C → RT	48 h	10%
22 eq	/	H ₂ O	0°C	3 h	15%
2 eq	20 eq	H ₂ O	0°C → RT	12 h	40%
2 eq	20 eq	H ₂ O	0°C	3 h	20%
2 eq	20 eq	H ₂ O/TFE 4:1	0°C → RT	3 h	58%

Table 20

Summary of reaction conditions employed for Balz-Schiemann fluorination of **212**.

Having established that the use of a cosolvent increased the yield of the Balz-Schiemann reaction, the conditions were considered satisfactory. Compound **213** was converted into **214** under standard TFA/TFE conditions. Removal of the benzyl protecting group, however, proved unexpectedly difficult. As shown in **Table 21**, catalytic hydrogenation was attempted under a variety of conditions, but the formation of compound **209** was not observed.

Catalyst/conditions (solvent: methanol)	Result
10% Pd/C	No reaction
Pd(OH) ₂	
10% Pd/C, H-cube: 60°C, room press.	
Pd(OH) ₂ , H-cube: 60°C, 30 bar → 60 bar	
10% Pd/C, H-cube: 60°C, 60 bar	
Pd(OH) ₂ , H-cube: 60°C, 60 bar	

Table 21

Summary of reaction conditions employed for catalytic hydrogenation of **214**.

Compound **214** was submitted for biological evaluation and was found to inhibit CDK2 with an IC₅₀ value of 5.6 μ M and CDK7 with an IC₅₀ value of 7.5 μ M. All attempts at synthesising compound **209** were subsequently abandoned.

5.2.2 The ‘Cyclacel’ analogue of NU6247 (**44**)

2-Anilino-4-(thiazol-5-yl)pyrimidines were identified by Wu *et al.*²⁰⁰ as CDK2 inhibitors using virtual screening methods. Wang *et al.* then developed the series⁸⁸ and discovered compound **36**, which was reported to be active against CDK family members with the values shown in **Table 22**.

Protein kinase	K _i (nM)
CDK1/Cyclin B	80 \pm 40
CDK2/Cyclin E	2 \pm 0.6
CDK4/Cyclin D1	53 \pm 5
CDK7/Cyclin H	70 \pm 10
CDK9/Cyclin T1	4 \pm 3

Table 22

Kinase inhibition for **36** against CDK family members.⁸⁸

Crystal structure studies of **36** bound within the CDK2 ATP-binding site⁸⁸ (**Figure 47**) revealed that the pyrimidine H⁴ donates a hydrogen bond to the Glu81 backbone carbonyl; the NH proton at the pyrimidine 2-position and the nitrogen atom at the 3-position form hydrogen bonds with the Leu83 backbone carbonyl and NH respectively.²⁷ The nitrophenyl moiety interacts with Gln131 via the nitro group and an alternative conformation is observed where a weaker interaction with Lys89 takes place. The thiazole ring binds within the ribose binding pocket and interactions are observed between the NH₂ at the thiazole 2-position and Asp145, and between the nitrogen atom at the thiazole 3-position and Asn132.

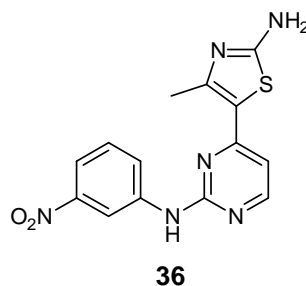
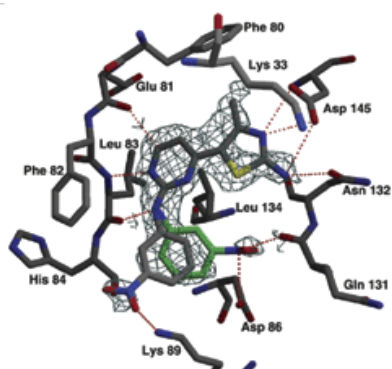


Figure 47

Crystal structure of **36** bound within the CDK2 ATP-binding site.⁸⁸

Studies carried out by Kim *et al.*²⁰¹ identified *N*-phenylacetyl-2-aminothiazoles as potent CDK2 inhibitors, and subsequent development of a related series of *N*-(cycloalkylamino)acyl-2-aminothiazoles²⁰² resulted in the identification of **215**, reported to inhibit CDK family members with IC₅₀ values shown in **Table 23**.²⁰³

Protein kinase	IC ₅₀ (μM)
CDK1/Cyclin B	0.48
CDK2/Cyclin E	0.038
CDK4/Cyclin D1	0.93
CDK7/Cyclin H	0.062
CDK9/Cyclin T1	0.004

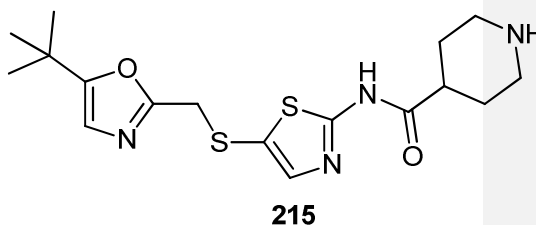


Table 23

Kinase inhibition for compound **215** against CDK family members.

Crystal structure studies of **215** bound to CDK2²⁰² showed the thiazole ring binding to the hinge region and the piperidine ring extending towards the specificity pocket and Leu134. The *t*-butyloxazole ring folds back towards the ribose-binding pocket to avoid unfavourable interactions with the gatekeeper residue Phe80 (**Figure 14**).

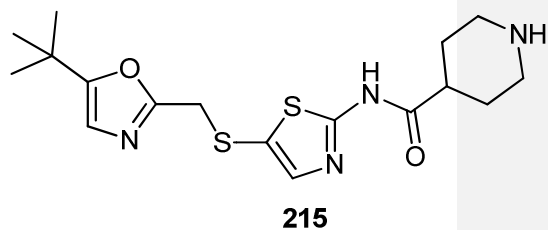
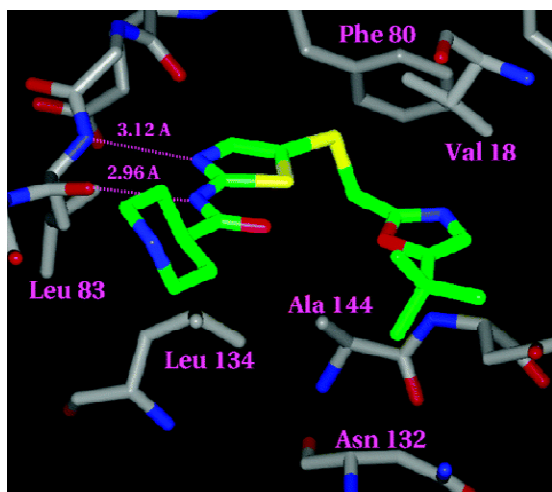
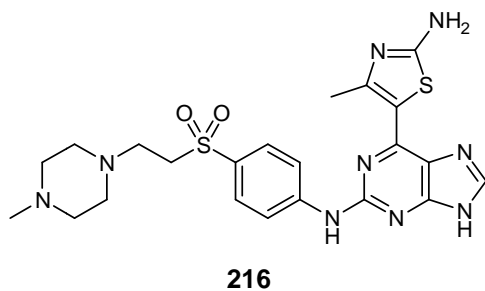


Figure 48

Crystal structure of **215** bound within the CDK2 ATP-binding site.²⁰²

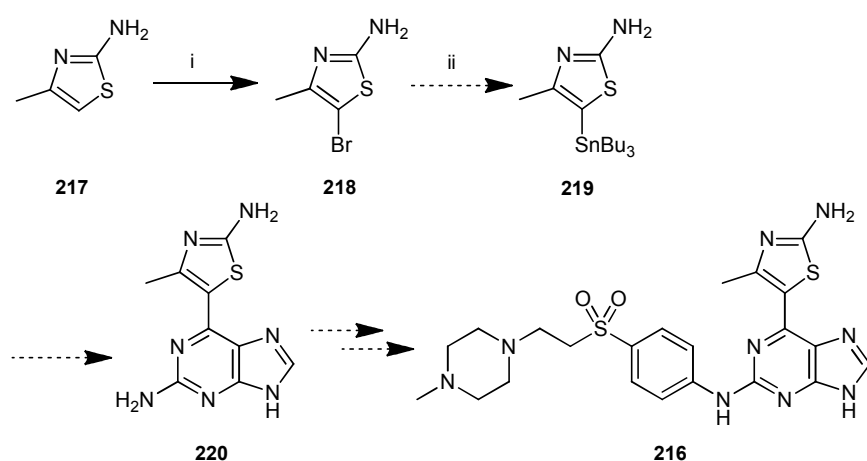
Compounds **36** and **215** are also potent against CDK7 and this could be explained by a similar binding mode to that observed with CDK2. If the assumption that the thiazole ring of **36** and the oxazole ring of **215** bind within the ribose-binding pocket of CDK7 is correct, replacing the cyclohexylmethoxy group of NU6247 (**44**) with an aminothiazole may confer favourable interactions and lead to enhanced potency against CDK7.



To approach **216** as a synthetic target, a literature method based on the palladium-catalysed Stille coupling reaction was considered, where a purine was successfully coupled to either a thiophene, a pyrrole, or a simple thiazole derivative.²⁰³⁻²¹¹ No

reports were found in the literature of a purine or a pyrimidine being coupled to a thiazole using a Suzuki approach.

Starting from commercially available 2-amino-4-methylthiazole (**217**) the route described in **Scheme 33** was initially devised for the synthesis of **216**.



Scheme 33

Reagents and conditions: (i) NBS, AcOH, 3 h, RT; (ii) *n*BuLi, Bu₃SnCl, THF, 2 h, -78 °C.

A literature procedure²¹² involving the use of *N*-bromosuccinimide in acetic acid was used to convert **217** into the brominated derivative **218**, and the reaction proceeded successfully. It was not possible, however, to convert **218** into the stannyl derivative **219**.

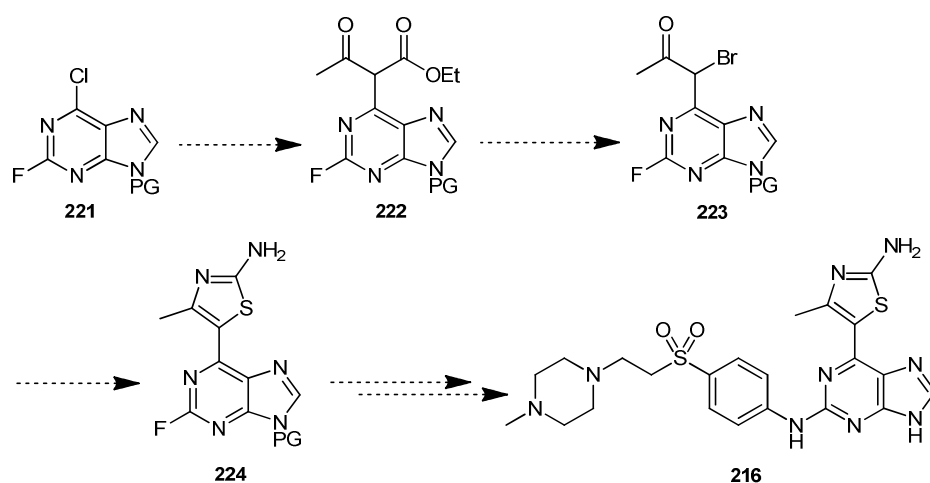
Compound **219** is not reported in the literature; a standard stannylation reaction involving lithiation at the 5-bromo position of **218** using an alkyllithium reagent (*n*BuLi), followed by tin-lithium exchange using an alkyltin halide (Bu₃SnCl) as reported for a simple thiazole,²¹¹ was tried without success. The reaction was attempted using increasing amounts of *n*-butyllithium, taking into consideration the possibility of deprotonation at both the 2-amino and the 4-methyl moiety of **218** (Wang *et al.*, unpublished observations), but in no case was the formation of the desired product (**219**) observed. The results are summarised in **Table 24**.

Equivalents of <i>n</i> BuLi	Temperature	Result
1	-78 °C	Complex reaction mixture; no product detected by NMR or LC-MS analysis.
2	-78 °C → RT	
3	-78 °C → RT	
4	-78 °C → RT	

Table 24

Attempted reaction conditions for lithiation of compound **218**.

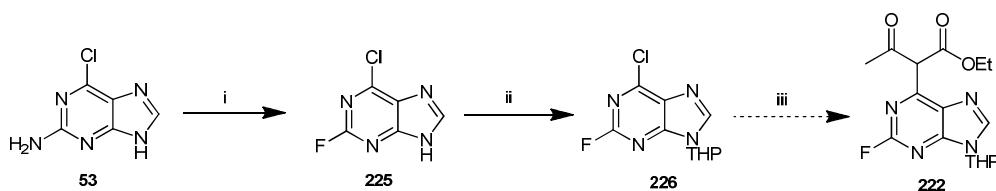
As a result of these observations, the Stille approach to compound **216** was abandoned; a stepwise approach to the 2-fluoro derivative **224** was then investigated as shown in **Scheme 34**.



Scheme 34

Proposed synthetic strategy to target molecule **216**.

The synthesis of **224** (where PG = THP) was attempted following a literature procedure²¹³ as exemplified in **Scheme 35**, where 2-amino-6-chloropurine (**53**) was converted into the 2-fluoro derivative (**225**) under standard Balz-Schiemann conditions and subsequently protected at the *N*⁹-position using DHP in EtOAc. Alkylation of **226** at the 6-chloro position was unsuccessful. Compound **226** was observed to degrade under the reaction conditions and no formation of product was observed; this route, too, was therefore abandoned.

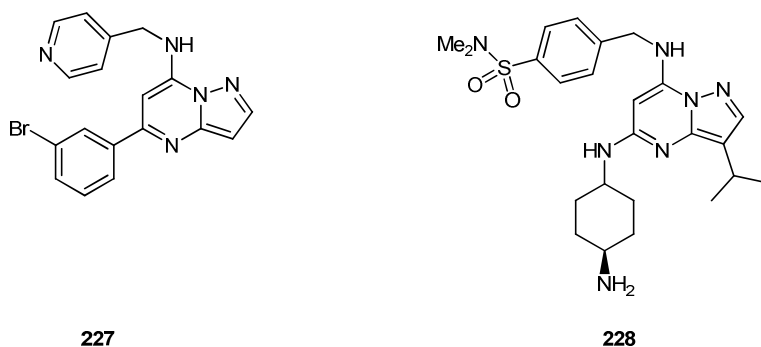


Scheme 35

Reagents and conditions: (i) HBF_4 , NaNO_2 , H_2O , 75 min, RT; (ii) DHP, EtOAc, 24 h, 60 °C; (iii) Ethyl acetate, sodium salt, THF, 3 h, RT

5.2.3 Replacement of the purine core pharmacophore of NU6247 (44) by a pyrazolo-pyrimidine

The pyrazolo[1,5 α]pyrimidine pharmacophore was first reported as a scaffold for CDK inhibitors by Williamson *et al.* in 2005,²¹⁴ from a high-throughput screen of a commercially available kinase-directed compound library. The authors discovered that compound **227** had an IC_{50} value of 1.8 μM against CDK2 but inhibited GSK-3 β kinase with similar potency. Due to the structural similarity of **227** with (*R*)-roscovitine (**13**) and other purine-based inhibitors such as NU6102 (**31**), SAR studies around the pyrazolo[1,5 α]pyrimidine core pharmacophore ultimately resulted in the identification of compounds such as **228**, which exhibited similar potency and selectivity for CDK2 as NU6102 (**31**) and a binding mode analogous to roscovitine (**Figure 49**).



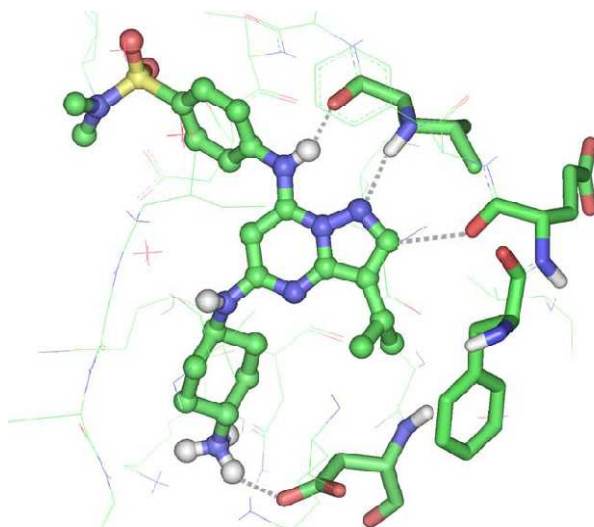
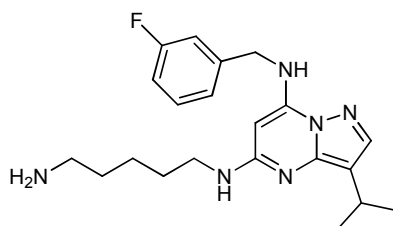


Figure 49

Crystal structure of **228** bound within the CDK2 ATP-binding site.²¹⁴

Researchers at Emory University and Imperial College recently developed a series of compounds with CDK inhibitory activity based on the pyrazolo[1,5 α]pyrimidine core pharmacophore.¹³⁷ The results obtained, while varying quite widely in the selectivity for specific members of the CDK family, proved of interest due to the discovery of compound BS-181 (**39**), an inhibitor of CDK7 with 40-fold selectivity over CDK2.

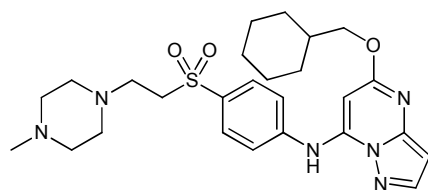


BS-181 (**39**)
 IC_{50} μ M = 0.018 (CDK7), 0.75 (CDK2)

No structural data have been published to date concerning the binding mode of **39** within CDK7 or CDK2, but the structural similarity with **13** would suggest a binding orientation similar to that shown in **Figure 49**. The sidechain at the 5-position of the heterocycle is similar in both cases; a lack of a sulfonamide moiety in the *para*-

position of the aromatic ring at the 7-position would account for the loss of CDK2-inhibitory activity with respect to both **228** and NU6102 (**31**), but identifying a structural feature which would account for the selectivity of compound **39** for CDK7 over CDK2 is not straightforward without the aid of structural biology studies.

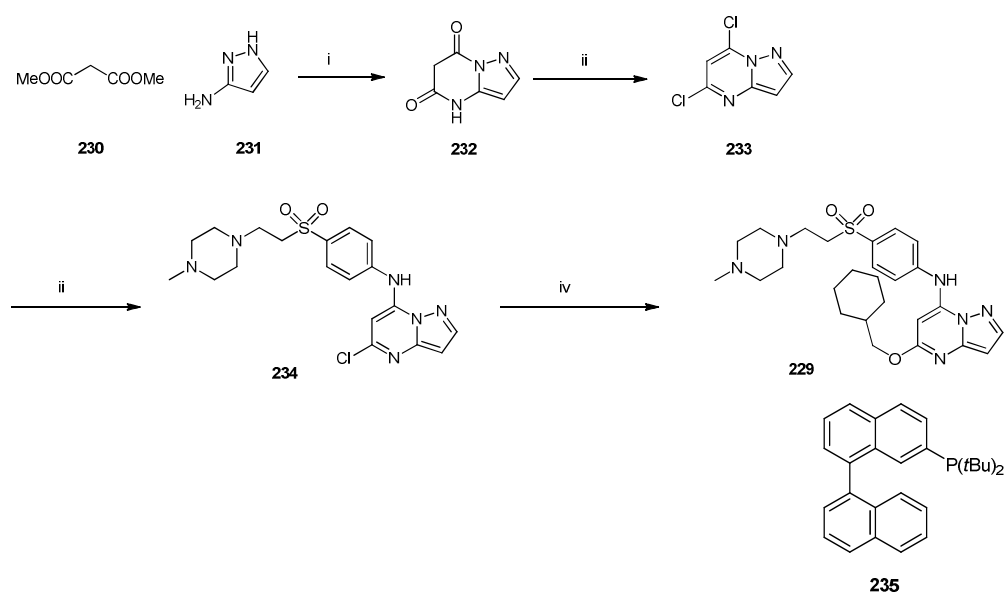
In order to establish a direct comparison between **39** and NU6247 (**44**), compound **229** was identified as a synthetic target.



229

From available information regarding the binding orientation of the Newcastle purines within the CDK2 ATP-binding site, it was decided that a cyclohexylmethoxy substituent at the 5-position, an ethylsulfone sidechain at the 7-position, and removal of the isopropyl substituent at the 3-position would provide the closest overlay with NU6247 (**44**).

To synthesise target **229**, dimethyl malonate and 3-amino-pyrazole were reacted in the presence of sodium etoxide, followed by phosphoryl chloride-mediated reaction to generate 5,7-dichloropyrazolo[1,5 α]pyrimidine **233** (**Scheme 36**). Compound **233** could selectively be coupled with an aniline at the 5-position,²¹⁵ enabling the introduction of the desired aniline sidechain *via* standard TFA/TFE conditions. No 7-addition product was observed in the reaction mixture at this stage. With compound **234** in hand, a palladium-catalysed C-O bond formation reaction was attempted to introduce the cyclohexylmethoxy substituent at the 5-position of the heterocycle.²¹⁶



Scheme 36

Reagents and conditions: (i) EtONa, EtOH, 24 h, reflux; (ii) POCl₃, μ W; (iii) **187**, TFA, TFE, 48 h, reflux; (iv) **235**, Pd(OAc)₂, Cs₂CO₃, CyCH₂OH, μ W

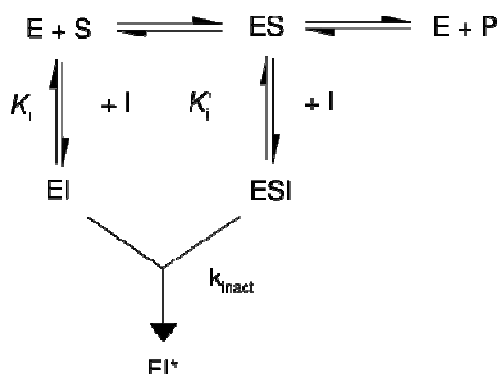
Inhibitor **229** was tested for CDK2- and 7-inhibitory activity and found to exhibit IC₅₀ values of 1.6 μ M and a 19.1 μ M, respectively. The results show that the compound does not interact with the ATP-binding domain of CDK7 as effectively as BS-181 (**39**), and the useful interactions made by **31** and **44** with the ATP-binding sites of CDK2 and CDK7 respectively are also not replicated. Structural biology studies would be needed to assess whether **39** and **229** bind in a similar orientation to **13** or to **31**.

Chapter 6 – NU6300, an irreversible CDK2 inhibitor

6.1 Irreversible enzyme inhibition

Enzyme inhibitors can interact with their intended protein target in either a reversible or an irreversible manner. Reversible inhibitors form non-covalent interactions with their target enzyme such as hydrogen bonds, hydrophobic and Van Der Waals interactions and ionic bonds. Multiple weak bonds between the inhibitor and the binding site can combine to produce strong and specific binding. Reversible inhibitors generally do not undergo chemical reactions when bound to the enzyme and can be removed by dilution or dialysis.²¹⁷

Irreversible inhibitors invariably react with a specific site on the target protein to form one or more covalent bonds. This results in chemical modification and subsequent inactivation of the enzyme. The formation of the covalent bond is normally relatively slow, and so irreversible inhibitors display time-dependent inhibition. Their potency cannot be characterised by an IC_{50} value, because at any time the amount of active enzyme at a given concentration of inhibitor will be dependent on the time the enzyme is pre-incubated with the inhibitor. Instead, k_{obs}/C values are used²¹⁸ where k_{obs} is the observed pseudo-first order rate of inactivation (obtained by plotting the log of % activity vs. time) and C is the concentration of inhibitor.



Scheme 37

Representation of the kinetic constants for reversible and irreversible enzyme inhibition. E = enzyme, I = inhibitor, S = substrate.

Scheme 37 summarises the kinetic constants involved in reversible and irreversible enzyme inhibition. The rate at which the Enzyme-Inhibitor covalent adduct is formed is called k_{inact} . At the point where the enzyme is saturated with the inhibitor, $k_{\text{obs}} = k_{\text{inact}}$.

Irreversible inhibitors can be classified into two groups depending on their mode of action.²¹⁹ **Active site-directed inhibitors**, or affinity labels, contain an element of recognition that can initially interact with the target enzyme in a reversible manner. The reactive group, or 'warhead', subsequently reacts with what is usually a nucleophilic residue on the target protein such as hydroxyl (serine, threonine, [tyrosine](#)) or sulfhydryl ([tyrosine](#), cysteine) to form the irreversible enzyme-inhibitor complex. **Mechanism-based inhibitors**, or suicide inhibitors, are initially competitive inhibitors that bind to the active site where they are chemically modified through the enzyme's own catalytic mechanism to produce a reactive group that covalently binds to the enzyme to form a stable complex.²²⁰ Mechanism-based inhibitors exploit some component of the target enzyme's catalytic mechanism to promote enzyme inactivation, usually by covalently modifying a key amino acid involved in the catalytic mechanism.²²¹

Mechanism-based irreversible enzyme inhibition was first reported in 1968²²² and active site-directed irreversible enzyme inhibition in 1976.²²³

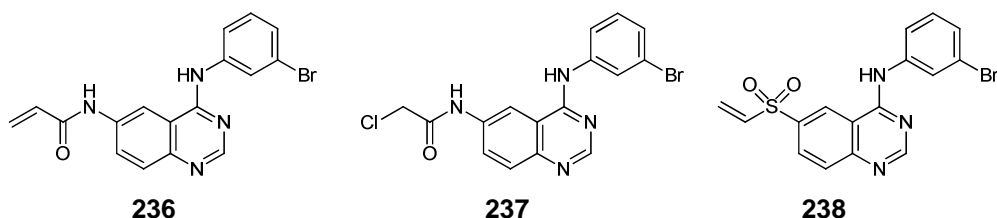
Active site-directed inhibitors have the ability to bind selectively to individual enzymes or specific enzyme families. This enables them to be used as tools to elucidate characteristics such as abundance, interactions, cellular localisation and function of a protein under investigation.²²⁴

The vinyl sulfone moiety is known for its ability to participate in Michael-type additions and has therefore been widely employed in irreversible cysteine protease inhibitors.²²⁵ Vinyl sulfones are less reactive toward nucleophiles than the analogous vinyl ketones or esters,²²⁶ which allows the design of inhibitors that are unreactive toward other proteases, non-active-site cysteines and circulating thiols such as glutathione. The vinyl sulfone moiety also exhibits the capability to form a hydrogen bond with the active site, which helps to align the warhead for attack by the catalytic cysteine residue. Examples of cysteine proteases that have been irreversibly inhibited by vinyl sulfones are the cathepsins, caspases, de-ubiquitinases and falciparin-2.²²⁷⁻²³⁰

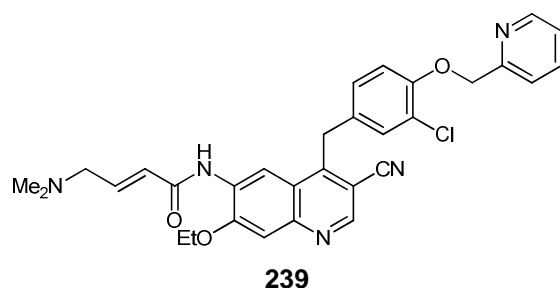
An advantage of affinity labelling is that permanent inactivation of the enzyme provides a long duration of action, since *de novo* protein synthesis is required for restoration of enzyme activity, and such a process is usually slow. Plasma levels of the irreversible inhibitor can then decrease between treatments without enzyme inactivation being reduced, allowing reduced dosages of the drug and longer intervals between doses.²³¹ On the other hand, if the affinity label is too reactive, it can interact with low-molecular-weight nucleophiles or other cellular macromolecules prior to reaching its intended target, diminishing specificity and increasing the risk of off-target activity and toxicity.²³²

A recent example of irreversible kinase inhibition is the development of ErbB or epidermal growth factor receptor (EGFR) tyrosine kinase inhibitors. The synthesis of a library of irreversible EGFR inhibitors based on the 4-anilinoquinazoline pharmacophore was undertaken to overcome the problem of resistance associated with gefitinib (**4**) and erlotinib (**6**), arising as a result of a mutation (T790M) within the kinase domain of EGFR.²³³ Reversible analogues where the 'warhead' functionality was removed for control purposes were also synthesised. The library included compounds such as **236** and **237** (earlier work by Kwak *et al.* identified vinyl sulfone **238**²³⁴) but, ultimately, the results showed that this new generation of inhibitors were not as effective as initially hoped, and their activity required combination with either

cytotoxic agents or inhibitors of other kinases acting downstream of EGFR, such as MEK or PI3K.



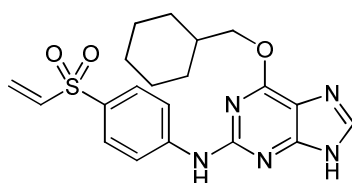
Another recent example of an irreversible ErbB receptor tyrosine kinase inhibitor is neratinib (**239**).²³⁵ Neratinib is a potent, low-molecular-weight, orally administered irreversible pan-ErbB (*i.e.* Erb 1, 2 and 4) receptor tyrosine kinase inhibitor currently in Phase II clinical trials. Recent results have shown that Neratinib is clinically active both on its own and in combination with trastuzumab, a monoclonal antibody that binds specifically to the ErbB-2 tyrosine kinase receptor, or cytotoxic drugs such as taxanes and anthracyclines.²³⁶



There is currently no known irreversible cyclin-dependent kinase inhibitor in the literature.²³⁷⁻²³⁹ CDK2 does not have a catalytic cysteine, although a catalytic aspartic acid and two lysines (Lys88 and Lys89) are present and may be correctly positioned to react with a Michael acceptor within the ATP-binding site.

6.2 NU6300 as an irreversible inhibitor of CDK2

The vinyl sulfone purine intermediate NU6300 (**63**), generated as part of the Cope elimination reaction (see **Chapter 4**), has the potential to irreversibly inhibit CDK2. As noted above, the vinyl sulfone moiety can be involved in Michael addition-type reactions with nucleophilic cysteines, although no precedent for a similar reaction with a nucleophilic lysine appears to exist.



NU6300 (**63**)

IC₅₀ (CDK2) = 22.4 nM

Early studies to test vinyl sulfone **63** as an irreversible inhibitor of CDK2 were aimed at demonstrating that the compound showed a time-dependent inhibition of the enzyme, with enzyme activity decreasing as a function of the time of exposure to the inhibitor.

To do this, the catalytically active enzyme (pCDK2/cyclin A) was incubated with NU6300 and, at various time intervals, an aliquot was taken and assayed for enzymatic activity.²⁴⁰ The results (**figure 50a**) showed that, comparing with a non-incubated control, the kinase loses activity proportionally to the inhibitor exposure time, suggesting that a covalent modification is taking place.

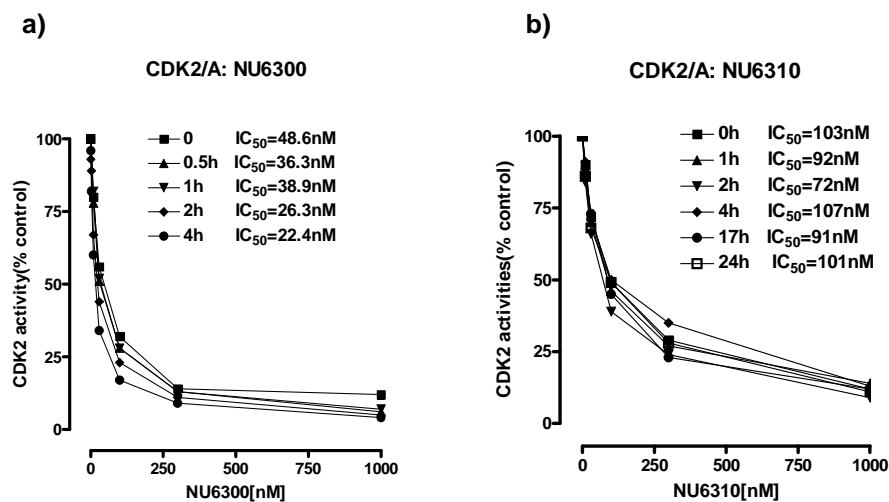
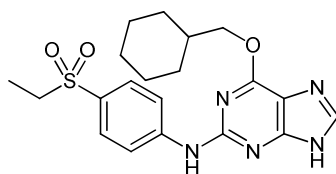


Figure 50

a) Time-dependent inhibition of CDK2 by NU6300. b) The same experiment run with NU6310 shows no decrease in activity over time

To further validate the hypothesis that the vinyl sulfone moiety is covalently modifying a nucleophilic residue of CDK2, a parallel experiment was run on NU6310 (**240**), in which the vinyl sulfone has been replaced with an unreactive ethyl sulfone. As expected for a reversible inhibitor, the activity of CDK2/Cyclin A did not decrease in a time-dependent manner after incubation with NU6310 (**Figure 50b**).



NU6310 (**240**)
IC₅₀ CDK2 = 160 nM

6.2.1 Surface Plasmon Resonance experiments

Formatted: Font: 14 pt, Bold, Italic

Through a collaboration with Beactica, Sweden the interaction of the same two compounds with CDK2 was investigated using a surface plasmon resonance biosensor. Exposure to NU6300 for several hours decreased the binding capacity of CDK2 for NU6310 (**Figure 51**).

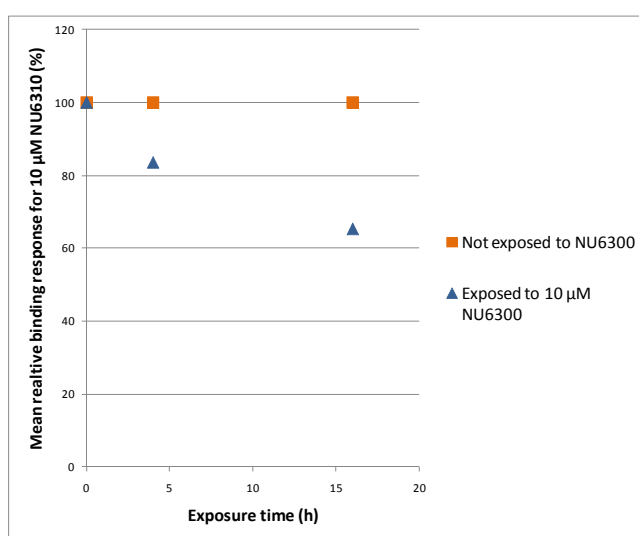


Figure 51

Binding responses for 10 μM NU6310 to CDK2 surfaces. CDK2 showed a decreased binding capacity for NU6310 when incubated with 10 μM NU6300.

At the interface between two transparent media of different refractive index (e.g. glass and water, or glass and air, or glass and vacuum), when the angle at which the light strikes the interface (the angle of incidence, or θ) is greater than a critical value (the critical angle, or θ_c), the light is completely reflected. If the surface of the glass is coated with a thin layer of a noble metal (e.g. gold), the reflection is not total. Energy from the incident light is absorbed by mobile electrons on the gold surface (or “plasma”), which oscillate resulting in a wave called a **surface plasmon**. There exists an angle, greater than the critical angle, at which the quantity of absorbed energy is greatest and the intensity of the reflected light reaches a minimum. This

angle is called the **surface plasmon resonance angle**, or θ_{spr} . If incident light is monochromatic and p-polarised, and has the same wavelength of the surface plasmon, the electrons 'resonate', resulting in the phenomenon of **surface plasmon resonance (SPR)**.

Since the wave is on the boundary of the metal and the external medium (e.g. water, air or vacuum), the oscillations are very sensitive to any change of this boundary, such as the adsorption of molecules to the metal surface. Linear relationship is found between resonance energy and mass concentration of biochemically relevant molecules. The SPR signal, expressed in resonance units, is therefore a measure of mass concentration at the sensor surface. In order to detect an interaction, one molecule (the ligand; in the present case, CDK2) is immobilised onto the sensor surface. A binding partner (the analyte; in the present case, a reversible CDK2 inhibitor) is injected in solution (sample buffer) under continuous flow. As the analyte binds to the ligand, the accumulation on the surface results in an increase in the refractive index. This change in refractive index is measured in real time, and the result plotted as response or resonance units (RUs) versus time (a sensorgram). This means that the analyte and ligand association and dissociation can be observed and rate constants as well as equilibrium constants can be calculated.

A CDK2 crystal surface incubated with 10 μM NU6300 was tested for binding capacity for NU6310 after various time intervals (0, 4, 20 h) and the results compared with a CDK2 surface incubated with buffer. The surface exposed to NU6300 displayed only 55% of the binding capacity after 20 h (**Figure 52**).

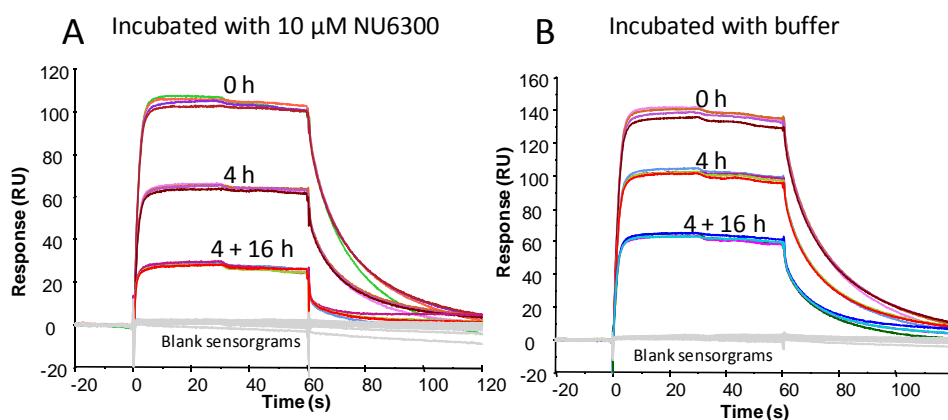


Figure 52

SPR sensorgrams (reference subtracted) for the interaction between immobilised CDK2 and 10 µM NU6310 after incubation with A) buffer including 10 µM NU6300 and B) buffer.

6.2.2 Band shift assays

As a means to confirm that prolonged exposure to NU6300 covalently modifies and therefore inactivates pCDK2/cyclin A, a standard band shift assay versus pRb was implemented. Three aliquots of enzyme were incubated overnight with 100 µM NU6300, 100 µM NU6310 and DMSO respectively. They were then transferred to a dialysis unit whereby any non-covalent inhibitors would be eliminated from the active site by means of successive dilutions. The dialysed enzyme samples were then utilised to catalyse a test phosphorylation reaction of the substrate pRb, carried out in the presence of ATP and monitored over a time course of 15 min.

pRb is a natural substrate of CDK2/Cyclin E and D-dependent CDKs (see **Chapter 2**).²⁴¹ CDK1 and 2 phosphorylate pRb on at least five recognised sites (Ser249, Thr252, Thr373, Ser807 and Ser811).²⁴²⁻²⁴³ Mass and charge increase sensibly in pRb as a result of hyperphosphorylation, rendering this protein a useful tool for detecting CDK2-mediated phosphorylation in standard band shift assays by sodium dodecyl sulfate polyacrylamide gel electrophoresis (SDS-PAGE).

As shown in **Figure 53**, pRb was phosphorylated by CDK2 previously incubated with

Formatted: Font: 14 pt, Bold, Italic

Formatted: Font: 14 pt, Bold, Italic

DMSO, and (at a slightly lower rate) by CDK2 previously incubated with NU6310, suggesting that after dialysis NU6310, the reversible inhibitor, is almost completely removed from the active site. The enzyme incubated with NU6300, however, remained inactive after dialysis and phosphorylation of pRb was not observed during the time course. This appeared to-suggested a possible covalent modification, likely within the ATP-binding site of CDK2, which eliminated-could be responsible for the elimination of kinase activity.

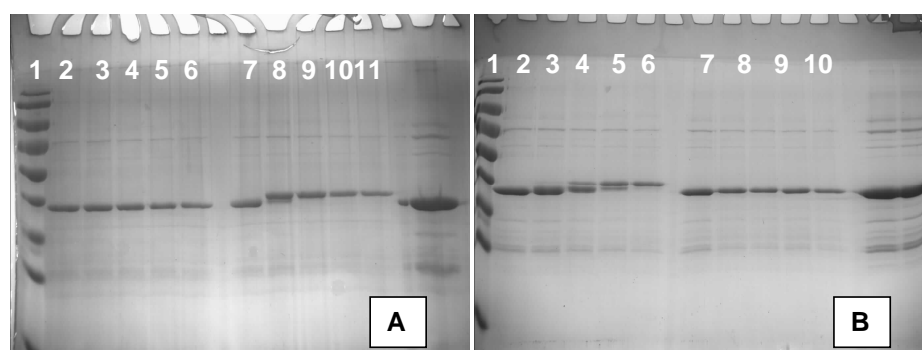


Figure 53

Phosphorylation of GST-pRb by wild type CDK2/A. **A)** Lane 1, molecular weight markers (170, 130, 95, 72, 55, 43, 34, 26 and 17 kDa). Lanes 2-6, negative control. GST-pRb incubated with 50 mM Tris-HCl pH 7.5, 10 mM magnesium chloride, 1.0 mM ATP after 0', 1', 5', 10', 15'. In the absence of CDK2/A, no phosphorylation occurs resulting in no band shift. Lanes 7-11, positive control. GST-pRb incubated with the same as above and 8 ng/μl CDK2/A, at the same time intervals as above. Hyperphosphorylated GST-pRb has a lower electrophoretic mobility. **B)** Lane 1, molecular weight markers; lanes 2-6, phosphorylation of GST-pRb carried out using a sample of CDK2/A incubated overnight with 100 μM NU6310 and then dialysed. Enzyme activity is recovered after dialysis and phosphorylation of GST-pRb is achieved, resulting in a band shift; lanes 7-11, phosphorylation reaction carried out using a CDK2/A sample incubated overnight with 100 μM NU6300 and then dialysed. Enzyme activity is not recovered after dialysis and GST-pRb is not phosphorylated. Proteins were visualized by Coomassie stain following 15% SDS-PAGE. Reactions were carried out under the conditions described in **Chapter 7**.

6.2.3 Mass spectrometry experiments

Formatted: Font: 14 pt, Bold, Italic

A mass spectrometry experiment performed on CDK2/Cyclin A samples incubated with 2.5 mM NU6300 demonstrated covalent modification by showing a 414 Da increase in the mass of the protein after overnight incubation with NU6300 (**Figure 54c**). This result is compatible with one nucleophilic residue from CDK2 (a lysine NH_2 , cysteine SH or aspartate COO^-) reacting with the vinyl sulfone moiety of NU6300 (molecular weight 413 Da) in a Michael-type addition to the double bond, resulting in the formation of a covalent bond. A similarly prepared sample incubated overnight with NU6310 at the same concentration did not show any increase in the mass with respect to the control sample incubated with DMSO (**Figure 54a and b**).

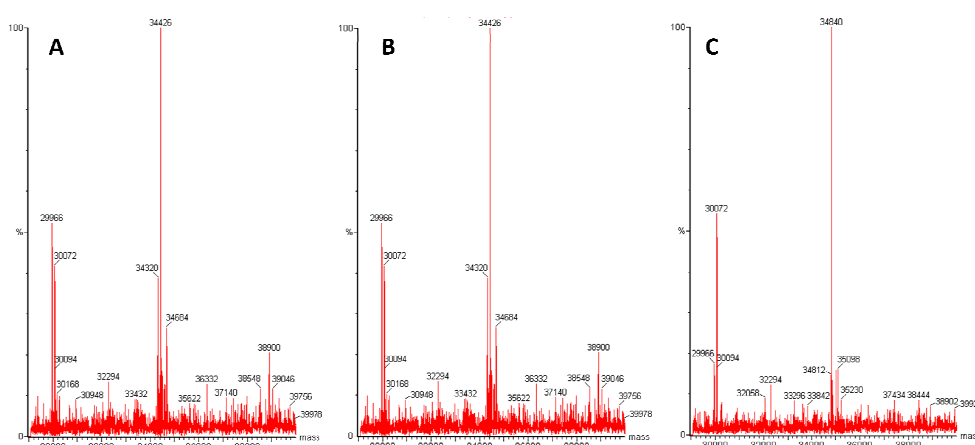


Figure 54

Mass spectra of 3 mg/ml CDK2/A pre-incubated overnight with **A)** DMSO; **B)** 2.5 mM NU6310; **C)** 2.5 mM NU6300.

It should be noted that, despite the high concentration [of NU6300 \(calculated to be in a 50:1 stoichiometric excess with respect to CDK2\)](#), only one molecule of NU6300 was incorporated after overnight incubation. This suggested that the vinyl sulfone of NU6300 does not react promiscuously with any solvent-exposed nucleophilic residues, such as Cys327 in Cyclin A, but is attacked only by an appropriately

positioned amino acid after having assumed the correct orientation within the CDK2 ATP-binding site.

Assuming a similar binding orientation of NU6300 within the ATP-binding site of CDK2 to that observed with NU6102,⁴³ the potential nucleophilic residues that could react with the vinyl sulfone group to form a covalent bond were Asp86, Lys88 and Lys89.

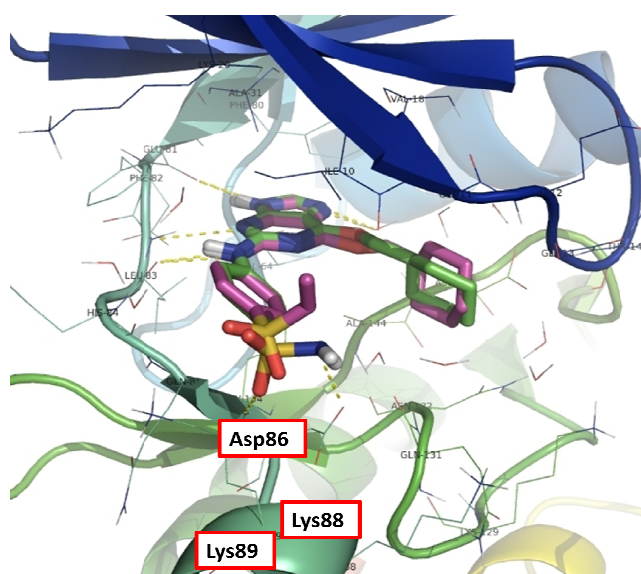


Figure 55

Superposition of the crystal conformation of NU6102 (green sticks) with the best-scoring docking pose of NU6300 (magenta sticks).

In a first attempt to determine the exact site of covalent modification, a Coomassie-stained gel band corresponding to the CDK2-NU6300 covalent adduct and one corresponding to unmodified CDK2 were proteolysed with trypsin. The lysates were analysed by MALDI-TOF MS/MS, and the resulting spectra were compared. The peak at 1664 Da, corresponding to the Asp86 and Lys88-containing digested peptide, was present in the control spectrum and appeared unaltered in the spectrum of the adduct, suggesting that Asp86 and Lys88 did not participate in the formation of the covalent bond.

Unfortunately, the Lys89-containing peptide (expected mass 1686 Da) was only seen in traces in the control spectrum, due to a markedly hydrophobic nature that prevents this peptide from being ionised under MALDI conditions. The expected mass for the same peptide if Lys89 were the site of covalent modification would be 2230 Da, and again only traces of this appeared in the spectrum of the CDK2-NU6300 adduct (**Figure 56**).

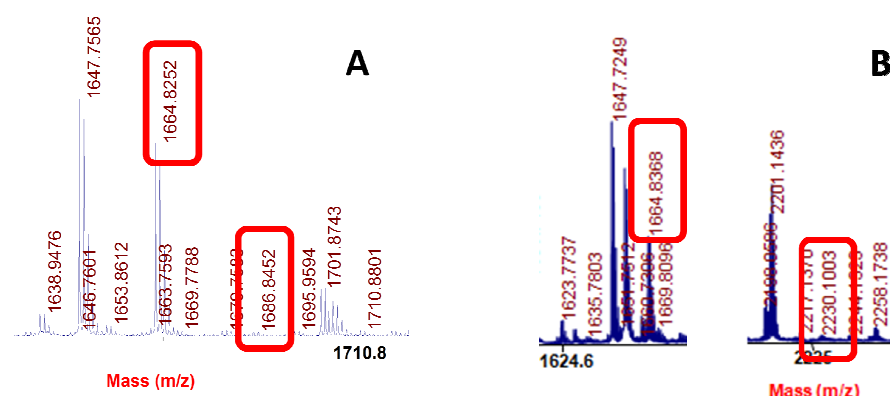


Figure 56

A) Detail of MALDI-TOF TOF spectrum of wild type CDK2, highlighting the peaks 1664 and 1686 Da.
B) Detail of MALDI-TOF TOF spectrum of the CDK2-NU6300 covalent adduct, highlighting the peaks at 1664 and 2230 Da.

The evidence from the MALDI-TOF TOF experiment suggested a reaction between NU6300 and Lys89, but this hypothesis needs further confirmation. Additional evidence excluding any involvement of Asp86 was provided by site-directed mutagenesis studies. A CDK2 mutant enzyme, where Lys88 and Lys89 were substituted by a glutamic acid and a valine, respectively, was synthesised. Overnight incubation of this mutant enzyme with 2.5 mM NU6300 did not result in an increase in the mass of the protein (**Figure 57**). This result suggested that the residue involved in the Michael addition to the vinyl sulfone moiety of NU6300 was either Lys88 or Lys89. As a consequence, the K88E K89V mutant CDK2 does not possess any nucleophilic residue correctly positioned for Michael-type addition to NU6300, which therefore acts as a purely reversible inhibitor of this mutant kinase.

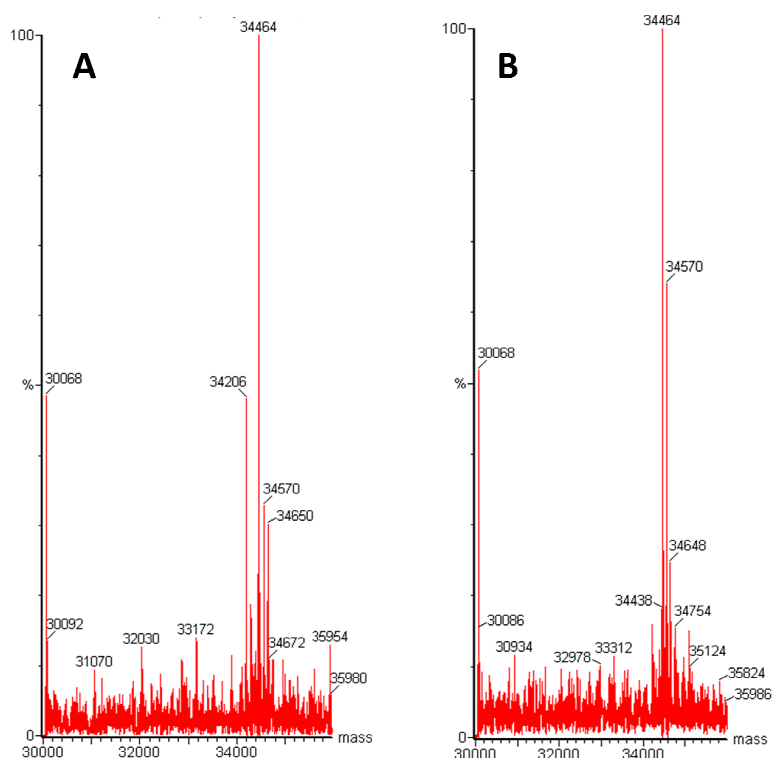


Figure 58

Mass spectra of 3 mg/ml K88E K89V CDK2/cyclin A pre-incubated overnight with **A)** DMSO; **B)** 2.5 mM NU6300.

To confirm that NU6300 acts purely as a reversible inhibitor of the K88E K89V mutant CDK2, three aliquots of mutant enzyme were incubated overnight with 100 μ M NU6300, 100 μ M NU6310 and DMSO, respectively, and then dialysed, mirroring the experiment already conducted on the wild-type enzyme. This time, the test phosphorylation reaction of the substrate pRb, carried out and monitored under the same conditions as for the wild-type enzyme, proceeded smoothly in all cases. The NU6300-incubated sample of mutant CDK2 recovered activity following dialysis, confirming the hypothesis that no irreversible inactivation of the enzyme was taking place (**Figure 58**).

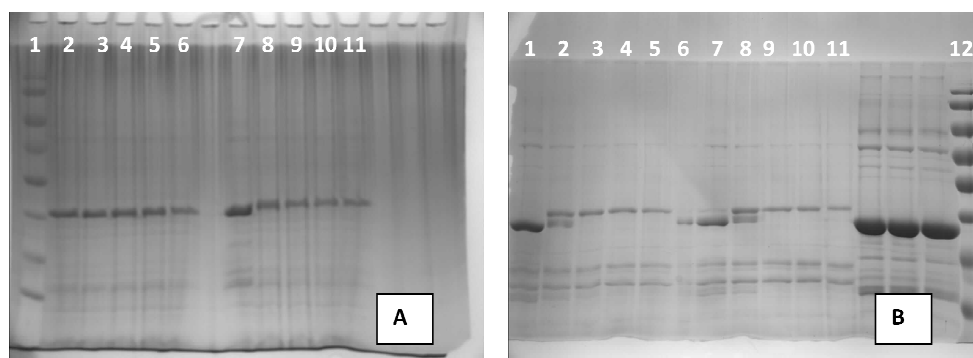


Figure 58

Phosphorylation of GST-pRb by K88E K89V mutant CDK2/cyclin A. **A)** Lane 1, molecular weight markers (170, 130, 95, 72, 55, 43, 34, 26 and 17 kDa). Lanes 2-6, negative control. Lanes 7-11, positive control. Hyperphosphorylated GST-pRb has a lower electrophoretic mobility. **B)** Lanes 1-5, phosphorylation of GST-pRb carried out using a sample of mutant CDK2/A incubated overnight with 100 μ M NU6310 and then dialysed. Enzyme activity is recovered after dialysis; lanes 7-11, phosphorylation reaction carried out using a mutant CDK2/A sample incubated overnight with 100 μ M NU6300 and then dialysed. Enzyme activity is recovered after dialysis and GST-pRb is phosphorylated. Lane 12, molecular weight markers. Proteins were visualized by Coomassie stain following 15% SDS-PAGE. Reactions were carried out under the conditions described under "Experimental Details".

The results obtained from the MS experiments and enzyme activity assays on both the wild-type and K88E K89V mutant CDK2/Cyclin A confirmed the hypothesis that vinyl sulfone NU6300 is an irreversible inhibitor of CDK2. The MS/MS experiments conducted on the wild-type enzyme, and the MS experiments and enzyme activity assays conducted on the K88E K89V mutant CDK2, excluded any involvement of Asp86 in the formation of the covalent bond. These results also suggested an involvement of Lys89 over Lys88, although this hypothesis needs further corroboration.

The formation of a covalent bond between NU6300 and each of these lysines was modelled starting from the crystal structure of NU6102 within CDK2. The resulting structures were minimised and comparison of the total energies of the minimised complexes showed that a Lys88 complex would be 9.2 kcal/mol lower in energy than a Lys89 complex, and therefore more favourable (**Figure 59**), due to a network of

hydrogen bonds formed between the sulfone oxygens, the Lys88 NH₂ and the Asp86 COO⁻.

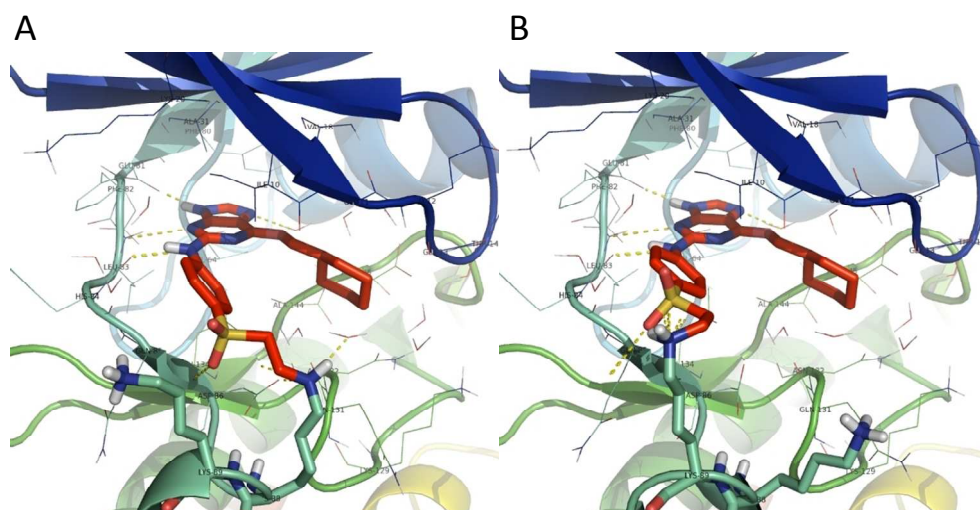


Figure 59

NU6300 (red sticks) docked into the ATP-binding pocket of CDK2 while covalently bound to **A)** Lys88 and **B)** Lys89. The neighbouring lysine residues 88 and 89 are rendered as green sticks in the foreground.

The issue could possibly be resolved by further site-directed mutagenesis experiments. The synthesis of the K88E and K89V CDK2 single mutants is in progress, and MS experiments on NU6300-incubated samples of these single mutant enzymes may clarify which residue is involved in the formation of the covalent bond. Crystallography studies with NU6300 and wild-type CDK2/A are also in progress, and a cocrystal structure may provide evidence for the formation of the covalent bond and its location.

6.3 CDK2 redundancy

The results obtained with NU6300 and CDK2, in combination with CDK redundancy patterns discussed in **Chapter 2**, raise the question of whether a permanent inactivation of CDK2 through irreversible inhibition would cause cell cycle arrest, and

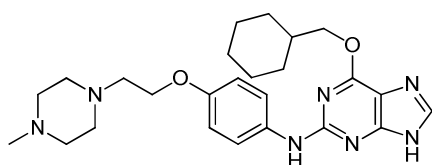
whether an irreversible CDK2 inhibitor would be considered a useful investigative tool.

A series of studies published between 2003 and 2005^{141-142, 244-245} has questioned the essentiality of the role played by CDK2 in the regulation of the cell cycle. A possible mechanism behind this redundancy was further investigated in 2006²⁴⁶ when it was shown that when transcription of either CDK2 or CDK1 is eliminated using siRNA, there were complex shifts of cyclin A towards its reciprocal partner, *i.e.* when CDK2 is ablated, cyclin A redistributes to CDK1; when CDK1 is absent, cyclin A forms more abundant complexes with CDK2. Knockdown of both CDK1 and CDK2 using siRNA results in G₂ arrest.

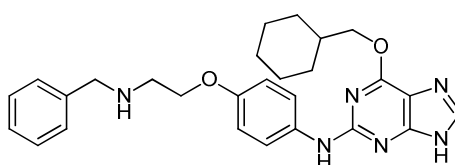
CDK2 has shown emerging roles in DNA damage response,²⁴⁷ proliferation of melanoma cells,²⁴⁸ mitosis,²⁴⁹ S-phase histone gene transcription²⁵⁰ and centrosome duplication,²⁵¹⁻²⁵² but to what extent these roles are conserved in different cell types, and which kinase takes over these roles in the absence of CDK2, is not known. It is suggested²⁵³ that selective chemical inactivation of CDK1 and CDK2 (as well as CDK4) in different conditions, and across different cell types, would be a worthwhile endeavour towards elucidating how different cells have evolved diverse requirements for CDK activity.

Conclusions

Previous structure-activity relationship studies had identified NU6247 (**44**) as a promising purine-based CDK7 inhibitor. Research was thus conducted to expand the purine series, leading to the synthesis of compounds, e.g. **94** and **133**, with improved selectivity for CDK7 over CDK2.

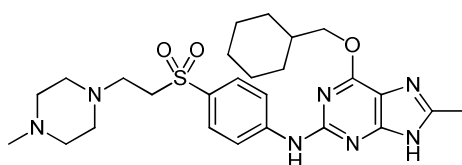


NU6451 (**94**)
 IC_{50} μ M = 0.63 (CDK2), 0.37 (CDK7)



NCL-00013804 (**133**)
 IC_{50} μ M = 2.6 (CDK2), 0.56 (CDK7)

Guided by a structure-based inhibitor design approach, systematic structural modifications have been made at the purine 2-, 6- and 8-positions. A versatile and efficient route to 8-alkylpurines has been discovered, leading to the synthesis of compound **192** and analogues. Purine **192** is a selective, albeit not very potent, CDK7 inhibitor with growth-inhibitory activity in a cancer cell line. The apparent ability of CDK7 to accommodate 2- and 8-substituted purines with higher flexibility with respect to CDK2 opens a number of new perspectives in the pursuit of CDK7-selective, purine-based inhibitors.



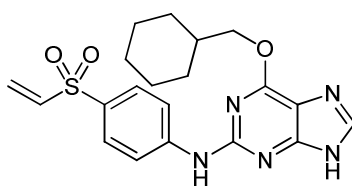
NCL-00016768 (**192**)
47% inhibition at 100 μ M (CDK2)
 IC_{50} μ M = 5.3 (CDK7)

The initial objective of this research, namely the enhancement of CDK7 activity and selectivity over CDK2 of NU6247 (**44**) *via* specific sidechain modifications, was

unsuccessful for the inhibitors tested to date. However, the results obtained for compounds **192** and **39** indicated that the identification of different binding modes, as well as the modification of the purine core pharmacophore, may offer new possibilities for the achievement of a CDK7-selective inhibitor in the future.

The possible redundancy of CDK2 and other members of the CDK family in proliferating cells has raised the question of the validity of CDK inhibition for the treatment of cancer. The emerging issue in the discovery of such inhibitors is the selectivity within the CDK family. The development of inhibitors selective for individual CDKs is important in further assessing the potential of CDK inhibition in cancer therapeutics. Evaluation of the 8-substituted purine series against CDK2 and CDK7 may reveal potential opportunities for achieving kinase selectivity within the CDK family. Elucidation of their binding mode via the co-crystallisation with both enzymes should provide a starting point for the rational design of CDK7-selective inhibitors.

Additionally, the isolation and biological evaluation of the vinyl sulfone intermediate NU6300 (**62**) indicated time-dependent inhibition of CDK2 (from radioactive kinase assays), loss of enzymatic activity following incubation (from SPR and bandshift assays) and covalent modification of the kinase following incubation (from mass spectrometry experiments). These results are in accordance with NU6300 being the first irreversible inhibitor of CDK2 to be reported. A selective, covalent inhibitor of CDK2 would potentially be a powerful tool towards a better understanding of the role of CDK2 in both normal and cancer cells.



NU6300 (**63**)

Chapter 7 - Experimental

7.1 Chemicals and Solvents

Reagents were purchased from reputable suppliers. Unless otherwise stated, laboratory grade reagents and solvents (dichloromethane, diethyl ether, ethyl acetate and petrol) were used. Petrol (petroleum ether) refers to that fraction of pentanes and hexanes in the boiling range 40-60 °C.

Anhydrous solvents such as acetonitrile, *N,N*-dimethylformamide, 1,2-dimethoxyethane, dimethyl sulfoxide, dioxane, ethanol, methanol, pyridine, tetrahydrofuran and toluene were obtained from Sigma-Aldrich in SureSeal™ bottles. HPLC gradient acetonitrile and methanol were employed for chromatography. Moisture sensitive reagents such as sodium hydride were stored in a dry box under a nitrogen atmosphere. *m*CPBA (ca. 75% purity from Sigma-Aldrich, confirmed by iodometric titration) was obtained and used directly without further purification.

7.2 Chromatography

Thin layer chromatography (TLC) was conducted on Merck aluminium backed plates pre-coated with 0.2 mm of silica gel 60F₂₅₄ using a variety of mobile phase solvents. TLC plates were subsequently dried and visualised either by using short (254 nm) and long (365 nm) wave ultraviolet light or by treatment with additional agents, defined generally as 'stains', such as ninhydrin, potassium permanganate or iodine.

Column chromatography was carried out in glass columns under medium pressure using Davisil silica gel (particle size of 40-63 µm, porosity of 60 Å). A Biotage SP1 automated parallel chromatography system was employed as well, using prepacked cartridges of different kinds: FLASH+ Silica columns (40-63 µm, 60 Å), KP-NH FLASH+ cartridges (40-75 µm, 100 Å) and reverse phase C18 FLASH+ cartridges (40-63 µm, 90 Å). The crude product was either loaded onto the column directly (as

an oil or dissolved in the minimum amount of suitable solvent) or pre-loaded onto silica or prepacked samplets.

Purification by semi-preparative HPLC was conducted on a Jones C18 column (15 × 22.5 cm) using a Varian Prostar Model 410 Autosampler, in combination with a Model 320 UV-VIS Detector, Model 710 Fraction Collector and a Model 210 Solvent Delivery Module. Both H₂O:MeOH and H₂O:MeCN were used as gradient solvent systems.

7.3 Analytical Techniques and Instrumentation

Liquid chromatography-mass spectra (LC-MS) were recorded on a Micromass Platform LC, in combination with a Waters 996 Photodiode Array Detector, a Waters 600 Controller and a Waters 2700 Sample Manager. The instrument was run in positive or negative ion electrospray mode. Chromatography was carried out using either a 5 min or a 12 min method.

- 5 min method:

Column: Waters Symmetry Shield RP18 3 µm, 4.6 x 20 mm (P/No. 186002092).

Mobile Phase: A/ 0.1 %v/v formic acid (aqueous), B/ acetonitrile.

Flow Rate: 3.0 mL/min.

Gradient:

Time (min)	% A	% B
0.0	95	5
3.3	5	95
4.0	5	95
4.05	95	5
5.0	95	5

- 12 min method:

Column: Waters Atlantis dC18 3 µm, 4.6 x 50 mm (P/No. 186001329).

Mobile Phase: A/ 0.1 %v/v formic acid (aqueous), B/ acetonitrile.

Flow Rate: 1.0 mL/min.

Gradient:

Time (min)	% A	% B
0.0	95	5
4.0	5	95
9.3	5	95
10.0	95	5
12.0	95	5

Accurate mass analyses were measured using a Finnigan MAR 95 XP or a Finnigan MAR 900 XLT at Swansea EPSRC National Mass Spectrometry Service Centre (EPSRC, Chemistry Department, University of Wales Swansea, Wales, SA2 8PP).

Proton (^1H) and Carbon (^{13}C) Nuclear Magnetic Resonance (NMR) spectra were recorded using a Bruker Spectrospin AC 300E (^1H at 300 MHz, ^{13}C at 75 MHz), Bruker Spectrospin AC 500E (^1H at 500 MHz, ^{13}C at 125 MHz), or a Jeol JNM-LA500 spectrometer (^1H at 500 MHz, ^{13}C at 125 MHz), using as solvents CDCl_3 , d_6 -DMSO, d_3 -MeCN or d_4 -MeOH.

Chemical shifts (δ) are reported in parts per million (ppm), referenced to the known signals of the deuterated solvent employed as internal standards. Coupling constants (J) are given in Hertz (Hz) units. Multiplicities are indicated by s (singlet), d (doublet), t (triplet), q (quartet), quint (quintet), sept (septet), m (multiplet) and br (broad).

Melting points were determined using a Stuart-Scientific SMP3 apparatus and are uncorrected. Infrared (IR) spectra were recorded as a neat sample on a Bio-Rad Excalibur FTS 3000MX diamond ATR spectrometer, equipped with a solid sampling device, in the range $4000\text{--}600\text{ cm}^{-1}$. UV spectra were recorded on a Hitachi U-2001 spectrophotometer with samples prepared as solutions in HPLC ethanol.

Elemental combustion analyses were either recorded on Carlo-Erba instrument 1106 analyser, in-house, or were performed either by Medac Ltd (Brunel Science Centre, Egham, Surrey, TW20 0JZ) or by the School of Pharmacy at London University (29-

39 Brunswick Square, London, WC1N 1AX) using an Elemental Analyser, Model 1108 (Carlo-Erba) and a Sartorius Ultra Micro Balance 4504MP8.

Parallel syntheses were carried out in a 'Green House' system (Radleys). Reactions needing microwave irradiation were carried out in a Biotage InitiatorTM Sixty Microwave apparatus. The 'hold temperature' mode was activated in all the experiments, unless otherwise stated. All samples were prepared under argon and pre-stirred in the reactor for 30 seconds before being irradiated.

7.4 Index of Compounds Synthesised

6-Cyclohexylmethoxy-9H-purin-2-ylamine (32).....	180
6-(Cyclohexylmethoxy)-N-(4-((2-(4-isopropylpiperazin-1-yl)ethyl)sulfonyl)phenyl)-9H-purin-2-amine (48).....	185
6-(Cyclohexylmethoxy)-N-(4-((2-(4-(4-methoxyphenyl)piperazin-1-yl)ethyl)sulfonyl)phenyl)-9H-purin-2-amine (50).....	187
N-(4-((2-(4-(4-Chlorophenyl)piperazin-1-yl)ethyl)sulfonyl)phenyl)-6-(cyclohexylmethoxy)-9H-purin-2-amine (51).....	188
6-(Cyclohexylmethoxy)-N-(4-((2-(4-(4-(trifluoromethyl)phenyl)piperazin-1-yl)ethyl)sulfonyl)phenyl)-9H-purin-2-amine (52).....	188
1-(2-Amino-(H-purin-6-yl)-4-aza-1-azoniabicyclo[2.2.2]octane chloride (54).....	180
6-Cyclohexylmethoxy-2-fluoro-9H-purine (55).....	181
2-(4-(Tert-butoxycarbonylamino)phenylthio)acetic acid (57).....	182
Tert-butyl 4-(2-oxo-2-(piperidin-1-yl)ethylthio)phenylcarbamate (58).....	182
2-(4-(6-(Cyclohexylmethoxy)-7H-purin-2-ylamino)phenylthio)-1-(piperidin-1-yl)ethanone (59).....	183
6-(Cyclohexylmethoxy)-N-(4-(2-(piperidin-1-yl)ethylthio)phenyl)-7H-purin-2-amine (60).....	184
3-Cyclohexyl-2-[4-(6-cyclohexylmethoxy-9H-purin-2-ylamino)-benzenesulfonyl]-propan-1-ol (63).....	193
3-Cyclohexyl-2-[4-(6-cyclohexylmethoxy-9H-purin-2-ylamino)-benzenesulfonyl]-propionic acid methyl ester (64).....	193
4-Cyclohexyl-2-[4-(6-cyclohexylmethoxy-9H-purin-2-ylamino)-phenyl]-butan-1-ol (65).....	198
Methyl-4-cyclohexyl-2-(4-(6-(cyclohexylmethoxy)-9H-purin-2-ylamino)phenyl)butanoate (66).....	197
Methyl 2-(4-aminophenylthio)acetate (67).....	189
Methyl 2-(4-(tert-butoxycarbonylamino)phenylthio)acetate (68).....	190
Methyl 2-(4-(tert-butoxycarbonylamino)phenylsulfonyl)acetate (69).....	190
Methyl-2-(4-(tert-butoxycarbonylamino)phenylsulfonyl)-3-cyclohexylpropanoate (70).....	191

[4-(1-Cyclohexyl-3-hydroxy-propane-2-sulfonyl)-phenyl]-carbamic acid tert-butyl ester (71).....	192
(4-Nitro-phenyl)-acetic acid methyl ester (73).....	194
2-Cyclohexylacetaldehyde (79).....	195
4-Cyclohexyl-2-(4-nitro-phenyl)-but-2-enoic acid methyl ester (78).....	195
2-(4-Amino-phenyl)-4-cyclohexyl-butyric acid methyl ester (83).....	196
2-(4-Amino-phenyl)-4-cyclohexyl-butan-1-ol (84)	197
1-(4-(6-(Cyclohexylmethoxy)-9H-purin-2-ylamino)phenyl)-3-(3-(4-methylpiperazin-1-yl)ethyl)urea (88).....	212
1-(4-(6-(Cyclohexylmethoxy)-9H-purin-2-ylamino)phenyl)-3-(3-(4-methylpiperazin-1-yl)propyl)urea (89).....	206
4-(6-(Cyclohexylmethoxy)-9H-purin-2-ylamino)-N-(3-(4-methylpiperazin-1-yl)ethyl)benzenesulfonamide (90).....	209
4-(6-(Cyclohexylmethoxy)-9H-purin-2-ylamino)-N-(3-(4-methylpiperazin-1-yl)propyl)benzenesulfonamide (91).....	203
4-(6-(Cyclohexylmethoxy)-9H-purin-2-ylamino)-N-(3-(4-methylpiperazin-1-yl)ethyl)benzamide (92)	210
4-(6-(Cyclohexylmethoxy)-9H-purin-2-ylamino)-N-(3-(4-methylpiperazin-1-yl)propyl)benzamide (93).....	203
6-(Cyclohexylmethoxy)-N-(4-(2-(4-methylpiperazin-1-yl)ethoxy)phenyl)-9H-purin-2-amine (94).....	204
N-(4-(3-(4-Methylpiperazin-1-yl)propoxy)phenyl)-6-(cyclohexylmethoxy)-9H-purin-2-amine (95).....	214
1-(3-(4-Methylpiperazin-1-yl)propyl)-3-(4-nitrophenyl)urea (97).....	205
1-(3-(4-Methylpiperazin-1-yl)ethyl)-3-(4-nitrophenyl)urea (98).....	211
1-(4-Aminophenyl)-3-(3-(4-methylpiperazin-1-yl)propyl)urea (99).....	205
1-(4-Aminophenyl)-3-(3-(4-methylpiperazin-1-yl)ethyl)urea (100).....	211
N-[3-(4-Methyl-piperazin-1-yl)-ethyl]-4-nitro-benzamide (103).....	207
N-[3-(4-Methyl-piperazin-1-yl)-propyl]-4-nitro-benzenesulfonamide (104).....	199
N-[3-(4-Methyl-piperazin-1-yl)-propyl]-4-nitro-benzamide (105).....	199
N-[3-(4-Methyl-piperazin-1-yl)-ethyl]-4-nitro-benzenesulfonamide (106).....	207
4-Amino-N-[3-(4-methyl-piperazin-1-yl)-ethyl]-benzamide (107).....	209
4-Amino-N-[3-(4-methyl-piperazin-1-yl)-propyl]-benzenesulfonamide (108)	201

4-Amino-N-[3-(4-methyl-piperazin-1-yl)-propyl]-benzamide (109)	202
4-Amino-N-[3-(4-methyl-piperazin-1-yl)-ethyl]-benzenesulfonamide (110).....	208
1-(2-Chloro-ethoxy)-4-nitro-benzene (112)	200
1-Methyl-4-[2-(4-nitro-phenoxy)-ethyl]-piperazine (113)	201
4-[2-(4-Methyl-piperazin-1-yl)-ethoxy]-phenylamine (114).....	202
1-(3-Bromopropoxy)-4-nitrobenzene (116).....	213
1-(3-(4-Nitrophenoxy)propyl)-4-methylpiperazine (117).....	213
4-(3-(4-Methylpiperazin-1-yl)propoxy)benzenamine (118).....	214
N,N-dimethyl-2-(4-nitrophenoxy)ethanamine (119).....	217
1-(2-(4-Nitrophenoxy)ethyl)pyrrolidine (120).....	218
1-(2-(4-Nitrophenoxy)ethyl)piperidine (121).....	218
4-(2-(4-Nitrophenoxy)ethyl)morpholine (122).....	219
2-(4-Nitrophenoxy)-N-benzylethanamine (123).....	219
4-(2-(Dimethylamino)ethoxy)benzenamine (124).....	220
4-(2-(Pyrrolidin-1-yl)ethoxy)benzenamine (125).....	220
4-(2-(Piperidin-1-yl)ethoxy)benzenamine (126).....	221
4-(2-Morpholinoethoxy)benzenamine (127).....	221
4-(2-(Benzylamino)ethoxy)benzenamine (128).....	222
N-(4-(2-(Dimethylamino)ethoxy)phenyl)-6-(cyclohexylmethoxy)-9H-purin-2-amine (129).....	222
N-(4-(2-(Pyrrolidin-1-yl)ethoxy)phenyl)-6-(cyclohexylmethoxy)-9H-purin-2-amine (130).....	223
N-(4-(2-(Piperidin-1-yl)ethoxy)phenyl)-6-(cyclohexylmethoxy)-9H-purin-2-amine (131).....	224
N-(4-(2-Morpholinoethoxy)phenyl)-6-(cyclohexylmethoxy)-9H-purin-2-amine (132).....	225
N-(4-(2-(Benzylamino)ethoxy)phenyl)-6-(cyclohexylmethoxy)-9H-purin-2-amine (133).....	225
N-(4-(2-(4-Methylpiperazin-1-yl)ethylthio)phenyl)-6-(cyclohexylmethoxy)-9H-purin-2- amine (134).....	228
N1-(6-(cyclohexylmethoxy)-9H-purin-2-yl)-N4-(2-(4-methylpiperazin-1- yl)ethyl)benzene-1,4-diamine (135)	232

6-(Cyclohexylmethoxy)-N-(4-(3-(4-methylpiperazin-1-yl)propyl)phenyl)-9H-purin-2-amine (136).....	230
(2-Chloroethyl)(4-nitrophenyl)sulfane (138).....	226
1-(2-(4-Nitrophenylthio)ethyl)-4-methylpiperazine (139).....	227
4-(2-(4-Methylpiperazin-1-yl)ethylthio)benzenamine (140).....	227
N-(2-(4-Methylpiperazin-1-yl)ethyl)-4-nitrobenzenamine (142).....	231
N1-(2-(4-Methylpiperazin-1-yl)ethyl)benzene-1,4-diamine (143).....	231
1-(3-Chloropropyl)-4-nitrobenzene (145).....	228
1-Methyl-4-(3-(4-nitrophenyl)propyl)piperazine (146).....	229
1-Methyl-4-(3-(4-nitrophenyl)propyl)piperazine (147).....	229
N-(4-(2-(3,4-Dihydroisoquinolin-2(1H)-yl)ethoxy)phenyl)-6-(cyclohexylmethoxy)-9H-purin-2-amine (148).....	248
N-(4-(2-(Isoindolin-2-yl)ethoxy)phenyl)-6-(cyclohexylmethoxy)-9H-purin-2-amine (149).....	249
N-(4-((1-Benzylpiperidin-3-yl)oxy)phenyl)-6-(cyclohexylmethoxy)-9H-purin-2-amine (150).....	253
2-(2-(4-Nitrophenoxy)ethyl)isoindoline (151).....	246
2-(2-(4-Nitrophenoxy)ethyl)-1,2,3,4-tetrahydroisoquinoline (152).....	246
4-(2-(Isoindolin-2-yl)ethoxy)benzenamine (153).....	247
4-(2-(3,4-Dihydroisoquinolin-2(1H)-yl)ethoxy)benzenamine (154).....	247
tert-Butyl 4-((1-benzylpiperidin-3-yl)oxy)phenylcarbamate (157).....	252
3-Aminopiperidin-2-one (167).....	249
3-Diazo-piperidin-2-one (168).....	250
tert-Butyl 4-(2-oxopiperidin-3-yloxy)phenylcarbamate (169).....	251
tert-Butyl 4-(2-oxopiperidin-3-yloxy)phenylcarbamate (170).....	251
N-(4-((2-(4-Methylpiperazin-1-yl)ethylsulfonyl)methyl)phenyl)-6-(cyclohexylmethoxy)-9H-purin-2-amine (174).....	236
Benzyl(2-chloroethyl)sulfane (176).....	233
1-((2-Chloroethylsulfonyl)methyl)benzene (177).....	233
1-((2-Chloroethylsulfonyl)methyl)-4-nitrobenzene (178).....	234
1-(2-(4-Nitrobenzylsulfonyl)ethyl)-4-methylpiperazine (179).....	234
4-((2-(4-methylpiperazin-1-yl)ethylsulfonyl)methyl)benzenamine (180).....	235
N-(4-(2-(4-Methylpiperazin-1-yl)ethylsulfonyl)phenyl)-9H-purin-2-amine (183).....	238

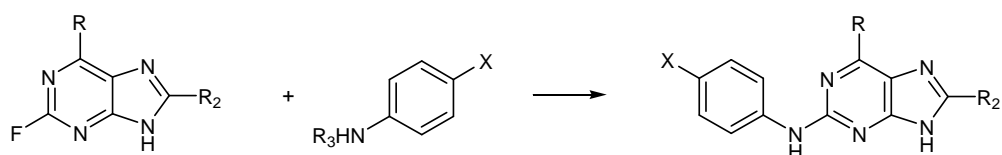
6-Chloro-2-fluoro-9H-purine (184).....	236
2-Fluoro-9H-purine (185).....	237
N-(4-(2-Cyclohexylethylsulfonyl)phenyl)-6-(cyclohexylmethoxy)-9H-purin-2-amine (188).....	217
(2-Cyclohexylethyl)(4-nitrophenyl)sulfane (189).....	215
1-(2-Cyclohexylethylsulfonyl)-4-nitrobenzene (190).....	215
6-(Cyclohexylmethoxy)-8-methyl-N-(4-(2-(4-methylpiperazin-1-yl)ethylsulfonyl)phenyl)-9H-purin-2-amine (192).....	245
6-(Cyclohexylmethoxy)pyrimidine-2,4-diamine (194).....	242
6-(Cyclohexylmethoxy)-5-nitrosopyrimidine-2,4-diamine (195).....	242
N-(2-Amino-6-(cyclohexylmethoxy)-5-nitrosopyrimidin-4-yl)acetamide (196).....	243
6-(Cyclohexylmethoxy)-8-methyl-9H-purin-2-amine (197).....	244
6-(Cyclohexylmethoxy)-2-fluoro-8-methyl-9H-purine (198).....	244
6-(Cyclohexylmethoxy)-8-methyl-N-(4-(2-(4-methylpiperazin-1-yl)ethoxy)phenyl)-9H- purin-2-amine (199).....	261
6-(Cyclohexylmethoxy)-8-ethyl-N-(4-(2-(4-methylpiperazin-1-yl)ethoxy)phenyl)-9H- purin-2-amine (200).....	262
6-(Cyclohexylmethoxy)-8-isopropyl-N-(4-(2-(4-methylpiperazin-1-yl)ethoxy)phenyl)- 9H-purin-2-amine (201).....	263
6-(Cyclohexylmethoxy)-2-fluoro-9-(tetrahydro-2H-pyran-2-yl)-9H-purine (202).....	257
6-(Cyclohexylmethoxy)-2-fluoro-8-methyl-9-(tetrahydro-2H-pyran-2-yl)-9H-purine (203).....	257
6-(Cyclohexylmethoxy)-2-fluoro-8-ethyl-9-(tetrahydro-2H-pyran-2-yl)-9H-purine (204).....	258
6-(Cyclohexylmethoxy)-2-fluoro-8-isopropyl-9-(tetrahydro-2H-pyran-2-yl)-9H-purine (205).....	259
6-(Cyclohexylmethoxy)-2-fluoro-8-methyl-9H-purine (206).....	260
6-(Cyclohexylmethoxy)-2-fluoro-8-ethyl-9H-purine (207).....	260
6-(Cyclohexylmethoxy)-2-fluoro-8-isopropyl-9H-purine (208).....	261
4-(2-Cyclohexylethylsulfonyl)benzenamine.....	216
1-(Benzyloxy)-3-methylbutan-2-ol (211).....	238
6-(1-(Benzyloxy)-3-methylbutan-2-yloxy)-9H-purin-2-amine (212).....	239
6-(1-(Benzyloxy)-3-methylbutan-2-yloxy)-2-fluoro-9H-purine (213).....	240

6-(1-(Benzyloxy)-3-methylbutan-2-yloxy)-N-(4-(2-(4-methylpiperazin-1-yl)ethylsulfonyl)phenyl)-9H-purin-2-amine (214).....	241
Pyrazolo[1,5-a]pyrimidine-5,7(4H,6H)-dione (232).....	254
5,7-Dichloropyrazolo[1,5-a]pyrimidine (233).....	254
5-Chloro-N-(4-((2-(4-methylpiperazin-1-yl)ethyl)sulfonyl)phenyl)pyrazolo[1,5-a]pyrimidin-7-amine (234).....	255
5-(Cyclohexylmethoxy)-N-(4-((2-(4-methylpiperazin-1-yl)ethyl)sulfonyl)phenyl)pyrazolo[1,5-a]pyrimidin-7-amine (229).....	256

7.5 General Procedures

Several related compounds have been synthesised using similar procedures. These general protocols are described below. All experiments were conducted under an inert atmosphere (N_2 or Ar), unless otherwise stated. Any variation to these specifications is indicated within the synthetic procedure and analytical characterisation of a specific compound.

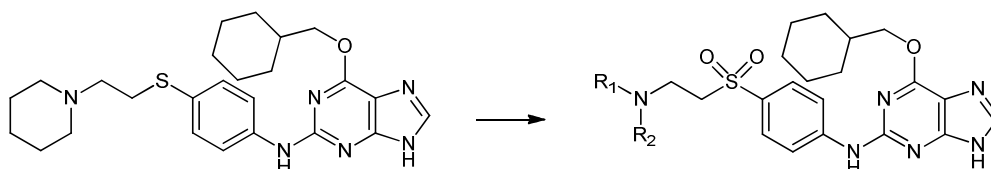
7.5.1 General procedure I: TFA/TFE coupling of anilines to fluoropurines



R = H or *o*-cyclohexylmethyl;
R₂ = H or *tert*-butoxycarbonyl;
R₃ = H, methyl, ethyl or isopropyl;
X = Sidechain.

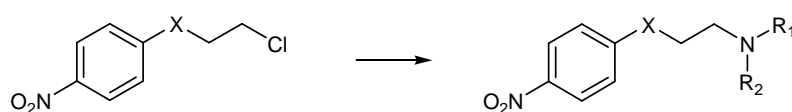
To a stirred solution of the appropriate free or Boc-protected aniline (2 equiv.) in a 5% solution of TFA in TFE (5 mL) was added the appropriate 2-fluoropurine (1 equiv.). The reaction mixture was heated to reflux and stirred for 48 h. The mixture was concentrated under reduced pressure, and the residue was taken up in saturated aqueous $NaHCO_3$ (15 mL) and extracted with CH_2Cl_2 (2 x 15 mL). The combined organic layers were dried over Na_2SO_4 and evaporated, and the crude product was purified by column chromatography on either silica or KP-NH FLASH+ cartridges. In some cases further purification by preparative HPLC ($CH_3CN/0.1\%$ aqueous formic acid 1:1) was required to obtain the title compound as a white solid.

7.5.2 General procedure II: Solution-Phase Library Synthesis of 6-(cyclohexylmethoxy)-*N*-(4-((2-aminoethyl)sulfonyl)phenyl)-9*H*-purin-2-amines



To a stirred solution of 6-(cyclohexylmethoxy)-*N*-(4-(2-(piperidin-1-yl)ethylthio)phenyl)-7*H*-purin-2-amine (**59**) (100 mg, 0.21 mmol) in CH₂Cl₂ (5 mL) was added *m*CPBA (170 mg, 1.0 mmol) and the reaction was stirred at room temperature for 5 min. The appropriate amine (1.29 mmol) was added and the reaction mixture was stirred at room temperature for 18 h. The reaction mixture was diluted with CH₂Cl₂ (30 mL) and washed with saturated aqueous NaHCO₃ (2 x 30 mL), dried over Na₂SO₄ and concentrated under reduced pressure to yield a crude product that was purified by flash chromatography on KP-NH silica cartridges (EtOAc or EtOAc/MeOH 9:1).

7.5.3 General procedure III: Solution-phase library synthesis of 4-nitroarylethyleneamines

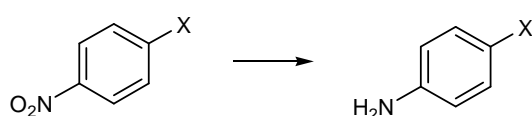


X = O, NH, S, CH₂, CH₂SO₂

In a microwave vial, to a stirred solution of the appropriate chloride (1 equiv.) in acetonitrile (10 mL) was added the appropriate amine (6 equiv.). The reaction mixture was heated for 30 min at 140 °C under micro wave irradiation. The mixture

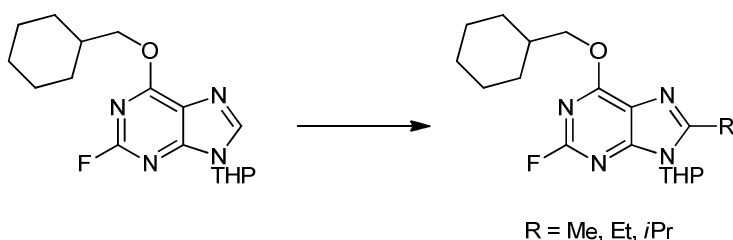
was concentrated under reduced pressure and the residue was taken up in water (20 mL) and extracted with CH_2Cl_2 (2 x 30 mL). The combined organic layers were dried over Na_2SO_4 and evaporated. Unless otherwise stated, the product obtained was used in the following step without further purification.

7.5.4 General procedure IV: Catalytic hydrogenation of nitroarenes



To a stirred solution of the appropriate nitrobenzene derivative in MeOH (25 mL) was added a catalytic amount of palladium on activated carbon (10% w/w). The system was stirred at room temperature under a hydrogen atmosphere for 18 h. The reaction mixture was filtered through a pad of celite and the filtrate was evaporated *in vacuo* to yield the desired product in quantitative yield and without need for further purification unless otherwise stated.

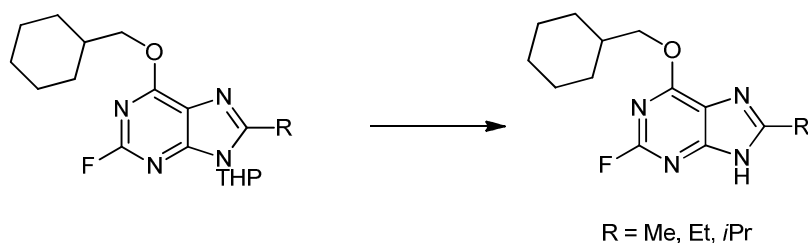
7.5.5 General procedure V: 8-alkylation of purines



To a stirred solution of diisopropylamine in THF (1.5 mL) at -78°C was added *n*BuLi (2.5 M in hexane). The mixture was stirred at -78°C for 5 minutes before adding dropwise to a stirred solution of 6-(cyclohexylmethoxy)-2-fluoro-9-(tetrahydro-2H-

pyran-2-yl)-9*H*-purine (**55**) in THF (2.5 mL) at -78 °C. After 5 minutes, a solution of MeI in THF (1 mL) was added dropwise, and the mixture was allowed to warm up to room temperature and stirred for 18 h. The mixture was concentrated under reduced pressure and the crude product was purified by flash chromatography on silica (EtOAc/Hexane 3:7).

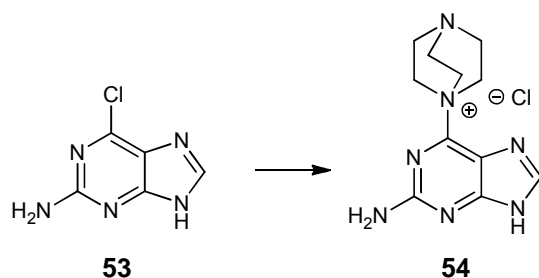
7.5.6 General procedure VI: Deprotection of 9-THP purines



To a solution of the starting purine in 5 mL of isopropanol were added 0.5 mL TFA and 0.5 mL water. The solution was heated at 75 °C for 2 h. The mixture was concentrated under reduced pressure and the crude product was purified by flash chromatography on silica (EtOAc/Hexane 1:1).

7.6 Experimental procedures

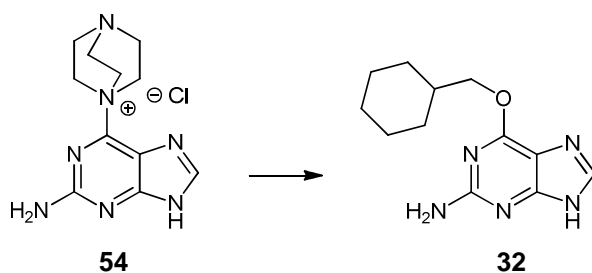
1-(2-Amino-(*H*-purin-6-yl)-4-aza-1-azoniabicyclo[2.2.2]octane chloride (**54**)²⁵⁴



DABCO (6.6 g, 0.58 mol) was added to a solution of 2-amino-6-chloropurine (**54**) (5 g, 0.29 mol) in DMSO (75 mL) and the mixture was stirred at room temperature for 18 h. The precipitate formed was filtered, washed with ether and dried to give the title compound as a white solid (10.5 g, 100%).

mp: decomposes at 230 °C; ¹H NMR (300 MHz, D₂O) δ 3.37 (6H, t, *J* = 10 Hz, N(CH₂)₃), 4.15 (3H, t, *J* = 10 Hz, N⁺(CH₂)₃), 8.17 (1H, s, H-8); ¹³C NMR (75 MHz, D₂O) δ 38.7 (NCH₂), 53.4 (NCH₂), 116.0, 143.7, 151.2, 158.2 (C-2).

6-Cyclohexylmethoxy-9*H*-purin-2-ylamine (**32**)²⁵⁴

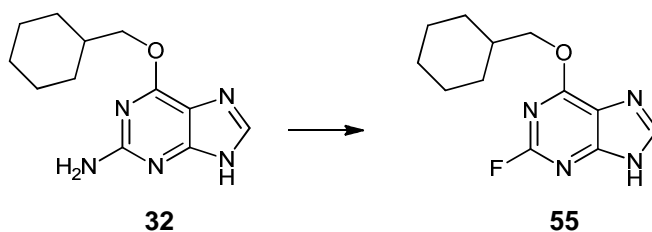


Cyclohexylmethanol (17.6 mL, 0.14 mol) was added dropwise to a suspension of NaH (2.6 g, 0.10 mol) in DMSO (50 mL), and the mixture was stirred at room temperature for 1 h. **54** (9.9 g, 0.34 mol) was added in portions and the mixture was stirred at room temperature for 24 h. The reaction was quenched with water (250

mL) and glacial acetic acid was added until pH neutral. The white precipitate formed was filtered, washed with water and ether and dried, yielding the title compound as a white solid (6.9 g, 84%).

R_f = 0.41 (EtOAc/MeOH 9:1); m.p.: 195-197 °C ^1H NMR (300 MHz, DMSO) δ 1.21 (5H, m, cyclohexyl), 1.74 (6H, m, cyclohexyl), 4.21 (2H, d, J = 6 Hz, CH_2O), 6.21 (2H, s, NH_2), 7.81 (1H, s, H-8); ^{13}C NMR (75 MHz, DMSO) δ 25.6, 26.4, 29.6, 37.2, 70.8 ($\text{CH}_2\text{-O}$), 153.3, 142.9, 159.3 (C-2), 160.1 (C-O); MS(ES+) m/z 248.2 $[\text{M} + \text{H}]^+$.

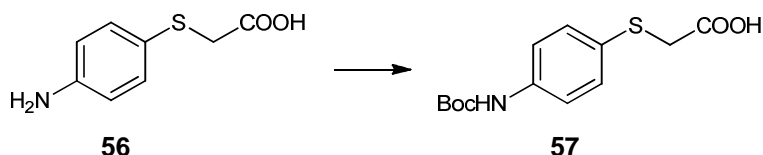
6-Cyclohexylmethoxy-2-fluoro-9H-purine (55)⁹⁵



A 50% (w/w) aqueous solution of HBF_4 (40 mL) was brought to -5 °C. **32** (6.9 g, 0.28 mol) was then added in one portion. NaNO_2 (4.2 g, 0.76 mol) was dissolved in water (50 mL) and added dropwise, ensuring that the temperature remained below 0 °C. The temperature was raised to 20 °C and the mixture was stirred for 18 h. The solution was neutralised with Na_2CO_3 and the resulting precipitate was filtered and stirred in EtOAc (3 x 100 mL). The combined filtrates were concentrated under reduced pressure, yielding the title compound as a white solid (2.3 g, 35%).

R_f = 0.45 (EtOAc/MeOH 9:1); m.p.: 173-175 °C ^1H NMR (300 MHz, DMSO) δ 1.20 (5H, m, cyclohexyl), 1.79 (6H, m, cyclohexyl), 4.33 (2H, d, J = 6 Hz, CH_2O), 8.38 (1H, s, H-8); ^{13}C NMR (75 MHz, DMSO) δ 24.5, 25.8, 30.1, 36.8, 72.9 ($\text{CH}_2\text{-O}$), 154.5, 144.2, 160.1 (C-2), 162.0 (C-O), 168.0 (C-F); MS(ES+) m/z 251.2 $[\text{M} + \text{H}]^+$.

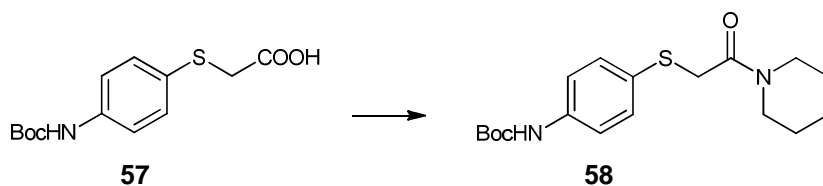
2-(4-(*Tert*-butoxycarbonylamino)phenylthio)acetic acid (**57**)²⁵⁵



To 2-(4-aminophenylthio)acetic acid (5.0 g, 0.27 mol) in a 2:1 mixture of dioxane and water (75 mL) was added triethylamine (7.2 mL, 0.54 mol), followed by di-*tert*-butyl dicarbonate (11.9 g, 0.54 mol). The reaction mixture was stirred at room temperature for 18 h. The mixture was concentrated under reduced pressure and 3 M HCl was added until pH neutral. The resulting precipitate was filtered, washed with water and dried, yielding the title compound as a light yellow solid (7.2 g, 93%).

R_f = 0.54 (EtOAc/MeOH 9:1); m.p.: 153-155 °C ^1H NMR (300 MHz, DMSO) δ 1.47 (9H, s, *t*Bu), 3.66 (2H, s, SCH₂), 7.30 (2H, d, J = 10 Hz, Ar-H), 7.40 (2H, d, J = 10 Hz, Ar-H), 9.42 (1H, s, NH); ^{13}C NMR (75 MHz, DMSO) δ 28.4, 36.9, 79.5, 127.6, 130.7, 138.7, 153.0, 175.5 (NHCO), 181.1 (COOH); MS(ES+) m/z 284.5 [M + H]⁺.

Tert-butyl 4-(2-oxo-2-(piperidin-1-yl)ethylthio)phenylcarbamate (**58**)¹⁶⁷

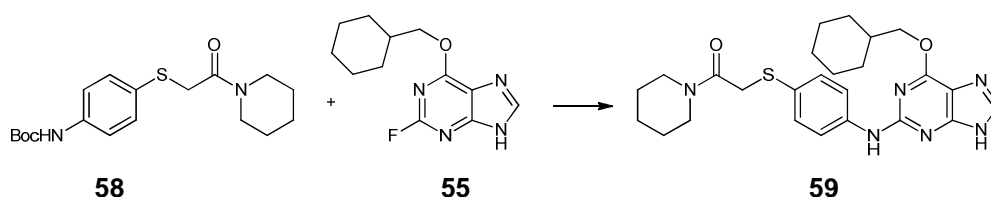


To 2-(4-(*tert*-butoxycarbonylamino)phenylthio)acetic acid (9.85 g, 0.25 mol) in THF (25 mL) was added thionyl chloride (17.6 mL, 0.38 mol), followed by DMF (0.1 mL). The mixture was stirred for 3 h at room temperature, then concentrated under reduced pressure and the residue was taken up in THF (25 mL). The resulting solution was added dropwise to piperidine (10 mL, 0.10 mol) in THF (10 mL). The mixture was stirred for 18 h at room temperature, concentrated under reduced

pressure and the residue was dissolved in CH₂Cl₂ (30 mL). The solution was washed with brine (30 mL) and the organic phase was dried over Na₂SO₄ and evaporated to give an orange oil. The crude product was purified by flash chromatography using a gradient solvent system (EtOAc/Hexane 3:7 → 1:1), yielding the title compound as a white solid (5.4 g, 77%).

R_f = 0.31 (EtOAc/MeOH 9:1); mp: 118-120 °C; IR (cm⁻¹) 3233, 3048, 2940, 2162, 1697, 1593; ¹H NMR (300 MHz, CDCl₃) δ 1.43 (9H, s, *t*Bu), 1.54 (6H, m, piperidine), 3.32 (2H, t, J = 6 Hz, NCH₂), 3.46 (2H, t, J = 6 Hz, NCH₂), 3.60 (2H, s, SCH₂), 6.80 (1H, s, NH), 7.26 (2H, d, J = 9 Hz, Ar-H), 7.31 (2H, d, J = 9 Hz, Ar-H); ¹³C NMR (75 MHz, CDCl₃) δ 24.7, 25.9, 26.8, 28.7, 38.4, 43.5, 48.0, 81.0, 119.3, 128.1, 132.9, 138.7, 153.0 (CONR₂), 167.4 (NHCOO*t*Bu); MS(ES+) m/z 351.2 [M + H]⁺.

2-(4-(6-(Cyclohexylmethoxy)-7*H*-purin-2-ylamino)phenylthio)-1-(piperidin-1-yl)ethanone (59)¹⁶⁷

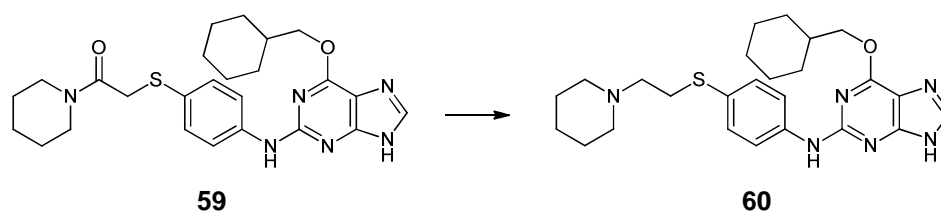


The compound was prepared according to General Procedure I from *tert*-butyl 4-(2-oxo-2-(piperidin-1-yl)ethylthio)phenylcarbamate (3.6 g, 0.10 mol) and 6-(cyclohexylmethoxy)-2-fluoro-9*H*-purine (1.3 g, 0.05 mol). The crude product was purified by flash chromatography on silica (EtOAc/MeOH 9:1), yielding the title compound as an off-white solid (1.4 g, 61%).

R_f = 0.41 (EtOAc/MeOH 9:1); mp: 198-200 °C; IR (cm⁻¹) 3302, 2916, 1580, 1592, 1447; ¹H NMR (300 MHz, CDCl₃) δ 1.05-1.85 (17H, m, cyclohexyl + piperidine), 3.40 (2H, t, J = 6 Hz, NCH₂), 3.49 (2H, t, J = 6 Hz, NCH₂), 3.81 (2H, s, SCH₂), 4.33 (2H, d, J = 6 Hz, CH₂O), 7.34 (2H, d, J = 9 Hz, Ar-H), 7.81 (2H, d, J = 9 Hz, Ar-H), 7.99 (1H, s, H-8), 9.41 (1H, s, NH); ¹³C NMR (75 MHz, CDCl₃) δ 25.5, 25.7, 26.3, 29.6,

37.2, 37.6, 42.6, 47.0, 71.4, 119.1, 131.6, 155.5 (purine C-2), 166.5 (CONR₂); MS(ES+) *m/z* 481.8 [M + H]⁺.

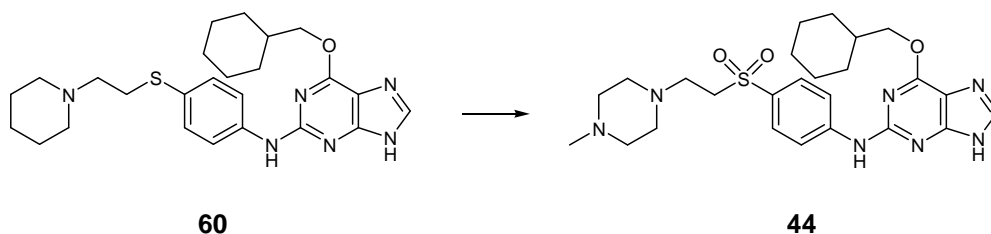
6-(Cyclohexylmethoxy)-*N*-(4-(2-(piperidin-1-yl)ethylthio)phenyl)-7*H*-purin-2-amine (60) ¹⁶⁷



To 2-(4-(6-(cyclohexylmethoxy)-9*H*-purin-2-ylamino)phenylthio)-1-(piperidin-1-yl)ethanone (1.4 g, 0.29 mol) in anhydrous THF (20 mL) cooled to 0 °C was added LiAlH₄ (1M in THF, 6 mL, 0.05 mol) dropwise. The reaction mixture was allowed to warm to room temperature and stirred for 3 h. The mixture was quenched adding dropwise: water (0.2 mL), 15% (w/v) aqueous NaOH (0.2 mL) and water (0.6 mL). The resulting grey suspension was stirred for 30 min. The white precipitate was filtered through a pad of celite and the filtrate was evaporated to give an oil. This was taken up in CH₂Cl₂ (20 mL) and the solution was washed with water (2 x 20 mL), dried over Na₂SO₄, evaporated and the resulting beige solid was purified by flash chromatography (CH₂Cl₂/MeOH 95:5), yielding the title compound as an off-white solid (0.8 g, 60%).

*R*_f = 0.25 (EtOAc/MeOH 9:1); mp: 125-126 °C; ¹H NMR (300 MHz, CDCl₃) δ 1.08-1.68 (11H, m, cyclohexyl), 1.75-1.86 (6H, m, piperidine), 2.39 (2H, t, *J* = 6 Hz, NCH₂), 2.52 (2H, t, *J* = 6 Hz, NCH₂), 2.65 (2H, t, *J* = 6 Hz, NCH₂), 2.94 (2H, t, *J* = 6 Hz, SCH₂), 4.24 (2H, d, *J* = 6 Hz, CH₂O), 7.21 (2H, d, *J* = 9 Hz, Ar-H), 7.42 (2H, d, *J* = 9 Hz, Ar-H), 8.02 (1H, s, H-8), 9.36 (1H, s, NH); ¹³C NMR (75 MHz, CDCl₃) δ 24.4, 25.5, 25.9, 26.4, 29.6, 32.2, 37.3, 54.2, 58.5, 71.5, 119.5, 126.9, 131.0, 140.3, 155.7 (purine C-2); MS(ES+) *m/z* 467.2 [M + H]⁺.

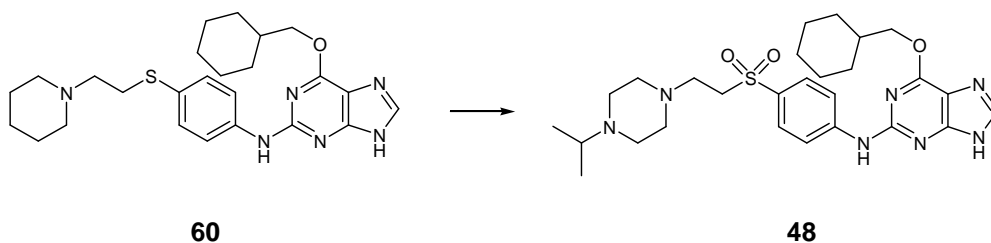
6-(Cyclohexylmethoxy)-*N*-(4-((2-(4-methylpiperazin-1-yl)ethyl)sulfonyl)phenyl)-9*H*-purin-2-amine (44).



Compound **44** was prepared from *N*-methylpiperazine (0.14 mL, 1.29 mmol) according to General Procedure II and was obtained as an off-white solid (92 mg, 75%).

R_f = 0.28 (EtOAc/MeOH 9:1); mp: 135-137 °C; IR (cm^{-1}) 2926, 2844, 1590, 1535, 1499, 1444; λ_{max} (EtOH)/nm: 312; ^1H NMR (300 MHz, CDCl_3) δ 0.78-1.18 (5H, m, cyclohexyl), 1.65-1.84 (6H, m, cyclohexyl), 2.18 (3H, s, NMe), 2.37 (8H, m, piperazine ring), 2.73 (2H, t, J = 7 Hz, CH_2N), 3.29 (2H, t, J = 7 Hz, CH_2SO_2), 4.27 (2H, d, J = 6 Hz, CH_2Cy), 7.41 (1H, s, NH), 7.72 (2H, d, J = 9 Hz, Ar-H), 7.76 (2H, d, J = 9 Hz, Ar-H), 7.83 (1H, s, H-8); ^{13}C NMR (75 MHz, CDCl_3) δ 26.0, 26.7, 30.1, 37.6, 46.0, 51.6, 52.8, 54.1, 55.0, 72.9, 115.6, 118.0, 129.6, 130.8, 139.6, 145.8, 155.1, 161.1; MS(ES+) m/z 514.3 [$\text{M} + \text{H}$] $^+$; anal. calcd for $\text{C}_{25}\text{H}_{35}\text{N}_7\text{O}_3\text{S}$: C, 58.46, H, 6.87, N, 19.09%; found: C, 58.65, H, 6.49, N, 19.11%.

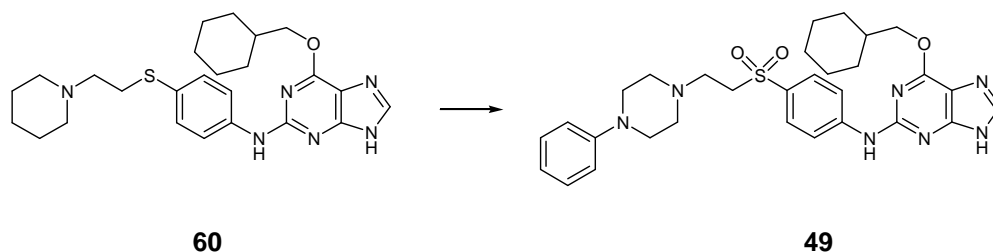
6-(Cyclohexylmethoxy)-*N*-(4-((2-(4-isopropylpiperazin-1-yl)ethyl)sulfonyl)phenyl)-9*H*-purin-2-amine (48).



Compound **48** was prepared from *N*-isopropylpiperazine (0.19 mL, 1.29 mmol) according to General Procedure II and was obtained as an off-white solid (90 mg, 51%).

R_f = 0.16 (EtOAc/MeOH 9:1); mp: 110-112 °C; IR (cm^{-1}) 2924, 2851, 1589, 1531, 1496, 1446; λ_{max} (EtOH)/nm 313; ^1H NMR (300 MHz, CDCl_3) δ 1.0 (6H, d, J = 6 Hz, $\text{CH}(\text{CH}_3)_2$), 1.27-1.78 (11H, m, cyclohexyl), 2.50 (8H, m, piperazine), 2.71 (1H, septet, J = 6 Hz, $\text{CH}(\text{CH}_3)_2$), 2.80 (2H, t, J = 7 Hz, CH_2N), 3.31 (2H, t, J = 7 Hz, CH_2SO_2), 4.33 (2H, d, J = 6 Hz, CH_2Cy), 7.61 (1H, s, NH), 7.78 (2H, d, J = 9 Hz, Ar-H), 7.82 (2H, d, J = 9 Hz, Ar-H), 7.93 (1H, s, H-8); ^{13}C NMR (75 MHz, CDCl_3) δ 18.8, 27.3, 28.0, 31.2, 39.1, 46.5, 53.0, 53.8, 54.6, 56.2, 73.6, 119.1, 130.7, 132.0, 141.7, 148.1, 157.1, 161.7; MS(ES+) m/z 542.4 $[\text{M} + \text{H}]^+$; anal. calcd for $\text{C}_{27}\text{H}_{39}\text{N}_7\text{O}_3\text{S}$: C, 59.86, H, 7.26, N, 18.10%; found: C, 59.68, H, 7.01, N, 16.25%.

6-(Cyclohexylmethoxy)-*N*-(4-((2-(4-phenylpiperazin-1-yl)ethyl)sulfonyl)phenyl)-9*H*-purin-2-amine (49).

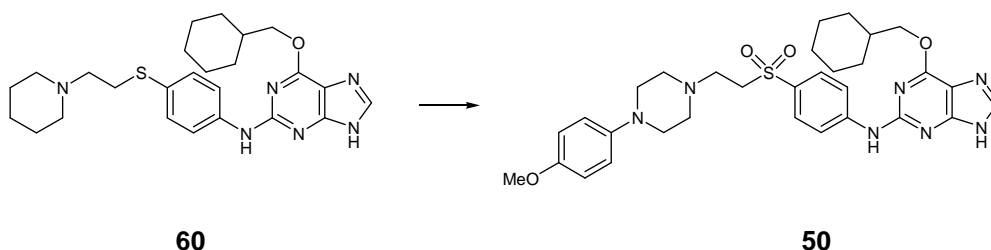


Compound **49** was prepared from *N*-phenylpiperazine (0.195 mL, 1.29 mmol) according to General Procedure II and was obtained as a light yellow solid (125 mg, 92%).

R_f = 0.27 (EtOAc); mp: 140-142 °C; IR (cm^{-1}): 2925, 2848, 1591, 1531, 1495, 1448; λ_{max} (EtOH)/nm: 312.5; ^1H NMR (300 MHz, CDCl_3): δ 1.00-1.81 (11H, m, cyclohexyl), 2.47 (4H, t, J = 5 Hz, NCH_2), 2.77 (2H, t, J = 7 Hz, CH_2N), 3.02 (4H, t, J = 5 Hz, NCH_2), 3.28 (2H, t, J = 7 Hz, CH_2SO_2), 4.26 (2H, d, J = 6 Hz, CH_2Cy), 6.77 (2H, t, J = 8 Hz, Ar-H), 7.14 (2H, t, J = 7 Hz, Ar-H), 7.75 (6H, m, Ar-H + H-8); ^{13}C NMR (125 MHz, CDCl_3): δ 5.1, 8.2, 9.0, 15.1, 18.5, 25.7, 26.4, 29.8, 37.3, 48.7, 48.9,

49.1, 51.5, 52.9, 72.7, 76.8, 77.1, 77.3, 100.0, 109.0, 116.2, 117.9, 120.1, 129.22, 129.5, 145.3, 151.0, 154.9; MS(ES+) m/z 576.3 $[M + H]^+$; anal. calcd for $C_{30}H_{37}N_7O_3S$: C, 62.59, H, 6.48, N, 17.03%; found: C, 62.58, H, 6.47, N, 17.01%.

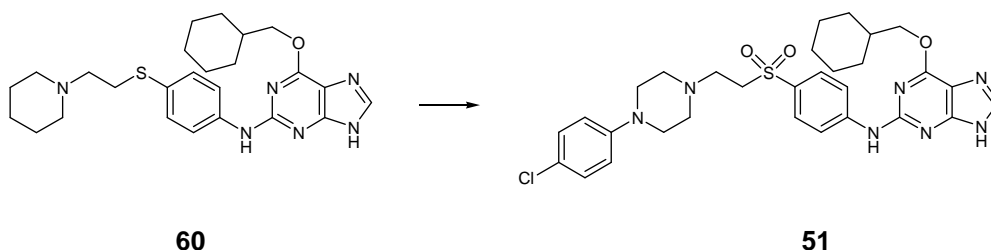
6-(Cyclohexylmethoxy)-*N*-(4-((2-(4-(4-methoxyphenyl)piperazin-1-yl)ethyl)sulfonyl)phenyl)-9*H*-purin-2-amine (50).



Compound **50** was prepared from 1-(4-methoxyphenyl)piperazine (0.245 g, 1.29 mmol) according to General Procedure II and was obtained as a yellow solid (122 mg, 91%).

R_f = 0.30 (EtOAc); mp: 185-187 °C; IR (cm^{-1}): 2927, 2848, 2158, 2023, 1980, 1591, 1531, 1496, 1448; λ_{max} (EtOH)/nm : 313; 1H NMR (300 MHz, $CDCl_3$): δ 1.11-1.92 (11H, m, cyclohexyl), 2.57 (4H, t, J = 5 Hz, NCH_2), 2.89 (2H, t, J = 7 Hz, CH_2N), 3.00 (4H, t, J = 5 Hz, NCH_2), 3.37 (2H, t, J = 7 Hz, CH_2SO_2), 3.75 (3H, s, OMe), 4.35 (2H, d, J = 6 Hz, CH_2Cy), 6.82 (2H, d, J = 9 Hz, Ar-H), 6.86 (2H, d, J = 9 Hz, Ar-H), 7.40 (1H, s, NH), 7.83 (2H, d, J = 9 Hz, Ar-H), 7.87 (2H, d, J = 9 Hz, Ar-H), 7.95 (1H, s, H-8); ^{13}C NMR (125 MHz, $CDCl_3$): δ 25.7, 26.4, 29.8, 37.3, 48.8, 50.4, 51.4, 52.9, 53.8, 55.6, 66.5, 72.7, 76.9, 114.5, 117.8, 118.4, 129.4, 130.8, 145.4, 154.1, 154.9; MS(ES+) m/z 606.4 $[M + H]^+$; anal. calcd for $C_{31}H_{39}N_7O_4S$: C, 61.47, H, 6.49, N, 16.19%; found: C, 61.18, H, 6.41, N, 16.01%.

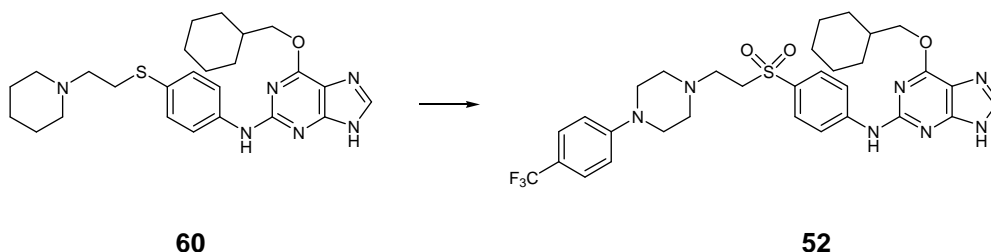
***N*-(4-((2-(4-(4-Chlorophenyl)piperazin-1-yl)ethyl)sulfonyl)phenyl)-6-(cyclohexylmethoxy)-9*H*-purin-2-amine (51).**



Compound **51** was prepared from 1-(4-chlorophenyl)piperazine (0.250 g, 1.29 mmol) according to General Procedure II and was obtained as a light yellow solid (102 mg, 84%).

R_f = 0.23 (EtOAc); mp: 149-151 °C; IR (cm^{-1}): 2924, 1726, 1591, 1532, 1494, 1449; λ_{max} (EtOH)/nm: 292; ^1H NMR (300 MHz, CDCl_3): δ 1.14-1.95 (11H, m, cyclohexyl), 2.55 (4H, t, J = 5 Hz, NCH_2), 2.86 (2H, t, J = 8 Hz, CH_2N), 3.06 (4H, t, J = 5 Hz, NCH_2), 3.35 (2H, t, J = 8 Hz, CH_2SO_2), 4.37 (2H, d, J = 6 Hz, CH_2Cy), 6.80 (2H, d, J = 9 Hz, Ar-H), 7.19 (2H, d, J = 9 Hz, Ar-H), 7.35 (1H, s, NH), 7.83 (2H, d, J = 9 Hz, Ar-H), 7.87 (2H, d, J = 9 Hz, Ar-H), 10.0 (1H, s, H-8); ^{13}C NMR (125 MHz, CDCl_3): δ 15.0, 19.0, 21.0, 21.5, 23.0, 25.7, 26.4, 29.8, 37.3, 48.9, 49.0, 51.4, 52.6, 53.8, 60.5, 64.5, 72.6, 117.4, 117.8, 124.9, 129.0, 129.4, 129.6, 130.7, 145.5, 149.6, 154.8; MS(ES+) m/z 610.3 [$\text{M}(^{35}\text{Cl}) + \text{H}$] $^+$, 612.3 [$\text{M}(^{37}\text{Cl}) + \text{H}$] $^+$; anal. calcd for $\text{C}_{30}\text{H}_{36}\text{ClN}_7\text{O}_3\text{S}$: C, 59.05, H, 5.95, N, 16.07%; found: C, 59.08, H, 6.15, N, 16.03%.

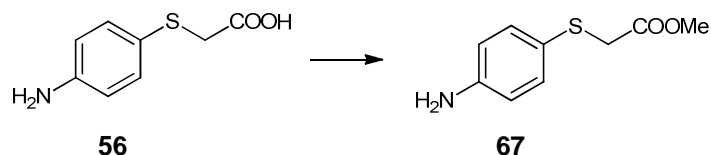
6-(Cyclohexylmethoxy)-*N*-(4-((2-(4-(4-(trifluoromethyl)phenyl)piperazin-1-yl)ethyl)sulfonyl)phenyl)-9*H*-purin-2-amine (52).



Compound **52** was prepared from 1-(4-(trifluoromethyl)phenyl)piperazine (0.30 g, 1.29 mmol) according to General Procedure II and was obtained as a yellow solid (120 mg, 95%).

R_f = 0.28 (EtOAc); mp: 160-162 °C; IR (cm^{-1}) 2937, 2338, 2112, 2083, 1596, 1524, 1494, 1448; λ_{max} (EtOH)/nm: 292; ^1H NMR (500 MHz, CDCl_3): δ 1.28-1.78 (11H, m, cyclohexyl), 2.56 (4H, t, J = 5 Hz, NCH_2), 2.87 (2H, t, J = 8 Hz, CH_2N), 3.19 (4H, t, J = 5 Hz, NCH_2), 3.36 (2H, t, J = 8 Hz, CH_2SO_2), 4.38 (2H, d, J = 6 Hz, CH_2Cy), 6.89 (2H, d, J = 9 Hz, Ar-H), 7.33 (1H, s, NH), 7.48 (2H, d, J = 8.7, Ar-H), 7.83 (2H, d, J = 9 Hz, Ar-H), 7.87 (2H, d, J = 9 Hz, Ar-H), 9.58 (1H, s, H-8). ^{13}C NMR (125 MHz, CDCl_3): δ 15.2, 18.7, 25.7, 26.4, 29.8, 37.3, 47.8, 48.8, 51.4, 52.6, 53.9, 66.5, 66.7, 72.7, 76.8, 77.1, 77.3, 114.7, 117.8, 121.0, 124.5, 126.4, 129.4, 130.9, 145.3, 153.1, 154.9; MS(ES+) m/z 644.3 $[\text{M} + \text{H}]^+$; anal. calcd for $\text{C}_{31}\text{H}_{36}\text{F}_3\text{N}_7\text{O}_3\text{S}$: C, 57.84, H, 5.69, N, 14.38%; found: C, 57.69, H, 5.69, N, 14.38%.

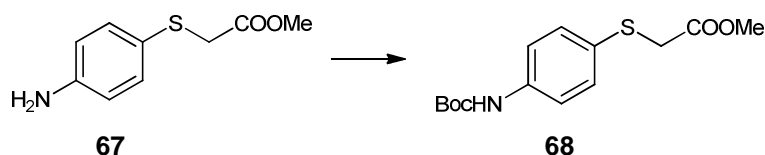
Methyl 2-(4-aminophenylthio)acetate (**67**)²⁵⁶



To a stirred solution of 2-(4-aminophenylthio)acetic acid (4 g, 14 mmol) in MeOH (50 mL) at 0 °C was added thionyl chloride (5 mL, 70 mmol). After 10 min at 0 °C, the reaction mixture was heated to reflux and stirred for 4 h. The mixture was concentrated under reduced pressure and the residue was taken up in saturated aqueous NaHCO_3 (30 mL) and extracted with EtOAc (2 x 30 mL). The combined organic layers were dried over Na_2SO_4 and evaporated to yield the title compound as a light yellow solid (4.1 g, 99%).

R_f = 0.35 (EtOAc/Hexane 2:3); mp: 166-170 °C ^1H NMR (300 MHz, CDCl_3) δ 3.39 (2H, s, SCH_2), 3.67 (3H, s, COOMe), 6.53 (2H, d, J = 9 Hz, Ar-H), 7.21 (2H, d, J = 9 Hz, Ar-H); ^{13}C NMR (125 MHz, CDCl_3) δ 32.1, 51.2, 115.4, 126.4, 142.1, 170.4; MS(ES+) m/z 199.0 $[\text{M} + \text{H}]^+$.

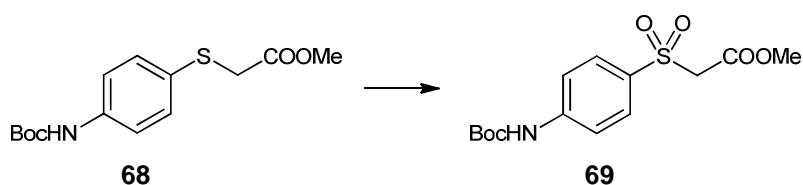
Methyl 2-(4-(*tert*-butoxycarbonylamino)phenylthio)acetate (68) ²⁵⁷⁻²⁵⁸



To a stirred solution of methyl-2-(4-aminophenylthio)acetate (400 mg, 2 mmol) in a 2:1 solution of dioxane and water (15 mL) was added triethylamine (0.5 mL, 4 mmol), then di-*tert*-butyldicarbonate (873 mg, 4 mmol). The mixture was stirred at room temperature for 18 h. The mixture was concentrated under reduced pressure and 3 M HCl was added until pH neutral. The resulting white precipitate was filtered, washed with water and dried, to give the title compound as a white solid (610 mg, 99%).

R_f = 0.35 (EtOAc/Hexane 2:3); mp: 146-149 °C ^1H NMR (300 MHz, CDCl_3) δ 3.47 (2H, s, SCH_2), 3.57 (3H, s, COOMe), 7.03 (2H, d, J = 9 Hz, Ar-H), 7.81 (2H, d, J = 9 Hz, Ar-H); ^{13}C NMR (125 MHz, CDCl_3) δ 28.4, 33.0, 52.8, 116.6, 122.5, 144.4, 172.7; MS(ES+) m/z 298.7 $[\text{M} + \text{H}]^+$.

Methyl 2-(4-(*tert*-butoxycarbonylamino)phenylsulfonyl)acetate (69) ²⁵⁷⁻²⁵⁸

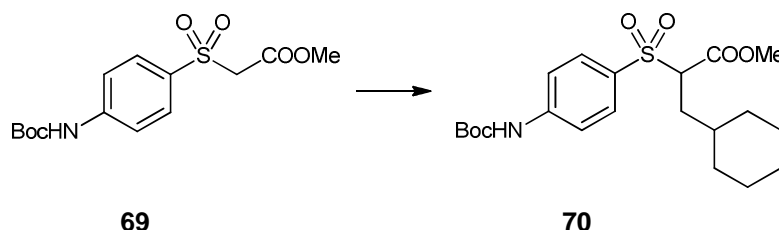


To a stirred solution of methyl 2-(4-(*tert*-butoxycarbonylamino)phenylthio) acetate (400 mg, 1.35 mmol) in CH_2Cl_2 (10 mL) was added *m*CPBA (1.2 g, 6 mmol). The mixture was stirred at room temperature for 2 h. The mixture was concentrated under reduced pressure and the residue was taken up in EtOAc (15 mL) and washed with saturated aqueous NaHCO_3 (2 x 20 mL). The organic layer was dried over

Na₂SO₄ and evaporated. The crude product was purified by column chromatography (EtOAc/Hexane 1:2) to yield the title compound as a white solid (300 mg, 75%).

R_f = 0.35 (EtOAc/Hexane 2:3); mp: 158-160 °C ¹H NMR (300 MHz, CDCl₃) δ 3.72 (2H, s, SCH₂), 4.11 (3H, s, COOMe), 6.99 (2H, d, *J* = 9 Hz, Ar-H), 7.91 (2H, d, *J* = 9 Hz, Ar-H); ¹³C NMR (125 MHz, CDCl₃) δ 28.4, 33.0, 52.8, 79.7, 118.2, 128.5, 132.1, 143.0, 152.7; MS(ES+) *m/z* 330.9 [M + H]⁺.

Methyl 2-(4-(*tert*-butoxycarbonylamino)phenylsulfonyl)-3-cyclohexylpropanoate (70)

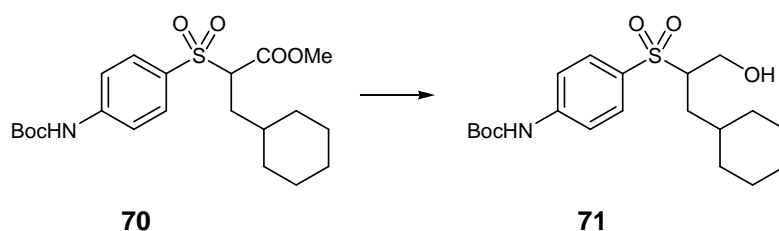


To stirred methyl 2-(4-(*tert*-butoxycarbonylamino)phenylsulfonyl) acetate (200 mg, 0.6 mmol) in DMF (10 mL) at 0°C was added NaH (14 mg, 0.6 mmol). After 10 min, (bromomethyl)cyclohexane (0.33 mL, 2.4 mmol) was added and the mixture was allowed to warm up to room temperature and stirred for 18 h. Saturated aqueous NH₄Cl (25 mL) was added and the mixture was extracted with Et₂O (2 x 30 mL). The combined organic layers were dried over Na₂SO₄ and evaporated. The crude product was purified by medium pressure column chromatography (EtOAc/Hexane 2:3) to give the title compound as a white solid (154 mg, 61%).

R_f = 0.8 (EtOAc/Hexane 2:3); mp: decomposes > 211.7 °C; IR (cm⁻¹) 2924, 2850, 2333, 2360, 1737, 1579, 1523, 1446; λ_{max} (EtOH)/nm: 245.5; ¹H NMR (300 MHz, CDCl₃) δ 0.89-1.85 (13H, m, CH₂Cy + Cy), 3.72 (3H, s, COOMe), 4.03 (1H, dd, *J* = 10; 4 Hz, SO₂CH), 6.92 (1H, s, NH), 7.57 (2H, d, *J* = 9 Hz, Ar-H), 7.76 (2H, d, *J* = 9 Hz, Ar-H); ¹³C NMR (125 MHz, CDCl₃): δ 25.5, 25.6, 25.9, 26.2, 29.4, 33.2, 37.3, 47.8, 68.8, 71.9, 113.4, 117.3, 127.4, 130.0, 139.9, 146.9, 155.1, 155.3, 160.0,

167.2; MS(ES+) m/z 426.3 $[M + H]^+$; anal. calcd for $C_{21}H_{31}NO_6S$: C, 59.27, H, 7.34, N, 3.29%; found: C, 59.29, H, 7.38, N, 3.28%.

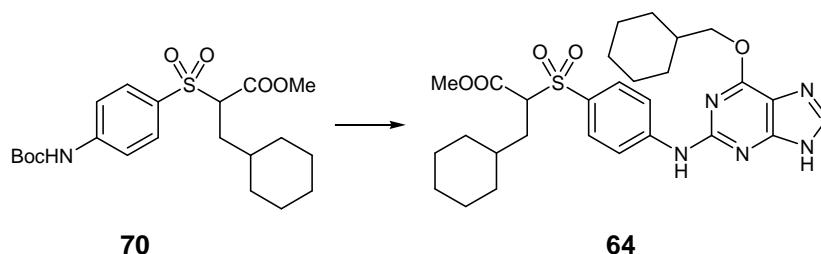
[4-(1-Cyclohexyl-3-hydroxy-propane-2-sulfonyl)-phenyl]-carbamic acid *tert*-butyl ester (71)



To stirred methyl 2-(4-(*tert*-butoxycarbonylamino)phenylsulfonyl)-3-cyclohexylpropanoate (100 mg, 0.2 mmol) in THF (5 mL) at $-78\text{ }^{\circ}\text{C}$ was added 1 M DIBAH in THF (0.25 mL, 0.2 mmol). After 3 h of stirring at $-78\text{ }^{\circ}\text{C}$, the reaction mixture was allowed to warm to room temperature. DIBAH (0.77 mL) was added and the reaction mixture was stirred for 18 h. Saturated aqueous potassium sodium tartrate (70 mL) was added to the mixture, which was extracted with CH_2Cl_2 (6 x 50 mL). The combined organic layers were dried over Na_2SO_4 and evaporated. The crude product was purified by medium pressure column chromatography (EtOAc/Hexane 1:2) and the title compound was isolated as a white solid (56 mg, 55%).

R_f = 0.5 (EtOAc/Hexane 2:3); mp: $251.1\text{--}252.6\text{ }^{\circ}\text{C}$; IR (cm^{-1}) 2900, 2842, 2633, 2450, 1700, 1580, 1577, 1540, 1484; λ_{max} (EtOH)/nm: 245.0; ^1H NMR (300 MHz, CDCl_3) δ 0.68–1.64 (13H, m, $\text{CH}_2\text{Cy} + \text{Cy}$), 3.00 (1H, t, $J = 5\text{ Hz}$, OH), 3.10 (1H, m, SO_2CH), 3.82 (2H, t, $J = 5\text{ Hz}$, CH_2OH), 7.06 (1H, s, NH), 7.60 (2H, d, $J = 9\text{ Hz}$, Ar-H), 7.86 (2H, d, $J = 9\text{ Hz}$, Ar-H); ^{13}C NMR (125 MHz, CDCl_3): δ 25.5, 25.6, 25.9, 26.2, 29.4, 33.2, 37.3, 47.8, 68.8, 71.9, 113.4, 117.3, 127.4, 130.0, 139.9, 146.9, 155.1, 155.3, 160.0, 167.18; MS(ES+) m/z 398.5 $[M + H]^+$; anal. calcd for $\text{C}_{20}\text{H}_{31}\text{NO}_5\text{S}$: C, 60.43, H, 7.86, N, 3.52%; found: C, 59.69, H, 7.88, N, 3.58%.

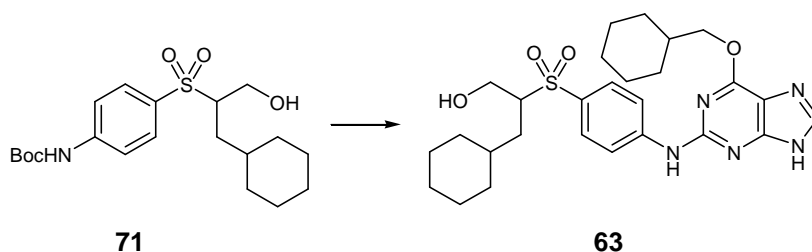
3-Cyclohexyl-2-[4-(6-cyclohexylmethoxy-9H-purin-2-ylamino)-benzenesulfonyl]-propionic acid methyl ester (64)



The compound was prepared according to General Procedure I from methyl 2-(4-(*tert*-butoxycarbonylamino)phenylsulfonyl)-3-cyclohexylpropanoate (500 mg, 1.18 mmol) and 6-cyclohexylmethoxy-2-fluoro-9H-purine (150 mg, 0.6 mmol). The crude product was purified by flash chromatography on silica (EtOAc) and then by preparative HPLC (CH₃CN/0.1% aqueous formic acid 1:1). The title compound was isolated as a white solid (51 mg, 32%).

R_f = 0.28 (EtOAc/MeOH 9:1); mp: decomposes >211 °C; IR (cm⁻¹): 2924, 2850, 2333, 2360, 1737, 1579, 1523, 1446; λ_{max} (EtOH)/nm: 315; ¹H NMR (300 MHz, CD₃OD) δ 1.0-2.05 (25H, m, 2 x cyclohexyl + CyCH₂CHSO₂), 3.66 (3H, s, COOMe), 4.15 (1H, dd, J = 11; 4 Hz, SO₂CHCOOMe), 4.40 (2H, d, J = 6 Hz, OCH₂Cy), 7.73 (1H, d, J = 9 Hz, Ar-H), 8.06 (2H, d, J = 9 Hz, Ar-H), 8.10 (1H, s, H-8); ¹³C NMR (125 MHz, CDCl₃) δ 25.5, 25.6, 25.9, 26.2, 29.4, 33.2, 37.3, 47.8, 68.8, 71.9, 113.4, 117.3, 127.4, 130.0, 139.9, 146.9, 155.1, 155.3, 160.0, 167.1; MS(ES+) m/z 556.5 [M + H]⁺; HRMS calcd for C₂₈H₂₆NO₃S [M + H]⁺ 556.2588, found 556.2589.

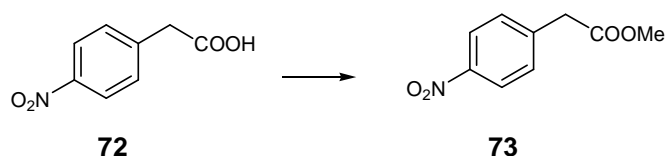
3-Cyclohexyl-2-[4-(6-cyclohexylmethoxy-9H-purin-2-ylamino)-benzenesulfonyl]-propan-1-ol (63)



The compound was prepared according to General Procedure I from [4-(1-cyclohexyl-3-hydroxy-propane-2-sulfonyl)-phenyl]-carbamic acid tert-butyl ester (270 mg, 0.68 mmol) and 6-cyclohexylmethoxy-2-fluoro-9*H*-purine (170 mg, 0.68 mmol). The crude product was purified by flash chromatography on silica (EtOAc) and then by preparative HPLC (CH₃CN/0.1% aqueous formic acid 1:1). The title compound was isolated as a white solid (54 mg, 39%).

R_f = 0.28 (EtOAc/MeOH 9:1); mp: decomposes >236.1 °C; IR (cm⁻¹): IR: 3329, 3146, 2921, 2850, 1580, 1529, 1496, 1446; λ_{max} (EtOH)/nm: 313.5; ¹H NMR (300 MHz, CD₃OD) δ 1.0-1.96 (25H, m, 2 x cyclohexyl + CyCH₂CHSO₂), 3.21 (1H, m, SO₂CHCH₂OH), 3.83 (2H, dd, J = 12; 5 Hz, CH₂OH), 3.87 (2H, dd, J = 12; 5 Hz, CH₂OH), 4.39 (2H, d, J = 6 Hz, OCH₂Cy), 7.78 (1H, d, J = 9 Hz, Ar-H), 8.08 (2H, d, J = 9 Hz, Ar-H), 8.10 (1H, s, H-8); ¹³C NMR (125 MHz, CDCl₃) δ 15.0, 15.1, 15.9, 16.2, 19.4, 23.2, 27.3, 37.1, 58.2, 61.0, 65.8, 103.0, 107.3, 117.5, 120.4, 129.5, 136.9, 145.1, 155.1, 159.2; MS(ES+) m/z 528.5 [M + H]⁺; HRMS calcd for C₂₇H₃₇N₅O₄S [M + H]⁺ 528.2639, found 528.2639.

(4-Nitro-phenyl)-acetic acid methyl ester (73) ²⁵⁹

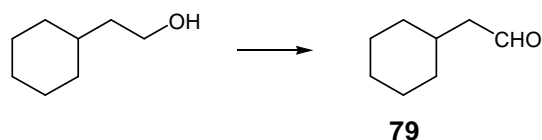


To a stirred solution of (4-nitro-phenyl)-acetic acid (5 g, 27 mmol) in methanol (50 mL) at 0 °C was added thionyl chloride (9.2 mL, 124 mmol). After 10 min at 0 °C, the reaction mixture was heated to reflux and stirred for 4 h. The mixture was concentrated under reduced pressure and the residue was taken up in saturated aqueous NaHCO₃ (25 mL) and extracted with EtOAc (2 x 25 mL). The combined organic layers were dried over Na₂SO₄ and evaporated to yield the title compound as a yellow solid (5.2 g, 99%).

R_f = 0.25 (EtOAc/MeOH 9:1); mp: 53-55 °C; ¹H NMR (300 MHz, CDCl₃) δ 3.70 (3H, s, COOMe), 3.74 (2H, s, CH₂COOMe), 7.45 (2H, d, J = 9 Hz, Ar-H), 8.16 (2H, d, J =

9 Hz, Ar-H); ^{13}C NMR (75 MHz, CDCl_3) δ 45.1, 53.3, 128.8, 129.9, 134.1, 135.1, 168.2; MS(ES+) m/z 197.2 $[\text{M} + \text{H}]^+$.

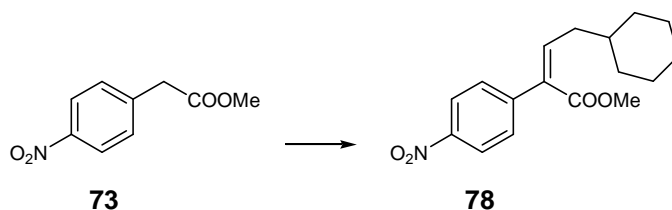
2-Cyclohexylacetaldehyde (**79**)²⁶⁰



To a stirred solution of 2-cyclohexylethanol (0.5 mL, 3.6 mmol) in CH_2Cl_2 (5 mL) was added PCC (1.5 g, 7.2 mmol). The mixture was stirred at room temperature for 3 h. The reaction mixture was diluted with ether (35 mL) and stirred vigorously for 30 min, then filtered over a pad of celite. The filtrate was washed with saturated aqueous NaHCO_3 (2 x 20 mL) and dried over Na_2SO_4 before evaporating the solvent. The crude product was purified by taking up in EtOAc (50 mL), filtering through a pad of silica and then evaporating the filtrate, affording the title compound as a colourless oil (485 mg, 76%).

R_f = 0.25 (EtOAc/Hexane 1:9); bp: 90-100 $^\circ\text{C}$; ^1H NMR (300 MHz, CDCl_3) δ 0.9-1.65 (11H, m, cyclohexyl), 2.01 (2H, d, J = 4.5 Hz, CH_2CHO), 9.7 (1H, s, CHO); ^{13}C NMR (75 MHz, CDCl_3) δ 26.6, 36.7, 51.0, 201.5; MS(ES+) m/z 127.2 $[\text{M} + \text{H}]^+$.

4-Cyclohexyl-2-(4-nitro-phenyl)-but-2-enoic acid methyl ester (**78**)

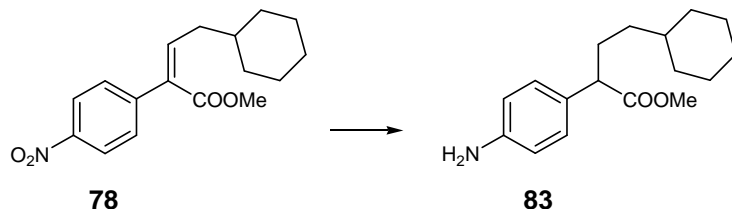


In a microwave vial, to a stirred solution of (4-nitro-phenyl)-acetic acid methylester (900 mg, 4.6 mmol) in CH_3CN (5 mL) at 0 $^\circ\text{C}$ was added cyclohexylacetaldehyde (3.5 g, 27 mmol) and tetramethylguanidine (0.02 mL, 0.01 mmol). The reaction

mixture was heated for 1 h at 120 °C under microwave irradiation. 3 M HCl was added until pH < 4 and the mixture was diluted with water (20 mL) and extracted with CH₂Cl₂ (2 x 25 mL). The combined organic layers were dried over Na₂SO₄ and evaporated. The crude product was purified by medium pressure column chromatography (EtOAc/Hexane 2:3) and the title compound was obtained as a yellow solid (0.9 g, 54%).

R_f = 0.8 (EtOAc/Hexane 1:3); mp: 211 °C; IR (cm⁻¹): 2924, 2851, 1589, 1531, 1497, 1445; λ_{max} (EtOH)/nm: 275; ¹H NMR (300 MHz, CDCl₃) δ 0.9-1.9 (11H, m, cyclohexyl), 2.23 (2H, d, J = 7.5 Hz, CHCH₂Cy), 3.76 (3H, s, COOMe), 7.22 (1H, t, J = 7.5 Hz, CHCH₂Cy), 7.34 (2H, d, J = 9 Hz, Ar-H), 8.23 (2H, d, J = 9 Hz, Ar-H); ¹³C NMR (125 MHz, CDCl₃) δ 21.4, 27.3, 28.0, 31.2, 39.1, 42.7, 47.5, 53.0, 53.6, 54.1, 54.6, 73.6, 119.2, 130.7, 131.4, 148.1, 157.1, 171.9; MS(ES+) m/z 307.0 [M + H]⁺; HRMS calcd for C₁₇H₂₁NO₄ [M + H]⁺ 307.2544, found 307.2543.

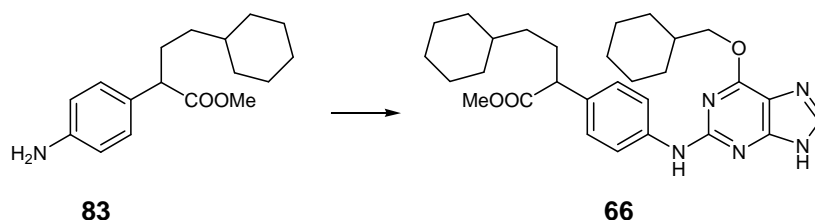
2-(4-Amino-phenyl)-4-cyclohexyl-butyric acid methyl ester (83)



The compound was prepared according to General Procedure IV from 4-cyclohexyl-2-(4-nitro-phenyl)-but-2-enoic acid methyl ester (1.5 g, 5 mmol), and was obtained as a yellow oil (1.2 g, 99%).

R_f = 0.8 (EtOAc/Hexane 1:3); IR (cm⁻¹): 2942, 2581, 1836, 1731, 1426; λ_{max} (EtOH)/nm 210; ¹H NMR (300 MHz, CDCl₃) δ 2.03-0.90 (11H, m, cyclohexyl), 2.23 (2H, d, J = 7.5 Hz, CHCH₂Cy), 3.39 (1H, t, J = 8 Hz, CHCOOMe), 3.64 (3H, s, COOMe), 6.68 (2H, d, J = 9 Hz, Ar-H), 7.10 (2H, d, J = 9 Hz, Ar-H), 7.22 (2H, s, NH₂); ¹³C NMR (125 MHz, CDCl₃) δ 25.4, 28.6, 30.0, 31.9, 33.3, 36.1, 50.5, 52.2, 116.6, 129.8, 145.3, 173.8; MS(ES+) m/z 276.7 [M + H]⁺; HRMS calcd for C₁₇H₂₅NO₂ [M + H]⁺ 276.7657, found 276.7651.

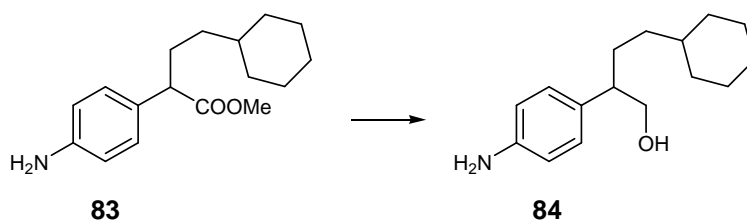
Methyl 4-cyclohexyl-2-(4-(6-(cyclohexylmethoxy)-9H-purin-2-ylamino)phenyl)butanoate (66)



The compound was prepared according to General Procedure I from 2-(4-amino-phenyl)-4-cyclohexyl-butyric acid methyl ester (500 mg, 1.8 mmol) and 6-(cyclohexylmethoxy)-2-fluoro-9H-purine (230 mg, 0.9 mmol). The crude product was purified by flash chromatography on silica (EtOAc) and then by semi-preparative HPLC (CH₃CN/water 1:1), yielding the title compound as a white solid (205 mg, 43%).

R_f = 0.2 (EtOAc/Hexane 1:1); mp: 110.0-111.7 °C; IR (cm⁻¹): 3107, 2922, 2848, 2212, 1730, 1583, 1526, 1446; λ_{max} (EtOH)/nm 274.0; ¹H NMR (300 MHz, CD₃OD) δ 1.79-1.05 (26H, m, 2 x cyclohexyl + 2 x CH₂), 3.40 (1H, t, J = 7 Hz, CHCOOMe), 3.59 (3H, s, COOMe), 4.23 (2H, d, J = 6 Hz, OCH₂Cy), 7.19 (2H, d, J = 9 Hz, Ar-H) 7.48 (2H, d, J = 9 Hz, Ar-H), 7.80 (1H, s, NH); ¹³C NMR (125 MHz, CDCl₃) δ 27.2, 27.7, 27.9, 28.1, 31.2, 32.3, 34.7, 34.8, 36.6, 39.1, 39.2, 52.6, 53.0, 73.4, 121.0, 129.4, 134.2, 140.8, 141.6, 158.3, 161.9, 177.0; MS(ES+) m/z 506.5 [M + H]⁺; HRMS calcd for C₂₉H₃₉N₅O₃ [M + H]⁺ 506.3126, found 506.3128.

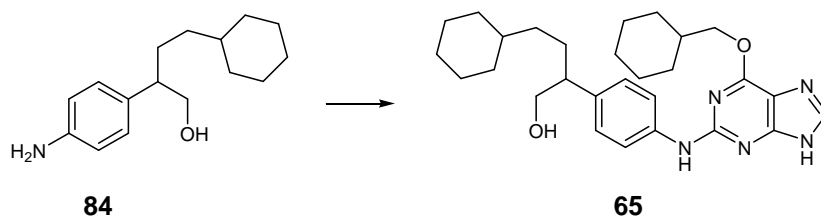
2-(4-Amino-phenyl)-4-cyclohexyl-butan-1-ol (84)



To a stirred solution of 2-(4-amino-phenyl)-4-cyclohexyl-butyric acid methyl ester (1 g, 3.6 mmol) in THF (10 mL) at -78 °C was added 1 M DIBALH in THF (11 mL, 11 mmol). The mixture was stirred at -78 °C for 3 h and then at room temperature for 16 h. Saturated aqueous sodium potassium tartrate (40 mL) was added to the mixture, which was extracted with CH₂Cl₂ (6 x 40 mL). The combined organic layers were dried over Na₂SO₄ and evaporated *in vacuo*, and the crude product was purified by medium pressure column chromatography (EtOAc/Hexane 1:1) yielding the title compound as a white solid (0.9 g, 89%).

R_f = 0.2 (EtOAc); IR (cm⁻¹): 2942, 2924, 2851, 2581, 1836, 1731, 1426; λ_{\max} (EtOH)/nm 211.5; ¹H NMR (300 MHz, CDCl₃) δ 0.68-1.64 (15H, m, Cy + 2 x CH₂), 2.45 (1H, m, CHCH₂OH), 2.00 (2H, s, NH₂), 3.64 (2H, m, CH₂OH), 6.67 (2H, d, J = 9 Hz, Ar-H), 6.99 (2H, d, J = 9 Hz, Ar-H); ¹³C NMR (125 MHz, CDCl₃) δ 24.8, 28.1, 29.3, 30.9, 32.1, 35.8, 50.0, 51.7, 65.9, 116.0, 129.1, 144.2; MS(ES+) m/z 248.3 [M + H]⁺; HRMS calcd for C₁₆H₂₅NO [M + H]⁺ 248.3487, found 248.3480.

4-Cyclohexyl-2-[4-(6-cyclohexylmethoxy-9H-purin-2-ylamino)-phenyl]-butan-1-ol (65)

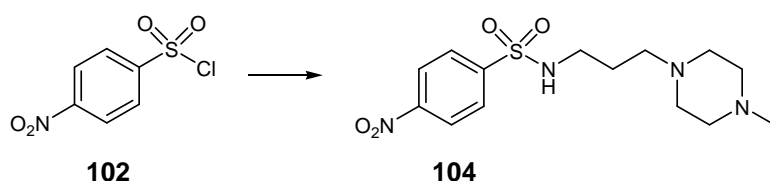


The compound was prepared according to General Procedure I from 2-(4-amino-phenyl)-4-cyclohexyl-butan-1-ol (200 mg, 0.8 mmol) and 6-(cyclohexylmethoxy)-2-fluoro-9H-purine (101 mg, 0.4 mmol). The crude product was purified by flash chromatography on silica (EtOAc) and then by preparative HPLC (CH₃CN/water 1:1), yielding the title compound as a white solid (105 mg, 42%).

R_f = 0.2 (EtOAc/Hexane 1:1); mp: 129.4-129.8 °C; IR (cm⁻¹): 3439, 2918, 2846, 2164, 1753, 1604, 1582, 1527, 1449; λ_{\max} (EtOH)/nm 272.0; ¹H NMR (300 MHz, CD₃OD) δ 0.72-1.83 (26H, m, 2 x cyclohexyl + CH₂CH₂Cy), 2.63 (1H, m, CHCH₂OH),

3.64 (2H, ddd, $J = 20; 10; 5$ Hz, CH_2OH), 4.24 (2H, d, $J = 6$ Hz, OCH_2Cy), 6.93 (1H, s, H-8), 7.09 (2H, d, $J = 9$ Hz, Ar-H), 7.41 (2H, d, $J = 9$ Hz, Ar-H); ^{13}C NMR (125 MHz, CDCl_3) δ 27.2, 27.8, 27.8, 27.9, 28.1, 31.0, 31.2, 34.7, 35.1, 36.6, 39.7, 39.5, 68.8, 68.8, 73.4, 78.7, 79.5, 121.2, 129.5, 138.5, 140.6; MS(ES+) m/z 478.7 $[\text{M} + \text{H}]^+$; HRMS calcd for $\text{C}_{28}\text{H}_{39}\text{N}_5\text{O}_2$ $[\text{M} + \text{H}]^+$ 478.3177, found 478.3178.

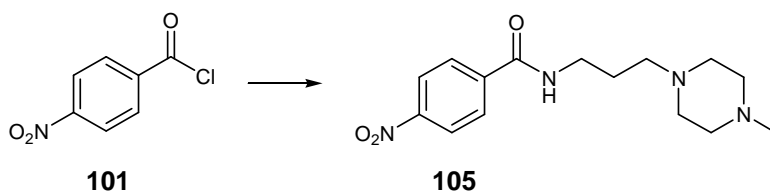
***N*-[3-(4-Methyl-piperazin-1-yl)-propyl]-4-nitro-benzenesulfonamide (104)**



To a stirred solution of *p*-nitro benzenesulfonyl chloride (2 g, 9 mmol) in CH_2Cl_2 (20 mL) at 0 °C was added K_2CO_3 (2.7 g, 19.8 mmol) and 3-(4-methyl-piperazin-1-yl)-propylamine (1.7 mL, 9.9 mmol). The reaction mixture was stirred at room temperature for 18 h. The mixture was filtered and the filtrates were combined, dried over Na_2SO_4 and evaporated *in vacuo* to yield the title compound as a yellow oil (2.8 g, 92%).

$R_f = 0.5$ (EtOAc/MeOH 9:1); ^1H NMR (300 MHz, CDCl_3) δ 1.60 (2H, t, $J = 6$ Hz, $\text{CH}_2\text{CH}_2\text{CH}_2$), 2.25 (3H, s, NMe), 2.38 (8H, m, piperazine), 2.40 (2H, t, $J = 6$ Hz, CH_2N), 3.05 (2H, t, $J = 6$ Hz, CH_2NH), 7.96 (2H, d, $J = 9$ Hz, Ar-H), 8.29 (2H, d, $J = 9$ Hz, Ar-H); ^{13}C NMR (125 MHz, CDCl_3) δ 28.4, 36.8, 53.7, 57.8, 66.5, 79.8, 117.4, 128.2, 128.3, 142.5, 152.9, 166.0; MS(ES+) m/z 343.9 $[\text{M} + \text{H}]^+$.

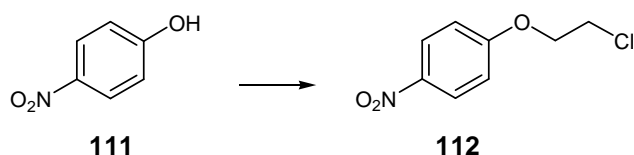
***N*-[3-(4-Methyl-piperazin-1-yl)-propyl]-4-nitro-benzamide (105)**



To a stirred solution of *p*-nitro benzoyl chloride (2 g, 10.8 mmol) in CH₂Cl₂ (20 mL) at 0 °C was added K₂CO₃ (3.3 g, 23.8 mmol) and 3-(4-methyl-piperazin-1-yl)-propylamine (2 mL, 11.8 mmol). The reaction mixture was stirred at room temperature for 18 h. The mixture was filtered and the filtrates were combined, dried over Na₂SO₄ and evaporated *in vacuo* to yield the title compound as a yellow oil (2.9 g, 94%).

*R*_f = 0.5 (EtOAc/MeOH 9:1); ¹H NMR (300 MHz, CDCl₃) δ 1.91 (2H, t, *J* = 6 Hz, CH₂CH₂CH₂), 2.34 (3H, s, NMe), 2.38 (8H, m, piperazine), 2.40 (2H, t, *J* = 6 Hz, CH₂N), 2.65 (8H, m, piperazine), 2.74 (2H, t, *J* = 6 Hz, CH₂N), 3.52 (2H, t, *J* = 6 Hz, CH₂NH), 8.04 (2H, d, *J* = 9 Hz, Ar-H), 8.57 (1H, s, NH); 8.20 (2H, d, *J* = 9 Hz, Ar-H); ¹³C NMR (125 MHz, CDCl₃) δ 28.4, 60.5, 69.3, 72.5, 79.8, 117.4, 128.1, 128.3, 142.5, 152.9, 166.1; MS(ES+) *m/z* 307.9 [M + H]⁺.

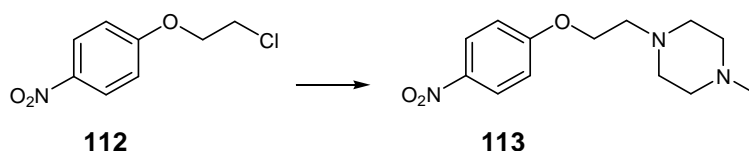
1-(2-Chloro-ethoxy)-4-nitro-benzene (112) ²⁶¹



To a stirred solution of *p*-nitro phenol (10 g, 72 mmol) in acetonitrile (100 mL) was added K₂CO₃ (25 g, 180 mmol) and dichloroethane (56 mL, 720 mmol). The mixture was heated to reflux and stirred for 48 h. The excess base was filtered and the filtrate was evaporated *in vacuo* to yield the title compound as a yellow solid (15 g, 99%).

*R*_f = 0.7 (EtOAc); mp: 63-64 °C ¹H NMR (300 MHz, CDCl₃) δ 3.79 (2H, t, *J* = 6 Hz, CH₂Cl), 4.26 (2H, t, *J* = 6 Hz, OCH₂), 6.91 (2H, d, *J* = 9 Hz, Ar-H), 8.14 (2H, d, *J* = 9 Hz, Ar-H); ¹³C NMR (125 MHz, CDCl₃) δ 40.4, 45.0, 110.6, 125.5, 140.4, 172.7; MS(ES+) *m/z* 202.7 [M + H]⁺.

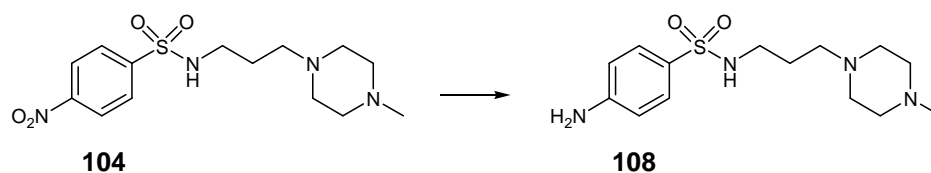
1-Methyl-4-[2-(4-nitro-phenoxy)-ethyl]-piperazine (113)²⁶²



The compound was prepared according to General Procedure III from 1-(2-chloroethoxy)-4-nitro-benzene (2 g, 10 mmol) and *N*-methyl piperazine (5.5 mL, 50 mmol), and was obtained as a yellow solid (2.8 g, 91%).

R_f = 0.5 (EtOAc/MeOH 9:1); ¹H NMR (300 MHz, CDCl₃) δ 2.22 (3H, s, NMe), 2.55-2.40 (8H, m, piperazine), 2.78 (2H, t, J = 6 Hz, CH₂N), 4.12 (2H, t, J = 6 Hz, OCH₂), 6.89 (2H, d, J = 9 Hz, Ar-H), 8.16 (2H, d, J = 9 Hz, Ar-H); ¹³C NMR (125 MHz, CDCl₃) δ 45.6, 47.0, 58.6, 60.8, 70.9, 115.5, 130.2, 145.8, 165.7; MS(ES+) m/z 266.7 [M + H]⁺.

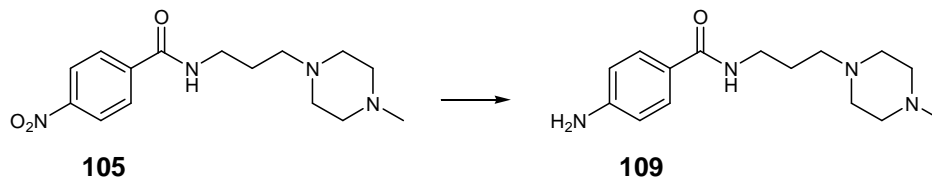
4-Amino-*N*-[3-(4-methyl-piperazin-1-yl)-propyl]-benzenesulfonamide (108)²⁶³



The compound was prepared according to General Procedure IV from *N*-[3-(4-methyl-piperazin-1-yl)-propyl]-4-nitro-benzenesulfonamide (2.5 g, 7.3 mmol), and was obtained as an orange oil (2.3 g, 99%).

R_f = 0.4 (EtOAc); ¹H NMR (300 MHz, CDCl₃) δ 1.53 (2H, t, J = 6 Hz, CH₂CH₂CH₂), 2.22 (3H, s, NMe), 2.31 (2H, t, J = 6 Hz, CH₂N), 2.40 (8H, m, piperazine), 2.92 (2H, t, J = 6 Hz, CH₂NH), 4.20 (2H, s, NH₂), 6.60 (2H, d, J = 9 Hz, Ar-H), 7.52 (2H, d, J = 9 Hz, Ar-H); ¹³C NMR (125 MHz, CDCl₃) δ 15.4, 28.5, 40.5, 44.3, 51.7, 59.1, 111.5, 120.5, 128.7, 140.3, 141.5, 159.8; MS(ES+) m/z 313.2 [M + H]⁺.

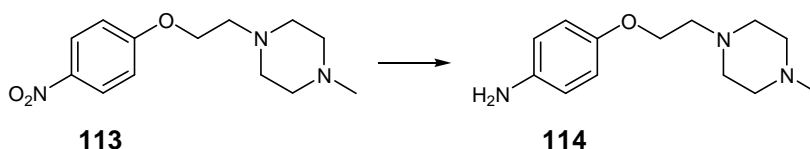
4-Amino-*N*-[3-(4-methyl-piperazin-1-yl)-propyl]-benzamide (109)²⁶⁴



The compound was prepared according to General Procedure IV from 4-[3-(4-methyl-piperazin-1-yl)-propyl]-4-nitro-benzamide (2.5 g, 8.2 mmol), and was obtained as an orange oil (2.3 g, 98%).

R_f = 0.4 (EtOAc); ^1H NMR (300 MHz, CDCl_3) δ 1.83 (2H, t, J = 6 Hz, $\text{CH}_2\text{CH}_2\text{CH}_2$), 2.42 (3H, s, NMe), 2.61 (2H, t, J = 6 Hz, CH_2N), 2.80 (8H, m, piperazine), 3.25 (2H, t, J = 6 Hz, CH_2NH), 3.40 (2H, s, NH_2), 6.60 (2H, d, J = 9 Hz, Ar-H), 7.58 (2H, d, J = 9 Hz, Ar-H); ^{13}C NMR (125 MHz, CDCl_3) δ 16.5, 29.5, 41.6, 43.2, 50.6, 58.0, 112.6, 121.6, 129.8, 139.2, 140.4, 158.7; MS(ES+) m/z 277.2 $[\text{M} + \text{H}]^+$.

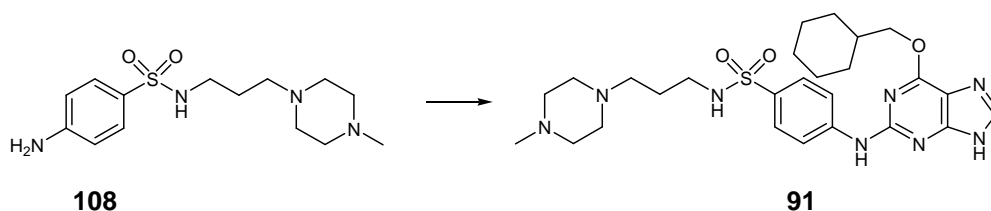
4-[2-(4-Methyl-piperazin-1-yl)-ethoxy]-phenylamine (114)²⁶⁵



The compound was prepared according to General Procedure IV from 1-methyl-4-[2-(4-nitro-phenoxy)-ethyl]-piperazine (2.5 g, 9.4 mmol), and was obtained as an orange oil (2.3 g, 99%).

R_f = 0.35 (EtOAc); ^1H NMR (300 MHz, CDCl_3) δ 2.23 (3H, s, NMe), 2.50 (8H, m, piperazine), 2.72 (2H, t, J = 6 Hz, CH_2N), 3.36 (2H, s, NH_2), 3.97 (2H, t, J = 6 Hz, OCH_2), 6.52 (2H, d, J = 9 Hz, Ar-H), 6.69 (2H, d, J = 9 Hz, Ar-H); ^{13}C NMR (125 MHz, CDCl_3) δ 44.5, 46.9, 57.5, 61.9, 71.0, 114.4, 131.3, 146.9, 167.8; MS(ES+) m/z 236.7 $[\text{M} + \text{H}]^+$.

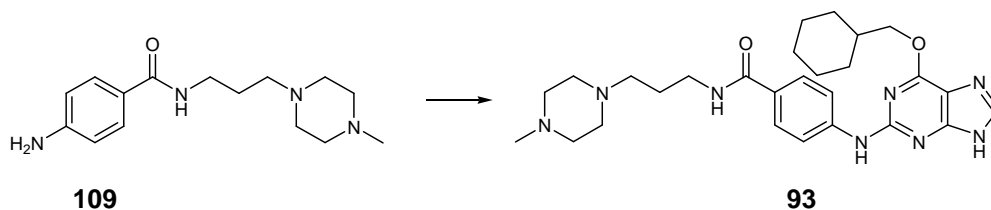
4-(6-(Cyclohexylmethoxy)-9H-purin-2-ylamino)-N-(3-(4-methylpiperazin-1-yl)propyl)benzenesulfonamide (91)



The compound was prepared according to General Procedure I from 4-amino-*N*-[3-(4-methyl-piperazin-1-yl)-propyl]-benzenesulfonamide (250 mg, 0.8 mmol) and 6-cyclohexylmethoxy-2-fluoro-9*H*-purine (100 mg, 0.4 mmol). The crude product was purified by flash chromatography on silica (EtOAc/MeOH 9:1) yielding the title compound as a white solid (105 mg, 42%).

R_f = 0.25 (EtOAc/MeOH 9:1); mp: 142.4-144.0 °C; IR (cm^{-1}): 2848, 1758, 1596, 1529, 1460, 1425; λ_{max} (EtOH)/nm 307.0; ^1H NMR (300 MHz, CDCl_3) δ 1.03-2.04 (13H, m, cyclohexyl + $\text{CH}_2\text{CH}_2\text{CH}_2$), 2.24 (3H, s, NMe), 2.34 (2H, t, J = 4 Hz, NCH_2), 2.31-2.50 (8H, m, piperazine), 2.98 (2H, t, J = 4 Hz, CH_2NHSO_2), 4.27 (2H, d, J = 6 Hz, OCH_2Cy), 7.38 (1H, s, NH), 7.74 (2H, d, J = 9 Hz, Ar-H), 7.70 (2H, d, J = 9 Hz, Ar-H), 7.78 (1H, s, H-8); ^{13}C NMR (125 MHz, CDCl_3) δ 25.6, 26.6, 26.7, 26.9, 30.3, 37.4, 43.2, 46.5, 53.8, 55.4, 57.0, 72.6, 118.3, 128.7, 132.9, 144.1, 155.3; MS(ES+) m/z 543.6 $[\text{M} + \text{H}]^+$; HRMS calcd for $\text{C}_{26}\text{H}_{38}\text{N}_8\text{O}_3\text{S}$ $[\text{M} + \text{H}]^+$ 543.2860, found 543.2855.

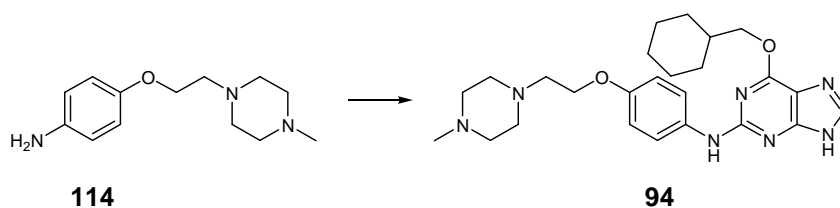
4-(6-(Cyclohexylmethoxy)-9H-purin-2-ylamino)-N-(3-(4-methylpiperazin-1-yl)propyl)benzamide (93)



The compound was prepared according to General Procedure I from 4-amino-*N*-[3-(4-methyl-piperazin-1-yl)-propyl]-benzamide (250 mg, 0.9 mmol) and 6-cyclohexylmethoxy-2-fluoro-9*H*-purine (113 mg, 0.45 mmol). The crude product was purified by flash chromatography on silica (EtOAc/MeOH 9:1) yielding the title compound as a white solid (102 mg, 42%).

R_f = 0.25 (EtOAc/MeOH 9:1); mp: 145.5-146.9 °C; IR (cm⁻¹): 3095, 2924, 2849, 2805, 2160, 1603, 1525, 1603, 1525, 1496, 1447; λ_{max} (EtOH)/nm 314.0; ¹H NMR (300 MHz, CDCl₃) δ 1.00-2.06 (13H, m, cyclohexyl + CH₂CH₂CH₂), 2.22 (3H, s, NMe), 2.48 (2H, t, J = 4 Hz, NCH₂), 2.41-2.63 (8H, m, piperazine), 3.46 (2H, t, J = 4 Hz, CH₂NH), 4.24 (2H, d, J = 6 Hz, OCH₂Cy), 7.37 (1H, s, NH), 7.67 (2H, d, J = 9 Hz, Ar-H), 7.71 (2H, d, J = 9 Hz, Ar-H), 7.76 (1H, s, NH), 8.10 (1H, s, H-8); ¹³C NMR (125 MHz, CDCl₃) δ 25.5, 26.0, 26.7, 30.1, 37.7, 40.5, 46.1, 53.4, 55.3, 57.9, 72.6, 115.6, 118.2, 128.4, 139.2, 143.7, 155.7, 161.2, 167.7; MS(ES+) m/z 507.6 [M + H]⁺; HRMS calcd for C₂₇H₃₈N₈O₂ [M + H]⁺ 507.3190, found 507.3189.

6-(Cyclohexylmethoxy)-*N*-(4-(2-(4-methylpiperazin-1-yl)ethoxy)phenyl)-9*H*-purin-2-amine (94)

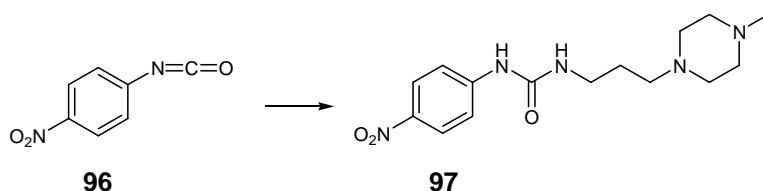


The compound was prepared according to General Procedure I from 4-(2-(4-methylpiperazin-1-yl)ethoxy)benzenamine (250 mg, 1 mmol) and 6-cyclohexylmethoxy-2-fluoro-9*H*-purine (133 mg, 0.5 mmol). The crude product was purified by flash chromatography on silica (EtOAc/MeOH 9:1) yielding the title compound as a white solid (106 mg, 44%).

R_f = 0.25 (EtOAc/MeOH 9:1); mp: 156.0-156.9 °C; IR (cm⁻¹): 3626, 3416, 2916, 2848, 2789, 2160, 1624, 1584, 1538, 1497, 1445, 1406; λ_{max} (EtOH)/nm 272.0; ¹H NMR (300 MHz, CDCl₃) δ 1.07-1.81 (11H, m, cyclohexyl), 2.23 (3H, s, NMe), 2.43-

2.57 (8H, m, piperazine), 2.74 (2H, t, $J = 6$ Hz, $\text{OCH}_2\text{CH}_2\text{N}$), 3.99 (2H, t, $J = 6$ Hz, $\text{OCH}_2\text{CH}_2\text{N}$), 4.21 (2H, d, $J = 6$ Hz, OCH_2Cy), 6.78 (2H, d, $J = 9$ Hz, Ar-H), 6.87 (1H, s, H-8), 7.05 (1H, s, NH), 7.34 (1H, d, $J = 9$ Hz, Ar-H); ^{13}C NMR (125 MHz, CDCl_3) δ 26.0, 26.7, 30.1, 37.7, 46.1, 53.7, 55.3, 57.5, 66.9, 72.4, 115.6, 122.6, 133.7, 138.2, 155.3, 157.0, 161.5; MS(ES+) m/z 466.6 $[\text{M} + \text{H}]^+$; HRMS calcd for $\text{C}_{25}\text{H}_{35}\text{N}_7\text{O}_2$ $[\text{M} + \text{H}]^+$ 466.2925, found 466.2923.

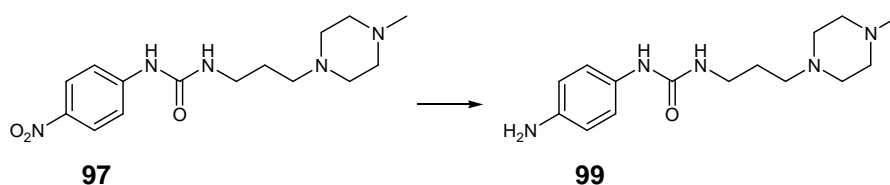
1-(3-(4-Methylpiperazin-1-yl)propyl)-3-(4-nitrophenyl)urea (97) ²⁶⁶



To a stirred solution of *p*-nitrophenyl isocyanate (2 g, 12.2 mmol) in THF (25 mL) was added 3-(4-methyl-piperazin-1-yl)-propylamine (2.7 mL, 16 mmol). The mixture was stirred at room temperature for 3 h. The solvent was evaporated *in vacuo* yielding the title compound as a yellow solid (3.5 g, 75%).

$R_f = 0.35$ (EtOAc/MeOH 9:1); mp: 97-100 °C ^1H NMR (300 MHz, CDCl_3) δ 1.64 (2H, t, $J = 6.5$ Hz, $\text{CH}_2\text{CH}_2\text{CH}_2$), 2.19 (3H, s, NMe), 2.34 (8H, m, piperazine), 3.27 (2H, t, $J = 6.5$ Hz, CH_2N), 3.69 (2H, t, $J = 6.5$ Hz, NHCH_2), 6.15 (1H, s, NH), 7.46 (2H, d, $J = 9$ Hz, Ar-H), 8.06 (2H, d, $J = 9$ Hz, Ar-H); ^{13}C NMR (125 MHz, CDCl_3) δ 26.5, 40.2, 43.3, 50.0, 52.6, 55.5, 121.1, 122.9, 142.7, 144.8; MS(ES+) m/z 322.2 $[\text{M} + \text{H}]^+$.

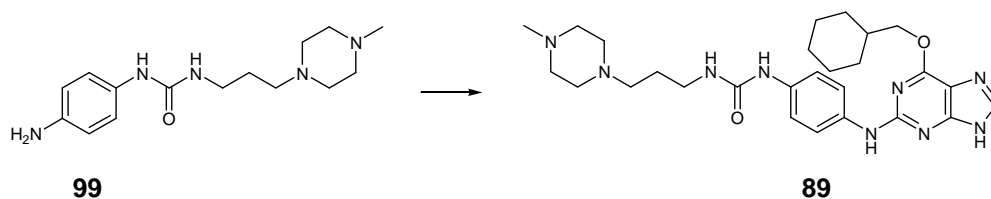
1-(4-Aminophenyl)-3-(3-(4-methylpiperazin-1-yl)propyl)urea (99) ²⁶⁶



The compound was prepared according to General Procedure III from 1-(3-(4-methylpiperazin-1-yl)propyl)-3-(4-nitrophenyl)urea (1 g, 3.1 mmol), to yield the title compound as an orange solid (0.87 g, quantitative).

R_f (EtOAc/MeOH 9:1) = 0.5 mp: 132.9-133.9 °C ^1H NMR (300 MHz, CDCl_3) δ 1.55 (2H, t, J = 6.5 Hz, $\text{CH}_2\text{CH}_2\text{CH}_2$), 2.16 (3H, s, NMe), 2.20 (8H, m, piperazine), 2.27 (2H, t, J = 6 Hz, CH_2N), 3.15 (2H, t, J = 6 Hz, NHCH_2), 6.53 (2H, d, J = 9 Hz, Ar-H), 6.96 (2H, d, J = 9 Hz, Ar-H); ^{13}C NMR (125 MHz, CDCl_3) δ 12.0, 24.8, 43.1, 117.5, 124.0, 131.9, 145.0, 159.7; MS(ES+) m/z 292.2 $[\text{M} + \text{H}]^+$.

1-(4-(6-(Cyclohexylmethoxy)-9H-purin-2-ylamino)phenyl)-3-(3-(4-methylpiperazin-1-yl)propyl)urea (89)

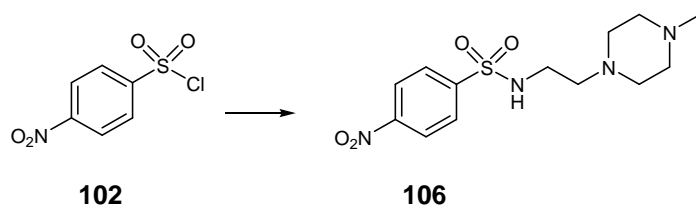


The compound was prepared according to General Procedure I from 1-(4-aminophenyl)-3-(3-(4-methylpiperazin-1-yl)propyl)urea (500 mg, 1.7 mmol) and 6-cyclohexylmethoxy-2-fluoro-9H-purine (215 mg, 0.85 mmol). The crude product was purified by flash chromatography on silica (EtOAc/MeOH 9:1) yielding the title compound as a white solid (208 mg, 43%).

R_f = 0.25 (EtOAc/MeOH 9:1); mp: 146.0-147.2 °C; IR (cm^{-1}): 2922, 2843, 1587, 1502, 1445; λ_{max} (EtOH)/nm 277.0; ^1H NMR (300 MHz, CDCl_3) δ 1.04-2.01 (13H, m, cyclohexyl + $\text{CH}_2\text{CH}_2\text{CH}_2$), 2.21 (3H, s, NMe), 2.37 (2H, t, J = 4 Hz, CH_2), 2.25-2.45 (8H, m, piperazine), 3.29 (2H, t, J = 4 Hz, CH_2NH), 4.31 (2H, d, J = 6 Hz, OCH_2Cy), 6.96 (2H, d, J = 9 Hz, Ar-H), 7.37 (2H, d, J = 9 Hz, Ar-H), 7.76 (1H, s, NH), 8.10 (1H, s, H-8); ^{13}C NMR (125 MHz, CDCl_3) δ 26.0, 26.7, 27.1, 29.7, 30.1, 37.7, 39.1, 45.8, 49.0, 49.2, 49.5, 49.8, 50.1, 53.0, 55.0, 55.1, 56.3, 72.4, 114.9, 120.8, 120.9, 122.4, 122.5, 122.6, 133.7, 133.7, 136.5, 136.5, 138.6, 155.3, 156.5, 156.6, 157.3, 157.4,

161.2; MS(ES+) m/z 522.5 $[M + H]^+$; HRMS calcd for $C_{27}H_{39}N_9O_2$ $[M + H]^+$ 522.3299, found 522.3301.

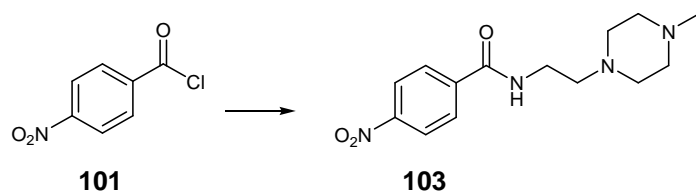
***N*-[3-(4-Methyl-piperazin-1-yl)-ethyl]-4-nitro-benzenesulfonamide (106)** ²⁶⁷



To a stirred solution of *p*-nitro benzenesulfonyl chloride (2 g, 9 mmol) in CH_2Cl_2 (20 mL) at 0 °C was added K_2CO_3 (2.7 g, 19.8 mmol) and 3-(4-methyl-piperazin-1-yl)-ethylamine (1.42 mL, 9.9 mmol). The reaction mixture was stirred at room temperature for 18 h. The mixture was filtered and the filtrates were combined, dried over Na_2SO_4 and evaporated *in vacuo* to yield the title compound as a yellow oil (2.7 g, 94%).

R_f = 0.5 (EtOAc/MeOH 9:1); 1H NMR (300 MHz, $CDCl_3$) δ 2.25 (3H, s, NMe), 2.38 (8H, m, piperazine), 2.40 (2H, t, J = 6 Hz, CH_2N), 3.05 (2H, t, J = 6 Hz, CH_2NH), 7.96 (2H, d, J = 9 Hz, Ar-H), 8.29 (2H, d, J = 9 Hz, Ar-H); ^{13}C NMR (125 MHz, $CDCl_3$) δ 28.4, 36.8, 53.7, 57.8, 66.5, 79.8, 117.4, 128.2, 128.3, 142.5, 152.9, 166.0; MS(ES+) m/z 343.9 $[M + H]^+$.

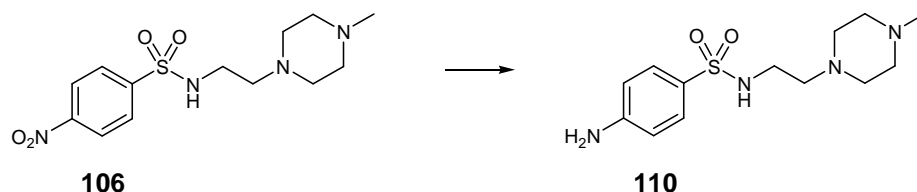
***N*-[3-(4-Methyl-piperazin-1-yl)-ethyl]-4-nitro-benzamide (103)** ²⁶⁸



To a stirred solution of *p*-nitro benzoyl chloride (2 g, 10.9 mmol) in CH₂Cl₂ (20 mL) at 0 °C was added K₂CO₃ (3.3 g, 24.0 mmol) and 3-(4-methyl-piperazin-1-yl)-ethylamine (1.72 mL, 11.9 mmol). The reaction mixture was stirred at room temperature for 18 h. The mixture was filtered and the filtrates were combined, dried over Na₂SO₄ and evaporated *in vacuo* to yield the title compound as a yellow oil (2.7 g, 92%).

R_f = 0.5 (EtOAc/MeOH 9:1); ¹H NMR (300 MHz, CDCl₃) δ 2.34 (3H, s, NMe), 2.38 (8H, m, piperazine), 2.40 (2H, t, *J* = 6 Hz, CH₂N), 2.65 (8H, m, piperazine), 2.74 (2H, t, *J* = 6 Hz, CH₂N), 3.52 (2H, t, *J* = 6 Hz, CH₂NH), 8.04 (2H, d, *J* = 9 Hz, Ar-H), 8.57 (1H, s, NH); 8.20 (2H, d, *J* = 9 Hz, Ar-H); ¹³C NMR (125 MHz, CDCl₃) δ 28.4, 60.5, 69.3, 72.5, 79.8, 117.4, 128.1, 128.3, 142.5, 152.9, 166.1; MS(ES+) *m/z* 307.9 [M + H]⁺.

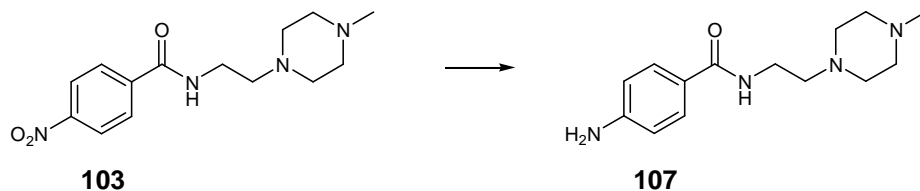
4-Amino-*N*-[3-(4-methyl-piperazin-1-yl)-ethyl]-benzenesulfonamide (110) ²⁶⁷



The compound was prepared according to General Procedure IV from *N*-[3-(4-methyl-piperazin-1-yl)-ethyl]-4-nitro-benzenesulfonamide (2 g, 6.1 mmol), and was obtained as an orange oil (1.85 g, 99%).

R_f = 0.4 (EtOAc); ¹H NMR (300 MHz, CDCl₃) δ 2.22 (3H, s, NMe), 2.31 (2H, t, *J* = 6 Hz, CH₂N), 2.40 (8H, m, piperazine), 2.92 (2H, t, *J* = 6 Hz, CH₂NH), 4.20 (2H, s, NH₂), 6.60 (2H, d, *J* = 9 Hz, Ar-H), 7.52 (2H, d, *J* = 9 Hz, Ar-H); ¹³C NMR (125 MHz, CDCl₃) δ 15.4, 28.5, 40.5, 44.3, 51.7, 59.1, 111.5, 120.5, 128.7, 140.3, 141.5, 159.8; MS(ES+) *m/z* 313.2 [M + H]⁺.

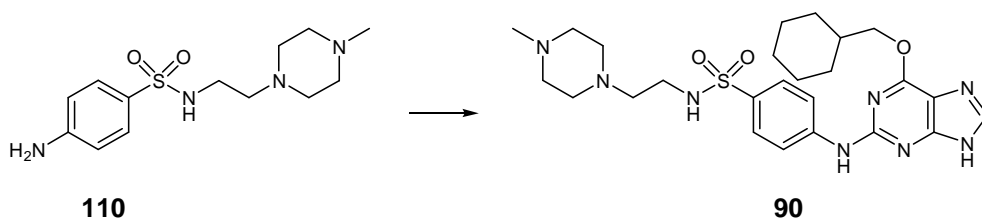
4-Amino-*N*-[3-(4-methyl-piperazin-1-yl)-ethyl]-benzamide (107)²⁶⁸



The compound was prepared according to General Procedure IV from 4-[3-(4-methyl-piperazin-1-yl)-ethyl]-4-nitro-benzamide (2 g, 6.8 mmol), and was obtained as an orange oil (1.87 g, 99%).

R_f = 0.4 (EtOAc); ^1H NMR (300 MHz, CDCl_3) δ 2.42 (3H, s, NMe), 2.61 (2H, t, J = 6 Hz, CH_2N), 2.80 (8H, m, piperazine), 3.25 (2H, t, J = 6 Hz, CH_2NH), 3.40 (2H, s, NH_2), 6.60 (2H, d, J = 9 Hz, Ar-H), 7.58 (2H, d, J = 9 Hz, Ar-H); ^{13}C NMR (125 MHz, CDCl_3) δ 16.5, 29.5, 41.6, 43.2, 50.6, 58.0, 112.6, 121.6, 129.8, 139.2, 140.4, 158.7; MS(ES+) m/z 277.2 $[\text{M} + \text{H}]^+$.

4-(6-(Cyclohexylmethoxy)-9*H*-purin-2-ylamino)-*N*-(3-(4-methylpiperazin-1-yl)ethyl)benzenesulfonamide (90)

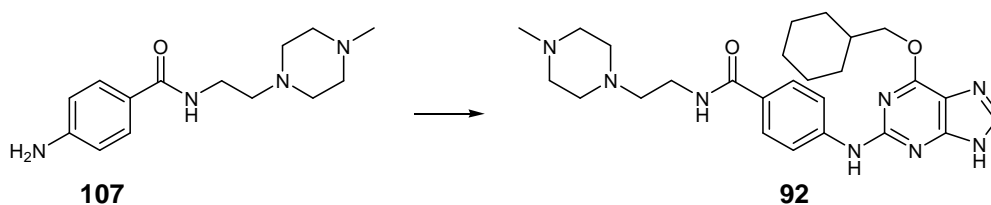


The compound was prepared according to General Procedure I from 4-amino-*N*-[3-(4-methyl-piperazin-1-yl)-ethyl]-benzenesulfonamide (500 mg, 1.7 mmol) and 6-cyclohexylmethoxy-2-fluoro-9*H*-purine (210 mg, 0.8 mmol). The crude product was purified by flash chromatography on silica (EtOAc/MeOH 9:1) yielding the title compound as a white solid (65 mg, 22%).

R_f = 0.25 (EtOAc/MeOH 9:1); mp: 142.4-144.0 °C; IR (cm^{-1}): 2848, 1758, 1596, 1529, 1460, 1425; λ_{max} (EtOH)/nm 307.0; ^1H NMR (300 MHz, CDCl_3) δ 1.03-2.04 (11H, m, cyclohexyl), 2.24 (3H, s, NMe), 2.34 (2H, t, J = 4 Hz, NCH_2), 2.31-2.50 (8H,

m, piperazine), 2.98 (2H, t, $J = 4$ Hz, $\text{CH}_2\text{NH}\text{SO}_2$), 4.27 (2H, d, $J = 6$ Hz, OCH_2Cy), 7.38 (1H, s, NH), 7.74 (2H, d, $J = 9$ Hz, Ar-H), 7.70 (2H, d, $J = 9$ Hz, Ar-H), 7.78 (1H, s, H-8); ^{13}C NMR (125 MHz, CDCl_3) δ 25.6, 26.6, 26.7, 26.9, 30.3, 37.4, 43.2, 46.5, 53.8, 55.4, 57.0, 72.6, 118.3, 128.7, 132.9, 144.1, 155.3; MS(ES+) m/z 543.6 $[\text{M} + \text{H}]^+$; HRMS calcd for $\text{C}_{26}\text{H}_{38}\text{N}_8\text{O}_3\text{S}$ $[\text{M} + \text{H}]^+$ 543.2860, found 543.2855.

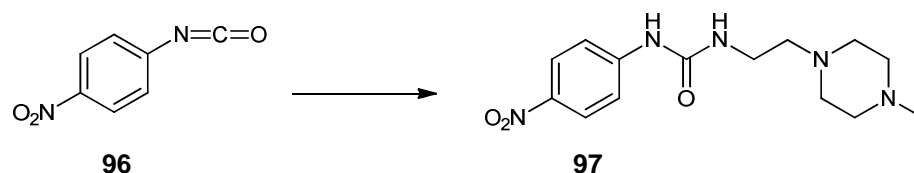
4-(6-(Cyclohexylmethoxy)-9H-purin-2-ylamino)-N-(3-(4-methylpiperazin-1-yl)ethyl)benzamide (92)



The compound was prepared according to General Procedure I from 4-amino-*N*-[3-(4-methyl-piperazin-1-yl)-ethyl]-benzamide (500 mg, 1.9 mmol) and 6-cyclohexylmethoxy-2-fluoro-9*H*-purine (240 mg, 0.95 mmol). The crude product was purified by flash chromatography on silica (EtOAc/MeOH 9:1) yielding the title compound as a white solid (152 mg, 45%).

R_f = 0.25 (EtOAc/MeOH 9:1); mp: 145.5-146.9 °C; IR (cm^{-1}): 3095, 2924, 2849, 2805, 2160, 1603, 1525, 1603, 1525, 1496, 1447; λ_{max} (EtOH)/nm 314.0; ^1H NMR (300 MHz, CDCl_3) δ 1.00-2.06 (11H, m, cyclohexyl), 2.22 (3H, s, NMe), 2.48 (2H, t, $J = 4$ Hz, NCH_2), 2.41-2.63 (8H, m, piperazine), 3.46 (2H, t, $J = 4$ Hz, CH_2NH), 4.24 (2H, d, $J = 6$ Hz, OCH_2Cy), 7.37 (1H, s, NH), 7.67 (2H, d, $J = 9$ Hz, Ar-H), 7.71 (2H, d, $J = 9$ Hz, Ar-H), 7.76 (1H, s, NH), 8.10 (1H, s, H-8); ^{13}C NMR (125 MHz, CDCl_3) δ 25.5, 26.0, 26.7, 30.1, 37.7, 40.5, 46.1, 53.4, 55.3, 57.9, 72.6, 115.6, 118.2, 128.4, 139.2, 143.7, 155.7, 161.2, 167.7; MS(ES+) m/z 507.6 $[\text{M} + \text{H}]^+$; HRMS calcd for $\text{C}_{27}\text{H}_{38}\text{N}_8\text{O}_2$ $[\text{M} + \text{H}]^+$ 507.3190, found 507.3189.

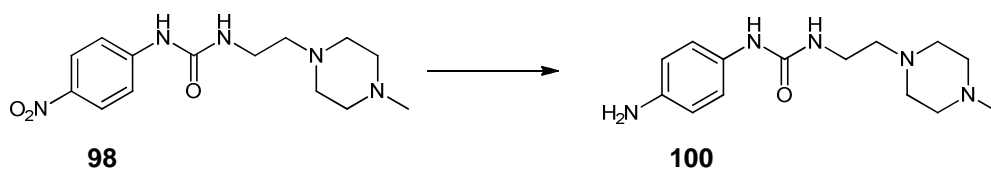
1-(3-(4-Methylpiperazin-1-yl)ethyl)-3-(4-nitrophenyl)urea (98) ²⁶⁹



To a stirred solution of *p*-nitrophenyl isocyanate (2 g, 12.2 mmol) in THF (25 mL) was added 3-(4-methylpiperazin-1-yl)ethylamine (2.3 mL, 15.8 mmol). The mixture was stirred at room temperature for 3 h. The solvent was evaporated *in vacuo* yielding the title compound as a yellow solid (3.8 g, 82%).

R_f = 0.35 (EtOAc/MeOH 9:1); mp: 97-100 °C; ^1H NMR (300 MHz, CDCl_3) δ 1.91 (2H, quint, J = 6.5 Hz, $\text{CH}_2\text{CH}_2\text{CH}_2$), 2.34 (3H, s, NMe), 2.74 (8H, m, piperazine), 2.80 (2H, t, J = 6.5 Hz, CH_2N), 3.54 (2H, t, J = 6.5 Hz, CH_2NH), 7.46 (2H, d, J = 9 Hz, Ar-H), 8.06 (2H, d, J = 9 Hz, Ar-H); ^{13}C NMR (125 MHz, CDCl_3) δ 26.5, 40.2, 43.3, 50.0, 52.6, 55.5, 121.1, 122.9, 142.7, 144.8; MS(ES+) m/z 308.2 $[\text{M} + \text{H}]^+$.

1-(4-Aminophenyl)-3-(3-(4-methylpiperazin-1-yl)ethyl)urea (100) ²⁶⁹

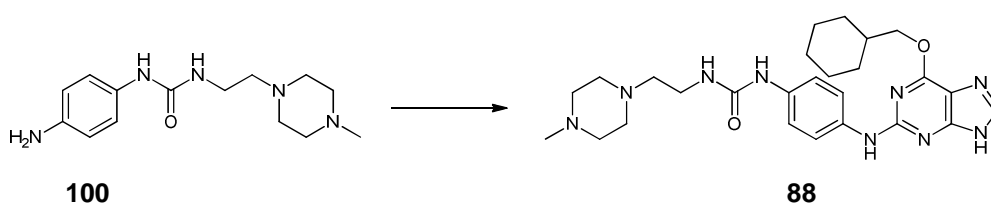


The compound was prepared according to General Procedure III from 1-(3-(4-methylpiperazin-1-yl)ethyl)-3-(4-nitrophenyl)urea (2 g, 6.5 mmol), to yield the title compound as an orange solid (1.78 g, 99%).

R_f (EtOAc/MeOH 9:1) = 0.5 mp: 132.9-133.9 °C ^1H NMR (300 MHz, CDCl_3) δ 2.16 (3H, s, NMe), 2.20 (8H, m, piperazine), 2.27 (2H, t, J = 6 Hz, CH_2N), 3.15 (2H, t, J = 6 Hz, NHCH_2), 6.53 (2H, d, J = 9 Hz, Ar-H), 6.96 (2H, d, J = 9 Hz, Ar-H); ^{13}C NMR

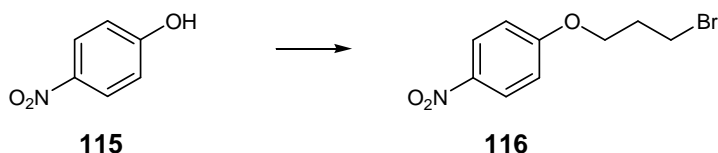
(125 MHz, CDCl₃) δ 12.0, 24.8, 43.1, 117.5, 124.0, 131.9, 145.0, 159.7; MS(ES+) m/z 278.2 [M + H]⁺.

1-(4-(6-(Cyclohexylmethoxy)-9H-purin-2-ylamino)phenyl)-3-(3-(4-methylpiperazin-1-yl)ethyl)urea (88)



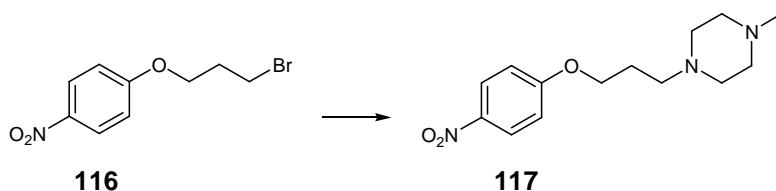
The compound was prepared according to General Procedure I from 1-(4-aminophenyl)-3-(3-(4-methylpiperazin-1-yl)ethyl)urea (500 mg, 1.8 mmol) and 6-cyclohexylmethoxy-2-fluoro-9H-purine (225 mg, 0.9 mmol). The crude product was purified by flash chromatography on silica (EtOAc/MeOH 9:1) yielding the title compound as a white solid (132 mg, 44%).

R_f = 0.25 (EtOAc/MeOH 9:1); mp: 146.0-147.2 °C; IR (cm⁻¹): 2922, 2843, 1587, 1502, 1445; λ_{\max} (EtOH)/nm 277.0; ¹H NMR (300 MHz, CDCl₃) δ 1.04-2.01 (11H, m, cyclohexyl), 2.21 (3H, s, NMe), 2.37 (2H, t, J = 4 Hz, CH₂), 2.25-2.45 (8H, m, piperazine), 3.29 (2H, t, J = 4 Hz, CH₂NH), 4.31 (2H, d, J = 6 Hz, OCH₂Cy), 6.96 (2H, d, J = 9 Hz, Ar-H), 7.37 (2H, d, J = 9 Hz, Ar-H), 7.76 (1H, s, NH), 8.10 (1H, s, H-8); ¹³C NMR (125 MHz, CDCl₃) δ 26.0, 26.7, 27.1, 29.7, 30.1, 37.7, 39.1, 45.8, 49.0, 49.2, 49.5, 49.8, 50.1, 53.0, 55.0, 55.1, 56.3, 72.4, 114.9, 120.8, 120.9, 122.4, 122.5, 122.6, 133.7, 133.7, 136.5, 136.5, 138.6, 155.3, 156.5, 156.6, 157.3, 157.4, 161.2; MS(ES+) m/z 508.5 [M + H]⁺; HRMS calcd for C₂₆H₃₇N₉O₂ [M + H]⁺ 508.3299, found 508.3301.

1-(3-Bromopropoxy)-4-nitrobenzene (116) ²⁷⁰⁻²⁷¹

To a stirred solution of *p*-nitro phenol (2 g, 14.3 mmol) in acetonitrile (25 mL) was added K_2CO_3 (5 g, 35.7 mmol) and dibromopropane (15 mL, 140 mmol). The mixture was heated to reflux and stirred for 48 h. The excess base was filtered and the filtrate was evaporated *in vacuo* to yield the title compound as a yellow solid (3.5 g, quantitative).

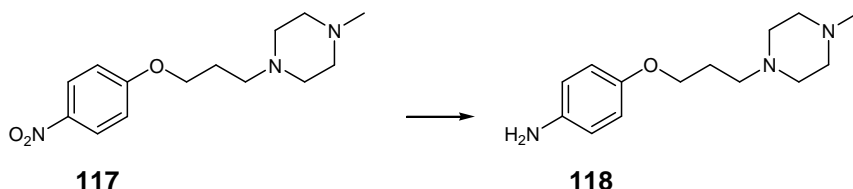
R_f = 0.7 (EtOAc); mp: 63-64 °C 1H NMR (300 MHz, $CDCl_3$) δ 1.97 (2H, t, J = 6 Hz, $CH_2CH_2CH_2$) 3.79 (2H, t, J = 6 Hz, CH_2Br), 4.26 (2H, t, J = 6 Hz, OCH_2), 6.91 (2H, d, J = 9 Hz, Ar-H), 8.14 (2H, d, J = 9 Hz, Ar-H); ^{13}C NMR (125 MHz, $CDCl_3$) δ 40.4, 45.0, 110.6, 125.5, 140.4, 172.7; MS(ES+) m/z 259.98 [$M(^{79}Br) + H$], 261.98 [$M(^{81}Br) + H$]⁺.

1-(3-(4-Nitrophenoxy)propyl)-4-methylpiperazine (117) ^{262, 272}

The compound was prepared according to General Procedure III from 1-(3-bromopropoxy)-4-nitrobenzene (2.5 g, 9.6 mmol) and *N*-methyl piperazine (5.5 mL, 48 mmol), and was obtained as an orange solid (2.3 g, 85%).

R_f = 0.5 (EtOAc/MeOH 9:1); 1H NMR (300 MHz, $CDCl_3$) δ 1.97 (2H, quint, J = 6 Hz, $CH_2CH_2CH_2$), 2.25 (3H, s, NMe), 2.55-2.40 (8H, m, piperazine), 2.52 (2H, t, J = 6 Hz, CH_2N), 4.08 (2H, t, J = 6 Hz, OCH_2), 6.90 (2H, d, J = 9 Hz, Ar-H), 8.12 (2H, d, J = 9 Hz, Ar-H); ^{13}C NMR (125 MHz, $CDCl_3$) δ 45.6, 47.0, 58.6, 60.8, 70.9, 115.5, 130.2, 145.8, 165.7; MS(ES+) m/z 280.7 [$M + H$]⁺.

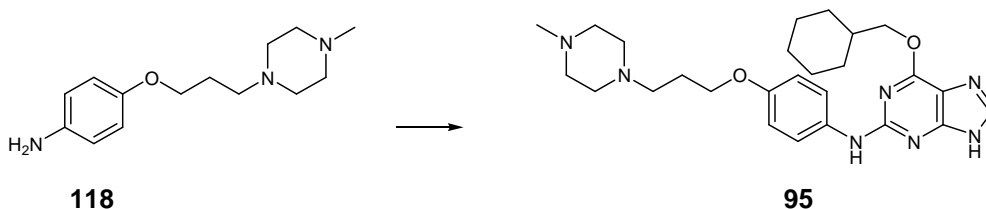
4-(3-(4-Methylpiperazin-1-yl)propoxy)benzenamine (118) ²⁶²



The compound was prepared according to General Procedure IV from 21-(3-(4-nitrophenoxy)propyl)-4-methylpiperazine (2.5 g, 10.02 mmol) and obtained as a clear yellow oil (2.0 g, 96%).

R_f = 0.5 (EtOAc/MeOH 9:1); bp 168-169 °C (lit.); ¹H NMR (300 MHz, CDCl₃): δ 1.97 (2H, quint, J = 6 Hz, CH₂CH₂CH₂), 2.30 (3H, s, NMe), 2.45-2.50 (8H, m, piperazine), 2.52 (2H, t, J = 6 Hz, CH₂N), 3.98 (2H, t, J = 6 Hz, OCH₂), 6.61 (2H, d, J = 9 Hz, Ar-H), 6.82 (2H, d, J = 9 Hz, Ar-H); ¹³C NMR (125 MHz, MeOD) δ 45.6, 61.0, 69.4, 111.8, 114.9, 142.5, 148.4. MS(ES+) m/z 250.6 [M + H]⁺.

N-(4-(3-(4-Methylpiperazin-1-yl)propoxy)phenyl)-6-(cyclohexylmethoxy)-9H-purin-2-amine (95)

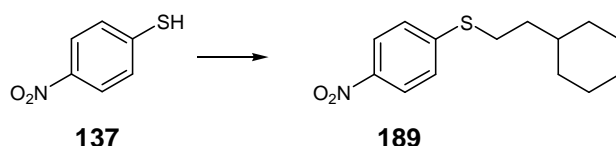


The compound was prepared according to General Procedure I from 4-(3-(4-methylpiperazin-1-yl)propoxy)benzenamine (500 mg, 2.27 mmol) and 6-cyclohexylmethoxy-2-fluoro-9H-purine (285 mg, 1.14 mmol). The crude product was purified by flash chromatography on silica (EtOAc/MeOH 9:1) yielding the title compound as a white solid (307 mg, 43%).

R_f = 0.25 (EtOAc/MeOH 9:1); mp: 116.0-116.9 °C; IR (cm⁻¹): 2924, 2849, 2776, 1618, 1583, 1543, 1504, 1443; λ_{max} (EtOH)/nm 272.0; ¹H NMR (300 MHz, CDCl₃) δ 1.1-1.9 (11H, m, cyclohexyl), 1.98 (2H, t, J = 6 Hz, CH₂CH₂CH₂), 2.30 (3H, s, NMe),

2.45-2.50 (8H, m, piperazine), 2.72 (2H, t, $J = 6$ Hz, CH_2N), 3.98 (2H, t, $J = 6$ Hz, OCH_2), 4.3 (2H, d, $J = 6$ Hz, CH_2Cy), 6.61 (2H, d, $J = 9$ Hz, Ar-H), 6.82 (2H, d, $J = 9$ Hz, Ar-H), 6.89 (1H, s, H-8); ^{13}C NMR (125 MHz, CDCl_3) δ 26.0, 26.8, 30.1, 37.8, 46.0, 58.7, 67.0, 72.4, 115.4, 115.5, 115.6, 116.7, 122.6, 122.7, 133.5, 137.8, 155.4, 157.1, 161.6; MS(ES+) m/z 480.52 $[\text{M} + \text{H}]^+$; HRMS calcd for $\text{C}_{26}\text{H}_{37}\text{N}_7\text{O}_2$ $[\text{M} + \text{H}]^+$ 480.2503, found 480.2498.

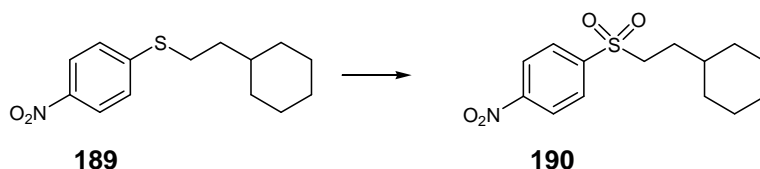
(2-Cyclohexylethyl)(4-nitrophenyl)sulfane (189) ²⁷³



To a stirred solution of 4-nitrobenzenethiol (2 mL, 15.5 mmol) in acetonitrile (10 mL) was added K_2CO_3 (2.3 g, 14.7 mmol). The temperature was lowered to 0 °C and cyclohexylethyl bromide (2.2 mL, 14.7 mmol) was added dropwise. The mixture was heated to reflux and stirred for 48 h. The excess base was filtered and the filtrate was evaporated *in vacuo* to yield the title compound as a white solid (2.8 g, quantitative).

$R_f = 0.7$ (EtOAc); mp: 139 °C (lit. 138 °C); ^1H NMR (300 MHz, CDCl_3) δ 0.94-1.69 (13H, m, cyclohexyl + CH_2Cy), 2.95 (2H, t, $J = 6$ Hz, CH_2S), 7.24 (2H, d, $J = 9$ Hz, Ar-H), 8.03 (2H, d, $J = 9$ Hz, Ar-H); ^{13}C NMR (125 MHz, CDCl_3) δ 34.4, 38.5, 43.0, 127.9, 128.0, 128.4, 137.1; MS(ES+) m/z 266.1 $[\text{M} + \text{H}]^+$.

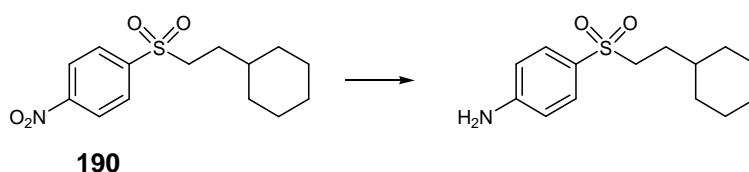
1-(2-Cyclohexylethylsulfonyl)-4-nitrobenzene (190) ²⁷⁴



To a stirred solution of (2-cyclohexylethyl)(4-nitrophenyl)sulfane (2 g, 7.5 mmol) in CH_2Cl_2 (10 mL) was added *m*CPBA (3 g, 16.6 mmol). The reaction mixture was stirred at room temperature for 48 h. The solvent was removed under reduced pressure and the residue was taken up in EtOAc (20 mL) and washed with saturated aqueous NaHCO_3 (6 x 20 mL). The combined organic layers were dried over Na_2SO_4 and the solvent was removed under reduced pressure, yielding the title compound as a white solid (2.1 g, 76%).

R_f = 0.5 (EtOAc/Hexane 1:9); mp: 95-96 °C (lit. 96 °C); ^1H NMR (300 MHz, CDCl_3) δ 0.94-1.69 (13H, m, cyclohexyl + CH_2Cy), 3.35 (2H, t, J = 6 Hz, CH_2S), 8.04 (2H, d, J = 9 Hz, Ar-H), 8.44 (2H, d, J = 9 Hz, Ar-H); ^{13}C NMR (125 MHz, CDCl_3) δ 35.4, 57.5, 58.0, 124.6, 129.1, 130.6, 137.1; MS(ES+) m/z 298.2 $[\text{M} + \text{H}]^+$.

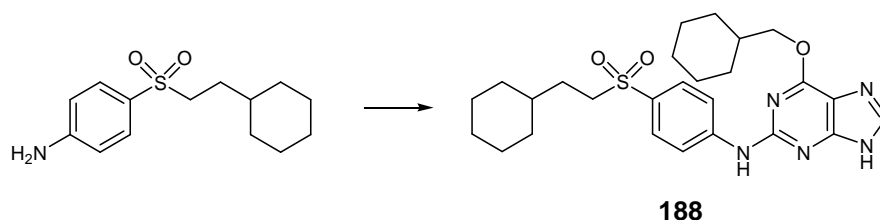
4-(2-Cyclohexylethylsulfonyl)benzenamine ²⁷⁴



The compound was prepared according to General Procedure IV from 1-(2-cyclohexylethylsulfonyl)-4-nitrobenzene (3 g, 10 mmol) and obtained as a clear yellow oil (2.8 g, 95%).

R_f 0.5 (EtOAc/MeOH 9:1); mp: 83-84 °C (lit. 85 °C); ^1H NMR (300 MHz, CDCl_3) δ 0.91-1.70 (13H, m, cyclohexyl + CH_2Cy), 3.05 (2H, t, J = 6 Hz, CH_2S), 6.02 (2H, s, NH_2), 6.64 (2H, d, J = 9 Hz, Ar-H), 7.41 (2H, d, J = 9 Hz, Ar-H); ^{13}C NMR (125 MHz, MeOD) δ 50.0, 55.8, 79.8, 61.0, 65.6, 69.4, 115.8, 116.9, 129.9, 136.0, 139.5, 144.4, 145.4, 149.3; MS(ES+) m/z 268.2 $[\text{M} + \text{H}]^+$.

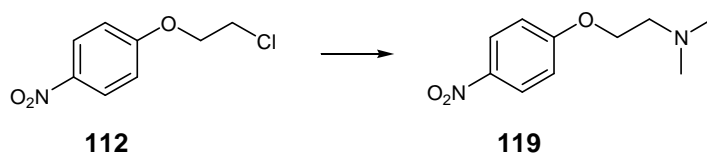
***N*-(4-(2-Cyclohexylethylsulfonyl)phenyl)-6-(cyclohexylmethoxy)-9*H*-purin-2-amine (188)**



The compound was prepared according to General Procedure I from 4-(2-cyclohexylethylsulfonyl)benzenamine (1 g, 3.74 mmol) and 6-cyclohexylmethoxy-2-fluoro-9*H*-purine (500 mg, 1.87 mmol). The crude product was purified by flash chromatography on silica (EtOAc/Petrol 7:3) yielding the title compound as a white solid (511 mg, 41%).

R_f = 0.25 (EtOAc/MeOH 9:1); mp: 116.0-116.9 °C; IR (cm^{-1}): 2924, 2849, 2776, 1618, 1583, 1543, 1504, 1443; λ_{max} (EtOH)/nm 272.0; ^1H NMR (300 MHz, CDCl_3) δ 0.91-1.70 (13H, m, cyclohexyl + CH_2Cy), 3.05 (2H, t, J = 6 Hz, CH_2S), 4.35 (2H, d, J = 6 Hz, CH_2Cy), 6.81 (1H, s, H-8), 6.94 (2H, d, J = 9 Hz, Ar-H), 7.21 (1H, s, NH), 7.45 (1H, d, J = 9 Hz, Ar-H); ^{13}C NMR (125 MHz, CDCl_3) δ 26.0, 26.8, 30.1, 37.8, 46.0, 58.7, 67.0, 72.4, 115.4, 115.5, 115.6, 116.7, 122.6, 122.7, 133.5, 137.8, 155.4, 157.1, 161.6; MS(ES+) m/z 498.3 $[\text{M} + \text{H}]^+$; HRMS calcd for $\text{C}_{26}\text{H}_{35}\text{N}_5\text{O}_3\text{S}$ $[\text{M} + \text{H}]^+$ 498.2503, found 498.2498.

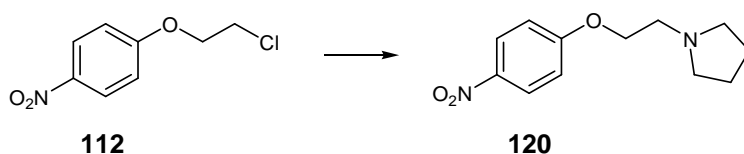
***N,N*-dimethyl-2-(4-nitrophenoxy)ethanamine (119) ²⁷⁵**



The compound was prepared according to General Procedure III from 1-(2-chloroethoxy)-4-nitrobenzene (1 g, 4.96 mmol) and 2 M dimethylamine in methanol (10 mL). The compound was obtained as a yellow solid (1.12 g, 89%).

$R_f = 0.5$ (EtOAc/MeOH 9:1); mp: 79-80 °C (lit. 82 °C) ^1H NMR (300 MHz, CDCl_3) δ 2.81 (6H, s, NMe_2), 3.54 (2H, t, $J = 6$ Hz, CH_2N), 4.64 (2H, t, $J = 6$ Hz, OCH_2), 7.18 (2H, d, $J = 9$ Hz, Ar-H), 8.16 (2H, d, $J = 9$ Hz, Ar-H); ^{13}C NMR (125 MHz, CDCl_3) δ 45.9, 59.5, 66.4, 115.5, 124.8, 139.0, 163.4. MS(ES+) m/z 211.1 $[\text{M}+\text{H}]^+$.

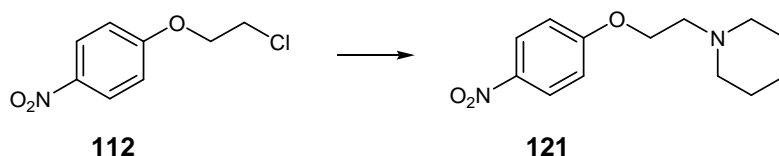
1-(2-(4-Nitrophenoxy)ethyl)pyrrolidine (120) ²⁷⁵



The compound was prepared according to General Procedure III from 1-(2-chloroethoxy)-4-nitrobenzene (1 g, 4.96 mmol) and 2 mL of pyrrolidine. The compound was obtained as a yellow solid (1.03 g, 84%).

$R_f = 0.5$ (EtOAc/MeOH 9:1); mp: 71-72 °C (lit. 74 °C); ^1H NMR (300 MHz, CDCl_3) δ 2.65 (2H, t, $J = 6$ Hz, NCH_2), 3.24 (2H, t, $J = 6$ Hz, NCH_2), 3.44 (2H, t, $J = 6$ Hz, CH_2N), 4.82 (2H, t, $J = 6$ Hz, OCH_2), 7.01 (2H, d, $J = 9$ Hz, Ar-H), 8.27 (2H, d, $J = 9$ Hz, Ar-H); ^{13}C NMR (125 MHz, CDCl_3) δ 25.6, 58.9, 59.0, 66.9, 115.5, 121.0, 140.4, 161.5; MS(ES+) m/z 237.6 $[\text{M}+\text{H}]^+$.

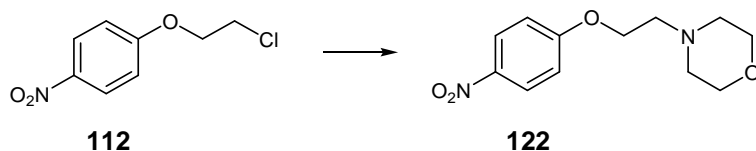
1-(2-(4-Nitrophenoxy)ethyl)piperidine (121) ²⁷⁶



The compound was prepared according to General Procedure III from 1-(2-chloroethoxy)-4-nitrobenzene (1 g, 4.96 mmol) and 2 mL of piperidine. The compound was obtained as a yellow solid (1.05 g, 81%).

$R_f = 0.5$ (EtOAc/MeOH 9:1); mp: 63-64 °C (lit. 65 °C); ^1H NMR (300 MHz, CDCl_3) δ 1.3 (2H, m, CH_2), 1.5 (4H, m, CH_2), 2.4 (4H, m, NCH_2), 2.6 (2H, t, $J = 6$ Hz, CH_2N), 3.9 (2H, t, $J = 6$ Hz, OCH_2), 7.1 (2H, d, $J = 9$ Hz, Ar-H), 8.4 (2H, d, $J = 9$ Hz, Ar-H); ^{13}C NMR (125 MHz, CDCl_3) δ 25.6, 54.7, 60.0, 68.4, 110.8, 122.5, 138.4, 158.7; MS(ES+) m/z 251.3 $[\text{M}+\text{H}]^+$.

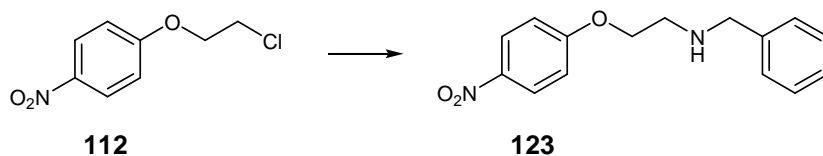
4-(2-(4-Nitrophenoxy)ethyl)morpholine (122) ²⁷⁵



The compound was prepared according to General Procedure III from 1-(2-chloroethoxy)-4-nitrobenzene (1 g, 4.96 mmol) and 2 mL of morpholine. The compound was obtained as a yellow solid (1.09 g, 87%).

$R_f = 0.5$ (EtOAc/MeOH 9:1); mp: 83-84 °C (lit. 82 °C); ^1H NMR (300 MHz, CDCl_3) δ 2.6 (4H, m, NCH_2), 2.9 (2H, t, $J = 6$ Hz, CH_2N), 3.9 (2H, t, $J = 6$ Hz, CH_2O), 4.2 (2H, t, $J = 6$ Hz, OCH_2), 7.0 (2H, d, $J = 9$ Hz, Ar-H), 8.2 (2H, d, $J = 9$ Hz, Ar-H); ^{13}C NMR (125 MHz, CDCl_3) δ 22.6, 54.9, 57.0, 68.9, 117.5, 125.7, 143.1, 166.9. MS(ES+) m/z 253.1 $[\text{M}+\text{H}]^+$.

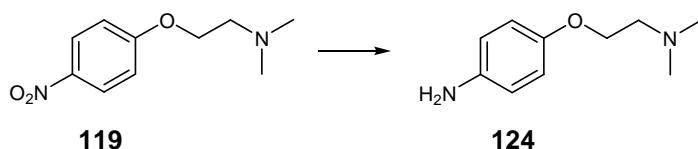
2-(4-Nitrophenoxy)-N-benzylethanamine (123) ²⁷⁶



The compound was prepared according to General Procedure III from 1-(2-chloroethoxy)-4-nitrobenzene (1 g, 4.96 mmol), 2.5 mL of benzylamine and 0.56 g of NaI. The compound was obtained as a yellow solid (1.04 g, 88%).

R_f = 0.5 (EtOAc/MeOH 9:1); mp: 63-64 °C (lit. 65 °C); ^1H NMR (300 MHz, CDCl_3) δ 2.9 (2H, t, J = 6 Hz, CH_2NH), 3.8 (2H, s, NHCH_2), 4.0 (2H, t, J = 6 Hz, OCH_2), 6.8 (2H, d, J = 9 Hz, Ar-H), 7.2 (1H, m, NH), 7.2 (5H, s, Ar-H), 8.0 (2H, d, J = 9 Hz, Ar-H); ^{13}C NMR (125 MHz, CDCl_3) δ 45.9, 49.5, 55.5, 70.4, 115.5, 124.8, 128.3, 129.6, 133.3, 139.0, 163.4. MS(ES+) m/z 273.6 $[\text{M}+\text{H}]^+$.

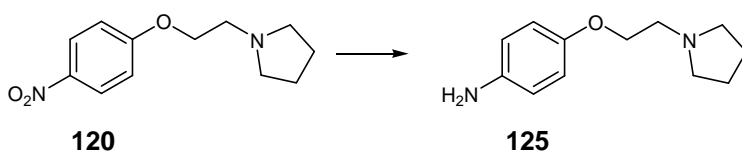
4-(2-(Dimethylamino)ethoxy)benzenamine (124)²⁷⁵



The compound was prepared according to General Procedure IV from 2-(4-nitrophenoxy)-*N,N*-dimethylethanamine (700 mg, 3.32 mmol) and obtained as a clear yellow oil (651 mg, quantitative).

R_f = 0.5 (EtOAc/MeOH 9:1); bp 168-169 °C (lit.); ^1H NMR (300 MHz, CDCl_3): δ 2.2 (6H, s, NMe_2), 2.6 (2H, t, J = 6 Hz, CH_2N), 3.9 (2H, t, J = 6 Hz, OCH_2), 6.5 (2H, d, J = 9 Hz, Ar-H), 6.6 (2H, d, J = 9 Hz, Ar-H); ^{13}C NMR (125 MHz, MeOD) δ 45.6, 61.0, 69.4, 111.8, 114.9, 142.5, 148.4. MS(ES+) m/z 181.6 $[\text{M}+\text{H}]^+$.

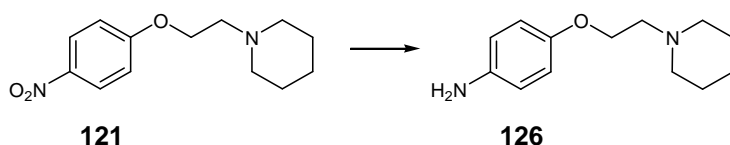
4-(2-(Pyrrolidin-1-yl)ethoxy)benzenamine (125)²⁷⁷



The compound was prepared according to General Procedure IV from 1-(2-(4-nitrophenoxy)ethyl)pyrrolidine (1 g, 4.22 mmol) and obtained as a clear yellow oil (898 mg, 98%).

$R_f = 0.5$ (EtOAc/MeOH 9:1); ^1H NMR (300 MHz, CDCl_3) δ 1.9 (4H, m, $2 \times \text{CH}_2$), 2.4 (4H, m, NCH_2), 6.4 (2H, d, $J = 9$ Hz, Ar-H), 6.7 (2H, d, $J = 9$ Hz, Ar-H). ^{13}C NMR (125 MHz, MeOD) δ 24.0, 55.6, 59.9, 67.0, 69.4, 111.8, 114.9, 142.5, 148.4; MS(ES+) m/z 207.5 $[\text{M}+\text{H}]^+$.

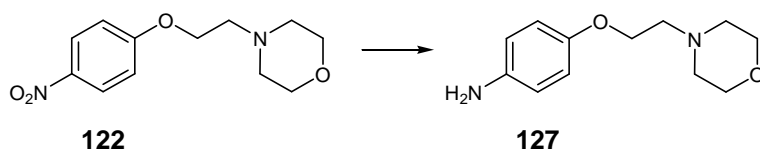
4-(2-(Piperidin-1-yl)ethoxy)benzenamine (126)²⁷⁸



The compound was prepared according to General Procedure IV from 1-(2-(4-nitrophenoxy)ethyl)piperidine (800 mg, 3.19 mmol) and obtained as a clear yellow oil (710 mg, 98%).

$R_f = 0.5$ (EtOAc/MeOH 9:1); ^1H NMR (300 MHz, CDCl_3): δ 1.3 (2H, m, CH_2), 1.5 (4H, m, CH_2), 2.4 (4H, m, NCH_2), 2.6 (2H, t, $J = 6$ Hz, CH_2N), 3.9 (2H, t, $J = 6$ Hz, OCH_2), 6.5 (2H, d, $J = 9$ Hz, Ar-H), 6.6 (2H, d, $J = 9$ Hz, Ar-H); ^{13}C NMR (125 MHz, MeOD) δ 22.9, 51.6, 59.6, 111.8, 113.9, 143.5, 149.4. MS(ES+) m/z 221.9 $[\text{M}+\text{H}]^+$.

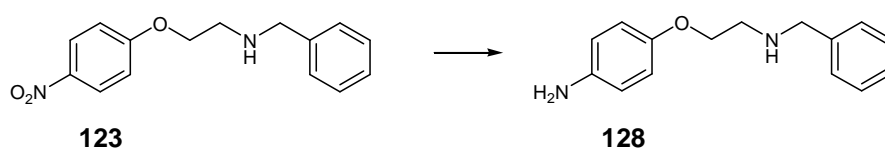
4-(2-(Morpholinoethoxy)benzenamine (127)²⁷⁵



The compound was prepared according to General Procedure IV from 4-(2-(4-nitrophenoxy)ethyl)morpholine (1 g, 3.96 mmol) and obtained as a clear yellow oil (909 mg, 99%).

$R_f = 0.5$ (EtOAc/MeOH 9:1); ^1H NMR (300 MHz, CDCl_3) δ 2.6 (4H, m, NCH_2), 2.7 (2H, t, $J = 6$ Hz, CH_2N), 3.7 (4H, t, $J = 6$ Hz, CH_2O), 4.0 (2H, t, $J = 6$ Hz, OCH_2), 6.6 (2H, d, $J = 9$ Hz, Ar-H), 6.7 (2H, d, $J = 9$ Hz, Ar-H). ^{13}C NMR (125 MHz, MeOD) δ 51.0, 55.6, 59.4, 61.0, 65.6, 69.4, 110.8, 115.9, 141.5, 149.4. MS(ES+) m/z 223.2 $[\text{M}+\text{H}]^+$.

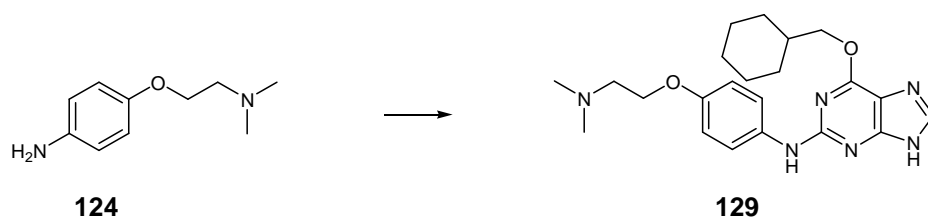
4-(2-(Benzylamino)ethoxy)benzenamine (128)²⁷⁶



The compound was prepared according to General Procedure IV from 2-(4-nitrophenoxy)-N-benzylethanamine (800 mg, 2.83 mmol) and obtained as a clear yellow oil (712 mg, 98%).

R_f 0.5 (EtOAc/MeOH 9:1); ^1H NMR (300 MHz, CDCl_3) δ 2.89 (2H, t, $J = 6$ Hz, CH_2NH), 3.7 (2H, s, CH_2Ph), 3.9 (2H, t, $J = 6$ Hz, OCH_2), 6.5 (2H, d, $J = 9$ Hz, Ar-H), 6.6 (2H, d, $J = 9$ Hz, Ar-H), 7.2 (5H, s, Ar-H); ^{13}C NMR (125 MHz, MeOD) δ 50.0, 55.8, 79.8, 61.0, 65.6, 69.4, 115.8, 116.9, 129.9, 136.0, 139.5, 144.4, 145.4, 149.3; MS(ES+) m/z 243.2 $[\text{M}+\text{H}]^+$.

N-(4-(2-(Dimethylamino)ethoxy)phenyl)-6-(cyclohexylmethoxy)-9H-purin-2-amine (129)

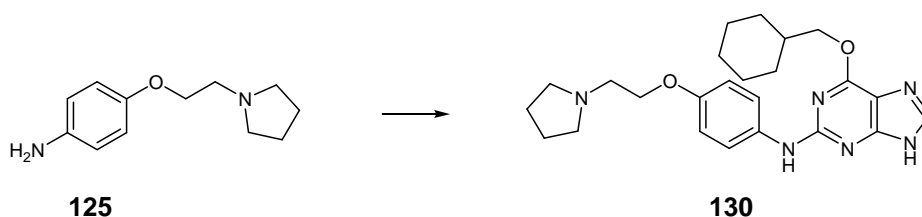


The compound was prepared according to General Procedure I from 4-(2-(dimethylamino)ethoxy)benzenamine (500 mg, 2.77 mmol) and 6-cyclohexylmethoxy-2-fluoro-9H-purine (312 mg, 1.25 mmol). The crude product was

purified by flash chromatography on silica (EtOAc/MeOH 9:1) yielding the title compound as a white solid (311 mg, 44%).

R_f = 0.25 (EtOAc/MeOH 9:1); mp: 116.0-116.9 °C; IR (cm^{-1}): 2924, 2849, 2776, 1618, 1583, 1543, 1504, 1443; λ_{max} (EtOH)/nm 272.0; ^1H NMR (300 MHz, CDCl_3) δ 1.1-1.9 (11H, m, cyclohexyl), 2.3 (6H, s, NMe_2), 2.7 (2H, t, J = 6 Hz, CH_2N), 4.1 (2H, t, J = 6 Hz, OCH_2), 4.3 (2H, d, J = 6 Hz, CH_2Cy), 6.8 (1H, s, H-8), 6.9 (2H, d, J = 9 Hz, Ar-H), 7.2 (1H, s, NH), 7.4 (1H, d, J = 9 Hz, Ar-H); ^{13}C NMR (125 MHz, CDCl_3) δ 26.0, 26.8, 30.1, 37.8, 46.0, 58.7, 67.0, 72.4, 115.4, 115.5, 115.6, 116.7, 122.6, 122.7, 133.5, 137.8, 155.4, 157.1, 161.6; MS(ES+) m/z 411.3 $[\text{M} + \text{H}]^+$; HRMS calcd for $\text{C}_{25}\text{H}_{35}\text{N}_7\text{O}_2$ $[\text{M} + \text{H}]^+$ 411.2503, found 411.2498.

***N*-(4-(2-(Pyrrolidin-1-yl)ethoxy)phenyl)-6-(cyclohexylmethoxy)-9*H*-purin-2-amine (130)**

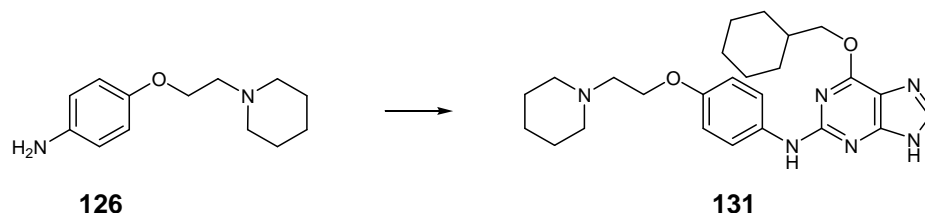


The compound was prepared according to General Procedure I from 4-(2-(pyrrolidin-1-yl)ethoxy)benzenamine (500 mg, 2.42 mmol) and 6-cyclohexylmethoxy-2-fluoro-9*H*-purine (312 mg, 1.25 mmol). The crude product was purified by flash chromatography on silica (EtOAc/MeOH 9:1) yielding the title compound as a white solid (308 mg, 45%).

R_f = 0.25 (EtOAc/MeOH 9:1); mp: 118.0-118.9 °C; IR (cm^{-1}): 2924, 2850, 1584, 1531, 1502, 1446; λ_{max} (EtOH)/nm 272.0; ^1H NMR (300 MHz, CDCl_3) δ 0.9-1.6 (11H, m, cyclohexyl), 1.7 (4H, m, CH_2CH_2 pyrrolidine), 2.5 (4H, m, NCH_2 pyrrolidine), 2.8 (2H, t, J = 6 Hz, CH_2N), 4.0 (2H, t, J = 6 Hz, OCH_2), 4.2 (2H, d, J = 6 Hz, CH_2Cy), 6.7 (2H, d, J = 9 Hz, Ar-H), 6.9 (1H, s, H-8), 7.1 (1H, s, NH), 7.3 (1H, d, J = 9 Hz, Ar-H); ^{13}C NMR (125 MHz, CDCl_3) δ 14.4, 23.9, 26.0, 26.7, 29.9, 30.0, 30.1, 37.7, 48.2, 54.8, 55.3, 60.5, 67.5, 72.4, 73.0, 115.5, 122.5, 133.9, 138.4, 140.9, 155.1, 155.2,

157.0, 161.5; MS(ES+) m/z 437.3 $[M + H]^+$; HRMS calcd for $C_{24}H_{32}N_6O_2$ $[M + H]^+$ 437.2660, found 437.2659.

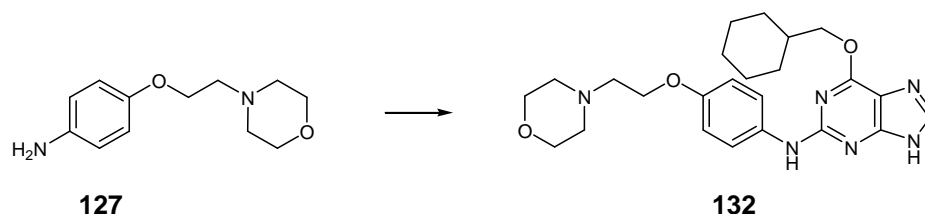
***N*-(4-(2-(Piperidin-1-yl)ethoxy)phenyl)-6-(cyclohexylmethoxy)-9*H*-purin-2-amine (131)**



The compound was prepared according to General Procedure I from 4-(2-(piperidin-1-yl)ethoxy)benzenamine (500 mg, 2.26 mmol) and 6-cyclohexylmethoxy-2-fluoro-9*H*-purine (312 mg, 1.25 mmol). The crude product was purified by flash chromatography on silica (EtOAc/MeOH 9:1) yielding the title compound as a white solid (298 mg, 43%).

R_f = 0.25 (EtOAc/MeOH 9:1); mp: 128.3-129.1 °C; IR (cm^{-1}): 3266, 2922, 2850, 2783, 1616, 1584, 1537, 1502, 1446; λ_{max} (EtOH)/nm 272.0; 1H NMR (300 MHz, $CDCl_3$) δ 1.2-1.9 (17H, m, cyclohexyl + piperidine), 2.5 (4H, m, piperidine), 2.7 (2H, t, J = 6 Hz, CH_2N), 4.1 (2H, t, J = 6 Hz, OCH_2), 4.3 (2H, d, J = 6 Hz, CH_2Cy), 6.8 (2H, d, J = 9 Hz, Ar-H), 7.1 (1H, s, NH), 7.2 (1H, s, H-8), 7.4 (1H, d, J = 9 Hz, Ar-H); ^{13}C NMR (125 MHz, $CDCl_3$) δ 24.5, 26.0, 26.2, 26.8, 30.1, 37.7, 55.3, 58.3, 66.8, 72.4, 115.6, 116.7, 122.7, 133.5, 138.2, 155.4, 157.5, 161.6; MS(ES+) m/z 451.5 $[M + H]^+$; HRMS calcd for $C_{25}H_{34}N_6O_2$ $[M + H]^+$ 451.2816, found 451.2819.

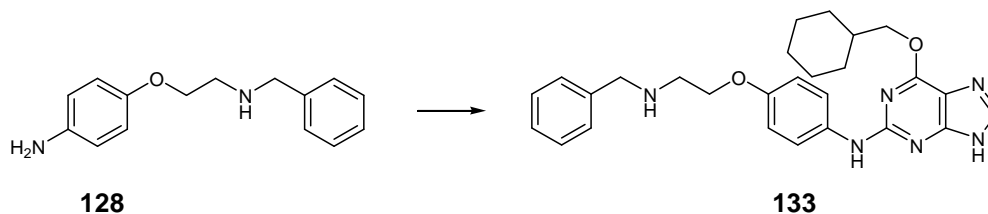
***N*-(4-(2-Morpholinoethoxy)phenyl)-6-(cyclohexylmethoxy)-9*H*-purin-2-amine (132)**



The compound was prepared according to General Procedure I from 4-(2-morpholinoethoxy)benzenamine (500 mg, 2.24 mmol) and 6-cyclohexylmethoxy-2-fluoro-9*H*-purine (312 mg, 1.25 mmol). The crude product was purified by flash chromatography on silica (EtOAc/MeOH 9:1) yielding the title compound as a white solid (315 mg, 46%).

R_f = 0.25 (EtOAc/MeOH 9:1); mp: 125.8-126.5 °C; IR (cm^{-1}): 2923, 2850, 2157, 2023, 1618, 1584, 1541, 1504, 1446; λ_{max} (EtOH)/nm 272.0; ^1H NMR (300 MHz, CDCl_3) δ 1.1-1.9 (11H, m, cyclohexyl), 2.6 (4H, m, NCH_2 morpholine), 2.8 (2H, t, J = 6 Hz, CH_2N), 3.7 (4H, t, J = 6 Hz, CH_2O morpholine), 4.1 (2H, t, J = 6 Hz, OCH_2), 4.3 (2H, d, J = 6 Hz, CH_2Cy), 6.8 (2H, d, J = 9 Hz, Ar-H), 7.0 (1H, s, NH), 7.2 (1H, s, H-8), 7.4 (1H, d, J = 9 Hz, Ar-H); ^{13}C NMR (125 MHz, CDCl_3) δ 26.0, 26.8, 30.2, 37.8, 54.4, 58.1, 67.2, 72.5, 115.7, 116.7, 122.9, 133.5, 137.7, 137.8, 155.5, 157.1, 161.7; MS(ES+) m/z 453.4 $[\text{M} + \text{H}]^+$; HRMS calcd for $\text{C}_{24}\text{H}_{32}\text{N}_6\text{O}_3$ $[\text{M} + \text{H}]^+$ 453.2609, found 453.2610.

***N*-(4-(2-(Benzylamino)ethoxy)phenyl)-6-(cyclohexylmethoxy)-9*H*-purin-2-amine (133)**

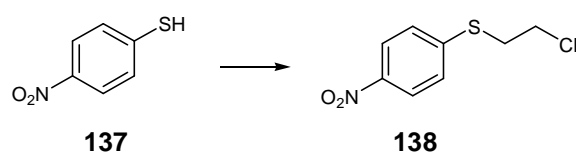


The compound was prepared according to General Procedure I from 4-(2-(benzylamino)ethoxy)benzenamine (500 mg, 2.06 mmol) and 6-cyclohexylmethoxy-

2-fluoro-9*H*-purine (312 mg, 1.25 mmol). The crude product was purified by flash chromatography on silica (EtOAc/MeOH 9:1) yielding the title compound as a white solid (355 mg, 51%).

R_f = 0.25 (EtOAc/MeOH 9:1); mp: 115.9-116.0 °C; IR (cm⁻¹): 3265, 2922, 2849, 2154, 1730, 1584, 1532, 1499, 1448; λ_{max} (EtOH)/nm 272.0; ¹H NMR (300 MHz, CDCl₃) δ 11.0-1.9 (11H, m, cyclohexyl), 3.0 (2H, t, J = 6 Hz, CH₂N), 3.9 (2H, s, PhCH₂), 4.0 (2H, t, J = 6 Hz, OCH₂), 4.3 (2H, d, J = 6 Hz, CH₂Cy), 6.8 (2H, d, J = 9 Hz, Ar-H), 7.1 (1H, s, NH), 7.3 (1H, s, H-8), 7.3 (5H, m, Ar-H), 7.4 (1H, d, J = 9 Hz, Ar-H); ¹³C NMR (125 MHz, CDCl₃) δ 26.0; 26.8, 30.1, 37.8, 48.6, 54.0, 68.6, 72.5, 115.4, 115.7, 116.7, 122.8, 127.3, 128.4, 128.7, 133.6, 137.8, 140.5, 154.9, 155.6, 157.1, 161.6; MS(ES+) m/z 473.1 [M + H]⁺; HRMS calcd for C₂₇H₃₂N₆O₂ [M + H]⁺ 473.2660, found 473.2659.

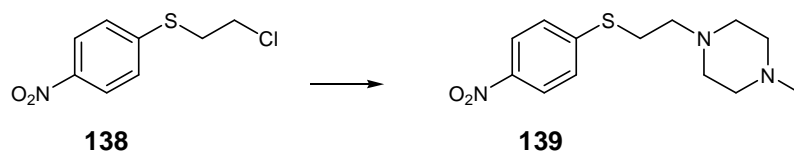
(2-Chloroethyl)(4-nitrophenyl)sulfane (**138**)²⁷⁹



To a stirred solution of *p*-nitro benzenethiol (2 g, 13 mmol) in acetonitrile (50 mL) was added K₂CO₃ (4.5 g, 32 mmol) and dichloroethane (10 mL, 130 mmol). The mixture was heated to reflux and stirred for 24 h. The excess base was filtered and the filtrate was evaporated *in vacuo* to yield the title compound as a yellow oil (2.8 g, quantitative).

R_f = 0.7 (EtOAc/MeOH 9:1); ¹H NMR (300 MHz, CDCl₃) δ 3.3 (2H, t, J = 6 Hz, CH₂Cl), 3.6 (2H, t, J = 6 Hz, SCH₂), 7.3 (2H, d, J = 9 Hz, Ar-H), 8.0 (2H, d, J = 9 Hz, Ar-H); ¹³C NMR (125 MHz, MeOD) δ 34.4, 43.0, 122.8, 130.0, 142.2, 142.6; MS(ES+) m/z 218.5 [M(³⁵Cl) + H]⁺; 220.5 [M(³⁷Cl) + H]⁺.

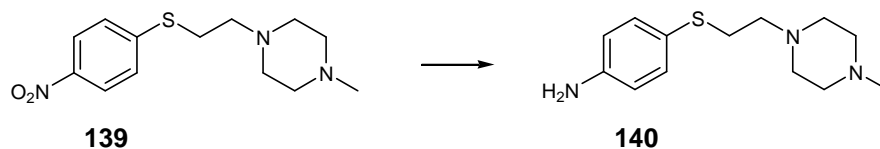
1-(2-(4-Nitrophenylthio)ethyl)-4-methylpiperazine (139) ²⁸⁰



The compound was prepared according to General Procedure III from (2-chloroethyl)(4-nitrophenyl)sulfane (2.94 g, 13 mmol) and *N*-methyl piperazine (7.5 mL, 67.5 mmol). The compound was obtained as a yellow solid (2.85 g, 91%).

R_f = 0.5 (EtOAc/MeOH 9:1); mp: 83-84 °C (lit. 86 °C) ; ^1H NMR (300 MHz, CDCl_3) δ 2.2 (3H, s, NMe), 2.4 (8H, m, NCH_2), 2.6 (2H, t, J = 6 Hz, CH_2N), 3.0 (2H, t, J = 6 Hz, SCH_2), 7.2 (2H, d, J = 9 Hz, Ar-H), 8.5 (2H, d, J = 9 Hz, Ar-H); ^{13}C NMR (125 MHz, CDCl_3) δ 34.4, 43.0, 44.4, 47.9, 53.7, 53.9, 57.6, 121.8, 133.4, 141.8, 142.7; MS(ES+) m/z 282.5 $[\text{M} + \text{H}]^+$.

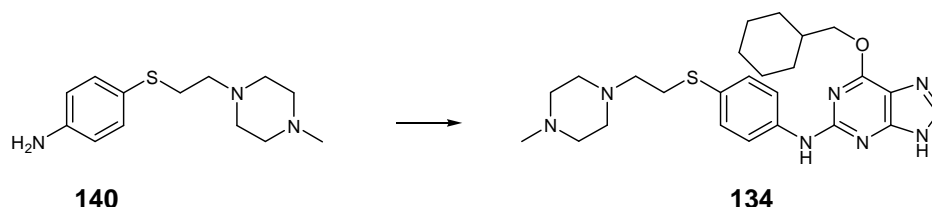
4-(2-(4-Methylpiperazin-1-yl)ethylthio)benzenamine (140) ²⁶⁵



The compound was prepared according to General Procedure IV from 1-methyl-4-(2-(4-nitrophenylthio)ethyl)piperazine (800 mg, 2.84 mmol) and obtained as a clear yellow oil (0.42 g, 48%).

R_f = 0.5 (EtOAc/MeOH 9:1); mp: 88.9-89.9 °C ^1H NMR (300 MHz, CDCl_3) δ 2.2 (3H, s, NMe), 2.4 (8H, m, CH_2), 2.5 (2H, t, J = 6 Hz, CH_2N), 2.8 (2H, t, J = 6 Hz, SCH_2), 3.7 (2H, s, NH_2), 6.6 (2H, d, J = 9 Hz, Ar-H), 7.2 (2H, d, J = 9 Hz, Ar-H); ^{13}C NMR (125 MHz, CDCl_3) δ 32.6, 42.9, 46.4, 48.1, 54.7, 56.7, 58.6, 123.4, 134.0, 143.8, 148.2; MS(ES+) m/z 252.3 $[\text{M} + \text{H}]^+$.

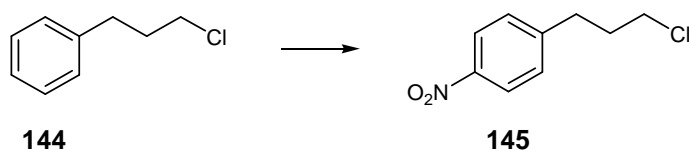
***N*-(4-(2-(4-Methylpiperazin-1-yl)ethylthio)phenyl)-6-(cyclohexylmethoxy)-9*H*-purin-2-amine (134)**



The compound was prepared according to General Procedure I from 4-(2-(4-methylpiperazin-1-yl)ethylthio)benzenamine (250 mg, 1 mmol) and 6-cyclohexylmethoxy-2-fluoro-9*H*-purine (125 mg, 0.55 mmol). The crude product was purified by flash chromatography on silica (EtOAc/MeOH 9:1) yielding the title compound as a white solid (108 mg, 47%).

R_f = 0.25 (EtOAc/MeOH 9:1); mp: 146.0-146.9 °C; IR (cm^{-1}): 3096, 2924, 2848, 2798, 2191, 1731, 1596, 1575, 1530, 1492, 1444; λ_{max} (EtOH)/nm 288.5; ^1H NMR (300 MHz, CDCl_3) δ 1.2-1.9 (11H, m, cyclohexyl), 2.3 (3H, s, NMe), 2.5 (8H, m, piperazine), 2.6 (2H, t, J = 6 Hz, CH_2N), 3.0 (2H, t, J = 6 Hz, SCH_2), 4.3 (2H, d, J = 6 Hz, OCH_2), 7.0 (1H, s, H-8), 7.3 (2H, d, J = 9 Hz, Ar-H), 7.5 (1H, d, J = 9 Hz, Ar-H), 7.6 (1H, s, NH); ^{13}C NMR (125 MHz, CDCl_3) δ 25.7, 26.4, 29.8, 37.3, 45.7, 52.7, 54.7, 57.7, 66.9, 72.2, 115.6, 119.6, 131.7, 138.2, 155.3, 157.0, 161.5; MS(ES+) m/z 482.5 $[\text{M} + \text{H}]^+$; HRMS calcd for $\text{C}_{25}\text{H}_{35}\text{N}_7\text{OS}$ $[\text{M} + \text{H}]^+$ 482.2697, found 482.26982.

1-(3-Chloropropyl)-4-nitrobenzene (145) ²⁸¹⁻²⁸²

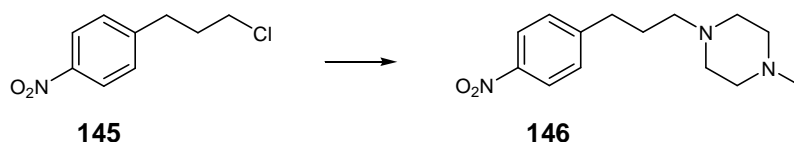


To stirred nitric acid (1.6 mL, 260 mmol) at 0 °C was added sulfuric acid (1.05 mL, 193.5 mmol) dropwise. 3-chloropropyl benzene (2 mL, 12.9 mmol) was then added dropwise. The mixture was stirred at 0 °C for 10 min, then allowed to warm up to

room temperature and stirred for further 3 h. Ice water (10 mL) was added to the mixture, which was then extracted with CH₂Cl₂ (3 x 10 mL). The crude product was purified by column chromatography on silica (Et₂O/Hexane 5:95) and the title compound was isolated as a colourless oil (1.4 g, 62%).

R_f = 0.5 (EtOAc); bp: 168-169 °C ¹H NMR (300 MHz, CDCl₃) δ 22.1 (2H, quint, J = 6 Hz, CH₂CH₂CH₂), 2.9 (2H, t, J = 6 Hz, PhCH₂), 3.5 (2H, t, J = 6 Hz, CH₂Cl), 7.3 (2H, d, J = 9 Hz, Ar-H), 8.1 (2H, d, J = 9 Hz, Ar-H); ¹³C NMR (125 MHz, CDCl₃) δ 26.9, 37.5, 44.4, 121.3, 129.4, 140.0, 145.23; MS(ES+) m/z 200.3 [M(³⁵Cl) + H]⁺; 202.3 [M(³⁷Cl) + H]⁺.

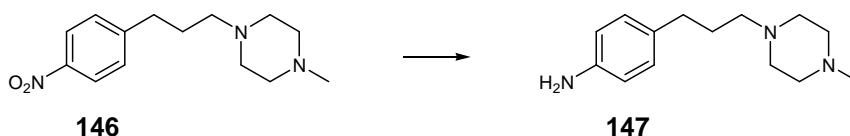
1-Methyl-4-(3-(4-nitrophenyl)propyl)piperazine (146)^{280, 283}



The compound was prepared according to General Procedure III from 1-(3-chloropropyl)-4-nitrobenzene (700 mg, 3.5 mmol) and *N*-methyl piperazine (2 mL, 17.5 mmol). The compound was obtained as a yellow solid (697 mg, 85%).

R_f = 0.5 (EtOAc/MeOH 9:1); mp: 76-77 °C (lit. 79 °C) ; ¹H NMR (300 MHz, CDCl₃) δ 1.9 (2H, quint, J = 6 Hz, CH₂CH₂CH₂), 2.2 (3H, s, NMe), 2.3 (2H, t, J = 6 Hz, PhCH₂), 2.4 (8H, m, CH₂ piperazine), 2.6 (2H, t, J = 6 Hz, CH₂N), 7.2 (2H, d, J = 9 Hz, Ar-H), 8.0 (2H, d, J = 9 Hz, Ar-H); ¹³C NMR (125 MHz, CDCl₃) δ 27.6, 33.4, 40.8, 50.7, 54.7, 56.7, 56.9, 57.0, 120.3, 128.4, 141.0, 147.7; MS(ES+) m/z 264.6 [M + H]⁺.

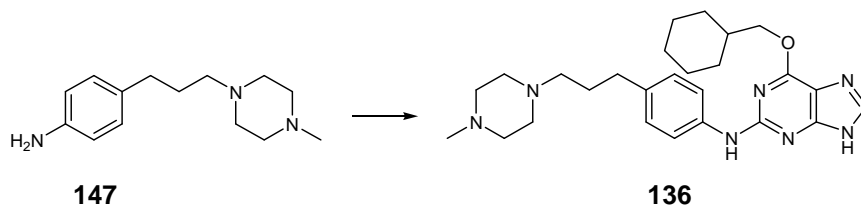
1-Methyl-4-(3-(4-nitrophenyl)propyl)piperazine (147)²⁸⁴



The compound was prepared according to General Procedure IV from 1-methyl-4-(3-(4-nitrophenyl)propyl)piperazine (700 mg, 2.66 mmol) and obtained as a clear yellow oil (0.65 g, 98%).

R_f = 0.5 (EtOAc/MeOH 9:1); mp: 83.0-84.1 °C (lit. 89 °C); ^1H NMR (300 MHz, CDCl_3) δ 1.9 (2H, quint, J = 6 Hz, $\text{CH}_2\text{CH}_2\text{CH}_2$), 2.0 (3H, s, NMe), 2.1 (2H, t, J = 6 Hz, PhCH_2), 2.2 (8H, m, CH_2 piperazine), 2.4 (2H, t, J = 6 Hz, CH_2N), 6.4 (2H, d, J = 9 Hz, Ar-H), 7.0 (2H, d, J = 9 Hz, Ar-H); ^{13}C NMR (125 MHz, CDCl_3) δ 30.5, 31.8, 39.6, 51.3, 53.6, 53.7, 58.9, 59.0, 121.3, 127.9, 142.6, 148.5; MS(ES+) m/z 234.1 [$\text{M} + \text{H}$] $^+$.

6-(Cyclohexylmethoxy)-*N*-(4-(3-(4-methylpiperazin-1-yl)propyl)phenyl)-9*H*-purin-2-amine (136)

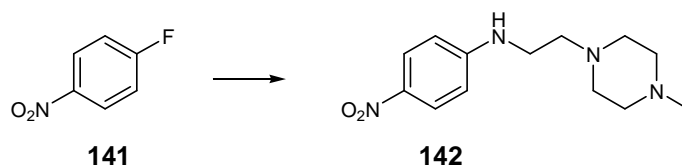


The compound was prepared according to General Procedure I from 4-(3-(4-methylpiperazin-1-yl)propyl)benzenamine (250 mg, 1 mmol) and 6-cyclohexylmethoxy-2-fluoro-9*H*-purine (125 mg, 0.55 mmol). The crude product was purified by flash chromatography on silica (EtOAc/MeOH 9:1) yielding the title compound as a white solid (102 mg, 52%).

R_f = 0.25 (EtOAc/MeOH 9:1); mp: 102.2-103.6 °C; IR (cm^{-1}): 2920, 2803, 1615, 1581, 1535, 1506, 1444; λ_{max} (EtOH)/nm 272.5; ^1H NMR (300 MHz, CDCl_3) δ 1.0-1.9 (13H, m, cyclohexyl + $\text{CH}_2\text{CH}_2\text{CH}_2$), 2.3 (3H, s, NMe), 2.3 (2H, t, J = 8 Hz, CH_2Ph), 2.5 (8H, m, CH_2 piperazine), 2.6 (2H, t, J = 9 Hz, CH_2N), 4.3 (2H, d, J = 6 Hz, OCH_2), 7.0 (1H, s, NH), 7.1 (2H, d, J = 9 Hz, Ar-H), 7.4 (2H, d, J = 9 Hz, Ar-H), 8.0 (1H, s, H-8); ^{13}C NMR (125 MHz, CDCl_3) δ 26.9, 27.5, 29.4, 30.8, 34.0, 38.7, 45.9, 48.5, 48.7, 48.8, 49.0, 49.2, 49.4, 49.5, 53.6, 55.5, 58.9, 72.9, 120.3, 129.4, 136.3, 140.0, 140.2,

157.4, 161.4; MS(ES+) m/z 464.7 $[M + H]^+$; HRMS calcd for $C_{26}H_{37}N_7O$ $[M + H]^+$ 464.3132, found 464.3134.

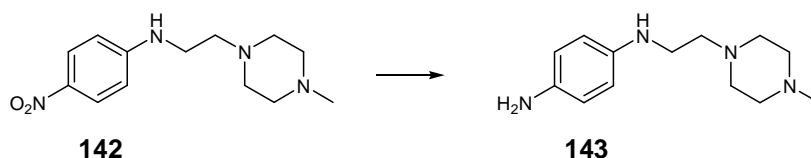
***N*-(2-(4-Methylpiperazin-1-yl)ethyl)-4-nitrobenzenamine (142)** ²⁸⁵



To a stirred solution of *p*-nitro fluorobenzene (1.63 mL, 15.4 mmol) in acetonitrile (10 mL) was added 2-(4-methylpiperazin-1-yl)ethanamine (2 mL, 14 mmol). The mixture was heated to reflux and stirred for 48 h. The solvent was removed under reduced pressure and the residue was taken up in water (20 mL) and extracted with CH₂Cl₂ (3 x 20 mL). The combined organic layers were dried over Na₂SO₄ and evaporated *in vacuo*, yielding the title compound as a yellow solid (2.2 g, 84%).

R_f = 0.7 (EtOAc); mp: 200-201 °C (lit. 201 °C); ¹H NMR (300 MHz, CDCl₃) δ 2.3 (3H, s, NMe), 2.5 (8H, m, CH₂ piperazine), 2.6 (2H, t, J = 6 Hz, CH₂N), 3.2 (2H, t, J = 6 Hz, NHCH₂), 5.3 (1H, s, PhNH), 6.5 (2H, d, J = 9 Hz, Ar-H), 8.0 (2H, d, J = 9 Hz, Ar-H); ¹³C NMR (125 MHz, CDCl₃) δ 43.8, 47.7, 53.5, 55.9, 58.1, 72.8, 114.6, 123.0, 132.6, 158.7; MS(ES+) m/z 265.1 $[M + H]^+$.

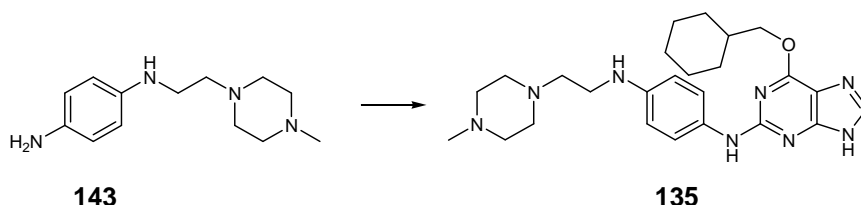
***N*1-(2-(4-Methylpiperazin-1-yl)ethyl)benzene-1,4-diamine (143)** ²⁸⁵



The compound was prepared according to General Procedure IV from *N*-(2-(4-methylpiperazin-1-yl)ethyl)-4-nitrobenzenamine (2 g, 7.56 mmol) and obtained as an orange solid (1.85 g, 98%).

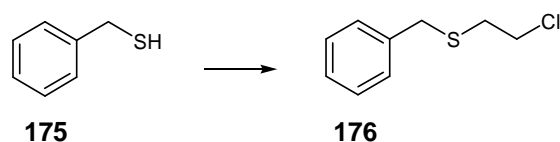
R_f = 0.5 (EtOAc/MeOH 9:1); mp: 200-201 °C (lit. 201 °C); ^1H NMR (300 MHz, CDCl_3) δ 2.2 (3H, s, NMe), 2.4 (8H, m, CH_2 piperazine), 2.5 (2H, t, J = 6 Hz, CH_2N), 3.0 (2H, t, J = 6 Hz, NHCH_2), 3.5 (2H, s, NH_2), 6.4 (2H, d, J = 9 Hz, Ar-H), 6.5 (2H, d, J = 9 Hz, Ar-H); ^{13}C NMR (125 MHz, CDCl_3) δ 43.8, 47.7, 53.5, 56.0, 58.1, 72.8, 112.4, 117.8, 132.6, 158.7; MS(ES+) m/z 235.6 $[\text{M} + \text{H}]^+$.

***N*1-(6-(cyclohexylmethoxy)-9*H*-purin-2-yl)-*N*4-(2-(4-methylpiperazin-1-yl)ethyl)benzene-1,4-diamine (135)**



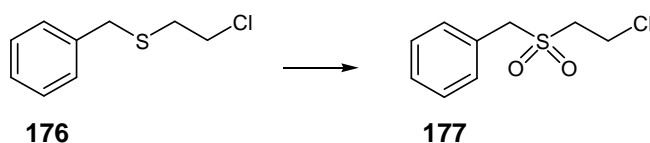
The compound was prepared according to General Procedure I from *N*1-(2-(4-methylpiperazin-1-yl)ethyl)benzene-1,4-diamine (250 mg, 1 mmol) and 6-cyclohexylmethoxy-2-fluoro-9*H*-purine (0.55 mmol, 125 mg). The crude product was purified by flash chromatography on silica (EtOAc/MeOH 9:1) yielding the title compound as a white solid (98 mg, 49%).

R_f = 0.25 (EtOAc/MeOH 9:1); mp: 143.1-144.0 °C; IR (cm^{-1}): 2922, 2846, 2803, 1732, 1618, 1582, 1500, 1446; λ_{max} (EtOH)/nm 279.0; ^1H NMR (300 MHz, CDCl_3) δ 1.0 -1.9 (11H, m, cyclohexyl), 2.3 (3H, s, NMe), 2.4 (8H, m, CH_2 piperazine), 2.6 (2H, t, J = 8 Hz, NCH_2), 3.1 (2H, t, J = 8 Hz, CH_2N), 4.2 (2H, d, J = 6 Hz, OCH_2), 6.6 (2H, d, J = 9 Hz, Ar-H), 6.7 (1H, s, NH), 7.2 (2H, d, J = 9 Hz, Ar-H), 7.3 (1H, s, H-8); ^{13}C NMR (125 MHz, CDCl_3) δ 26.9, 27.6, 30.8, 38.7, 42.5, 45.9, 48.5, 48.6, 48.8, 49.0, 49.2, 49.3, 49.5, 53.7, 55.6, 58.1, 72.8, 114.6, 123.0, 132.3, 158.7; MS(ES+) m/z 465.5 $[\text{M} + \text{H}]^+$; HRMS calcd for $\text{C}_{25}\text{H}_{36}\text{N}_8\text{O}$ $[\text{M} + \text{H}]^+$ 465.3085, found 465.3058.

Benzyl(2-chloroethyl)sulfane (176) ²⁸⁶⁻²⁸⁷

To a stirred solution of phenylmethanethiol (2 mL, 15.5 mmol) in acetonitrile (10 mL) was added K_2CO_3 (5.3 g, 38.7 mmol) and dichloroethane (12.2 mL, 155 mmol). The mixture was heated to reflux and stirred for 48 h. The excess base was filtered and the filtrate was evaporated *in vacuo* to yield the title compound (2.8 g, quantitative).

R_f = 0.7 (EtOAc); mp: 139 °C (lit. 138 °C); 1H NMR (300 MHz, $CDCl_3$) δ 2.7 (2H, t, J = 6 Hz, CH_2Cl), 3.5 (2H, t, J = 6 Hz, SCH_2), 3.7 (2H, s, $PhCH_2$), 7.3 (5H, br s, Ar-H); ^{13}C NMR (125 MHz, $CDCl_3$) δ 34.4, 38.5, 43.0, 127.9, 128.0, 128.4, 137.1; MS(ES+) m/z 187.3 [$M(^{35}Cl) + H$] $^+$; 189.3 [$M(^{37}Cl) + H$] $^+$.

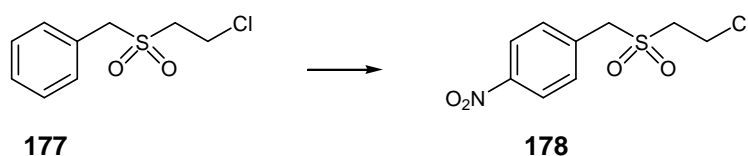
1-((2-Chloroethylsulfonyl)methyl)benzene (177) ²⁸⁸⁻²⁸⁹

To a stirred solution of *N*-(benzyl(2-chloroethyl)sulfane) (3 g, 16.07 mmol) in CH_2Cl_2 (50 mL) was added *m*CPBA (15 g, 80.34 mmol). The reaction mixture was stirred at room temperature for 48 h. The solvent was removed under reduced pressure and the residue was taken up in EtOAc (50 mL) and washed with saturated aqueous $NaHCO_3$ (6 x 30 mL). The combined organic layers were dried over Na_2SO_4 and the solvent was removed under reduced pressure, yielding the title compound as a white solid (2.7 g, 79%).

R_f = 0.5 (EtOAc/Hexane 1:9); mp: 95-96 °C (lit. 96 °C); 1H NMR (300 MHz, $CDCl_3$) δ 3.3 (2H, t, J = 6 Hz, CH_2Cl), 3.8 (2H, t, J = 6 Hz, SO_2CH_2), 4.3 (2H, s, $PhCH_2$), 7.4

(5H, s, Ar-H); ^{13}C NMR (125 MHz, CDCl_3) δ 35.4, 57.5, 58.0, 124.6, 129.1, 130.6, 137.1; MS(ES+) m/z 219.2 [$\text{M}(^{35}\text{Cl}) + \text{H}$] $^+$; 221.3 [$\text{M}(^{37}\text{Cl}) + \text{H}$] $^+$.

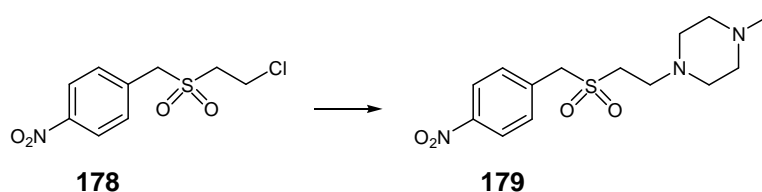
1-((2-Chloroethylsulfonyl)methyl)-4-nitrobenzene (178) ²⁸⁹



To stirred nitric acid (2 mL, 22.86 mmol) at 0 °C was added sulfuric acid (1 mL, 17.15 mmol) dropwise. ((2-chloroethylsulfonyl)methyl)benzene (2.5 g, 11.4 mmol) was then added in small portions. The mixture was stirred at 0 °C for 10 min, then allowed to warm up to room temperature and stirred for further 3 h. Ice water (10 mL) was added to the mixture, which was then extracted with CH_2Cl_2 (3 x 10 mL). The combined organic layers were dried over Na_2SO_4 and evaporated under reduced pressure, and the crude product was purified by column chromatography on silica using a gradient solvent system (EtOAc/Hex 1:9 \rightarrow 1:1). The title compound was isolated as a white solid (1.20 g, 51%).

R_f = 0.3 (EtOAc/Hexane 1:9); mp: 87 °C (lit. 89 °C); ^1H NMR (300 MHz, CDCl_3) δ 3.3 (2H, t, J = 6 Hz, CH_2Cl), 3.9 (2H, t, J = 6 Hz, SO_2CH_2), 4.4 (2H, s, PhCH_2), 7.6 (2H, d, J = 9 Hz, Ar-H), 8.2 (2H, d, J = 9 Hz, Ar-H); ^{13}C NMR (125 MHz, CDCl_3) δ 35.4, 57.5, 58.0, 121.6, 121.9, 131.0, 149.5; MS(ES+) m/z 264.1 [$\text{M}(^{35}\text{Cl}) + \text{H}$] $^+$; 266.1 [$\text{M}(^{37}\text{Cl}) + \text{H}$] $^+$.

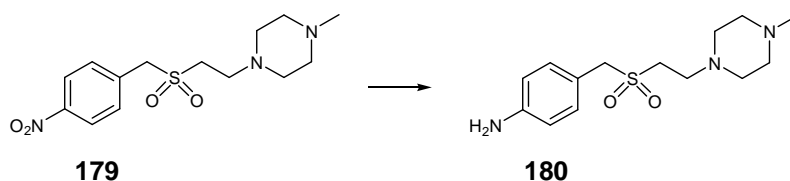
1-(2-(4-Nitrobenzylsulfonyl)ethyl)-4-methylpiperazine (179)



The compound was prepared according to General Procedure III from 1-((2-chloroethylsulfonyl)methyl)-4-nitrobenzene (800 mg, 3.0 mmol) and *N*-methyl piperazine (1.7 mL, 15 mmol). The compound was obtained as a yellow solid (784 mg, 86%).

R_f = 0.5 (EtOAc/MeOH 9:1); mp: 93-94 °C; IR (cm⁻¹): 3315, 3000, 2900, 2837, 1608, 1510, 1450; λ_{max} (EtOH)/nm 275.0; ¹H NMR (300 MHz, CDCl₃) δ 2.2 (3H, s, NMe), 2.2-2.8 (8H, m, CH₂ piperazine), 3.0 (2H, t, J = 6 Hz, CH₂N), 4.5 (2H, t, J = 6 Hz, SO₂CH₂), 5.2 (2H, s, PhCH₂), 7.5 (2H, d, J = 9 Hz, Ar-H), 8.2 (2H, d, J = 9 Hz, Ar-H); ¹³C NMR (125 MHz, CDCl₃) δ 43.7, 49.4, 50.0, 52.3, 55.2, 57.5, 58.0, 122.4, 123.0, 133.1, 150.6; MS(ES+) m/z 328.13 [M + H]⁺; HRMS calcd for C₁₄H₂₁N₃O₄S [M + H]⁺ 328.1489, found 328.1488.

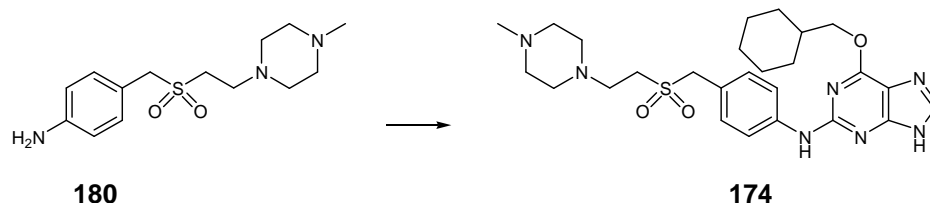
4-((2-(4-methylpiperazin-1-yl)ethylsulfonyl)methyl)benzenamine (180)



The compound was prepared according to General Procedure IV from 1-methyl-4-(2-(4-nitrobenzylsulfonyl)ethyl)piperazine (800 mg, 3.0 mmol) and obtained as a clear yellow oil (702 mg, 98%).

R_f = 0.5 (EtOAc/MeOH 9:1); mp: 98-99 °C; IR (cm⁻¹): 3407, 3332, 3224, 3094, 2959, 1683, 1597, 1514; λ_{max} (EtOH)/nm 290.6; ¹H NMR (300 MHz, CDCl₃) δ 2.3 (3H, s, NMe), 2.3-2.5 (8H, m, CH₂ piperazine), 2.5 (2H, t, J = 6 Hz, CH₂N), 3.5 (2H, t, J = 6 Hz, SO₂CH₂), 4.4 (2H, s, PhCH₂), 6.7 (2H, d, J = 9 Hz, Ar-H); 7.2 (2H, d, J = 9 Hz, Ar-H); ¹³C NMR (125 MHz, CDCl₃) δ 43.7, 49.4, 50.0, 52.3, 55.2, 57.5, 58.0, 114.8, 116.3, 132.4, 149.0, 150.1; MS(ES+) m/z 298.15 [M + H]⁺; HRMS calcd for C₁₄H₂₃N₃O₂S [M + H]⁺ 298.8712, found 298.5623.

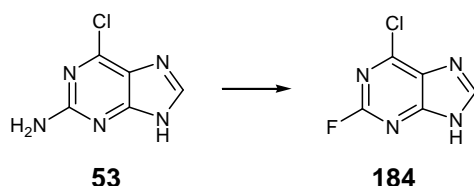
***N*-(4-((2-(4-Methylpiperazin-1-yl)ethylsulfonyl)methyl)phenyl)-6-(cyclohexylmethoxy)-9*H*-purin-2-amine (174)**



The compound was prepared according to General Procedure I from 4-((2-(4-methylpiperazin-1-yl)ethylsulfonyl)methyl)benzenamine (250 mg, 0.84 mmol) and 6-cyclohexylmethoxy-2-fluoro-9*H*-purine (75 mg, 0.42 mmol). The crude product was purified by flash chromatography on silica (EtOAc/MeOH 9:1) yielding the title compound as a white solid (116 mg, 47%).

R_f = 0.25 (EtOAc/MeOH 9:1); mp: 158-160 °C; IR (cm^{-1}): 3431, 2920, 2849, 2806, 1730, 1585, 1533, 1496, 1439; λ_{max} (EtOH)/nm 247.5; ^1H NMR (300 MHz, CDCl_3) δ 1.2-1.8 (11H, m, cyclohexyl), 2.2 (3H, s, NMe), 2.5 (8H, m, CH_2 piperazine), 2.9 (2H, t, J = 8 Hz, CH_2N), 3.0 (2H, t, J = 8 Hz, $\text{CH}_2\text{CH}_2\text{SO}_2$), 4.2 (2H, d, J = 6 Hz, OCH_2), 4.3 (2H, d, J = 6 Hz, $\text{SO}_2\text{CH}_2\text{Ph}$), 7.0 (1H, s, NH), 7.30 (2H, d, J = 9 Hz, Ar-H), 7.51 (2H, d, J = 9 Hz, Ar-H), 7.8 (1H, s, H-8); ^{13}C NMR (125 MHz, CDCl_3) δ 26.9, 27.5, 30.8, 38.7, 45.9, 48.5, 48.7, 48.8, 49.0, 49.2, 49.3, 49.5, 49.9, 50.0, 51.8, 51.9, 53.4, 55.6, 55.7, 60.6, 73.0, 73.1, 119.8, 120.3, 132.4; MS(ES+) m/z 528.4 $[\text{M} + \text{H}]^+$; HRMS calcd for $\text{C}_{26}\text{H}_{37}\text{N}_7\text{O}_3\text{S}$ $[\text{M} + \text{H}]^+$ 528.2751, found 528.27183.

6-Chloro-2-fluoro-9*H*-purine (184) ²⁹⁰

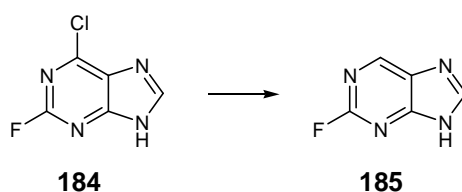


A 50% (w/w) aqueous solution of HBF_4 (40 mL) was brought to the temperature of -5 °C. 2-amino-6-chloro purine (6 g, 27.8 mmol) was then added in one portion. NaNO_2

(4.2 g, 0.76 mol) was dissolved in water (50 mL) and added dropwise, ensuring that the temperature remained below 0 °C. The temperature was raised to 20 °C and the mixture was stirred for 2 h. The solution was neutralised with Na₂CO₃ and the mixture was concentrated *in vacuo*. The crude product was purified by column chromatography (EtOAc/MeOH 9:1) yielding the title compound as a white solid (4.3 g, 64%).

R_f = 0.5 (EtOAc/Hexane 1:9); mp: 169-173 °C (lit. 173 °C); ¹H NMR (300 MHz, DMSO) δ 8.3 (1H, s, H-8); ¹³C NMR (125 MHz, DMSO) δ 131.5, 144.1, 151.5, 153.7, 158.9; MS(ES+) *m/z* 172.3 [M + H]⁺.

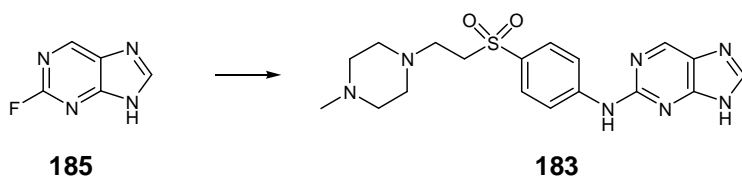
2-Fluoro-9H-purine (185)²⁹⁰



To a stirred solution of 6-chloro-2-fluoropurine (1 g, 5.8 mmol) in methanol (10 mL) was added ammonium formate (1.82 g, 30 mmol) followed by palladium hydroxide (20% on activated carbon, 1 g). The mixture was heated to reflux and stirred for 1 h. The reaction mixture was filtered through a pad of celite and the filtrate was evaporated *in vacuo* to yield the title compound as a white crystalline solid (702 mg, 92%).

R_f = 0.5 (EtOAc/Hexane 1:9); mp: 225-228 °C (lit. 228 °C); ¹H NMR (300 MHz, DMSO) δ 8.3 (1H, s, H-8), 9.3 (1H, s, H-6); ¹³C NMR (125 MHz, DMSO) δ 133.6, 145.0, 151.9, 152.2, 159.9; MS(ES+) *m/z* 138.66 [M + H]⁺.

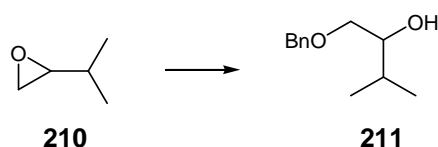
***N*-(4-(2-(4-Methylpiperazin-1-yl)ethylsulfonyl)phenyl)-9*H*-purin-2-amine (183)**



The compound was prepared according to General Procedure I from tert-butyl 4-(2-(4-methylpiperazin-1-yl)ethylsulfonyl)phenylcarbamate (250 mg, 0.65 mmol) and 2-fluoro-9*H*-purine (70 mg, 0.32 mmol). The crude product was purified by flash chromatography on silica (EtOAc/MeOH 9:1) yielding the title compound as a white solid (116 mg, 45%).

R_f = 0.25 (EtOAc/MeOH 9:1); mp: 118.7-120.0 °C; IR (cm^{-1}): 3277, 3180, 3101, 2920, 2849, 2808, 1596, 1541, 1506, 1458, 1408; λ_{max} (EtOH)/nm 247.5; ^1H NMR (300 MHz, CDCl_3) δ 2.0 (3H, s, NMe), 2.2 (8H, m, CH_2 piperazine), 2.6 (2H, t, J = 8 Hz, CH_2N), 3.3 (2H, t, J = 8 Hz, CH_2SO_2), 7.7 (2H, d, J = 9 Hz, Ar-H), 7.9 (2H, d, J = 9 Hz, Ar-H), 8.1 (1H, s, H-6), 8.7 (1H, s, H-8); ^{13}C NMR (125 MHz, CDCl_3) δ 45.9, 48.5, 48.7, 48.8, 49.0, 49.2, 49.4, 49.5, 49.9, 52.5, 53.1, 54.3, 55.5, 79.0, 118.8, 130.3, 144.9, 147.9, 157.6; MS(ES+) m/z 402.3 $[\text{M} + \text{H}]^+$; HRMS calcd for $\text{C}_{18}\text{H}_{23}\text{N}_7\text{O}_2\text{S}$ $[\text{M} + \text{H}]^+$ 402.17345, found 402.17345.

1-(Benzyloxy)-3-methylbutan-2-ol (211) ²⁹¹

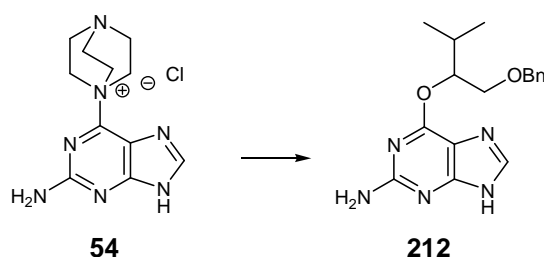


To stirred benzyl alcohol (25 mL, 0.23 mol) was added diced sodium (1.6 g, 69 mmol). The reaction mixture was heated to 150 °C and stirred until all the sodium had dissolved. The reaction mixture was cooled down to room temperature, then 2-isopropyloxirane (2 mL, 23 mmol) was added dropwise. The reaction mixture was heated to 180 °C and stirred for 48 h. Water (15 mL) was added to the mixture, then

acetic acid until pH neutral. The reaction mixture was then extracted with CH₂Cl₂ (3 x 30 mL). The combined organic layers were dried over Na₂SO₄ and evaporated *in vacuo*. The crude product was purified by fractioned distillation, affording the title compound as a colourless oil (2.1 g, 74%).

R_f = 0.25 (EtOAc/Hexane 1:9); bp: 291 °C (lit.); ¹H NMR (300 MHz, CDCl₃) δ 0.7 (3H, d, *J* = 6 Hz, (CH₃)₂), 1.1 (3H, d, *J* = 6 Hz, (CH₃)₂), 1.6 (1H, m, CH(CH₃)₂), 2.4 (1H, s, OH), 3.3 (1H, q, *J* = 6 Hz, CHOH), 3.5 (2H, t, *J* = 6 Hz, OCH₂), 4.4 (2H, s, PhCH₂). 7.3 (5H, br s, Ar-H); ¹³C NMR (125 MHz, MeOD) δ 17.4, 30.5, 75.0, 78.9, 127.9, 128.0, 128.4, 128.9, 129.0, 137.1; MS(ES+) *m/z* 194.6 [M + H]⁺.

6-(1-(Benzyloxy)-3-methylbutan-2-yloxy)-9H-purin-2-amine (212)

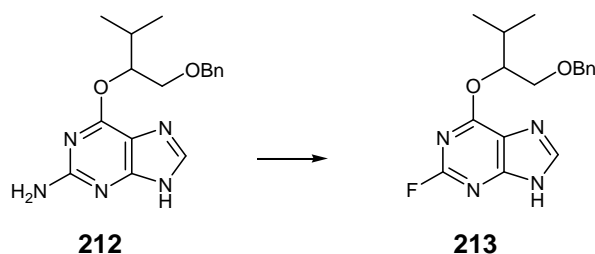


1-(Benzyloxy)-3-methylbutan-2-ol (2 g, 10.3 mmol) was added dropwise to a suspension of NaH (200 mg, 7.7 mmol) in DMSO (10 mL), and the mixture was stirred at room temperature for 1 hour. 1-(2-Amino-9H-purin-6-yl)-4-aza-1-azoniabicyclo[2.2.2]octane chloride (750 mg, 2.5 mmol) was then added in portions and the mixture was stirred at room temperature for 24 h. The mixture was concentrated *in vacuo* and the residue was taken up in water (10 mL) and acetic acid was added until pH neutral. The mixture was extracted with CH₂Cl₂ (3 x 20 mL). The combined organic layers were dried over Na₂SO₄ and the solvent was removed under reduced pressure. The crude product was purified by column chromatography (EtOAc/Petrol 1:1) to yield the title compound as a white solid (645 mg, 78%).

R_f = 0.25 (EtOAc); mp: decomposes > 258 °C; IR (cm⁻¹): 3471, 3323, 3186, 2962, 2870, 2791, 2560, 1616, 1575, 1497, 1452; λ_{max} (EtOH)/nm 282.0; ¹H NMR (300

MHz, CDCl₃) δ 0.9 (6H, d, J = 6 Hz, (CH₃)₂), 2.1 (1H, m, CH(CH₃)₂), 3.7 (2H, d, J = 6 Hz, CH₂O); 4.5 (1H, q, J = 6 Hz, CHO-Ar), 5.0 (2H, s, OCH₂Ph), 5.5 (1H, s, NH), 7.2 (5H, s, Ar-H), 7.7 (1H, s, H-8); ¹³C NMR (125 MHz, CDCl₃) δ 17.2, 30.7, 75.6, 79.0, 116.4, 127.9, 128.0, 128.4, 128.9, 129.0, 137.1, 144.8, 153.2, 159.9, 160.1; MS(ES+) m/z 328.0 [M + H]⁺; HRMS calcd for C₁₇H₂₁N₅O₂ [M + H]⁺ 328.1768, found 328.17586.

6-(1-(Benzyloxy)-3-methylbutan-2-yloxy)-2-fluoro-9H-purine (213)

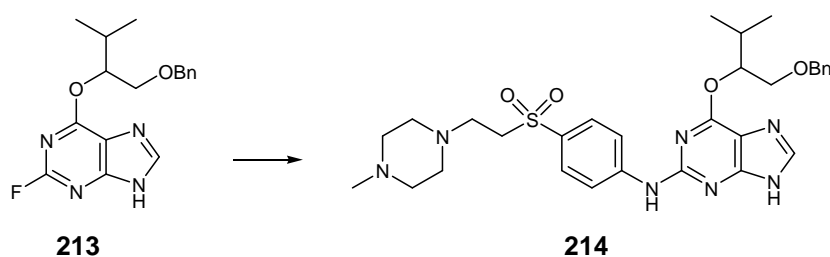


6-(1-(benzyloxy)-3-methylbutan-2-yloxy)-9H-purin-2-amine (400 mg, 1.22 mmol) was dissolved in TFE (2.5 mL) and water (5 mL), then brought to 5 °C. A 50% (w/w) aqueous solution of HBF₄ (0.25 mL, 2.44 mmol) was added dropwise, then LiBF₄ (2.3 g, 24.4 mmol) was added in one portion. NaNO₂ (170 mg, 2.5 mmol) was dissolved in water (3 mL) and added dropwise to the mixture, which was stirred at 5 °C for 1 h. The reaction was allowed to warm up to room temperature and stirred for further 3 h. Aqueous saturated NaHCO₃ was added to the mixture until pH neutral. The mixture was extracted with CH₂Cl₂ (3 x 15 mL) and the combined organic layers were dried over Na₂SO₄ and evaporated under reduced pressure. The crude product was purified by column chromatography (EtOAc/Petrol 1:1) yielding the title compound as a white solid (222 mg, 58%).

R_f = 0.5 (EtOAc); mp: 145-146 °C; IR (cm⁻¹): 3742, 3232, 3168, 2926, 2880, 2719, 2590, 1661, 1557, 1487, 1492; λ_{max} (EtOH)/nm 282.0; ¹H NMR (300 MHz, CDCl₃) δ 0.9 (6H, d, J = 6 Hz, (CH₃)₂), 2.2 (1H, m, CH(CH₃)₂), 3.4 (2H, s, CH₂Ph), 3.7 (1H, q, J = 6 Hz, CHO-Ar), 4.5 (2H, d, J = 6 Hz, CH₂O), 5.5 (1H, s, NH), 7.2 (5H, s, Ar-H), 8.1 (1H, s, H-8); ¹³C NMR (125 MHz, CDCl₃) δ 12.7, 37.0, 76.5, 79.6, 114.6, 129.7,

128.5, 128.9, 129.1, 130.0, 131.7, 148.4, 152.3, 159.8, 161.0; MS(ES+) m/z 331.2 [M + H]⁺; HRMS calcd for C₁₇H₁₉FN₄O₂ [M + H]⁺ 331.1565, found 331.1566.

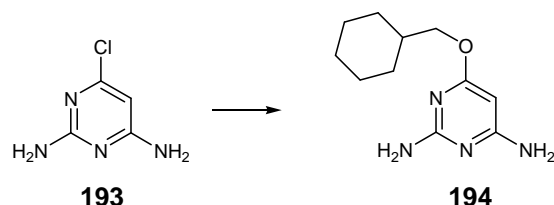
6-(1-(Benzyloxy)-3-methylbutan-2-yloxy)-*N*-(4-(2-(4-methylpiperazin-1-yl)ethylsulfonyl)phenyl)-9*H*-purin-2-amine (214)



The compound was prepared according to General Procedure I from *tert*-butyl 4-(2-(4-methylpiperazin-1-yl)ethylsulfonyl)phenylcarbamate (370 mg, 0.97 mmol) and 6-(1-(benzyloxy)-3-methylbutan-2-yloxy)-2-fluoro-9*H*-purine (160 mg, 0.48 mmol). The crude product was purified by flash chromatography on silica (EtOAc/MeOH 9:1) yielding the title compound as a white solid (155 mg, 46%).

R_f = 0.25 (EtOAc/MeOH 9:1); mp: 187.3-187.7 °C; IR (cm⁻¹): 2924, 2850, 1584, 1531, 1502, 1446; λ_{max} (EtOH)/nm 274.5; ¹H NMR (300 MHz, CDCl₃) δ 0.99 (6H, m, CH(CH₃)₂), 2.25 (1H, ept, J = 4 Hz, CH(CH₃)₂), 2.30 (3H, s, NMe), 2.41 (8H, m, piperazine), 2.72 (2H, t, J = 4 Hz, CH₂N), 3.21 (2H, t, J = 4 Hz, CH₂SO₂), 3.72 (2H, dd, J = 6; 2 Hz, CH₂OBn), 4.04 (2H, s, OCH₂Ph), 5.60 (1H, m, OCH), 6.62 (2H, d, J = 9 Hz, Ar-*H*), 7.19 (5H, m, Ar-*H*); 7.58 (2H, d, J = 9 Hz, Ar-*H*), 7.80 (1H, s, H-8); ¹³C NMR (125 MHz, CDCl₃) δ 45.9, 48.5, 48.7, 48.8, 49.0, 49.2, 49.4, 49.5, 49.9, 52.5, 53.1, 54.3, 55.5, 79.0, 118.8, 130.3, 144.9, 147.9, 157.6; MS(ES+) m/z 593.36 [M + H]⁺; HRMS calcd for C₃₀H₃₉N₇O₄S [M + H]⁺ 594.2852, found 594.28346.

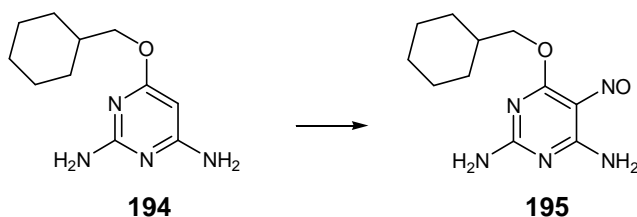
6-(Cyclohexylmethoxy)pyrimidine-2,4-diamine (194)¹⁹⁷



Sodium (0.84 g, 36 mmol) was added to cyclohexylmethanol (30 mL, 244 mmol) and the mixture was heated to 150 °C and stirred for 2 h. 4-Chloro-2,6-diaminopyrimidine (4.32 g, 30.0 mmol) was added, the temperature was increased to 180 °C and stirring was continued for 2 h. After cooling, the reaction mixture was neutralised with 1 M HCl. The excess of cyclohexylmethanol was removed by distillation under reduced pressure to yield a white viscous residue, which was taken up in methanol and filtered. The crude product was purified by chromatography on silica (EtOAc/MeOH 9:1). The title compound was obtained as a white solid (6.6 g, 95%).

R_f = 0.4 (EtOAc/MeOH 9:1); mp: 137-139 °C (lit. 142 °C); ^1H NMR (300 MHz, DMSO) δ 0.9-1.2 (5H, m, C_6H_{11}), 1.6-1.7 (6H, m, C_6H_{11}), 3.8 (2H, d, J = 6.0, OCH_2), 5.0 (1H, s, H-5), 5.8 (2H, s, NH_2), 5.9 (2H, s, NH_2); ^{13}C NMR (125 MHz, DMSO) δ 25.2, 26.0, 29.3, 36.9, 69.7, 75.9, 162.9, 165.9, 170.2; MS(ES+) m/z 223.01 [$\text{M} + \text{H}$] $^+$.

6-(Cyclohexylmethoxy)-5-nitrosopyrimidine-2,4-diamine (195)¹⁶⁴

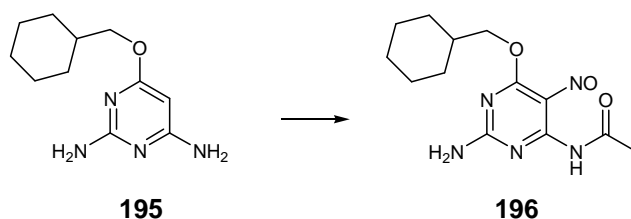


To a stirred solution of 6-(cyclohexylmethoxy)pyrimidine-2,4-diamine (1 g, 4.5 mmol) in 30% (v/v) aqueous acetic acid (10 mL) at 80 °C was added sodium nitrite (350 mg,

5 mmol). The reaction mixture was stirred at 80 °C for 40 min. The purple precipitate was collected by filtration resulting in 504 mg of the title compound (56%).

R_f = 0.7 (EtOAc/MeOH 9:1); mp: 242-246 °C (lit. 254 °C); ^1H NMR (300 MHz, DMSO) δ 1.0-1.2 (5H, m, C_6H_{11}), 1.6-1.8 (6H, m, C_6H_{11}), 4.2 (2H, d, J = 6 Hz, OCH_2), 7.7 (2H, s, NH_2), 8.0 (1H, s, NH), 10.1 (1H, s, NH); ^{13}C NMR (125 MHz, DMSO) δ 25.1, 25.9, 29.1, 36.7, 71.5, 139.5, 150.1, 163.5, 170.8; MS(ES+) m/z 252.26 $[\text{M} + \text{H}]^+$.

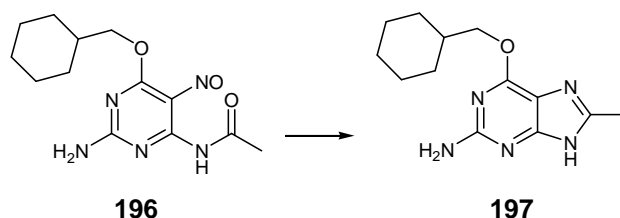
***N*-(2-Amino-6-(cyclohexylmethoxy)-5-nitrosopyrimidin-4-yl)acetamide (196)** ¹⁹⁷



6-(Cyclohexylmethoxy)-5-nitrosopyrimidine-2,4-diamine (500 mg, 2 mmol) was suspended in acetic anhydride (3 mL) and stirred at 80 °C for 30 min. The mixture was poured into water (10 mL) and extracted with CH_2Cl_2 (3 x 10 mL). The combined organic layers were dried over Na_2SO_4 and evaporated under reduced pressure. The crude product was purified by column chromatography on silica (EtOAc/Hexane 7:3) yielding the title compound as a blue solid (170 mg, 53%).

R_f = 0.8 (EtOAc); mp: 278-279 °C (lit. 274 °C); ^1H NMR (300 MHz, MeOD) δ 1.1-1.9 (11H, m, cyclohexyl), 2.4 (3H, s, CH_3CO), 4.4 (2H, d, J = 6 Hz, CH_2O), 5.9 (2H, s, NH_2), 6.5 (1H, s, NH); ^{13}C NMR (125 MHz, MeOD) δ 22.2, 25.8, 28.3, 29.9, 29.4, 38.4, 74.9, 84.9, 126.0, 131.2, 163.3, 165.7, 168.4; MS(ES+) m/z 294.8 $[\text{M} + \text{H}]^+$.

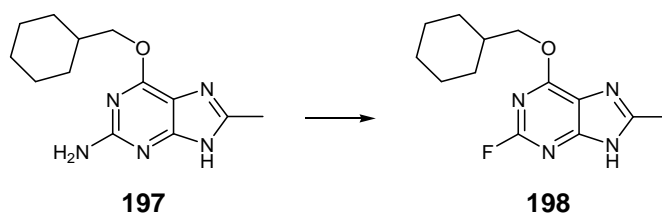
6-(Cyclohexylmethoxy)-8-methyl-9H-purin-2-amine (197)



N-(2-Amino-6-(cyclohexylmethoxy)-5-nitrosopyrimidin-4-yl)acetamide (100 mg, 0.34 mmol) was suspended in *o*-xylene (25 mL) and stirred at 100 °C for 30 min. Triphenylphosphine (250 mg, 0.85 mmol) was then added, and the mixture was heated to 200 °C and refluxed for 24 h. The mixture was concentrated *in vacuo* and the crude product was purified by column chromatography (EtOAc) yielding the title compound as a white solid (90 mg, 83%).

R_f = 0.2 (EtOAc); mp: 232-236 °C; IR (cm⁻¹): 3480, 3311, 3163, 2916, 1582; λ_{max} (EtOH)/nm 290.0; ¹H NMR (300 MHz, CDCl₃) δ 1.1-1.9 (11H, m, cyclohexyl), 2.4 (3H, s, Ar-CH₃), 4.4 (2H, d, J = 6 Hz, CH₂O), 6.2 (2H, s, NH₂); ¹³C NMR (125 MHz, CDCl₃) δ 25.6, 26.4, 29.6, 37.2, 70.8, 160.1; MS(ES+) m/z 262.8 [M + H]⁺; HRMS calcd for C₁₃H₂₀ON₅ [M + H]⁺ 262.1662, found 262.16507.

6-(Cyclohexylmethoxy)-2-fluoro-8-methyl-9H-purine (198)

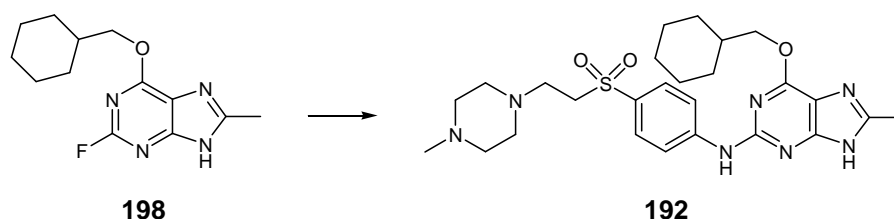


A 50% (w/w) aqueous solution of HBF₄ (5 mL, 19.8 mmol) was brought to the temperature of -5 °C. 6-(Cyclohexylmethoxy)-8-methyl-9H-purin-2-amine (235 mg, 0.9 mmol) was then added in one portion. NaNO₂ (124 mg, 1.8 mmol) was dissolved in water (50 mL) and added dropwise, ensuring that the temperature remained below

0 °C. The temperature was raised to 20 °C and the mixture was stirred for 18 h. The solution was neutralised with Na₂CO₃ and the mixture was extracted with CH₂Cl₂ (3 x 15 mL) and the combined organic layers were dried over Na₂SO₄ and evaporated under reduced pressure. The crude product was purified by column chromatography (EtOAc/Petrol 1:1) yielding the title compound as a white solid (41 mg, 41%).

R_f = 0.5 (EtOAc); mp: 171-173 °C; IR (cm⁻¹): 2916, 2777, 2538, 1597; λ_{max} (EtOH)/nm 291.0; ¹H NMR (300 MHz, DMSO) δ 1.2 (6H, m, cyclohexyl), 1.7 (5H, m, cyclohexyl), 2.4 (3H, s, Ar-CH₃), 4.3 (2H, d, *J* = 6 Hz, OCH₂); ¹³C NMR (125 MHz, CDCl₃) δ 18.0, 25.8, 28.3, 29.9, 29.4, 38.4, 74.9, 116.2, 147.6, 153.0, 158.9, 160.1; MS(ES+) *m/z* 264.1 [M + H]⁺; HRMS calcd for C₁₃H₁₇N₄O [M + H]⁺ 264.5622, found 264.56235.

6-(Cyclohexylmethoxy)-8-methyl-*N*-(4-(2-(4-methylpiperazin-1-yl)ethylsulfonyl)phenyl)-9*H*-purin-2-amine (192)

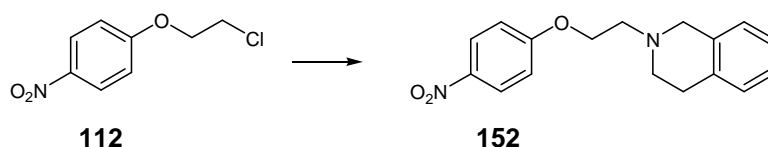


The compound was prepared according to General Procedure I from tert-butyl 4-(2-(4-methylpiperazin-1-yl)ethylsulfonyl)phenylcarbamate (250 mg, 0.65 mmol) and 6-(cyclohexylmethoxy)-2-fluoro-8-methyl-9*H*-purine (70 mg, 0.32 mmol). The crude product was purified by flash chromatography on silica (EtOAc/MeOH 9:1) yielding the title compound as a white solid (121 mg, 48%).

R_f = 0.25 (EtOAc/MeOH 9:1); mp: 112.2-113.6 °C; IR (cm⁻¹): 3455, 2923, 2848, 1674, 1620, 1591, 1531, 1452; λ_{max} (EtOH)/nm 313.0; ¹H NMR (300 MHz, CDCl₃) δ 1.1-1.8 (11H, m, cyclohexyl), 2.3 (3H, s, NMe), 2.4 (8H, m, CH₂ piperazine), 2.5 (3H, s, Ar-CH₃), 2.7 (2H, t, *J* = 6 Hz, CH₂N), 3.2 (2H, t, *J* = 6 Hz, CH₂SO₂), 4.2 (2H, d, *J* = 6 Hz, OCH₂), 7.3 (1H, s, NH), 7.6 (2H, d, *J* = 9 Hz, Ar-H), 7.7 (2H, d, *J* = 9 Hz, Ar-H); ¹³C NMR (125 MHz, CDCl₃) δ 15.2, 25.6, 26.4, 29.8, 37.2, 45.1, 50.8, 51.6, 53.7, 253

54.3, 54.4, 72.3, 114.0, 117.6, 129.3, 130.1; MS(ES+) m/z 528.3 $[M + H]^+$; HRMS calcd for $C_{26}H_{37}N_7O_3S$ $[M + H]^+$ 528.2751, found 528.27153.

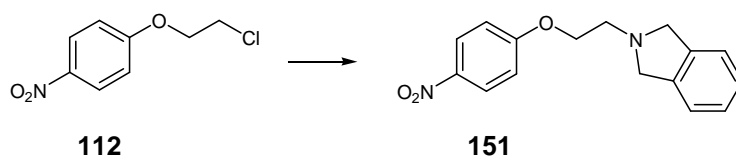
2-(2-(4-Nitrophenoxy)ethyl)-1,2,3,4-tetrahydroisoquinoline (152) ²⁹²



The compound was prepared according to General Procedure III from 1-(2-chloroethoxy)-4-nitrobenzene (500 mg, 2.5 mmol), NaI (560 mg, 3.73 mmol) and 1,2,3,4-tetrahydroisoquinoline (0.62 mL, 5 mmol). The compound was obtained as a yellow solid (521 mg, 81%).

R_f = 0.5 (EtOAc/MeOH 9:1); mp: 186-187 °C (lit. 189 °C); 1H NMR (300 MHz, $CDCl_3$) δ 2.85 (2H, t, J = 4.5 Hz, CH_2N), 2.88 (2H, t, J = 4.5 Hz, CH_2CH_2N), 3.74 (2H, s, $PhCH_2N$), 4.23 (2H, t, J = 5.5 Hz, OCH_2), 6.91 (2H, d, J = 9 Hz, Ar-H), 7.03 (4H, br s, Ar-H), 8.15 (2H, d, J = 9 Hz, Ar-H); ^{13}C NMR (125 MHz, $CDCl_3$) δ 27.1, 52.5, 54.3, 60.7, 66.9, 115.3, 121.7, 125.7, 127.2, 127.5, 128.8, 133.3, 137.1, 140.0, 163.6; MS(ES+) m/z 299.34 $[M + H]^+$.

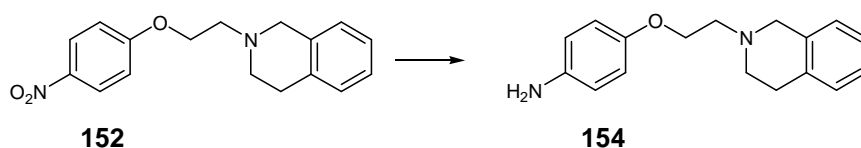
2-(2-(4-Nitrophenoxy)ethyl)isoindoline (151) ²⁹³



The compound was prepared according to General Procedure III from 1-(2-chloroethoxy)-4-nitrobenzene (500 mg, 2.5 mmol), NaI (560 mg, 3.73 mmol) and isoindoline (0.56 mL, 5 mmol). The compound was obtained as a yellow solid (598 mg, 91%).

R_f = 0.5 (EtOAc/MeOH 9:1); mp: 165-166 °C (lit. 169 °C); ^1H NMR (300 MHz, CDCl_3) δ 3.16 (2H, t, J = 5.5 Hz, CH_2N), 4.01 (4H, s, PhCH_2N), 4.21 (2H, t, J = 5.5 Hz, OCH_2), 6.93 (2H, d, J = 9 Hz, Ar-H), 7.14 (4H, br s, Ar-H), 8.15 (2H, d, J = 9 Hz, Ar-H); ^{13}C NMR (125 MHz, CDCl_3) δ 56.5, 60.3, 66.6, 115.3, 121.7, 125.7, 127.0, 127.5, 128.8, 133.3, 137.1, 140.0, 163.6; MS(ES+) m/z 285.31 $[\text{M} + \text{H}]^+$.

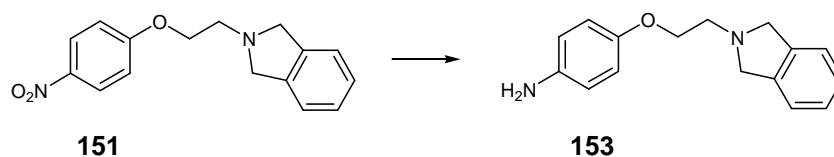
4-(2-(3,4-Dihydroisoquinolin-2(1*H*)-yl)ethoxy)benzenamine (154)²⁹²



The compound was prepared according to General Procedure IV from 2-(2-(4-nitrophenoxy)ethyl)-1,2,3,4-tetrahydroisoquinoline (600 mg, 2.01 mmol) and obtained as a clear yellow oil (584 mg, 99%).

R_f = 0.5 (EtOAc/MeOH 9:1); ^1H NMR (300 MHz, CDCl_3) δ 2.81 (2H, t, J = 4.5 Hz, CH_2N), 2.89 (2H, t, J = 4.5 Hz, $\text{CH}_2\text{CH}_2\text{N}$), 3.39 (2H, s, PhCH_2N), 3.69 (2H, s, NH_2), 4.07 (2H, t, J = 5.5 Hz, OCH_2), 6.56 (2H, d, J = 9 Hz, Ar-*H*), 6.71 (2H, d, J = 9 Hz, Ar-*H*), 7.03 (4H, m, Ar-*H*); ^{13}C NMR (125 MHz, CDCl_3) δ 27.1, 52.5, 54.3, 60.7, 66.9, 115.3, 121.7, 125.7, 127.2, 127.5, 128.8, 133.3, 137.1, 140.0; MS(ES+) m/z 269.35 $[\text{M} + \text{H}]^+$.

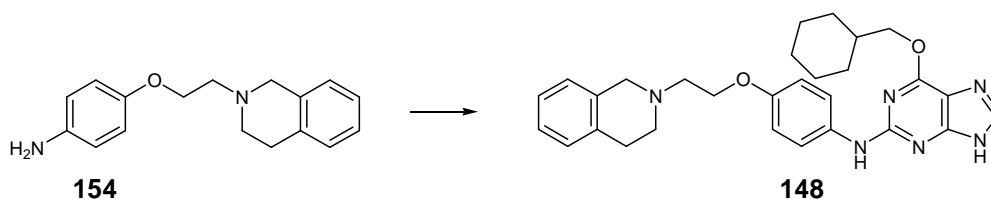
4-(2-(Isoindolin-2-yl)ethoxy)benzenamine (153)²⁹⁴



The compound was prepared according to General Procedure IV from 2-(2-(4-nitrophenoxy)ethyl)isoindoline (700 mg, 2.46 mmol) and obtained as a clear yellow oil (674 mg, 98%).

R_f = 0.5 (EtOAc/MeOH 9:1); ^1H NMR (300 MHz, CDCl_3) δ 3.07 (2H, t, J = 5.5 Hz, CH_2N), 3.98 (4H, s, PhCH_2N), 4.05 (2H, t, J = 5.5 Hz, OCH_2), 6.57 (2H, d, J = 9 Hz, Ar- H), 6.72 (2H, d, J = 9 Hz, Ar- H), 7.12 (4H, br s, Ar- H); ^{13}C NMR (125 MHz, CDCl_3) δ 56.5, 60.3, 66.6, 115.3, 116.9, 121.7, 125.7, 127.0, 127.5, 128.8, 133.3, 137.1, 140.0; MS(ES+) m/z 255.33 $[\text{M} + \text{H}]^+$.

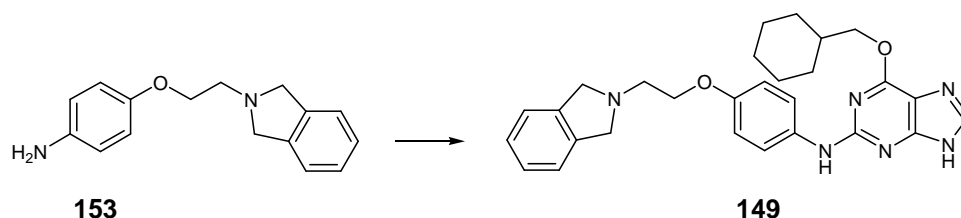
***N*-(4-(2-(3,4-Dihydroisoquinolin-2(1*H*)-yl)ethoxy)phenyl)-6-(cyclohexylmethoxy)-9*H*-purin-2-amine (148)**



The compound was prepared according to General Procedure I from 4-(2-(3,4-dihydroisoquinolin-2(1*H*)-yl)ethoxy)benzenamine (450 mg, 1.77 mmol) and 6-cyclohexylmethoxy-2-fluoro-9*H*-purine (221 mg, 0.88 mmol). The crude product was purified by flash chromatography on silica (EtOAc/MeOH 9:1) yielding the title compound as a white solid (311 mg, 57%).

R_f = 0.25 (EtOAc/MeOH 9:1); mp: 170.2-170.6 °C; IR (cm^{-1}): 2921, 2848, 1732, 1584, 1531, 1498, 1448; λ_{max} (EtOH)/nm 207.0; ^1H NMR (300 MHz, CDCl_3) δ 1.10-2.07 (11H, m, cyclohexyl), 2.94 (2H, t, J = 6 Hz, CH_2N), 3.03 (2H, t, J = 6 Hz, PhCH_2), 3.82 (2H, s, PhCH_2N), 4.17 (2H, t, J = 6 Hz, CH_2O), 4.33 (2H, d, J = 6 Hz, CH_2Cy), 6.87 (2H, d, J = 9 Hz, Ar- H), 6.87 (1H, s, H-8), 6.92 (2H, d, J = 9 Hz, Ar- H), 7.06 (4H, m, Ar- H), 6.89 (1H, s, NH), 7.49 (2H, d, J = 9 Hz, Ar); ^{13}C NMR (125 MHz, CDCl_3) δ 14.2, 21.0, 25.7, 26.4, 28.7, 29.8, 37.3, 51.3, 56.7, 56.8, 60.4, 66.4, 72.1, 76.7, 77.0, 115.1, 122.9, 125.7, 126.2, 126.6, 128.7, 133.8, 156.5; MS(ES+) m/z 499.36 $[\text{M} + \text{H}]^+$; HRMS calcd for $\text{C}_{29}\text{H}_{34}\text{N}_6\text{O}_2$ $[\text{M} + \text{H}]^+$ 499.2816, found 499.27919.

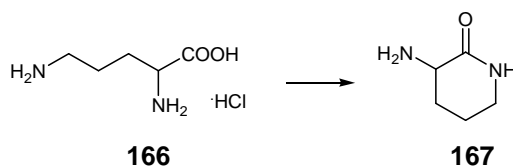
***N*-(4-(2-(Isoindolin-2-yl)ethoxy)phenyl)-6-(cyclohexylmethoxy)-9*H*-purin-2-amine (149)**



The compound was prepared according to General Procedure I from 4-(2-(isoindolin-2-yl)ethoxy)benzenamine (450 mg, 1.77 mmol) and 6-cyclohexylmethoxy-2-fluoro-9*H*-purine (221 mg, 0.88 mmol). The crude product was purified by flash chromatography on silica (EtOAc/MeOH 9:1) yielding the title compound as a white solid (308 mg, 56%).

R_f = 0.25 (EtOAc/MeOH 9:1); mp: 177.2-177.6 °C; IR (cm^{-1}): 2359, 2035, 1734, 1676, 1584, 1495, 1447; λ_{max} (EtOH)/nm 272.0; ^1H NMR (300 MHz, CDCl_3) δ 1.14-1.97 (11H, m, cyclohexyl), 3.13 (2H, t, J = 4 Hz, CH_2N), 4.03 (4H, s, PhCH_2N), 4.11 (2H, t, J = 6 Hz, CH_2O); 4.24 (2H, d, J = 6 Hz, CH_2Cy), 6.74 (1H, s, H-8), 6.86 (2H, d, J = 9 Hz, Ar-*H*), 7.13 (1H, s, NH), 7.14 (4H, m, Ar-*H*), 7.41 (2H, d, J = 9 Hz, Ar-*H*); ^{13}C NMR (125 MHz, CDCl_3) δ 25.7, 26.4, 29.8, 37.3, 54.7, 59.5, 60.4, 72.1, 76.7, 77.0, 115.1, 122.3, 126.8; MS(ES+) m/z 485.38 $[\text{M} + \text{H}]^+$; HRMS calcd for $\text{C}_{28}\text{H}_{32}\text{N}_6\text{O}_2$ $[\text{M} + \text{H}]^+$ 485.2660, found 485.26181.

3-Aminopiperidin-2-one (167) ¹⁸³

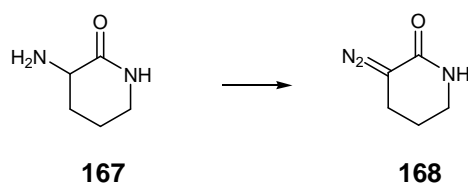


L-Ornithine hydrochloride (1 g, 5.9 mmol) was added to a stirred solution of sodium hydroxide pellets (0.23 g, 5.9 mmol) in water (5 mL). After 15 min, this solution was

added to a stirred mixture of alumina (3 g) and toluene (100 mL) and heated under reflux for 1.5 h. The water produced during the reaction was collected in a Dean–Stark trap. The reaction mixture was allowed to cool and the alumina was filtered off and washed with 10% MeOH/CH₂Cl₂ (30 mL). The filtrate and washings were combined and the solvent removed *in vacuo* to yield the title compound as a white solid (611 mg, 90%).

Mp 35–37°C; ¹H NMR (CDCl₃, 500 MHz) δ 1.5–2.1 (4H, m, CH₂CH₂), 1.75 (2H, bs, NH₂), 3.2 (2H, m, CH₂N), 3.2 (1H, dd, *J* = 3.8; 3.9 Hz, CHNH₂), 7.0 (1H, bs, NH); ¹³C NMR (125 MHz, CDCl₃) δ 20.6, 21.8, 29.6, 37.1, 51.0, 168.8; MS(ES+) *m/z* 115.15 [M + H]⁺.

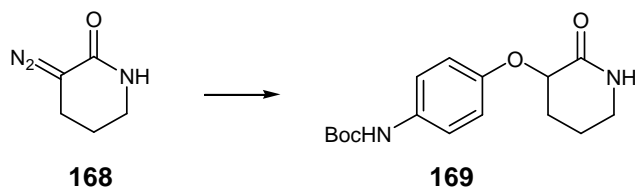
3-Diazo-piperidin-2-one (168) ¹⁸³



3-Amino-piperidin-2-one (1.6 g, 14 mmol) was dissolved in chloroform (30 mL). *iso*-Amyl nitrite (2.31 g, 18 mmol) and glacial acetic acid (0.126 g, 2.1 mmol) were added with stirring. The resulting solution was heated to reflux and stirred for 15 min, cooled in ice and washed with an ice-cold saturated solution of NaHCO₃ (10 mL). The organic layer was separated, dried over Na₂SO₄ and the solvent removed *in vacuo*. The solid was purified by column chromatography on silica (20% MeOH/CH₂Cl₂) to give the title compound as bright orange needles (1.07 g, 60%).

Mp 117–120°C; ¹H NMR (CDCl₃, 500 MHz) δ 1.9 (2H, m, CH₂), 2.7 (2H, t, *J* = 6.3 Hz, CH₂), 3.25 (2H, m, CH₂N), 6.5 (1H, bs, NH); ¹³C NMR (CDCl₃, 500 MHz) δ 20 (CH₂), 21 (CH₂), 41 (CH₂N), 53 (C=N₂), 167 (C=O); MS(ES+) *m/z* 126.13 [M + H]⁺.

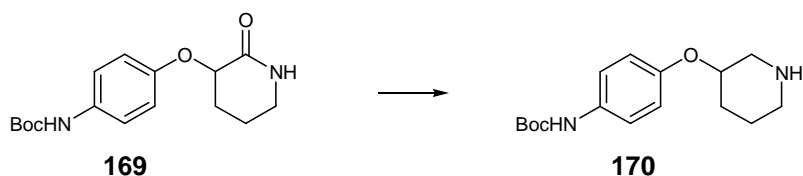
***tert*-Butyl 4-(2-oxopiperidin-3-yloxy)phenylcarbamate (169)**¹⁸³



3-Diazo-piperidin-2-one (1.5 g, 12 mmol) was dissolved in THF (25 mL). *tert*-Butyl 4-hydroxyphenylcarbamate (5 g, 72 mmol) was added in portions, then Rhodium(II)acetate (35 mg). The solution was stirred for 10 h. The solution was concentrated under reduced pressure and the residue taken up in CH₂Cl₂ (20 mL) and washed with saturated aqueous NaHCO₃. The organic layer was separated, dried over Na₂SO₄ and the solvent removed *in vacuo*. The solid was purified by column chromatography on silica (EtOAc/Petrol 1:1) to give the title compound as a white solid (502 mg, 41%).

Mp 156–158°C; ¹H NMR (CDCl₃, 500 MHz) δ 1.43 (4H, s, (CH₃)₃), 1.52 (5H, s, (CH₃)₃), 1.62–2.05 (4H, m, CH₂CH₂), 3.25 (2H, dd, *J* = 7.5; 5.5 Hz, CH₂NH), 4.51 (1H, dd, *J* = 7.5; 5.5 Hz, CHOAr), 5.75 (1H, s, NH), 6.25 (1H, s, NH), 6.93 (2H, d, *J* = 9 Hz, Ar-*H*), 7.19 (2H, d, *J* = 9 Hz, Ar-*H*); ¹³C NMR (CDCl₃, 500 MHz) δ 20 (CH₂), 21 (CH₂), 41 (CH₂N), 53 (C=N₂), 167 (C=O); MS(ES+) *m/z* 307.36 [M + H]⁺.

***tert*-Butyl 4-(2-oxopiperidin-3-yloxy)phenylcarbamate (170)**²⁹⁵

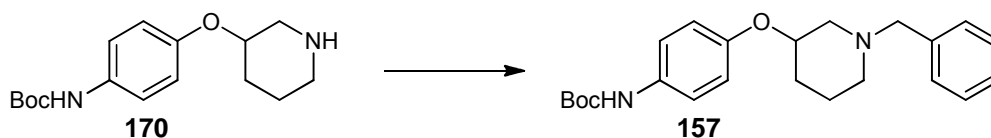


tert-Butyl 4-(2-oxopiperidin-3-yloxy)phenylcarbamate (129 mg, 0.49 mmol) was dissolved in anhydrous THF (10 mL) and cooled to 0 °C. LiAlH₄ (1M in THF, 1.4 mL, 1.2 mmol) was added dropwise and the reaction was allowed to warm up to room

temperature and stirred for 3 h. The reaction was quenched adding dropwise: water (0.2 mL), 15% (w/v) aqueous NaOH (0.2 mL) and then water again (0.6 mL). The resulting grey suspension was stirred for 30 min. The resulting white precipitate was filtered through a pad of celite and the filtrate was evaporated to give an oil which was taken up in CH₂Cl₂ (20 mL) and washed with water (2 x 20 mL). It was then dried over Na₂SO₄, evaporated and the resulting solid was purified by flash chromatography (EtOAc/MeOH 95:5), yielding the title compound as an off-white solid (44 mg, 38%).

R_f = 0.25 (EtOAc/MeOH 9:1); mp: 125-126 °C ¹H NMR (300 MHz, CDCl₃) δ 1.43 (9H, s, (CH₃)₃), 1.73 (4H, m, CH₂CH₂), 2.73 (2H, dd, J = 7.5; 5.5 Hz, NHCH₂), 2.85 (2H, dd, J = 7.5; 5.5 Hz, CH₂NH), 4.04 (1H, dd, J = 7.5; 5.5 Hz, CHOAr), 6.48 (1H, s, NH), 6.50 (2H, d, J = 9 Hz, Ar-H), 6.77 (2H, d, J = 9 Hz, Ar-H); ¹³C NMR (75 MHz, CDCl₃) δ 24.4, 25.5, 25.9, 26.4, 29.6, 32.2, 37.3, 54.2, 58.5, 71.5, 119.5, 126.9, 131.0, 140.3; MS(ES+) m/z 293.37 [M + H]⁺.

***tert*-Butyl 4-((1-benzylpiperidin-3-yl)oxy)phenylcarbamate (157)**

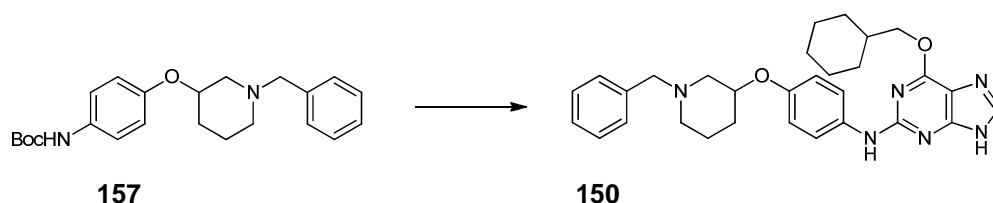


In a microwave vial, to a stirred solution of *tert*-butyl 4-(2-oxopiperidin-3-yloxy)phenylcarbamate (50 mg, 0.18 mmol) in THF (3 mL) were added benzaldehyde (12.6 μ L, 0.12 mmol), phenylsilane (13.1 μ L, 0.12 mmol) and dibutyldichlorostannane (3 mg, catalytic). The reaction mixture was heated for 15 min at 100 °C under microwave irradiation. The mixture was filtered through a thiol-based resin to eliminate excess tin, then concentrated under reduced pressure. The crude product was purified by flash chromatography (EtOAc), yielding the title compound as a white solid (21 mg, 74%).

R_f = 0.35 (EtOAc); mp: 101-102 °C; ¹H NMR (300 MHz, CDCl₃) δ 1.43 (9H, s, (CH₃)₃), 1.78 (4H, m, CH₂CH₂), 2.43 (2H, dd, J = 7.5; 5.5 Hz, NCH₂), 3.05 (2H, dd, J = 7.5; 5.5 Hz, CH₂NH), 4.04 (1H, dd, J = 7.5; 5.5 Hz, CHOAr), 6.48 (1H, s, NH), 6.50 (2H, d, J = 9 Hz, Ar-H), 6.77 (2H, d, J = 9 Hz, Ar-H); ¹³C NMR (75 MHz, CDCl₃) δ 24.4, 25.5, 25.9, 26.4, 29.6, 32.2, 37.3, 54.2, 58.5, 71.5, 119.5, 126.9, 131.0, 140.3; MS(ES+) m/z 293.37 [M + H]⁺.

= 7.5; 5.5 Hz, CH_2N), 3.5 (2H, 2 x d, $J = 6.5$, NCH_2Ph), 4.25 (1H, dd, $J = 7.5$; 5.5 Hz, CHOAr), 6.28 (1H, s, NH), 6.75 (2H, d, $J = 9$ Hz, Ar-H), 7.10 (5H, m, Ar-H), 7.27 (2H, d, $J = 9$ Hz, Ar-H); ^{13}C NMR (75 MHz, CDCl_3) δ 24.3, 25.8, 25.9, 27.1, 30.2, 33.7, 38.0, 54.2, 58.5, 79.5, 114.8, 119.5, 126.9, 131.0, 140.3, 152.8; MS(ES+) m/z 383.57 $[\text{M} + \text{H}]^+$.

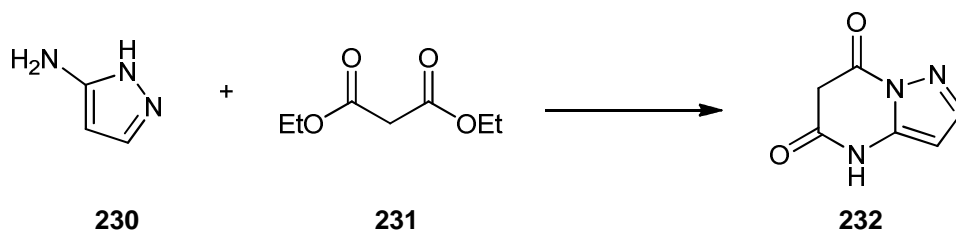
***N*-(4-((1-Benzylpiperidin-3-yl)oxy)phenyl)-6-(cyclohexylmethoxy)-9*H*-purin-2-amine (150)**



The compound was prepared according to General Procedure I from *tert*-butyl (4-((1-benzylpiperidin-3-yl)oxy)phenyl)carbamate (10 mg, 0.026 mmol) and 6-cyclohexylmethoxy-2-fluoro-9*H*-purine (32 mg, 0.013 mmol). The crude product was purified by flash chromatography on silica (EtOAc/MeOH 9:1) yielding the title compound as a white solid (38 mg, 46%).

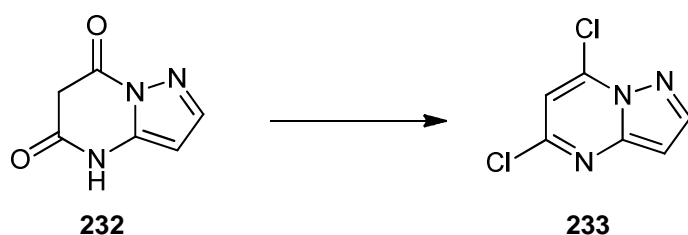
R_f = 0.25 (EtOAc/MeOH 9:1); mp: 177.2-177.6 °C; IR (cm^{-1}): 2539, 2053, 1743, 1667, 1548, 1459, 1474; λ_{max} (EtOH)/nm 272.0; ^1H NMR (300 MHz, CDCl_3) δ 0.84-1.90 (11H, m, cyclohexyl), 2.45 (2H, dd, $J = 7.5$; 5.5 Hz, NCH_2), 3.15 (2H, dd, $J = 7.5$; 5.5 Hz, CH_2N), 3.50 (2H, 2 x d, $J = 6.5$, NCH_2Ph), 4.27 (1H, dd, $J = 7.5$; 5.5 Hz, CHOAr), 6.78 (1H, s, NH), 7.15 (2H, d, $J = 9$ Hz, Ar-H), 7.20 (5H, m, Ar-H), 7.57 (2H, d, $J = 9$ Hz, Ar-H); ^{13}C NMR (125 MHz, CDCl_3) δ 26.0; 26.8, 30.1, 37.8, 48.6, 54.0, 68.6, 72.5, 115.4, 115.7, 116.7, 122.8, 127.3, 128.4, 128.7, 133.6, 137.8, 140.5, 154.9, 155.6, 157.1, 161.6; MS(ES+) m/z 513.28 $[\text{M} + \text{H}]^+$; HRMS calcd for $\text{C}_{28}\text{H}_{32}\text{N}_6\text{O}_2$ $[\text{M} + \text{H}]^+$ 513.65600, found 513.66530.

Pyrazolo[1,5-*a*]pyrimidine-5,7(4*H*,6*H*)-dione (232) ²⁹⁶



To 150 mL of stirred EtOH were added 2.3 g of sodium (0.1 mol) and the suspension was stirred until all the sodium had dissolved. 1*H*-Pyrazol-5-amine (4.2 g, 50 mmol) was added, followed by diethylmalonate (8.25 mL, 55 mmol). The solution was heated to reflux and stirred for 4 h. The white precipitate was collected and stirred in 1.2 M HCl for 2 h, then filtered and dried (3.8 g, 68%). Due to complete insolubility of the compound, only the measurement of melting point was possible (decomposed at 350 °C), therefore the compound was carried forward to the next step without characterisation.

5,7-Dichloropyrazolo[1,5-*a*]pyrimidine (233) ²⁹⁶

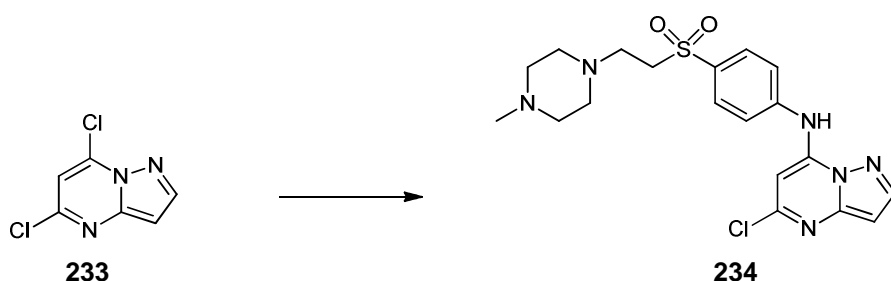


In a microwave vial, to pyrazolo[1,5-*a*]pyrimidine-5,7(4*H*,6*H*)-dione (200 mg, 6.61 mmol) was added POCl₃ (5 mL). The reaction mixture was heated for 30 min at 150 °C under microwave irradiation. The reaction mixture was poured onto ice, then 2.5 M NaOH was added until pH neutral. NaCl was added until saturation, and the resulting solution was extracted with THF (3 x 30 mL). The organic layers were collected, combined and dried over Na₂SO₄, and the solvent was removed *in vacuo*.

The crude product was purified by flash chromatography (EtOAc/Hexane 1:1) yielding the title compound as an off white solid (176 mg, 74%).

R_f = 0.35 (EtOAc); mp: 68-71 °C; ^1H NMR (300 MHz, CDCl_3) δ 6.68 (1H, s, H_3), 6.93 (1H, s, H_4), 8.16 (1H, s, H_8); ^{13}C NMR (75 MHz, CDCl_3) δ 96.3, 122.8, 144.9, 148.1, 164.2, 171.7; MS(ES+) m/z 187.57 $[\text{M} + \text{H}]^+$.

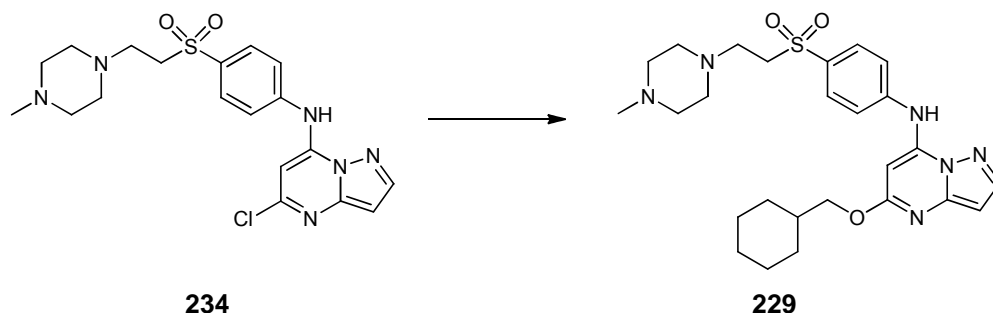
5-Chloro-*N*-(4-((2-(4-methylpiperazin-1-yl)ethyl)sulfonyl)phenyl)pyrazolo[1,5-*a*]pyrimidin-7-amine (234)



The compound was prepared according to General Procedure I from 5,7-dichloropyrazolo[1,5-*a*]pyrimidine (50 mg, 0.26 mmol) and *tert*-butyl 4-(2-(4-methylpiperazin-1-yl)ethylsulfonyl)phenylcarbamate (150 mg, 0.52 mmol). The crude product was purified by flash chromatography on silica (EtOAc/MeOH 9:1) yielding the title compound as a white solid (98 mg, 49%).

R_f = 0.28 (EtOAc/MeOH 9:1); mp: 135-137 °C; IR (cm^{-1}) 2926, 2844, 1590, 1535, 1499, 1444; λ_{max} (EtOH)/nm: 312; ^1H NMR (300 MHz, CDCl_3) δ 2.35 (3H, s, NMe), 2.67 (8H, m, piperazine ring), 2.69 (2H, t, J = 7 Hz, CH_2N), 3.19 (2H, t, J = 7 Hz, CH_2SO_2), 6.52 (2H, d, J = 18 Hz, H_3 het.), 6.90 (1H, s, H_4 het), 7.76 (2H, d, J = 9 Hz, Ar-H), 7.49 (2H, d, J = 9 Hz, Ar-H), 8.16 (1H, s, H_8 het); ^{13}C NMR (75 MHz, CDCl_3) δ 26.0, 26.7, 30.1, 37.6, 46.0, 51.6, 52.8, 54.1, 55.0, 72.9, 115.6, 118.0, 129.6, 130.8, 139.6, 145.8, 155.1, 161.1; MS(ES+) m/z 435.3 $[\text{M}(^{35}\text{Cl}) + \text{H}]^+$; 437.3 $[\text{M}(^{37}\text{Cl}) + \text{H}]^+$; anal. calcd for $\text{C}_{19}\text{H}_{23}\text{ClN}_6\text{O}_2\text{S}$: C, 52.46, H, 5.87, N, 19.09%; found: C, 52.65, H, 5.49, N, 19.11%.

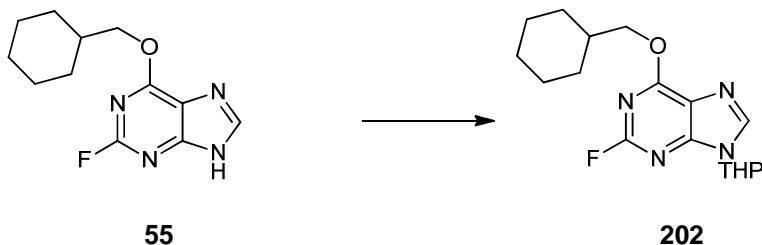
5-(Cyclohexylmethoxy)-*N*-(4-((2-(4-methylpiperazin-1-yl)ethyl)sulfonyl)phenyl)pyrazolo[1,5-*a*]pyrimidin-7-amine (229)



In a microwave vial, to 5-chloro-*N*-(4-((2-(4-methylpiperazin-1-yl)ethyl)sulfonyl)phenyl)pyrazolo[1,5-*a*]pyrimidin-7-amine (50 mg, 0.11 mmol) was added THF (5 mL) and cyclohexylmethanol (800 μ L, 1.14 mmol). In a second microwave vial, a catalytic amount of Pd(OAc)₂ (1.5 mg), ligand **A** (see **Chapter 5**, 1.3 mg) and cesium carbonate (60 mg, 0.171 mmol) were flushed with nitrogen for 1 h. The mixture from the first vial was added into the second vial, and the reaction mixture was heated for 30 min at 120 °C under micro wave irradiation. The reaction mixture was filtered through a celite pad and the solvent was removed *in vacuo*. The crude product was purified by flash chromatography (EtOAc) yielding the title compound as an off white solid (46 mg, 44%).

R_f = 0.28 (EtOAc/MeOH 9:1); mp: 146-148 °C; IR (cm⁻¹) 2999, 2996, 1690, 1630, 1598, 1567, 1834; λ_{max} (EtOH)/nm: 312; ¹H NMR (300 MHz, CDCl₃) δ 0.78-1.18 (5H, m, cyclohexyl), 1.65-1.84 (6H, m, cyclohexyl), 2.35 (3H, s, NMe), 2.67 (8H, m, piperazine ring), 2.69 (2H, t, J = 7 Hz, CH₂N), 3.19 (2H, t, J = 7 Hz, CH₂SO₂), 6.67 (2H, d, J = 18 Hz, H₃ het.), 6.91 (1H, s, H₄ het), 7.76 (2H, d, J = 9 Hz, Ar-H), 7.50 (2H, d, J = 9 Hz, Ar-H), 7.66 (1H, s, H₈ het); ¹³C NMR (75 MHz, CDCl₃) δ 26.0, 26.7, 30.1, 37.6, 46.0, 51.6, 52.8, 54.1, 55.0, 72.9, 115.6, 118.0, 129.6, 130.8, 139.6, 145.8, 155.1, 161.1; MS(ES+) m/z 513.3 [M + H]⁺; anal. calcd for C₂₆H₃₆N₆O₃S: C, 60.96, H, 7.07, N, 16.39%; found: C, 60.95, H, 7.09, N, 16.41%.

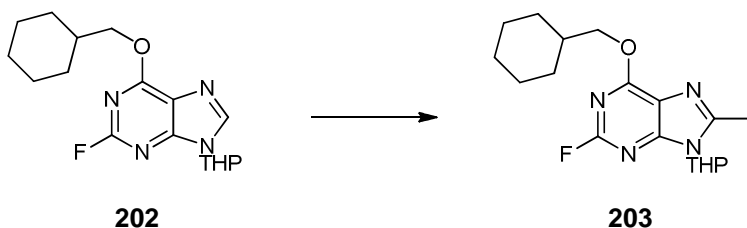
6-(Cyclohexylmethoxy)-2-fluoro-9-(tetrahydro-2H-pyran-2-yl)-9H-purine (202)



To 500 mg of 6-cyclohexylmethoxy-2-fluoropurine in 15 mL of EtOAc were added 313 μ L of 3,4-dihydro-2H-pyran and 30 mg of camphosulfonic acid (catalytic). The reaction mixture was heated at 60 $^{\circ}$ C for 18 h, then washed twice with 20 mL of saturated aqueous sodium bicarbonate. The combined organic layers were concentrated *in vacuo* and the crude product was purified by flash column chromatography (EtOAc/Hexane 1:1), yielding the title compound as a white solid (350 mg, 65%).

R_f = 0.51 (EtOAc/Hexane 3:1); mp: 146-148 $^{\circ}$ C; IR (cm^{-1}) 2999, 2996, 1690, 1630, 1598, 1567; λ_{max} (EtOH)/nm: 312; ^1H NMR (300 MHz, CDCl_3) δ 1.08-1.23 (5H, m, cyclohexyl), 1.54-2.02 (11H, m, cyclohexyl + THP), 3.71 (1H, t, J = 11 Hz, H_3 ax THP), 4.08 (1H, d, J = 11 Hz, H_3 eq THP), 4.31 (2H, d, J = 6 Hz, CH_2Cy), 5.58 (1H, d, J = 10.5 Hz, H_1 THP), 8.00 (1H, s, H_8 purine); ^{13}C NMR (75 MHz, CDCl_3) δ 22.7, 24.8, 25.6, 26.3, 29.6, 31.8, 37.1, 68.8, 73.3, 82.1, 140.0, 158.9, 162.9; MS(ES+) m/z 331.3 [$\text{M} + \text{H}$] $^+$; anal. calcd for $\text{C}_{17}\text{H}_{25}\text{N}_5\text{O}_2$: C, 61.96, H, 7.07, N, 21.39%; found: C, 61.95, H, 7.09, N, 21.41%.

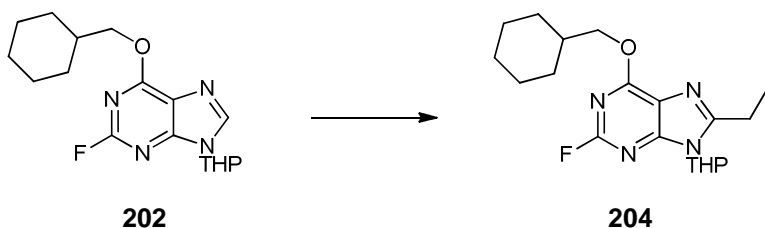
6-(Cyclohexylmethoxy)-2-fluoro-8-methyl-9-(tetrahydro-2H-pyran-2-yl)-9H-purine (203)



The compound was prepared according to General Procedure V using 300 mg (0.89 mmol) of **202**, 189 μL (1.34 mmol) of diisopropylamine, 536 μL of *n*BuLi solution and 167 μL (2.69 mmol) of MeI. The crude product was purified by flash chromatography on silica (EtOAc/Hexane 1:1) yielding the title compound as a white solid (154 mg, 51%).

R_f = 0.51 (EtOAc/Hexane 1:1); mp: 146-148 °C; IR (cm^{-1}) 2925, 2852, 2324, 1610, 1584, 1446; λ_{max} (EtOH)/nm: 257; ^1H NMR (300 MHz, CDCl_3) δ 1.17-1.20 (5H, m, cyclohexyl), 1.64-1.97 (11H, m, cyclohexyl + THP), 2.64 (3H, s, $\text{C}_8\text{-Me}$), 3.71 (1H, t, J = 11 Hz, H_3 ax THP), 4.11 (1H, d, J = 11 Hz, H_3 eq THP), 4.30 (2H, d, J = 6 Hz, CH_2Cy), 5.48 (1H, d, J = 10.5 Hz, H_1 THP); ^{13}C NMR (75 MHz, CDCl_3) δ 14.2, 16.1, 21.0, 23.1, 24.8, 25.6, 26.3, 29.6, 30.1, 37.1, 60.4, 69.1, 73.1, 82.9, 118.1, 151.6, 153.8, 154.0, 156.5, 158.2, 161.6, 161.7; MS(ES+) m/z 265.2 $[\text{M} + \text{H}]^+$.

6-(Cyclohexylmethoxy)-2-fluoro-8-ethyl-9-(tetrahydro-2H-pyran-2-yl)-9H-purine (204)

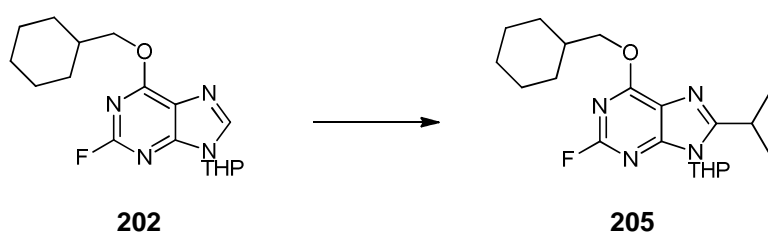


The compound was prepared according to General Procedure V using 300 mg (0.89 mmol) of **202**, 379 μL (2.69 mmol) of diisopropylamine, 1.07 mL of *n*BuLi solution and 334 μL (5.29 mmol) of MeI. The crude product was purified by flash chromatography on silica (EtOAc/Hexane 1:1) yielding the title compound as a white solid (210 mg, 80%).

R_f = 0.51 (EtOAc/Hexane 1:1); mp: 146-148 °C; IR (cm^{-1}) 2927, 2854, 1614, 1581, 1442; λ_{max} (EtOH)/nm: 258; ^1H NMR (300 MHz, CDCl_3) δ 1.13-1.21 (5H, m, cyclohexyl), 1.36 (3H, dd, J = 13; 2.5 Hz, $\text{C}_8\text{-CH}_2\text{CH}_3$), 1.64-1.81 (11H, m, cyclohexyl + THP), 2.97 (2H, dq, J = 13; 2.5 Hz, $\text{C}_8\text{-CH}_2\text{CH}_3$), 3.61 (1H, t, J = 11 Hz, H_3 ax THP), 4.09 (1H, d, J = 11 Hz, H_3 eq THP), 4.30 (2H, d, J = 6 Hz, CH_2Cy), 5.56 (1H,

d, $J = 10.5$ Hz, H_1 THP); ^{13}C NMR (75 MHz, CDCl_3) δ 12.1, 22.6, 23.2, 24.8, 25.6, 26.3, 29.6, 30.1, 37.0, 60.4, 69.1, 73.1, 83.1, 118.4, 153.8, 154.0, 156.3, 156.4, 158.1, 161.7, 161.8; MS(ES+) m/z 363.4 $[\text{M} + \text{H}]^+$.

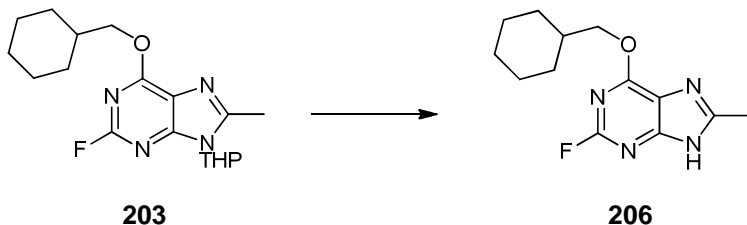
6-(Cyclohexylmethoxy)-2-fluoro-8-isopropyl-9-(tetrahydro-2H-pyran-2-yl)-9H-purine (205)



The compound was prepared according to General Procedure V using 100 mg (0.27 mmol) of **202**, 45 μL (0.38 mmol) of diisopropylamine, 160 μL of $n\text{BuLi}$ solution and 60 μL (0.76 mmol) of MeI. The crude product was purified by flash chromatography on silica (EtOAc/Hexane 1:1) yielding the title compound as a white solid (115 mg, 82%).

$R_f = 0.51$ (EtOAc/Hexane 1:1); mp: 146-148 $^{\circ}\text{C}$; IR (cm^{-1}) 2358, 2304, 2212, 2126, 1946, 1617; λ_{max} (EtOH)/nm: 258; ^1H NMR (300 MHz, CDCl_3) δ 0.93-1.18 (5H, m, cyclohexyl), 1.37 (6H, d, $J = 13$ Hz, $\text{C}_8\text{-CH}(\text{CH}_3)_2$), 1.66-1.71 (11H, m, cyclohexyl + THP), 2.57 (2H, dq, $J = 13; 2.5$ Hz, $\text{C}_8\text{-CH}(\text{CH}_3)_2$), 3.38 (1H, t, $J = 11$ Hz, H_3 ax THP), 3.69 (1H, d, $J = 11$ Hz, H_3 eq THP), 4.30 (2H, d, $J = 6$ Hz, CH_2Cy), 5.56 (1H, d, $J = 10.5$ Hz, H_1 THP); ^{13}C NMR (75 MHz, CDCl_3) δ 21.5, 22.0, 22.6, 23.2, 23.3, 24.8, 25.6, 26.4, 28.0, 29.6, 30.1, 37.1, 69.2, 73.1, 83.1, 160.1, 161.9; MS(ES+) m/z 293.4 $[\text{M} + \text{H}]^+$.

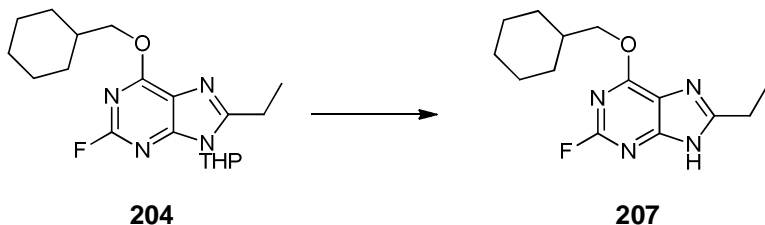
6-(Cyclohexylmethoxy)-2-fluoro-8-methyl-9H-purine (206)



The compound was prepared according to General Procedure VI from 150 mg (0.43 mmol) of **203**, yielding the title compound as a white solid (125 mg, 100%).

R_f = 0.21 (EtOAc/Hexane 1:1); mp: 169-170 °C; IR (cm^{-1}) 2925, 2852, 2324, 1610, 1584, 1446; λ_{max} (EtOH)/nm: 258; ^1H NMR (300 MHz, CDCl_3) δ 1.07-1.90 (11H, m, cyclohexyl), 2.62 (3H, s, $\text{C}_8\text{-Me}$), 4.30 (2H, d, J = 6 Hz, CH_2Cy); ^{13}C NMR (75 MHz, CDCl_3) δ 15.3, 25.6, 26.3, 29.6, 37.1, 73.4; MS(ES+) m/z 265.2 $[\text{M} + \text{H}]^+$.

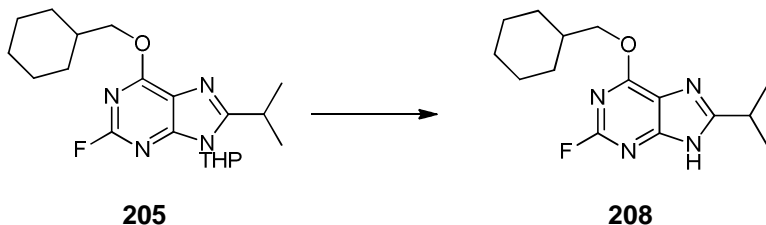
6-(Cyclohexylmethoxy)-2-fluoro-8-ethyl-9H-purine (207)



The compound was prepared according to General Procedure VI from 150 mg (0.43 mmol) of **204**, yielding the title compound as a white solid (131 mg, 100%).

R_f = 0.21 (EtOAc/Hexane 1:1); mp: 169-170 °C; IR (cm^{-1}) 2534, 2159, 2025, 1976, 1609, 1530, 1416; λ_{max} (EtOH)/nm: 258; ^1H NMR (300 MHz, CDCl_3) δ 0.98-1.21 (5H, m, cyclohexyl), 1.40 (3H, t, J = 10 Hz, $\text{C}_8\text{-CH}_2\text{CH}_3$), 1.66-1.83 (6H, m, cyclohexyl), 2.95 (2H, q, J = 10 Hz, $\text{C}_8\text{-CH}_2\text{CH}_3$), 4.30 (2H, d, J = 6 Hz, CH_2Cy); ^{13}C NMR (75 MHz, CDCl_3) δ 12.1, 23.0, 25.6, 26.3, 29.6, 37.1, 73.3; MS(ES+) m/z 279.3 $[\text{M} + \text{H}]^+$.

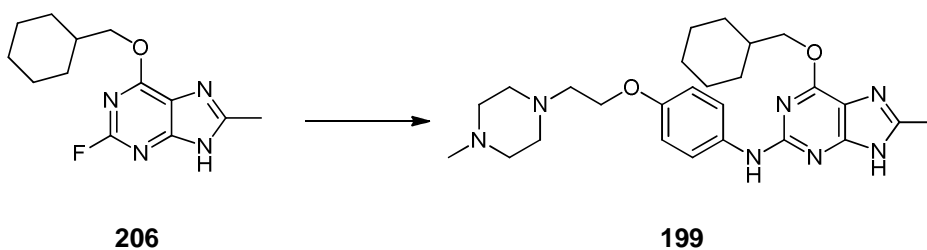
6-(Cyclohexylmethoxy)-2-fluoro-8-isopropyl-9H-purine (208)



The compound was prepared according to General Procedure VI from 100 mg (0.33 mmol) of **205**, yielding the title compound as a white solid (71 mg, 85%).

R_f = 0.21 (EtOAc/Hexane 1:1); mp: 169-170 °C; IR (cm^{-1}) 2923, 2854, 1604, 1524, 1442; λ_{max} (EtOH)/nm: 258; ^1H NMR (300 MHz, CDCl_3) δ 0.98-1.21 (5H, m, cyclohexyl), 1.41 (6H, d, J = 10 Hz, $\text{C}_8\text{-CH}(\text{CH}_3)_2$), 1.66-1.83 (6H, m, cyclohexyl), 3.25 (2H, ept, J = 10 Hz, $\text{C}_8\text{-CH}(\text{CH}_3)_2$), 4.32 (2H, d, J = 6 Hz, CH_2Cy); ^{13}C NMR (75 MHz, CDCl_3) δ 21.1, 25.6, 26.3, 29.5, 29.6, 37.1, 73.3; MS(ES+) m/z 291.3 $[\text{M} + \text{H}]^+$.

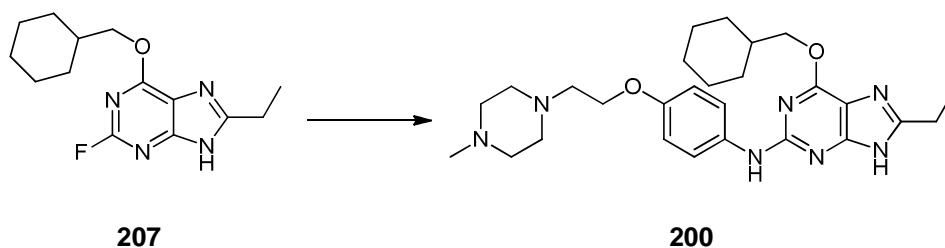
6-(Cyclohexylmethoxy)-8-methyl-*N*-(4-(2-(4-methylpiperazin-1-yl)ethoxy)phenyl)-9H-purin-2-amine (199)



The compound was prepared according to General Procedure I from 4-(2-(4-methylpiperazin-1-yl)ethoxy)benzenamine (215 mg, 0.88 mmol) and 6-cyclohexylmethoxy-2-fluoro-8-methyl-9H-purine (120 mg, 0.43 mmol). The crude product was purified by flash chromatography on silica (EtOAc/MeOH 9:1) yielding the title compound as a white solid (106 mg, 44%).

R_f = 0.25 (EtOAc/MeOH 9:1); mp: 156.0-156.9 °C; IR (cm⁻¹): 2977, 1805, 1753, 1737, 1672, 1624, 1586, 1529, 1505, 1452, 1401; λ_{\max} (EtOH)/nm 273.0; ¹H NMR (300 MHz, CDCl₃) δ 1.17-1.83 (11H, m, cyclohexyl), 2.23 (3H, s, NMe), 2.29 (3H, s, C₈-Me), 2.43-2.57 (8H, m, piperazine), 2.74 (2H, t, J = 6 Hz, OCH₂CH₂N), 3.99 (2H, t, J = 6 Hz, OCH₂CH₂N), 4.21 (2H, d, J = 6 Hz, OCH₂Cy), 6.78 (2H, d, J = 9 Hz, Ar-H), 7.05 (1H, s, NH), 7.34 (1H, d, J = 9 Hz, Ar-H); ¹³C NMR (125 MHz, CDCl₃) δ 25.7, 26.4, 29.8, 37.2, 46.0, 53.5, 55.0, 57.2, 66.1, 71.9, 114.9, 121.1; MS(ES+) m/z 480.4 [M + H]⁺; HRMS calcd for C₂₆H₃₇N₇O₂ [M + H]⁺ 480.3081, found 480.3076.

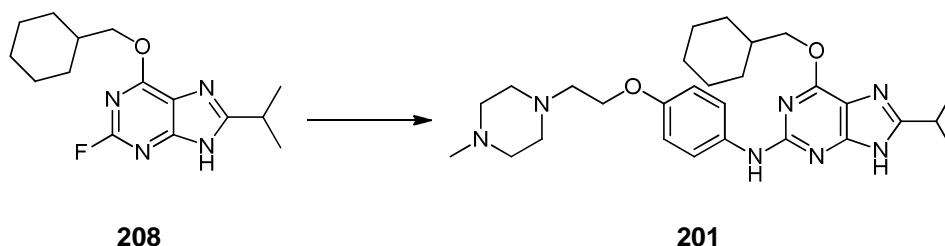
6-(Cyclohexylmethoxy)-8-ethyl-N-(4-(2-(4-methylpiperazin-1-yl)ethoxy)phenyl)-9H-purin-2-amine (200)



The compound was prepared according to General Procedure I from 4-(2-(4-methylpiperazin-1-yl)ethoxy)benzenamine (202 mg, 0.86 mmol) and 6-cyclohexylmethoxy-2-fluoro-8-ethyl-9H-purine (120 mg, 0.43 mmol). The crude product was purified by flash chromatography on silica (EtOAc/MeOH 9:1) yielding the title compound as a white solid (109 mg, 45%).

R_f = 0.25 (EtOAc/MeOH 9:1); mp: 156.0-156.9 °C; IR (cm⁻¹): 2924, 2847, 2800, 1810, 1745, 1740, 1682, 1665, 1587, 1535, 1507, 1450, 1400; λ_{\max} (EtOH)/nm 272.0; ¹H NMR (300 MHz, CDCl₃) δ 0.90-1.15 (5H, m, cyclohexyl), 1.16 (3H, t, J = 11 Hz, C₈-CH₂CH₃), 1.65-1.97 (6H, m, cyclohexyl), 2.28 (3H, s, NMe), 2.65 (8H, m, piperazine), 2.66 (2H, q, J = 11 Hz, C₈-CH₂CH₃), 2.74 (2H, t, J = 6 Hz, OCH₂CH₂N), 4.02 (2H, t, J = 6 Hz, OCH₂CH₂N), 4.22 (2H, d, J = 6 Hz, OCH₂Cy), 6.77 (2H, d, J = 9 Hz, Ar-H), 7.41 (1H, s, NH), 7.34 (1H, d, J = 9 Hz, Ar-H); ¹³C NMR (125 MHz, CDCl₃) δ 12.2, 22.6, 25.7, 26.4, 29.8, 37.2, 46.0, 53.5, 55.0, 57.2, 66.2, 71.99, 114.9, 121.1, 133.3, 152.2, 154.3; MS(ES+) m/z 494.4 [M + H]⁺; HRMS calcd for C₂₇H₃₉N₇O₂ [M + H]⁺ 494.3238, found 494.3232.

6-(Cyclohexylmethoxy)-8-isopropyl-*N*-(4-(2-(4-methylpiperazin-1-yl)ethoxy)phenyl)-9*H*-purin-2-amine (201)



The compound was prepared according to General Procedure I from 4-(2-(4-methylpiperazin-1-yl)ethoxy)benzenamine (112 mg, 0.48 mmol) and 6-cyclohexylmethoxy-2-fluoro-8-isopropyl-9*H*-purine (70 mg, 0.24 mmol). The crude product was purified by flash chromatography on silica (EtOAc/MeOH 9:1) yielding the title compound as a white solid (79 mg, 55%).

R_f = 0.25 (EtOAc/MeOH 9:1); mp: 156.0-156.9 °C; IR (cm⁻¹): 2337, 2254, 2126, 1749, 1738, 1727, 1710; λ_{max} (EtOH)/nm 274.0; ¹H NMR (300 MHz, CDCl₃) δ 0.90-1.15 (5H, m, cyclohexyl), 1.30 (6H, d, J = 11 Hz, C₈-CH(CH₃)₂), 1.65-1.97 (6H, m, cyclohexyl), 2.24 (3H, s, NMe), 2.71 (8H, m, piperazine), 2.75 (1H, ept, J = 11 Hz, C₈-CH(CH₃)₂), 2.76 (2H, t, J = 6 Hz, OCH₂CH₂N), 4.00 (2H, t, J = 6 Hz, OCH₂CH₂N), 4.24 (2H, d, J = 6 Hz, OCH₂Cy), 6.77 (2H, d, J = 9 Hz, Ar-H), 7.41 (1H, s, NH), 7.34 (1H, d, J = 9 Hz, Ar-H); ¹³C NMR (125 MHz, CDCl₃) δ 21.3, 25.7, 26.5, 29.1, 29.9, 37.1, 46.0, 53.6, 55.0, 57.2, 57.3, 66.3, 66.6, 114.9, 115.8, 116.3, 121.2, 140.1, 155.5, 155.8; MS(ES+) m/z 508.5 [M + H]⁺; HRMS calcd for C₂₈H₄₁N₇O₂ [M + H]⁺ 508.3395, found 508.3388.

7.7 Protein expression, kinase assays, MS and SPR

Protein expression and purification [\(performed by colleagues at the Department of Biochemistry, University of Oxford\)](#)

CDK2 phosphorylated at T160 (produced in *Escherichia coli* by coexpression of human GST-CDK2 and *S. cerevisiae* GST-Cak1), human cyclin A3 (residues 174-432), GST-3C-protease and GST-pRb (residues 792-928) were expressed and purified as previously described.²⁹⁷ *S. cerevisiae* GST-Cak1 (also called Civ1) was expressed and purified as previously described.²⁹⁸

GST-tagged K88E K89V mutant CDK2 (GST-CDK2*) was generated using a pGEX 6P-I expression plasmid. *E. coli* competent cells (strain BL21 (DE3) pLysS) were transformed with the plasmid (as per standard transformation protocol provided by supplier) and then grown in LB medium supplemented with 0.1 mg/ml ampicillin to an optical density of 0.9 at 37 °C and then at 20 °C for 2 h, before induction with 20 mM isopropyl- β -D-thiogalactoside (IPTG) and further incubation for 20–24 h at 20 °C. Centrifuged cells were resuspended in HEPES-buffered saline (HBS) containing protease inhibitors (10 mM HEPES, pH 7.4, 135 mM NaCl, 3 mM EDTA, 0.01% (v/v) monothioglycerol, and 0.01 % (w/v) sodium azide containing 0.1 mM phenylmethylsulphonyl fluoride (PMSF), 0.7 mg ml⁻¹ pepstatin A and 0.5 mg ml⁻¹ leupeptin) and stored at -20 °C.

Cells expressing GST-CDK2* were thawed and sonicated on ice. The clarified lysate was applied to a glutathione-Sepharose column (Amersham) equilibrated in HBS and washed with the same buffer. GST-CDK2* was eluted with freshly prepared 20 mM glutathione in HBS and phosphorylated on Thr160 in the presence of 1/10 w/w GST-Civ1, 50 mM Tris-HCl pH 7.5, 10 mM magnesium chloride, 1 mM ATP for 18 h at 4 °C. Phospho-T160-GST-CDK2* was purified from GST-Civ1 by gel filtration (Superdex SD-200). The pooled fractions from the gel filtration were applied to a second glutathione-Sepharose column, followed by a clarified lysate from thawed and sonicated cyclin-A3-expressing cells. The GST-pCDK2*/cyclin A complex was eluted with freshly prepared 20 mM glutathione in HBS and subjected to GST-3C-

protease digestion (1/50 w/w, 18 h, 4 °C). pCDK2*/cyclin A was further purified from GST dimer by gel filtration (Superdex SD-200) and a third glutathione–Sepharose column.

Band shift assays

Activity of both mutant and wild type CDK2/A was checked by gel shift on SDS-PAGE using 15% acrylamide. Enzyme concentration (except for negative controls) was at 8 µg/ml, against 50 µg/ml pRb as substrate. Kinase reactions were performed in 10 µl of buffer containing 50 mM Tris-HCl pH 7.5, 10 mM magnesium chloride, 1.0 mM ATP for 15 min at RT, monitoring at the following time intervals: 0', 1', 5', 10', 15'.

Radioactive kinase assays [\(kindly performed by Lan-Zhen Wang at the Northern Institute for Cancer Research, and by Elizabeth Anscombe at the department of Biochemistry, University of Oxford\)](#)

The assay conditions used for evaluating the time-dependent inhibitory activity of NU6300 and NU6310 against CDK2 were as previously described.¹⁹⁹

The purified enzyme was reacted with radiolabelled [³²P] ATP and the protein substrate. The assay involved detecting the transfer of the radiolabelled γ-phosphate group from ATP to the protein substrate.

IC₅₀ determinations were carried out at five different concentrations [of inhibitor to be tested](#). The IC₅₀ is the concentration required to inhibit enzyme activity by 50% under the assay conditions employed.

Compounds were dissolved in DMSO to give an initial 50 mM stock solution.

Inhibitors were tested in the assay at a final DMSO concentration of 1%, and hence were diluted with the buffer solution 1/50 from the original stock solution. It was assumed that employing a higher concentration of DMSO in the assays would denature the enzyme.

Radiolabelled [³²P] ATP was added to the buffered inhibitor, which was incubated for ten minutes at 30 °C. After incubation, the assay mixture was spotted onto

phosphocellulose filter paper to bind the protein, allowing a 20 second time interval for drying. The labelled filter paper was transferred to a stirred solution of 1% aqueous phosphoric acid to dilute the phosphate substrate, thereby terminating the reaction. The filters were washed a further 5-6 times for five minutes each and dried over paper towels, before being placed in a scintillation counter.

The amount of [³²P] incorporated into the histone was measured by counting the number of disintegrations per minute, giving an experimental measurement of enzyme activity.

Control assays (without inhibitor) were also carried out in 1% DMSO solution, with the control defined as having 100% enzyme activity. The percentage of remaining activity was derived from the ratio of inhibitor activity to the activity of the control assay (pure enzyme). The percentage inhibition was equal to 100 minus the percentage of the remaining activity.

$$\% \text{ Remaining Activity} = \text{Inhibitor Activity} / \text{Control Activity}$$

$$\% \text{ Inhibition} = 100 - \% \text{ Remaining Activity}$$

IC₅₀ values for the inhibitors were determined by plotting the percentage of inhibition against inhibitor concentration.

ESI Mass Spectrometry ([kindly performed by David Staunton at the Department of Biochemistry, University of Oxford](#))

Protein samples (at 3 mg/ml in HBS buffer) were desalted using C4 ZipTips (Millipore) as per manufacturer's instructions. The samples in 1:1 (v/v) acetonitrile and water + 0.1% formic acid were introduced at a flow rate of 10ul/min by electrospray ionisation (ESI) into a Micromass LCT orthogonal acceleration reflecting TOF mass spectrometer in positive ion mode. The mass spectrometer had been calibrated using myoglobin. The resultant m/z spectra were converted to mass spectra by using the maximum entropy analysis MaxEnt in the MassLynx suite of programmes.

Tryptic digest and MALDI-TOF TOF MS/MS ([kindly performed by Ben Thomas at the Sir William Dunn School of Pathology, University of Oxford](#))

Coomassie stained gel bands were excised and diced into 1 mm cubes before being destained with three washes of 25 mM ammonium bicarbonate (Fluka) in 50:50 (v/v) acetonitrile (Sigma) and water. Gel pieces were dehydrated with a wash of acetonitrile and reduced in 10 mM DTT (Fluka) for 30 minutes. Gel pieces were then washed twice with 25 mM ammonium bicarbonate and dehydrated with one wash of acetonitrile prior to being alkylated with 55 mM iodoacetamide (Fluka) for one hour. Gel pieces were washed twice with 25 mM ammonium carbonate and dehydrated with an acetonitrile wash. The gel pieces were dried in a SpeedVac (Thermo Savant). 3 µg of trypsin (Promega) in 25 mM ammonium bicarbonate were added to the gel pieces and the gel pieces were incubated at 37 °C overnight. The gel pieces were acidified to 1% formic acid. The supernatant was then collected in a fresh tube. The gel pieces were then incubated once with 0.1% formic acid (Sigma) in 5% aqueous acetonitrile for 30 min and once in 0.1% formic acid in 60% aqueous acetonitrile. The supernatants were pooled and dried to near dryness in a SpeedVac. The supernatant was then desalted using an in-house manufactured C18 reverse-phase tip consisting of a C18 plug (3M, Empore) packed into a pipette tip. The tip was wetted with several washes of acetonitrile containing 0.1% formic acid and then conditioned with several washes aqueous of 5% acetonitrile containing 0.1% formic acid. The sample was then bound by passing it twice over the tip. The salt was then washed off the tip with a wash of aqueous 5% acetonitrile containing 0.1% formic acid. The sample was then eluted in a small volume of aqueous 60% acetonitrile containing 0.1% formic acid and concentrated in a SpeedVac.

Mass spectrometry data were acquired on an Orbitrap mass spectrometer (Thermo) fitted with a nanospray source (Proxeon) coupled to a U3000 nano HPLC system (Dionex). The sample was loaded onto a 15 cm long, 100 µm ID, home-packed column manufactured by packing a Picotip emitter (New Objective) with ProntoSIL C18 phase (120 Å pore, 3 µm bead C18) (Bischoff Chromatography). The HPLC was run in a direct injection configuration. Buffer A consisted of 5% aqueous acetonitrile containing 0.1% formic acid and buffer B consisted of 95% aqueous acetonitrile

containing 0.1% formic acid. Samples were loaded onto the column at a flow rate of 700 nl/min, and resolved using a 180 minute gradient at a flow rate of 300 nl/min.

The Orbitrap was run in a data dependent acquisition mode in which the Orbitrap resolution was set at 60,000 and the top 5 multiply charged species were selected for MS/MS. The automatic gain control for the Orbitrap was set to 500,000 ions and the automatic gain control for the MS/MS in the ion trap was set at 10,000 ions. Maximum injection time into the ion trap in MS/MS was 200 ms and maximum accumulation time in the Orbitrap was 500 ms. Three MS/MS microscans were accumulated for each precursor. Dynamic exclusion was switched on and selected ions excluded for 180 s before they could be selected for another round of MS/MS.

Samples were typically injected in triplicate in order to increase the number of identifications.

Raw instrument data were converted into mzXML format using an in-house developed script. mzXML files were then submitted to an in-house developed proteomics data analysis pipeline based on Seattle Proteome Center's Trans Proteomic Pipeline (TPP). The data analysis pipeline incorporated three database search engines (Mascot, OMSSA and X!Tandem) in order to maximise the number of identifications and used various statistical tools (PeptideProphet, ProteinProphet and iProphet) in order to determine false discovery rates (FDR). Data were searched with the fixed modification carbamidomethyl cysteine and the variable modifications protein N-terminal acetylation, oxidised methionine and deamidated (NQ). Precursor mass tolerance was set at ± 10 ppm and MS/MS fragment tolerance at ± 0.5 Da. Strict Trypsin specificity was used and 2 missed cleavages were allowed. Data were then exported from the pipeline into Proteincenter (Proxeon) for filtering, annotation, classification and interpretation.

SPR experiments and data analysis [\(performed by colleagues at Beactica, Sweden\)](#)

The interaction experiments were performed using Biacore S51 and T100 instruments and CM5 biosensor chips (GE Healthcare/Biacore, Uppsala, Sweden). CDK2 was immobilised to activated carboxylated dextran surfaces by amine coupling to give surface densities of 6000-25000 RU. All interaction experiments

were performed at 25 °C in 10 mM phosphate pH 7.4, 137 mM NaCl, 3 mM KCl, with addition of 0.05 % Tween 20 (BDH/Prolabo), 5 % (v/v) DMSO (Riedel de Haën), and at a flow rate of 90 µl/min. For kinetic analysis the test compounds were diluted in the running buffer and injected for 30-240 s over the immobilised CDK2 at increasing concentrations. For analysis of the time dependence of the interaction, immobilised CDK2 was exposed to 10 µM NU6300 for 0 h, 4 h, and 4+16 h. A CDK2 surface incubated with buffer without NU6300 in parallel on the same chip was used as a reference. The binding capacity of the two surfaces was assayed by injections of 10 µM NU6310. Sensorgrams or extracted report points from reference surfaces and blank injections were subtracted from the raw data prior to data analysis, using Biacore T100 evaluation software 2.0. A 1:1 interaction model was fitted globally to sets of sensorgrams recorded with different contact times and at different inhibitor concentrations in multi-cycle experiments. Kinetic parameters were determined from sensorgrams with 30 s and 60 s contact time. Standard deviations were based on at least 4 measurement series.

Molecular modeling

All calculations were performed in Schrödinger Suite 2009 Update 2. Default settings were used throughout unless specified otherwise. Pictures were generated with PyMol 0.99. The structure of CDK2/cyclin A in complex with the purine-based inhibitor NU6102 (1H1S.pdb) was considered. The structure was prepared for docking using the Protein Preparation Wizard. Chains B, C, D and all waters beyond 5 Å of heterocyclic groups were removed. This left 10 water molecules surrounding NU6102. Docking grids were then calculated, using bound NU6102 to define the center of the grid box. Optional H-bond constraints were defined for the backbone carbonyl O's of Glu81 and Leu83, and the backbone NH of Leu83. NU6300 and NU6310 were built manually from the crystal conformation of NU6102 and then prepared with ligprep. The structures with the lowest Epik ionization state penalties were retained. The ligands were then docked with Glide XP. The Epik state penalties were added to the docking scores. 5 Poses were requested for each ligand.

References

1. Hanahan, D.; Weinberg, R. A., The hallmarks of cancer. *Cell* **2000**, *100* (1), 57-70.
2. Hanahan, D.; Weinberg, R. A., Hallmarks of cancer: the next generation. *Cell (Cambridge, MA, U. S.)* **2011**, *144* (Copyright (C) 2011 American Chemical Society (ACS). All Rights Reserved.), 646-674.
3. Baltimore, D., Our genome unveiled. *Nature* **2001**, *409* (6822), 814-816.
4. Lane, D. P.; Lain, S., Therapeutic exploitation of the p53 pathway. *Trends Mol. Med.* **2002**, *8* (4, Suppl.), S38-S42.
5. Chene, P., Inhibiting the p53-MDM2 interaction: An important target for cancer therapy. *Nat. Rev. Cancer* **2003**, *3* (2), 102-109.
6. Blume-Jensen, P.; Hunter, T., Oncogenic kinase signalling. *Nature* **2001**, *411* (6835), 355-365.
7. Cohen, P., The origins of protein phosphorylation. *Nat. Cell Biol.* **2002**, *4* (5), E127-E130.
8. Manning, G.; Whyte, D. B.; Martinez, R.; Hunter, T.; Sudarsanam, S., The Protein Kinase Complement of the Human Genome. *Science* **2002**, *298* (5600), 1912-1934.
9. Bridges, A. J., Chemical inhibitors of protein kinases. *Chem. Rev.* **2001**, *101* (8), 2541-2571.
10. Adams, J. A., Kinetic and catalytic mechanisms of protein kinases. *Chem. Rev.* **2001**, *101* (8), 2271-2290.
11. Khidekel, N.; Hsieh-Wilson, L. C., A 'molecular switchboard' - covalent modifications to proteins and their impact on transcription. *Org. Biomol. Chem.* **2004**, *2* (1), 1-7.
12. Sachsenmaier, C., Targeting protein kinases for tumor therapy. *Onkologie* **2001**, *24* (4), 346-55.
13. Hanks, S. K.; Quinn, A. M.; Hunter, T., The Protein-Kinase Family - Conserved Features and Deduced Phylogeny of the Catalytic Domains. *Science* **1988**, *241* (4861), 42-52.
14. Scott, J. W.; Oakhill, J. S.; van, D. B. J. W., AMPK/SNF1 structure: a menage a trois of energy-sensing. *Front. Biosci.* **2009**, *14*, 596-610.
15. Hinterding, K.; Alonso-Diaz, D.; Waldmann, H., Organic synthesis and biological signal transduction. *Angew. Chem. Int. Ed. Engl.* **1998**, *37* (6), 688-749.
16. Dancey, J.; Sausville, E. A., Issues and progress with protein kinase inhibitors for cancer treatment. *Nat. Rev. Drug Disc.* **2003**, *2* (4), 296-313.
17. Capdeville, H.; Pedoussat, C.; Pitchford, L. C., Ion and neutral energy flux distributions to the cathode in glow discharges in Ar/Ne and Xe/Ne mixtures. *J. Appl. Phys.* **2002**, *91* (3), 1026-1030.
18. Demetri, G. D.; van, O. A. T.; Garrett, C. R.; Blackstein, M. E.; Shah, M. H.; Verweij, J.; McArthur, G.; Judson, I. R.; Heinrich, M. C.; Morgan, J. A.; Desai, J.; Fletcher, C. D.; George, S.; Bello, C. L.; Huang, X.; Baum, C. M.; Casali, P. G., Efficacy and safety of sunitinib in patients with advanced gastrointestinal stromal tumour after failure of imatinib: a randomised controlled trial. *Lancet* **2006**, *368* (9544), 1329-1338.

19. Morin, M. J., From oncogene to drug: development of small molecule tyrosine kinase inhibitors as antitumor and antiangiogenic agents. *Oncogene* **2000**, *19* (56), 6574-6583.
20. Herbst, R. S.; Fukuoka, M.; Baselga, J., Timeline: Gefitinib - a novel targeted approach to treating cancer. *Nat. Rev. Cancer* **2004**, *4* (12), 956-965.
21. Spector, N. L.; Xia, W.; Burris, H., III; Hurwitz, H.; Dees, E. C.; Dowlati, A.; O'Neil, B.; Overmoyer, B.; Marcom, P. K.; Blackwell, K. L.; Smith, D. A.; Koch, K. M.; Stead, A.; Mangum, S.; Ellis, M. J.; Liu, L.; Man, A. K.; Bremer, T. M.; Harris, J.; Bacus, S., Study of the biologic effects of lapatinib, a reversible inhibitor of ErbB1 and ErbB2 tyrosine kinases, on tumor growth and survival pathways in patients with advanced malignancies. *J. Clin. Oncol.* **2005**, *23* (11), 2502-2512.
22. Eisen, T.; Ahmad, T.; Flaherty, K. T.; Gore, M.; Kaye, S.; Marais, R.; Gibbens, I.; Hackett, S.; James, M.; Schuchter, L. M.; Nathanson, K. L.; Xia, C.; Simantov, R.; Schwartz, B.; Poulin-Costello, M.; O'Dwyer, P. J.; Ratain, M. J., Sorafenib in advanced melanoma: a Phase II randomised discontinuation trial analysis. *Br. J. Cancer* **2006**, *95* (5), 581-586.
23. Melnikova, I.; Golden, J., From the analyst's couch: Targeting protein kinases. *Nat. Rev. Drug Disc.* **2004**, *3* (12), 993-994.
24. Hardcastle, I. R.; Golding, B. T.; Griffin, R. J., Designing inhibitors of cyclin-dependent kinases. *Annu. Rev. Pharmacol. Toxicol.* **2002**, *42*, 325-348.
25. Johnson, L. N.; Lewis, R. J., Structural Basis for Control by Phosphorylation. *Chem. Rev. (Washington, D. C.)* **2001**, *101* (8), 2209-2242.
26. Noble, M. E. M.; Endicott, J. A., Chemical inhibitors of cyclin-dependent kinases: insights into design from X-ray crystallographic studies. *Pharmacol. Ther.* **1999**, *82* (2-3), 269-278.
27. Fabbro, D.; Ruetz, S.; Buchdunger, E.; Cowan-Jacob, S. W.; Fendrich, G.; Liebetanz, J.; Mestan, J.; O'Reilly, T.; Traxler, P.; Chaudhuri, B.; Fretz, H.; Zimmermann, J.; Meyer, T.; Caravatti, G.; Furet, P.; Manley, P. W., Protein kinases as targets for anticancer agents: from inhibitors to useful drugs. *Pharmacol. Ther.* **2002**, *93* (Copyright (C) 2010 American Chemical Society (ACS). All Rights Reserved.), 79-98.
28. Laufer, S. A.; Domeyer, D. M.; Scior, T. R. F.; Albrecht, W.; Hauser, D. R. J., Synthesis and Biological Testing of Purine Derivatives as Potential ATP-Competitive Kinase Inhibitors. *J. Med. Chem.* **2005**, *48* (3), 710-722.
29. Heichman, K. A.; Roberts, J. M., Rules to Replicate By. *Cell* **1994**, *79* (4), 557-562.
30. Fischer, P. M.; Glover, D. M.; Lane, D. P., Targeting the cell cycle. *Drug Disc. Today: Ther. Strategies* **2004**, *1* (4), 417-423.
31. Zhou, J.; Yao, J.; Joshi, H. C., Attachment and tension in the spindle assembly checkpoint. *J. Cell Sci.* **2002**, *115* (18), 3547-3555.
32. Johnson, D. G.; Walker, C. L., Cyclins and cell cycle checkpoints. *Annu. Rev. Pharmacol. Toxicol.* **1999**, *39*, 295-312.
33. Elledge, S. J., Cell cycle checkpoints: Preventing an identity crisis. *Science* **1996**, *274* (5293), 1664-1672.
34. Malumbres, M.; Barbacid, M., Milestones in cell division: to cycle or not to cycle: a critical decision in cancer. *Nat. Rev. Cancer* **2001**, *1* (3), 222-231.
35. Marquez, R. T.; Wendlandt, E.; Galle, C. S.; Keck, K.; McCaffrey, A. P., MicroRNA-21 is upregulated during the proliferative phase of liver

- regeneration, targets Pellino-1, and inhibits NF- κ B signaling. *Am. J. Physiol.* **298** (4, Pt. 1), G535-G541.
36. Gavrilov, L. A.; Gavrilova, N. S., The reliability theory of aging and longevity. *J. Theor. Biol.* **2001**, *213* (4), 527-45.
 37. Huwe, A.; Mazitschek, R.; Giannis, A., Small molecules as inhibitors of cyclin-dependent kinases. *Angew. Chem., Int. Ed.* **2003**, *42* (19), 2122-2138.
 38. Toogood, P. L., Cyclin-dependent kinase inhibitors for treating cancer. *Med. Res. Rev.* **2001**, *21* (6), 487-498.
 39. Malumbres, M.; Barbacid, M., Cell cycle kinases in cancer. *Curr. Opin. Genet. Dev.* **2007**, *17* (1), 60-65.
 40. Schwartz, G. K.; Shah, M. A., Targeting the cell cycle: a new approach to cancer therapy. *J. Clin. Oncol.* **2005**, *23* (36), 9408-9421.
 41. Stern, B.; Nurse, P., A quantitative model for the cdc2 control of S phase and mitosis in fission yeast. *Trends in Genetics* **1996**, *12* (9), 345-350.
 42. Noble, M. E. M.; Endicott, J. A.; Johnson, L. N., Protein kinase inhibitors: Insights into drug design from structure. *Science* **2004**, *303* (5665), 1800-1805.
 43. Davies, T. G.; Bentley, J.; Arris, C. E.; Boyle, F. T.; Curtin, N. J.; Endicott, J. A.; Gibson, A. E.; Golding, B. T.; Griffin, R. J.; Hardcastle, I. R.; Jewsbury, P.; Johnson, L. N.; Mesguiche, V.; Newell, D. R.; Noble, M. E. M.; Tucker, J. A.; Wang, L.; Whitfield, H. J., Structure-based design of a potent purine-based cyclin-dependent kinase inhibitor. *Nat. Struct. Biol.* **2002**, *9* (10), 745-749.
 44. Fischer, P. M.; Gianella-Borradori, A., Recent progress in the discovery and development of cyclin-dependent kinase inhibitors. *Expert Opin. Invest. Drugs* **2005**, *14* (4), 457-477.
 45. Heitz, F.; Morris, M. C.; Fesquet, D.; Cavadore, J.-C.; Doree, M.; Divita, G., Interactions of cyclins with cyclin-dependent kinases: A common interactive mechanism. *Biochemistry* **1997**, *36* (16), 4995-5003.
 46. Hunter, T.; Pines, J., Cyclins and cancer II: cyclin D and CDK inhibitors come of age. *Cell (Cambridge, Mass.)* **1994**, *79* (4), 573-82.
 47. Weinberg, R. A., The Retinoblastoma Protein and Cell-Cycle Control. *Cell* **1995**, *81* (3), 323-330.
 48. Stillman, B., Cell Cycle Control of DNA replication. *Science* **1996**, *274* (5293), 1659-1664.
 49. Brugarolas, J.; Moberg, K.; Boyd, S. D.; Taya, Y.; Jacks, T.; Lees, J. A., Inhibition of cyclin-dependent kinase 2 by p21 is necessary for retinoblastoma protein-mediated G1 arrest after $\dot{\text{I}}^3$ -irradiation. *Proc. Natl. Acad. Sci. U. S. A.* **1999**, *96* (3), 1002-1007.
 50. Munger, K., Clefs, grooves, and (small) pockets: the structure of the retinoblastoma tumor suppressor in complex with its cellular target E2F unveiled. *Proc. Natl. Acad. Sci. U. S. A.* **2003**, *100* (5), 2165-2167.
 51. Sherr, C. J., Cancer cell cycles. *Science* **1996**, *274* (5293), 1672-1677.
 52. Knockaert, M.; Greengard, P.; Meijer, L., Pharmacological inhibitors of cyclin-dependent kinases. *Trends Pharmacol. Sci.* **2002**, *23* (9), 417-425.
 53. Meijer, L., Cyclin-dependent kinases inhibitors as potential anticancer, antineurodegenerative, antiviral and antiparasitic agents. *Drug Resist. Updates* **2000**, *3* (2), 83-88.
 54. Paglini, G.; Caceres, A., The role of the Cdk5-p35 kinase in neuronal development. *Eur. J. Biochem.* **2001**, *268* (6), 1528-1533.

55. Samuels, B. A.; Tsai, L.-H., Cdk5 is a dynamo at the synapse. *Nat. Cell Biol.* **2003**, 5 (8), 689-690.
56. Maccioni, R. B.; Otth, C.; Concha, I. I.; Munoz, J. P., The protein kinase Cdk5: structural aspects, roles in neurogenesis and involvement in Alzheimer's pathology. *Eur. J. Biochem.* **2001**, 268 (6), 1518-1527.
57. Leost, M.; Schultz, C.; Link, A.; Wu, Y.-Z.; Biernat, J.; Mandelkow, E.-M.; Bibb, J. A.; Snyder, G. L.; Greengard, P.; Zaharevitz, D. W.; Gussio, R.; Senderowicz, A. M.; Sausville, E. A.; Kunick, C.; Meijer, L., Paullones are potent inhibitors of glycogen synthase kinase-3 β and cyclin-dependent kinase 5/p25. *Eur. J. Biochem.* **2000**, 267 (19), 5983-5994.
58. Wang, S.; Fischer, P. M., Cyclin-dependent kinase 9: a key transcriptional regulator and potential drug target in oncology, virology and cardiology. *Trends Pharmacol. Sci.* **2008**, 29 (6), 302-313.
59. Rickert, P.; Corden, J. L.; Lees, E., Cyclin C/CDK8 and cyclin H/CDK7/p36 are biochemically distinct CTD kinases. *Oncogene* **1999**, 18 (4), 1093-1102.
60. Oelgeschlager, T., Regulation of RNA polymerase II activity by CTD phosphorylation and cell cycle control. *J. Cell. Physiol.* **2002**, 190 (2), 160-169.
61. Pavletich, N. P., Mechanisms of Cyclin-dependent Kinase Regulation: Structures of Cdks, their Cyclin Activators, and Cip and INK4 Inhibitors. *J. Mol. Biol.* **1999**, 287 (5), 821-828.
62. Jeffrey, P. D.; Russo, A. A.; Polyak, K.; Gibbs, E.; Hurwitz, J.; Massague, J.; Pavletich, N. P., Mechanism of CDK activation revealed by the structure of a cyclin A-CDK2 complex. *Nature (London)* **1995**, 376 (6538), 313-20.
63. Brown, N. R.; Noble, M. E. M.; Lawrie, A. M.; Morris, M. C.; Tunnah, P.; Divita, G.; Johnson, L. N.; Endicott, J. A., Effects of phosphorylation of threonine 160 on cyclin-dependent kinase 2 structure and activity. *J. Biol. Chem.* **1999**, 274 (13), 8746-8756.
64. Russo, A. A.; Jeffrey, P. D.; Pavletich, N. P., Structural basis of cyclin-dependent kinase activation by phosphorylation. *Nat. Struct. Biol.* **1996**, 3 (8), 696-700.
65. Harper, J. W.; Adams, P. D., Cyclin-dependent kinases. *Chem. Rev.* **2001**, 101 (8), 2511-2526.
66. Malumbres, M.; Barbacid, M., Is cyclin D1-CDK4 kinase a bona fide cancer target? *Cancer Cell* **2006**, 9 (1), 2-4.
67. Loog, M.; Morgan, D. O., Cyclin specificity in the phosphorylation of cyclin-dependent kinase substrates. *Nature (London, U. K.)* **2005**, 434 (7029), 104-108.
68. Sherr, C. J.; Roberts, J. M., CDK inhibitors: positive and negative regulators of G1-phase progression. *Genes Dev.* **1999**, 13 (12), 1501-1512.
69. Guo, Y.; Sklar, G. N.; Borkowski, A.; Kyprianou, N., Loss of the cyclin-dependent kinase inhibitor p27(Kip1) protein in human prostate cancer correlates with tumor grade. *Clin Cancer Res* **1997**, 3 (12 Pt 1), 2269-74.
70. Hall, M.; Peters, G., Genetic alterations of cyclins, cyclin-dependent kinases, and Cdk inhibitors in human cancer. *Adv. Cancer Res.* **1996**, 68, 67-108.
71. Russo, A. A.; Tong, L.; Lee, J.-O.; Jeffrey, P. D.; Pavletich, N. P., Structural basis for inhibition of the cyclin-dependent kinase Cdk6 by the tumor suppressor p16INK4a. *Nature (London)* **1998**, 395 (6699), 237-243.
72. Li, A.; Blow, J. J., The origin of CDK regulation. *Nat. Cell Biol.* **2001**, 3 (8), E182-E184.

73. Endicott, J. A.; Noble, M. E. M.; Tucker, J. A., Cyclin-dependent kinases: inhibition and substrate recognition. *Curr. Opin. Struct. Biol.* **1999**, 9 (6), 738-744.
74. Ryan, K. M.; Phillips, A. C.; Vousden, K. H., Regulation and function of the p53 tumor suppressor protein. *Curr. Opin. Cell Biol.* **2001**, 13 (3), 332-337.
75. Zhang, P.; Wong, C.; Depinho, R. A.; Harper, J. W.; Elledge, S. J., Cooperation between the Cdk inhibitors p27KIP1 and p57KIP2 in the control of tissue growth and development. *Genes Dev.* **1998**, 12 (20), 3162-3167.
76. Morgan, D. O., Cyclin-dependent kinases: engines, clocks, and microprocessors. *Annu. Rev. Cell Dev. Biol.* **1997**, 13, 261-291.
77. Huwe, A.; Mazitschek, R.; Giannis, A., Small molecules as inhibitors of cyclin-dependent kinases. *Angew. Chem.* **2003**, 42, 2122-2138.
78. Knockaert, M.; Greengard, P.; Meijer, L., Pharmacological inhibitors of cyclin-dependent kinases. *Trends Pharmacol. Sci.* **2002**, 23, 417-425.
79. Morgan, D. O., Principles of CDK regulation. *Nature (London)* **1995**, 374 (6518), 131-4.
80. Garrett, M. D.; Fattaey, A., CDK inhibition and cancer therapy. *Curr. Opin. Genet. Dev.* **1999**, 9 (1), 104-111.
81. Sielecki, T. M.; Boylan, J. F.; Benfield, P. A.; Trainor, G. L., Cyclin-dependent kinase inhibitors: useful targets in cell cycle regulation. *J. Med. Chem.* **2000**, 43 (1), 1-18.
82. de, C. G.; Perez, d. C. I.; Malumbres, M., Targeting cell cycle kinases for cancer therapy. *Curr. Med. Chem.* **2007**, 14 (9), 969-985.
83. Furet, P., X-ray crystallographic studies of CDK2, a basis for cyclin-dependent kinase inhibitor design in anti-cancer drug research. *Curr. Med. Chem.: Anti-Cancer Agents* **2003**, 3 (1), 15-23.
84. Chang, Y. T.; Gray, N. S.; Rosania, G. R.; Sutherlin, D. P.; Kwon, S.; Norman, T. C.; Sarohia, R.; Leost, M.; Meijer, L.; Schultz, P. G., Synthesis and application of functionally diverse 2,6,9-trisubstituted purine libraries as CDK inhibitors. *Chem. Biol.* **1999**, 6 (6), 361-375.
85. Gray, N. S.; Wodicka, L.; Thunnissen, A.; Norman, T. C.; Kwon, S. J.; Espinoza, F. H.; Morgan, D. O.; Barnes, G.; LeClerc, S.; Meijer, L.; Kim, S. H.; Lockhart, D. J.; Schultz, P. G., Exploiting chemical libraries, structure, and genomics in the search for kinase inhibitors. *Science* **1998**, 281 (5376), 533-538.
86. Sridhar, J.; Akula, N.; Pattabiraman, N., Selectivity and potency of cyclin-dependent kinase inhibitors. *Aaps J.* **2006**, 8 (1), E204-E221.
87. Barvian, M.; Boschelli, D. H.; Cossrow, J.; Dobrusin, E.; Fattaey, A.; Fritsch, A.; Fry, D.; Harvey, P.; Keller, P.; Garrett, M.; La, F.; Leopold, W.; McNamara, D.; Quin, M.; Trumpp-Kallmeyer, S.; Toogood, P.; Wu, Z. P.; Zhang, E. L., Pyrido[2,3-d]pyrimidin-7-one inhibitors of cyclin-dependent kinases. *J. Med. Chem.* **2000**, 43 (24), 4606-4616.
88. Wang, S. D.; Meades, C.; Wood, G.; Osnowski, A.; Anderson, S.; Yuill, R.; Thomas, M.; Mezna, M.; Jackson, W.; Midgley, C.; Griffiths, G.; Fleming, I.; Green, S.; McNae, I.; Wu, S. Y.; McInnes, C.; Zheleva, D.; Walkinshaw, M. D.; Fischer, P. M., 2-anilino-4-(thiazol-5-yl)pyrimidine CDK inhibitors: Synthesis, SAR analysis, X-ray crystallography, and biological activity. *J. Med. Chem.* **2004**, 47 (7), 1662-1675.
89. Wang, S. D.; Wood, G.; Meades, C.; Griffiths, G.; Midgley, C.; McNae, I.; McInnes, C.; Anderson, S.; Jackson, W.; Mezna, M.; Yuill, R.; Walkinshaw,

- M.; Fischer, P. M., Synthesis and biological activity of 2-anilino-4-(1H-pyrrol-3-yl) pyrimidine CDK inhibitors. *Bioorg. Med. Chem. Lett.* **2004**, *14* (16), 4237-4240.
90. Engler, T. A.; Furness, K.; Malhotra, S.; Sanchez-Martinez, C.; Shih, C.; Xie, W.; Zhu, G. X.; Zhou, X.; Conner, S.; Faul, M. M.; Sullivan, K. A.; Kolis, S. P.; Brooks, H. B.; Patel, B.; Schultz, R. M.; DeHahn, T. B.; Kirmani, K.; Spencer, C. D.; Watkins, S. A.; Considine, E. L.; Dempsey, J. A.; Ogg, C. A.; Stamm, N. B.; Anderson, B. D.; Campbell, R. M.; Vasudevan, V.; Lytle, M. L., Novel, potent and selective cyclin D1/CDK4 inhibitors: Indolo[6,7-a]pyrrolo[3,4-c]carbazoles. *Bioorg. Med. Chem. Lett.* **2003**, *13* (14), 2261-2267.
 91. Shimamura, T.; Shibata, J.; Kurihara, H.; Mita, T.; Otsuki, S.; Sagara, T.; Hirai, H.; Iwasawa, Y., Identification of potent 5-pyrimidinyl-2-aminothiazole CDK4, 6 inhibitors with significant selectivity over CDK1, 2, 5, 7, and 9. *Bioorg. Med. Chem. Lett.* **2006**, *16* (14), 3751-3754.
 92. Toogood, P. L.; Harvey, P. J.; Repine, J. T.; Sheehan, D. J.; VanderWel, S. N.; Zhou, H. R.; Keller, P. R.; McNamara, D. J.; Sherry, D.; Zhu, T.; Brodfuehrer, J.; Choi, C.; Barvian, M. R.; Fry, D. W., Discovery of a potent and selective inhibitor of cyclin-dependent kinase 4/6. *J. Med. Chem.* **2005**, *48* (7), 2388-2406.
 93. VanderWel, S. N.; Harvey, P. J.; McNamara, D. J.; Repine, J. T.; Keller, P. R.; Quin, J.; Booth, R. J.; Elliott, W. L.; Dobrusin, E. M.; Fry, D. W.; Toogood, P. L., Pyrido[2,3-d]pyrimidin-7-ones as specific inhibitors of cyclin-dependent kinase 4. *J. Med. Chem.* **2005**, *48* (7), 2371-2387.
 94. Zhu, G. X.; Conner, S. E.; Zhou, X.; Shih, C.; Li, T. C.; Anderson, B. D.; Brooks, H. B.; Campbell, R. M.; Considine, E.; Dempsey, J. A.; Faul, M. M.; Ogg, C.; Patel, B.; Schultz, R. M.; Spencer, C. D.; Teicher, B.; Watkins, S. A., Synthesis, structure-activity relationship, and biological studies of indolocarbazoles as potent cyclin D1-CDK4 inhibitors. *J. Med. Chem.* **2003**, *46* (11), 2027-2030.
 95. Hardcastle, I. R.; Arris, C. E.; Bentley, J.; Boyle, F. T.; Chen, Y. H.; Curtin, N. J.; Endicott, J. A.; Gibson, A. E.; Golding, B. T.; Griffin, R. J.; Jewsbury, P.; Menyerol, J.; Mesguiche, V.; Newell, D. R.; Noble, M. E. M.; Pratt, D. J.; Wang, L. Z.; Whitfield, H. J., N-2-substituted O-6-cyclohexylmethylguanine derivatives: Potent inhibitors of cyclin-dependent kinases 1 and 2. *J. Med. Chem.* **2004**, *47* (15), 3710-3722.
 96. Sayle, K. L.; Bentley, J.; Boyle, F. T.; Calvert, A. H.; Cheng, Y. Z.; Curtin, N. J.; Endicott, J. A.; Golding, B. T.; Hardcastle, I. R.; Jewsbury, P.; Mesguiche, V.; Newell, D. R.; Noble, M. E. M.; Parsons, R. J.; Pratt, D. J.; Wang, L. Z.; Griffin, R. J., Structure-based design of 2-arylamino-4-cyclohexylmethyl-5-nitroso-6-aminopyrimidine inhibitors of cyclin-dependent kinases 1 and 2. *Bioorg. Med. Chem. Lett.* **2003**, *13* (18), 3079-3082.
 97. Hirai, H.; Kawanishi, N.; Iwasawa, Y., Recent advances in the development of selective small molecule inhibitors for Cyclin-dependent kinases. *Curr. Top. Med. Chem. (Sharjah, United Arab Emirates)* **2005**, *5* (2), 167-179.
 98. Sausville, E. A., Complexities in the development of cyclin-dependent kinase inhibitor drugs. *Trends Mol. Med.* **2002**, *8* (4, Suppl.), S32-S37.
 99. Fisher, R. P., Secrets of a double agent: CDK7 in cell-cycle control and transcription. *J. Cell Sci.* **2005**, *118* (22), 5171-5180.
 100. Nigg, E. A., Cyclin-dependent kinase 7: At the cross-roads of transcription, DNA repair and cell cycle control? *Curr. Opin. Cell Biol.* **1996**, *8* (3), 312-317.

101. Gervais, V.; Busso, D.; Wasielewski, E.; Poterszman, A.; Egly, J.-M.; Thierry, J.-C.; Kieffer, B., Solution Structure of the N-terminal Domain of the Human TFIIH MAT1 Subunit. New insights into the ring finger family. *J. Biol. Chem.* **2001**, 276 (10), 7457-7464.
102. Busso, D.; Keriél, A.; Sandrock, B.; Poterszman, A.; Gileadi, O.; Egly, J. M., Distinct regions of MAT1 regulate cdk7 kinase and TFIIH transcription activities. *J. Biol. Chem.* **2000**, 275 (30), 22815-22823.
103. Yankulov, K. Y.; Bentley, D. L., Regulation of CDK7 substrate specificity by MAT1 and TFIIH. *EMBO J.* **1997**, 16 (7), 1638-1646.
104. Abbas, T.; Dutta, A., CDK2-activating kinase (CAK) - More questions than answers. *Cell Cycle* **2006**, 5 (10), 1123-1124.
105. Liu, Y.; Wu, C. W.; Galaktionov, K., p42, a novel cyclin-dependent kinase-activating kinase in mammalian cells. *J. Biol. Chem.* **2004**, 279 (6), 4507-4514.
106. Wohlbold, L.; Larochelle, S.; Liao, J. C. F.; Livshits, G.; Singer, J.; Shokat, K. M.; Fisher, R. P., The cyclin-dependent kinase (CDK) family member PNQALRE/CCRK supports cell proliferation but has no intrinsic CDK-activating kinase (CAK) activity. *Cell Cycle* **2006**, 5 (5), 546-554.
107. Larochelle, S.; Pandur, J.; Fisher, R. P.; Salz, H. K.; Suter, B., Cdk7 is essential for mitosis and for in vivo Cdk-activating kinase activity. *Genes & Development* **1998**, 12 (3), 370-381.
108. Harper, J. W.; Elledge, S. J., The role of Cdk7 in CAK function, a retro-retrospective. *Gen. Dev.* **1998**, 12 (3), 285-289.
109. Kim, K. K.; Chamberlin, H. M.; Morgan, D. O.; Kim, S.-H., Three-dimensional structure of human cyclin H, a positive regulator of the CDK-activating kinase. *Nat. Struct. Biol.* **1996**, 3 (10), 849-855.
110. Schneider, E.; Montenarh, M.; Wagner, P., Regulation of CAK kinase activity by p53. *Oncogene* **1998**, 17 (21), 2733-2741.
111. Akoulitchiev, S.; Chuikov, S.; Reinberg, D., TFIIH is negatively regulated by cdk8-containing mediator complexes. *Nature* **2000**, 407 (6800), 102-106.
112. Schneider, E.; Kartarius, S.; Schuster, N.; Montenarh, M., The cyclin H/cdk7/Mat1 kinase activity is regulated by CK2 phosphorylation of cyclin H. *Oncogene* **2002**, 21 (33), 5031-5037.
113. Allison, L. A.; Moyle, M.; Shales, M.; Ingles, C. J., Extensive Homology among the Largest Subunits of Eukaryotic and Prokaryotic Rna-Polymerases. *Cell* **1985**, 42 (2), 599-610.
114. Corden, J. L.; Cadena, D. L.; Ahearn, J. M.; Dahmus, M. E., A Unique Structure at the Carboxyl Terminus of the Largest Subunit of Eukaryotic Rna Polymerase-ii. *Proc. Natl. Acad. Sci. USA* **1985**, 82 (23), 7934-7938.
115. Meyer, P. A.; Ye, P.; Zhang, M.; Suh, M.-H.; Fu, J., Phasing RNA Polymerase II Using Intrinsically Bound Zn Atoms: An Updated Structural Model. *Structure (Cambridge, MA, U. S.)* **2006**, 14 (6), 973-982.
116. Prelich, G., RNA polymerase II carboxy-terminal domain kinases: Emerging clues to their function. *Eukaryotic Cell* **2002**, 1 (2), 153-162.
117. Lee, T. I.; Young, R. A., Transcription of eukaryotic protein-coding genes. *Annu. Rev. Genet.* **2000**, 34, 77-137.
118. Mydlikova, Z.; Gursky, J.; Pirscl, M., Transcription factor IIH - the protein complex with multiple functions. *Neoplasma* **57** (4), 287-290.
119. Patturajan, M.; Conrad, N. K.; Bregman, D. B.; Corden, J. L., Yeast carboxyl-terminal domain kinase I positively and negatively regulates RNA polymerase

- II carboxyl-terminal domain phosphorylation. *J. Biol. Chem.* **1999**, 274 (39), 27823-27828.
120. Kobayashi, H.; Stewart, E.; Poon, R. Y. C.; Hunt, T., Cyclin A and cyclin B dissociate from p34cdc2 with half-times of 4 and 15 h, respectively, regardless of the phase of the cell cycle. *J. Biol. Chem.* **1994**, 269 (46), 29153-60.
 121. Larochelle, S.; Chen, J.; Knights, R.; Pandur, J.; Morcillo, P.; Erdjument-Bromage, H.; Tempst, P.; Suter, B.; Fisher, R. P., T-loop phosphorylation stabilizes the CDK7-cyclin H-MAT1 complex in vivo and regulates its CTD kinase activity. *Embo J.* **2001**, 20 (14), 3749-3759.
 122. Bartkova, J.; Zemanova, M.; Bartek, J., Expression of CDK7/CAK in normal and tumour cells of diverse histogenesis, cell-cycle position and differentiation. *Int. J. Cancer* **1996**, 66 (6), 732-737.
 123. Kayaselcuk, F.; Erkanli, S.; Bolat, F.; Seydaoglu, G.; Kuscu, E.; Demirhan, B., Expression of cyclin H in normal and cancerous endometrium, its correlation with other cyclins, and association with clinicopathologic parameters. *Int. J. Gynecol. Cancer* **2006**, 16 (1), 402-408.
 124. Lolli, G.; Johnson, L. N., CAK-cyclin-dependent activating kinase: a key kinase in cell cycle control and a target for drugs? *Cell Cycle* **2005**, 4 (4), 572-577.
 125. Larochelle, S.; Pandur, J.; Fisher, R. P.; Salz, H. K.; Suter, B., Cdk7 is essential for mitosis and for in vivo Cdk-activating kinase activity. *Genes Dev.* **1998**, 12 (3), 370-381.
 126. Lee, K. M.; Saiz, J. E.; Barton, W. A.; Fisher, R. P., Cdc2 activation in fission yeast depends on Mcs6 and Csk1, two partially redundant Cdk-activating kinases (CAKs). *Curr. Biol.* **1999**, 9 (8), 441-444.
 127. Saiz, J. E.; Fisher, R. P., A CDK-activating kinase network is required in cell cycle control and transcription in fission yeast. *Curr. Biol.* **2002**, 12 (13), 1100-1105.
 128. Adamczewski, J. P.; Rossignol, M.; Tassan, J.-P.; Nigg, E. A.; Moncollin, V.; Egly, J.-M., MAT1, cdk7 and cyclin H form a kinase complex which is UV light-sensitive upon association with TFIIH. *EMBO J.* **1996**, 15 (8), 1877-1884.
 129. Rossignol, M.; Kolb-Cheynel, I.; Egly, J.-M., Substrate specificity of the cdk-activating kinase (CAK) is altered upon association with TFIIH. *EMBO J.* **1997**, 16 (7), 1628-1637.
 130. Chen, Y.; Jirage, D.; Caridha, D.; Kathcart, A. K.; Cortes, E. A.; Denuit, R. A.; Geyer, J. A.; Prigge, S. T.; Waters, N. C., Identification of an effector protein and gain-of-function mutants that activate Pfmrk, a malarial cyclin-dependent protein kinase. *Mol. Biochem. Parasitol.* **2006**, 149 (1), 48-57.
 131. Lee, K. M.; Miklos, I.; Du, H.; Watt, S.; Szilagyi, Z.; Saiz, J. E.; Madabhushi, R.; Penkett, C. J.; Sipiczki, M.; Baehler, J.; Fisher, R. P., Impairment of the TFIIH-associated CDK-activating kinase selectively affects cell cycle-regulated gene expression in fission yeast. *Mol. Biol. Cell* **2005**, 16 (6), 2734-2745.
 132. Lolli, G.; Johnson, L. N., CAK-cyclin-dependent activating kinase - A key kinase in cell cycle control and a target for drugs? *Cell Cycle* **2005**, 4 (4), 572-577.
 133. Korsisaari, N.; Rossi, D. J.; Paetau, A.; Charnay, P.; Henkemeyer, M.; Makela, T. P., Conditional ablation of the Mat1 subunit of TFIIH in Schwann cells provides evidence that Mat1 is not required for general transcription. *J. Cell Sci.* **2002**, 115 (22), 4275-4284.

134. Rossi, D. J.; Londesborough, A.; Korsisaari, N.; Pihlak, A.; Lehtonen, E.; Henkemeyer, M.; Makela, T. P., Inability to enter S phase and defective RNA polymerase II CTD phosphorylation in mice lacking Mat1. *EMBO J.* **2001**, *20* (11), 2844-2856.
135. Schwartz, B. E.; Larochelle, S.; Suter, B.; Lis, J. T., Cdk7 is required for full activation of Drosophila heat shock genes and RNA polymerase II phosphorylation in vivo. *Mol. Cell. Biol.* **2003**, *23* (19), 6876-6886.
136. Liang, Y. C.; Tsai, S. H.; Chen, L.; Lin-Shiau, S. Y.; Lin, J. K., Resveratrol-induced G(2) arrest through the inhibition of CDK7 and p34(CDC2) kinases in colon carcinoma HT29 cells. *Biochem. Pharmacol.* **2003**, *65* (7), 1053-1060.
137. Jogalekar, A. S.; Snyder, J. P.; Liotta, D. C.; Barrett, A. G. M.; Coombes, R.; Ali, S.; Siwicka, A.; Brackow, J.; Scheiper, B. Pyrazolopyrimidinamine compounds as selective inhibitors for cyclin-dependent kinases and their preparation, pharmaceutical compositions and use in the treatment of CDK-mediated diseases. **2008**.
138. Lolli, G.; Lowe, E. D.; Brown, N. R.; Johnson, L. N., The crystal structure of human CDK7 and its protein recognition properties. *Structure* **2004**, *12* (11), 2067-2079.
139. Malumbres, M.; Pevarello, P.; Barbacid, M.; Bischoff, J. R., CDK inhibitors in cancer therapy: what is next? *Trends Pharmacol. Sci.* **2008**, *29* (1), 16-21.
140. Grim, J. E.; Clurman, B. E., Cycling without CDK2? *Trends Cell Biol.* **2003**, *13* (8), 396-399.
141. Ortega, S.; Prieto, I.; Odajima, J.; Martin, A.; Dubus, P.; Sotillo, R.; Barbero, J. L.; Malumbres, M.; Barbacid, M., Cyclin-dependent kinase 2 is essential for meiosis but not for mitotic cell division in mice. *Nat. Genet.* **2003**, *35* (1), 25-31.
142. Tetsu, O.; McCormick, F., Proliferation of cancer cells despite CDK2 inhibition. *Cancer Cell* **2003**, *3* (3), 233-245.
143. Fischer, P. M.; Bell, G.; Midgley, C.; Sleight, R.; Glover, D. M., Cell cycle target validation: approaches and successes. *Targets* **2003**, *2* (4), 154-161.
144. Hu, B.; Mitra, J.; Van, d. H. S.; Enders, G. H., S and G2 phase roles for Cdk2 revealed by inducible expression of a dominant-negative mutant in human cells. *Mol. Cell. Biol.* **2001**, *21* (8), 2755-2766.
145. Zhu, Y.; Alvarez, C.; Doll, R.; Kurata, H.; Schebye, X. M.; Parry, D.; Lees, E., Intra-S-phase checkpoint activation by direct CDK2 inhibition. *Mol. Cell. Biol.* **2004**, *24* (14), 6268-6277.
146. Fabian, M. A.; Biggs, W. H.; Treiber, D. K.; Atteridge, C. E.; Azimioara, M. D.; Benedetti, M. G.; Carter, T. A.; Ciceri, P.; Edeen, P. T.; Floyd, M.; Ford, J. M.; Galvin, M.; Gerlach, J. L.; Grotzfeld, R. M.; Herrgard, S.; Insko, D. E.; Insko, M. A.; Lai, A. G.; Lelias, J.-M.; Mehta, S. A.; Milanov, Z. V.; Velasco, A. M.; Wodicka, L. M.; Patel, H. K.; Zarrinkar, P. P.; Lockhart, D. J., A small molecule-kinase interaction map for clinical kinase inhibitors. *Nat. Biotechnol.* **2005**, *23* (3), 329-336.
147. Benson, C.; Kaye, S.; Workman, P.; Garrett, M.; Walton, M.; de, B. J., Clinical anticancer drug development: targeting the cyclin-dependent kinases. *Br. J. Cancer* **2005**, *92* (1), 7-12.
148. Holstege, F. C. P.; Young, R. A. Dissecting the regulatory circuitry of a eukaryotic genome using HDAs to determine genome-wide effects of mutations in components of the transcriptional machinery. **2003**.

149. Lee, J.; Colwill, K.; Aneliunas, V.; Tennyson, C.; Moore, L.; Ho, Y.; Andrews, B., Interaction of yeast Rvs167 and Pho85 cyclin-dependent kinase complexes may link the cell cycle to the actin cytoskeleton. *Curr. Biol.* **1998**, *8* (24), 1310-1322.
150. McNeil, J. B.; Agah, H.; Bentley, D., Activated transcription independent of the RNA polymerase II holoenzyme in budding yeast. *Genes Dev.* **1998**, *12* (16), 2510-2521.
151. Pei, Y.; Shuman, S., Characterization of the *Schizosaccharomyces pombe* Cdk9/Pch1 Protein Kinase: Spt5 phosphorylation, autophosphorylation, and mutational analysis. *J. Biol. Chem.* **2003**, *278* (44), 43346-43356.
152. Pei, Y.; Schwer, B.; Shuman, S., Interactions between fission yeast Cdk9, its cyclin partner Pch1, and mRNA capping enzyme Pct1 suggest an elongation checkpoint for mRNA quality control. *J. Biol. Chem.* **2003**, *278* (9), 7180-7188.
153. Lindstrom, D. L.; Hartzog, G. A., Genetic interactions of Spt4-Spt5 and TFIIIS with the RNA polymerase II CTD and CTD modifying enzymes in *Saccharomyces cerevisiae*. *Genetics* **2001**, *159* (2), 487-497.
154. Neant, I.; Guerrier, P., 6-Dimethylaminopurine blocks starfish oocyte maturation by inhibiting a relevant protein kinase activity. *Exp. Cell Res.* **1988**, *176* (1), 68-79.
155. Meijer, L.; Raymond, E., Roscovitine and Other Purines as Kinase Inhibitors. From Starfish Oocytes to Clinical Trials. *Acc. Chem. Res.* **2003**, *36* (6), 417-425.
156. Raynaud, F. I.; Whittaker, S. R.; Fischer, P. M.; McClue, S.; Walton, M. I.; Barrie, S. E.; Garrett, M. D.; Rogers, P.; Clarke, S. J.; Kelland, L. R.; Valenti, M.; Brunton, L.; Eccles, S.; Lane, D. P.; Workman, P., In vitro and In vivo Pharmacokinetic-Pharmacodynamic Relationships for the Trisubstituted Aminopurine Cyclin-Dependent Kinase Inhibitors Olomoucine, Bohemine and CYC202. *Clin. Cancer Res.* **2005**, *11* (13), 4875-4887.
157. SchulzeGahmen, U.; DeBondt, H. L.; Kim, S. H., High-resolution crystal structures of human cyclin-dependent kinase 2 with and without ATP: Bound waters and natural ligand as guides for inhibitor design. *J. Med. Chem.* **1996**, *39* (23), 4540-4546.
158. Gray, N. S.; Wodicka, L.; Thunnissen, A.-M. W. H.; Norman, T. C.; Kwon, S.; Espinoza, F. H.; Morgan, D. O.; Barnes, G.; LeClerc, S.; Meijer, L.; Kim, S.-H.; Lockhart, D. J.; Schultz, P. G., Exploiting chemical libraries, structure, and genomics in the search for kinase inhibitors. *Science (Washington, D. C.)* **1998**, *281* (5376), 533-538.
159. DeAzevedo, W. F.; Leclerc, S.; Meijer, L.; Havlicek, L.; Strnad, M.; Kim, S. H., Inhibition of cyclin-dependent kinases by purine analogues - Crystal structure of human cdk2 complexed with roscovitine. *Eur. J. Biochem.* **1997**, *243* (1-2), 518-526.
160. Legraverend, M.; Ludwig, O.; Bisagni, E.; Leclerc, S.; Meijer, L.; Giocanti, N.; Sadri, R.; Favaudon, V., Synthesis and in vitro evaluation of novel 2,6,9-trisubstituted purines acting as cyclin-dependent kinase inhibitors. *Bioorg. Med. Chem.* **1999**, *7* (7), 1281-1293.
161. Bach, S.; Knockaert, M.; Reinhardt, J.; Lozach, O.; Schmitt, S.; Baratte, B.; Koken, M.; Coburn, S. P.; Tang, L.; Jiang, T.; Liang, D.-c.; Galons, H.; Dierick, J.-F.; Pinna, L. A.; Meggio, F.; Totzke, F.; Schaechtele, C.; Lerman, A. S.; Carnero, A.; Wan, Y.; Gray, N.; Meijer, L., Roscovitine Targets, Protein Kinases and Pyridoxal Kinase. *J. Biol. Chem.* **2005**, *280* (35), 31208-31219.

162. Senderowicz, A. M.; Sausville, E. A., Preclinical and clinical development of cyclin-dependent kinase modulators. *J. Natl. Cancer Inst.* **2000**, 92 (5), 376-387.
163. Griffin, R. J.; Arris, C. E.; Bleasdale, C.; Boyle, F. T.; Calvert, A. H.; Curtin, N. J.; Dalby, C.; Kanugula, S.; Lembicz, N. K.; Newell, D. R.; Pegg, A. E.; Golding, B. T., Resistance-Modifying Agents. 8. Inhibition of O6-Alkylguanine-DNA Alkyltransferase by O6-Alkenyl-, O6-Cycloalkenyl-, and O6-(2-Oxoalkyl)guanines and Potentiation of Temozolomide Cytotoxicity in Vitro by O6-(1-Cyclopentenylmethyl)guanine. *J. Med. Chem.* **2000**, 43 (22), 4071-4083.
164. Arris, C. E.; Boyle, F. T.; Calvert, A. H.; Curtin, N. J.; Endicott, J. A.; Garman, E. F.; Gibson, A. E.; Golding, B. T.; Grant, S.; Griffin, R. J.; Jewsbury, P.; Johnson, L. N.; Lawrie, A. M.; Newell, D. R.; Noble, M. E. M.; Sausville, E. A.; Schultz, R.; Yu, W., Identification of Novel Purine and Pyrimidine Cyclin-Dependent Kinase Inhibitors with Distinct Molecular Interactions and Tumor Cell Growth Inhibition Profiles. *J. Med. Chem.* **2000**, 43 (15), 2797-2804.
165. Gibson, A. E.; Arris, C. E.; Bentley, J.; Boyle, F. T.; Curtin, N. J.; Davies, T. G.; Endicott, J. A.; Golding, B. T.; Grant, S.; Griffin, R. J.; Jewsbury, P.; Johnson, L. N.; Mesguiche, V.; Newell, D. R.; Noble, M. E. M.; Tucker, J. A.; Whitfield, H. J., Probing the ATP ribose-binding domain of cyclin-dependent kinases 1 and 2 with O6()substituted guanine derivatives. *J. Med. Chem.* **2002**, 45 (16), 3381-3393.
166. Supuran, C. T.; Casini, A.; Scozzafava, A. In *Development of sulfonamide carbonic anhydrase inhibitors*, CRC Press LLC: 2004; pp 67-147.
167. Griffin, R. J.; Henderson, A.; Curtin, N. J.; Echalié, A.; Endicott, J. A.; Hardcastle, I. R.; Newell, D. R.; Noble, M. E. M.; Wang, L. Z.; Golding, B. T., Searching for cyclin-dependent kinase inhibitors using a new variant of the cope elimination. *J. Am. Chem. Soc.* **2006**, 128 (18), 6012-6013.
168. Lembicz, N. K.; Grant, S.; Clegg, W.; Griffin, R. J.; Heath, S. L.; Golding, B. T., Facilitation of displacements at the 6-position of purines by the use of 1,4-diazabicyclo[2.2.2]octane as leaving group. *J. Chem. Soc. Perkin Trans. 1* **1997**, (3), 185-186.
169. Suschitzky, H., The Balz-Schiemann reaction. *Advan. Fluorine Chem. (M. Stacey, J. C. Tatlow, and A. G. Sharpe, editors. Butterworths)* **1965**, 4 (Copyright (C) 2010 American Chemical Society (ACS). All Rights Reserved.), 1-27.
170. Seshadri, S., Vilsmeier-Haack reaction and its synthetic applications. *J. Sci. Ind. Res.* **1973**, 32 (Copyright (C) 2010 American Chemical Society (ACS). All Rights Reserved.), 128-49.
171. Cope, A. C.; Foster, T. T.; Towle, P. H., Thermal decomposition of amine oxides to olefins and dialkylhydroxylamines. *J. Am. Chem. Soc.* **1949**, 71 (Copyright (C) 2010 American Chemical Society (ACS). All Rights Reserved.), 3929-35.
172. Makosza, M.; Kwast, A., Direct nucleophilic addition versus a single-electron transfer pathway of *l*fH adduct formation in vicarious nucleophilic substitution of hydrogen. *Eur. J. Org. Chem.* **2004**, (10), 2125-2130.
173. Whitfield, H. J.; Griffin, R. J.; Hardcastle, I. R.; Henderson, A.; Meneyrol, J.; Mesguiche, V.; Sayle, K. L.; Golding, B. T., Facilitation of addition-elimination reactions in pyrimidines and purines using trifluoroacetic acid in trifluoroethanol. *Chem. Commun.* **2003**, (22), 2802-2803.

174. Henry, L., Nitro-alcohols. *Compt. rend.* **1895**, *120*, 1265-8.
175. Luzzio, F. A., The Henry reaction: recent examples. *Tetrahedron* **2001**, *57* (6), 915-945.
176. Simoni, D.; Rondanin, R.; Morini, M.; Baruchello, R.; Invidiata, F. P., 1,5,7-Triazabicyclo[4.4.0]dec-1-ene (TBD), 7-methyl-TBD (MTBD) and polymer-supported TBD (P-TBD): three efficient catalysts for the nitroaldol (Henry) reaction and for the addition of dialkyl phosphites to unsaturated systems. *Tetrahedron Lett.* **2000**, *41* (10), 1607-1610.
177. Jurczak, J.; Gryko, D.; Kobrzycka, E.; Gruza, H.; Prokopowicz, P., Effective and mild method for preparation of optically active 1 \pm -amino aldehydes via TEMPO oxidation. *Tetrahedron* **1998**, *54* (22), 6051-6064.
178. Righi, G.; Rumboldt, G.; Bonini, C., Stereoselective Preparation of Syn 1 \pm -Hydroxy-1 \pm -amino Ester Units via Regioselective Opening of 1 \pm ,1 \pm -Epoxy Esters: Enantioselective Synthesis of Taxol C-13 Side Chain and Cyclohexylnorstatine. *J. Org. Chem.* **1996**, *61* (10), 3557-60.
179. Martin, M. W.; Newcomb, J.; Nunes, J. J.; McGowan, D. C.; Armistead, D. M.; Boucher, C.; Buchanan, J. L.; Buckner, W.; Chai, L.; Elbaum, D.; Epstein, L. F.; Faust, T.; Flynn, S.; Gallant, P.; Gore, A.; Gu, Y.; Hsieh, F.; Huang, X.; Lee, J. H.; Metz, D.; Middleton, S.; Mohn, D.; Morgenstern, K.; Morrison, M. J.; Novak, P. M.; Oliveira-Dos-Santos, A.; Powers, D.; Rose, P.; Schneider, S.; Sell, S.; Tudor, Y.; Turci, S. M.; Welcher, A. A.; White, R. D.; Zack, D.; Zhao, H. L.; Zhu, L.; Zhu, X. T.; Ghiron, C.; Amouzegh, P.; Ermann, M.; Jenkins, J.; Johnston, D.; Napier, S.; Power, E., Novel 2-aminopyrimidine carbamates as potent and orally active inhibitors of Lck: Synthesis, SAR, and in vivo antiinflammatory activity. *J. Med. Chem.* **2006**, *49* (16), 4981-4991.
180. Sianesi, E.; Bonola, G.; Pozzi, R.; Da, R. P., Benzothiazines. III. 3,4-Dihydro-1H-2,1-, -2H-1,2-, and -1H-2,3-benzothiazine S,S-dioxides. *Chem. Ber.* **1971**, *104* (6), 1880-91.
181. Vedejs, E.; Engler, D. A.; Mullins, M. J., Reactive triflate alkylating agents. *J. Org. Chem.* **1977**, *42* (19), 3109-13.
182. Wolter, M.; Nordmann, G.; Job, G. E.; Buchwald, S. L., Copper-Catalyzed Coupling of Aryl Iodides with Aliphatic Alcohols. *Org. Lett.* **2002**, *4* (6), 973-976.
183. Hutchinson, I. S.; Matlin, S. A.; Mete, A., The synthesis and chemistry of 3-diazo-piperidin-2-one. *Tetrahedron* **2002**, *58* (16), 3137-3143.
184. Kangasmetsae, J. J.; Johnson, T., Microwave-Accelerated Methodology for the Direct Reductive Amination of Aldehydes. *Org. Lett.* **2005**, *7* (25), 5653-5655.
185. Flood, D. T., Fluorobenzene. *Org. Syn.* **1943**, *13*, 46.
186. Laali, K. K.; Gettewert, V. J., Fluorodediazoniation in ionic liquid solvents: new life for the Balz-Schiemann reaction. *J. Fluor. Chem.* **2001**, *107* (1), 31-34.
187. Wojciechowski, J., [A new method for the synthesis of theobromine, caffeine and 7-methylxanthine.]. *Acta Pol. Pharm.* **1961**, *18*, 409-13.
188. Schmidt, K., Strukturanaloga der natürlichen Purin-Derivate. *Angew. Chem.* **1961**, *73* (1), 15-22.
189. Xu, M.; De Giacomo, F.; Paterson, D. E.; George, T. G.; Vasella, A., An improved procedure for the preparation of 8-substituted guanines. *Chem. Commun.* **2003**, (12), 1452-1453.

190. Ghosh, A. K.; Lagisetty, P.; Zajc, B., Direct Synthesis of 8-Fluoro Purine Nucleosides via Metalation-Fluorination. *J. Org. Chem.* **2007**, *72* (22), 8222-8226.
191. Hocek, M., Syntheses of purines bearing carbon substituents in positions 2, 6 or 8 by metal- or organometal-mediated C-C bond-forming reactions. *Eur. J. Org. Chem.* **2003**, (2), 245-254.
192. Kumamoto, H.; Tanaka, H.; Tsukioka, R.; Ishida, Y.; Nakamura, A.; Kimura, S.; Hayakawa, H.; Kato, K.; Miyasaka, T., First Evident Generation of Purin-2-yllithium: Lithiation of an 8-Silyl-Protected 6-Chloropurine Riboside as a Key Step for the Synthesis of 2-Carbon-Substituted Adenosines. *J. Org. Chem.* **1999**, *64* (21), 7773-7780.
193. Tanaka, H.; Uchida, Y.; Shinozaki, M.; Hayakawa, H.; Matsuda, A.; Miyasaka, T., A simplified synthesis of 8-substituted purine nucleosides via lithiation of 6-chloro-9-(2,3-O-isopropylidene- β -D-ribofuranosyl)purine. *Chem. Pharm. Bull.* **1983**, *31* (2), 787-90.
194. Hayakawa, H.; Haraguchi, K.; Tanaka, H.; Miyasaka, T., Direct C-8 lithiation of naturally occurring purine nucleosides. A simple method for the synthesis of 8-carbon-substituted purine nucleosides. *Chem. Pharm. Bull.* **1987**, *35* (1), 72-9.
195. Havlicek, L.; Hanus, J.; Vesely, J.; Leclerc, S.; Meijer, L.; Shaw, G.; Strnad, M., Cytokinin-Derived Cyclin-Dependent Kinase Inhibitors: Synthesis and cdc2 Inhibitory Activity of Olomoucine and Related Compounds. *J. Med. Chem.* **1997**, *40* (4), 408-412.
196. Vesely, J.; Havlicek, L.; Strnad, M.; Blow, J. J.; Donella-Deana, A.; Pinna, L.; Letham, D. S.; Kato, J.-y.; Detivaud, L.; et, a., Inhibition of cyclin-dependent kinases by purine analogs. *Eur. J. Biochem.* **1994**, *224* (2), 771-86.
197. Mesguiche, V.; Parsons, R. J.; Arris, C. E.; Bentley, J.; Boyle, F. T.; Curtin, N. J.; Davies, T. G.; Endicott, J. A.; Gibson, A. E.; Golding, B. T.; Griffin, R. J.; Jewsbury, P.; Johnson, L. N.; Newell, D. R.; Noble, M. E. M.; Wang, L. Z.; Hardcastle, I. R., 4-alkoxy-2,6-diaminopyrimidine derivatives: Inhibitors of cyclin dependent kinases 1 and 2. *Bioorg. Med. Chem. Lett.* **2003**, *13* (2), 217-222.
198. Golding, B. T.; Hall, D. R.; Sakrikar, S., Reaction between Vicinal Diols and Hydrogen Bromide in Acetic-Acid - Synthesis of Chiral Propylene-Oxide. *J. Chem. Soc. Perkin Trans. 1* **1973**, (11), 1214-1220.
199. Arris, C. E.; Boyle, F. T.; Calvert, A. H.; Curtin, N. J.; Endicott, J. A.; Garman, E. F.; Gibson, A. E.; Golding, B. T.; Grant, S.; Griffin, R. J.; Jewsbury, P.; Johnson, L. N.; Lawrie, A. M.; Newell, D. R.; Noble, M. E. M.; Sausville, E. A.; Schultz, R.; Yu, W., Identification of novel purine and pyrimidine cyclin-dependent kinase inhibitors with distinct molecular interactions and tumor cell growth inhibition profiles. *J. Med. Chem.* **2000**, *43* (15), 2797-2804.
200. Wu, S. Y.; McNae, I.; Kontopidis, G.; McClue, S. J.; McInnes, C.; Stewart, K. J.; Wang, S. D.; Zheleva, D. I.; Marriage, H.; Lane, D. P.; Taylor, P.; Fischer, P. M.; Walkinshaw, M. D., Discovery of a novel family of CDK inhibitors with the program LIDAEUS: Structural basis for ligand-induced disordering of the activation loop. *Structure* **2003**, *11* (4), 399-410.
201. Kim, K. S.; Kimball, S. D.; Misra, R. N.; Rawlins, D. B.; Hunt, J. T.; Xiao, H. Y.; Lu, S. F.; Qian, L. G.; Han, W. C.; Shan, W. F.; Mitt, T.; Cai, Z. W.; Poss, M. A.; Zhu, H.; Sack, J. S.; Tokarski, J. S.; Chang, C. Y.; Pavletich, N.; Kamath, A.; Humphreys, W. G.; Marathe, P.; Bursuker, I.; Kellar, K. A.; Roongta, U.; Batorsky, R.; Mulheron, J. G.; Bol, D.; Fairchild, C. R.; Lee, F. Y.; Webster, K.

- R., Discovery of aminothiazole inhibitors of cyclin-dependent kinase 2: Synthesis, X-ray crystallographic analysis, and biological activities. *J. Med. Chem.* **2002**, 45 (18), 3905-3927.
202. Misra, R. N.; Xiao, H. Y.; Kim, K. S.; Lu, S. F.; Han, W. C.; Barbosa, S. A.; Hunt, J. T.; Rawlins, D. B.; Shan, W. F.; Ahmed, S. Z.; Qian, L. G.; Chen, B. C.; Zhao, R. L.; Bednarz, M. S.; Kellar, K. A.; Mulheron, J. G.; Batorsky, R.; Roongta, U.; Kamath, A.; Marathe, P.; Ranadive, S. A.; Sack, J. S.; Tokarski, J. S.; Pavletich, N. P.; Lee, F. Y. F.; Webster, K. R.; Kimball, S. D., N-(Cycloalkylamino)acyl-2-aminothiazole inhibitors of cyclin-dependent kinase - 2. N-[5-[[[5-(1,1-dimethylethyl)-2-oxazolyl]methyl]thio]-2-thiazolyl]-4-piperidinecarboxamide (BMS-387032), a highly efficacious and selective antitumor agent. *J. Med. Chem.* **2004**, 47 (7), 1719-1728.
 203. Junfa Fan, B. F., David Stockett, Erica Chan, Sravanthi Cheeti, Iana Serafimova, Yafan Lu., Phuongly Pham, D. H. W., Ute Hoch, Ingrid C. Choong, Modifications of the isonipecotic acid fragment of SNS-032: Analogs with improved permeability and lower efflux ratio. *Bioorg. Med. Chem. Lett.* **2008**, 18, 6236-6239.
 204. Gundersen, L. L., 6-Chloropurines and Organostannanes in Palladium-Catalyzed Cross-Coupling Reactions. *Tetrahedron Letters* **1994**, 35 (19), 3155-3158.
 205. Gillespie, R. J.; Cliffe, I. A.; Dawson, C. E.; Dourish, C. T.; Gaur, S.; Jordan, A. M.; Knight, A. R.; Lerpiniere, J.; Misra, A.; Pratt, R. M.; Roffey, J.; Stratton, G. C.; Upton, R.; Weiss, S. M.; Williamson, D. S., Antagonists of the human adenosine A(2A) receptor. Part 3: Design and synthesis of pyrazolo[3,4-d]pyrimidines, pyrrolo[2,3-d] pyrimidines and 6-aryl purines. *Bioorg. Med. Chem. Lett.* **2008**, 18 (9), 2924-2929.
 206. Hirao, I.; Fujiwara, T.; Kimoto, M.; Yokoyama, S., Unnatural base pairs between 2-and 6-substituted purines and 2-oxo(1H)pyridine for expansion of the genetic alphabet. *Bioorg. Med. Chem. Lett.* **2004**, 14 (19), 4887-4890.
 207. Hirao, I.; Harada, Y.; Kimoto, M.; Mitsui, T.; Fujiwara, T.; Yokoyama, S., A two-unnatural-base-pair system toward the expansion of the genetic code. *J. Am. Chem. Soc.* **2004**, 126 (41), 13298-13305.
 208. Kawai, R.; Kimoto, M.; Ikeda, S.; Mitsui, T.; Endo, M.; Yokoyama, S.; Hirao, L., Site-specific fluorescent labeling of RNA molecules by specific transcription using unnatural base pairs. *J. Am. Chem. Soc.* **2005**, 127 (49), 17286-17295.
 209. Mitsui, T.; Kimoto, M.; Harada, Y.; Yokoyama, S.; Hirao, L., An efficient unnatural base pair for a base-pair-expanded transcription system. *J. Am. Chem. Soc.* **2005**, 127 (24), 8652-8658.
 210. Mitsui, T.; Kimoto, M.; Kawai, R.; Yokoyama, S.; Hirao, I., Characterization of fluorescent, unnatural base pairs. *Tetrahedron* **2007**, 63 (17), 3528-3537.
 211. Zambon, A.; Borsato, G.; Brussolo, S.; Frascella, P.; Lucchini, V., Efficient access to 5-substituted thiazoles by a novel metallotropic rearrangement. *Tetrahedron Lett.* **2008**, 49 (1), 66-69.
 212. Augustine, J. K.; Naik, Y. A.; Mandal, A. B.; Chowdappa, N.; Praveen, V. B., gem-dibromomethylarenes: A convenient substitute for noncommercial aldehydes in the Knoevenagel-Doebner reaction for the synthesis of alpha,beta-unsaturated carboxylic acids. *J. Org. Chem.* **2007**, 72 (25), 9854-9856.

213. Ghorab, M. M.; Ismail, Z. H.; Abdel-Gawad, S. M.; Aziem, A. A., Antimicrobial activity of amino acid, imidazole, and sulfonamide derivatives of pyrazolo[3,4-d]pyrimidine. *Heteroatom Chem.* **2004**, 15 (1), 57-62.
214. Williamson, D. S.; Parratt, M. J.; Bower, J. F.; Moore, J. D.; Richardson, C. M.; Dokurno, P.; Cansfield, A. D.; Francis, G. L.; Hebdon, R. J.; Howes, R.; Jackson, P. S.; Lockie, A. M.; Murray, J. B.; Nunns, C. L.; Powles, J.; Robertson, A.; Surgenor, A. E.; Torrance, C. J., Structure-guided design of pyrazolo[1,5-a]pyrimidines as inhibitors of human cyclin-dependent kinase 2. *Bioorg. Med. Chem. Lett.* **2005**, 15 (4), 863-867.
215. Novinson, T.; Bhooshan, B.; Okabe, T.; Revankar, G. R.; Robins, R. K.; Senga, K.; Wilson, H. R., Novel heterocyclic nitrofurfural hydrazones. In vivo antitrypanosomal activity. *J. Med. Chem.* **1976**, 19 (4), 512-16.
216. Kuwabe, S.-i.; Torraca, K. E.; Buchwald, S. L., Palladium-Catalyzed Intramolecular C-O Bond Formation. *J. Am. Chem. Soc.* **2001**, 123 (49), 12202-12206.
217. Haefely, W.; Burkard, W. P.; Cesura, A. M.; Kettler, R.; Lorez, H. P.; Martin, J. R.; Richards, J. G.; Scherschlicht, R.; Da, P. M., Biochemistry and pharmacology of moclobemide, a prototype RIMA. *Psychopharmacology (Berlin)* **1992**, 106 (Suppl.), S6-S14.
218. Adam, G. C.; Cravatt, B. F.; Sorensen, E. J., Profiling the specific reactivity of the proteome with non-directed activity-based probes. *Chem. Biol.* **2001**, 8 (1), 81-95.
219. Krantz, A., A classification of enzyme inhibitors. *Bioorg. Med. Chem. Lett.* **1992**, 2 (11), 1327-34.
220. Pratt, R. F., On the definition and classification of mechanism-based enzyme inhibitors. *Bioorg. Med. Chem. Lett.* **1992**, 2 (11), 1323-6.
221. Penning, T. M.; Ricigliano, J. W., Mechanism-based inhibition of hydroxysteroid dehydrogenases. *J. Enzyme Inhib.* **1991**, 5 (3), 165-98.
222. Helmkamp, G. M., Jr.; Rando, R. R.; Brock, D. J. H.; Bloch, K., $\hat{1}^2$ -Hydroxydecanoyl thioester dehydrase. Specificity of substrates and acetylenic inhibitors. *J. Biol. Chem.* **1968**, 243 (12), 3229-31.
223. Hampton, A.; Sasaki, T.; Perini, F.; Slotin, L. A.; Kappler, F., Design of substrate-site-directed irreversible inhibitors of adenosine 5'-phosphate aminohydrolase. Effect of substrate substituents on affinity for the substrate site. *J. Med. Chem.* **1976**, 19 (8), 1029-33.
224. Campbell, D. A.; Szardenings, A. K., Functional profiling of the proteome with affinity labels. *Curr. Opin. Chem. Biol.* **2003**, 7 (2), 296-303.
225. Palmer, J. T.; Rasnick, D.; Klaus, J. L.; Bromme, D., Vinyl Sulfones as Mechanism-Based Cysteine Protease Inhibitors. *J. Med. Chem.* **1995**, 38 (17), 3193-6.
226. Simpkins, N. S., The chemistry of vinyl sulfones. *Tetrahedron* **1990**, 46 (20), 6951-84.
227. Pauly, T. A.; Sulea, T.; Ammirati, M.; Sivaraman, J.; Danley, D. E.; Griffor, M. C.; Kamath, A. V.; Wang, L. K.; Laird, E. R.; Seddon, A. P.; Menard, R.; Cygler, M.; Rath, V. L., Specificity determinants of human cathepsin S revealed by crystal structures of complexes. *Biochemistry* **2003**, 42 (11), 3203-3213.
228. Ng, S. L.; Yang, P. Y.; Chen, K. Y. T.; Srinivasan, R.; Yao, S. Q., Click synthesis of small-molecule inhibitors targeting caspases. *Org. Biomol. Chem.* **2008**, 6 (5), 844-847.

229. Hemelaar, J.; Borodovsky, A.; Kessler, B. M.; Reverter, D.; Cook, J.; Kolli, N.; Gan-Erdene, T.; Wilkinson, K. D.; Gill, G.; Lima, C. D.; Ploegh, H. L.; Ova, H., Specific and covalent targeting of conjugating and deconjugating enzymes of ubiquitin-like proteins. *Mol. Cell. Biol.* **2004**, *24* (1), 84-95.
230. Ettari, R.; Nizi, E.; Di Francesco, M. E.; Dude, M. A.; Pradel, G.; Vicik, R.; Schirmeister, T.; Micale, N.; Grasso, S.; Zappala, M., Development of peptidomimetics with a vinyl sulfone warhead as irreversible falcipain-2 inhibitors. *J. Med. Chem.* **2008**, *51* (4), 988-996.
231. Silverman, R. B. In *Enzyme inhibition*, John Wiley & Sons, Inc.: 2009; pp 663-681.
232. Tipton, K. F. In *Enzymes: irreversible inhibition*, John Wiley & Sons Ltd.: 2007; pp 490-503.
233. Sos, M. L.; Rode, H. B.; Heynck, S.; Peifer, M.; Fischer, F.; Klueter, S.; Pawar, V. G.; Reuter, C.; Heuckmann, J. M.; Weiss, J.; Ruddigkeit, L.; Rabiller, M.; Koker, M.; Simard, J. R.; Getlik, M.; Yuza, Y.; Chen, T.-H.; Greulich, H.; Thomas, R. K.; Rauh, D., Chemogenomic Profiling Provides Insights into the Limited Activity of Irreversible EGFR Inhibitors in Tumor Cells Expressing the T790M EGFR Resistance Mutation. *Cancer Res.* **70** (3), 868-874.
234. Kwak, E. L.; Sordella, R.; Bell, D. W.; Godin-Heymann, N.; Okimoto, R. A.; Brannigan, B. W.; Harris, P. L.; Driscoll, D. R.; Fidias, P.; Lynch, T. J.; Rabindran, S. K.; McGinnis, J. P.; Wissner, A.; Sharma, S. V.; Isselbacher, K. J.; Settleman, J.; Haber, D. A., Irreversible inhibitors of the EGF receptor may circumvent acquired resistance to gefitinib. *Proc. Natl. Acad. Sci. U. S. A.* **2005**, *102* (21), 7665-7670.
235. Rabindran, S. K.; Discifani, C. M.; Rosfjord, E. C.; Baxter, M.; Floyd, M. B.; Golas, J.; Hallett, W. A.; Johnson, B. D.; Nilakantan, R.; Overbeek, E.; Reich, M. F.; Shen, R.; Shi, X.; Tsou, H.-R.; Wang, Y.-F.; Wissner, A., Antitumor Activity of HKI-272, an Orally Active, Irreversible Inhibitor of the HER-2 Tyrosine Kinase. *Cancer Res.* **2004**, *64* (11), 3958-3965.
236. Burstein, H. J.; Sun, Y.; Dirix, L. Y.; Jiang, Z.; Paridaens, R.; Tan, A. R.; Awada, A.; Ranade, A.; Jiao, S.; Schwartz, G.; Abbas, R.; Powell, C.; Turnbull, K.; Vermette, J.; Zacharchuk, C.; Badwe, R., Neratinib, an irreversible ErbB receptor tyrosine kinase inhibitor, in patients with advanced ErbB2-positive breast cancer. *J. Clin. Oncol.* **28** (8), 1301-1307.
237. Galons, H.; Oumata, N.; Meijer, L., Cyclin-dependent kinase inhibitors: a survey of recent patent literature. *Expert Opin. Ther. Pat.* **20** (3), 377-404.
238. Knudsen, E. S.; Wang, J. Y. J., Targeting the RB-pathway in Cancer Therapy. *Clin. Cancer Res.* **16** (4), 1094-1099.
239. Krystof, V.; Uldrijan, S., Cyclin-dependent kinase inhibitors as anticancer drugs. *Curr. Drug Targets* **11** (3), 291-302.
240. Vesely, J.; Havlicek, L.; Strnad, M.; Blow, J. J.; Donelladeana, A.; Pinna, L.; Letham, D. S.; Kato, J.; Detivaud, L.; Leclerc, S.; Meijer, L., INHIBITION OF CYCLIN-DEPENDENT KINASES BY PURINE ANALOGS. *European Journal of Biochemistry* **1994**, *224* (2), 771-786.
241. Hatakeyama, M.; Weinberg, R. A., The role of RB in cell cycle control. *Prog. Cell Cycle Res.* **1995**, *1*, 9-19.
242. Lees, J. A.; Buchkovich, K. J.; Marshak, D. R.; Anderson, C. W.; Harlow, E., The retinoblastoma protein is phosphorylated on multiple sites by human cdc2. *EMBO J.* **1991**, *10* (13), 4279-90.

243. Lin, B. T. Y.; Gruenwald, S.; Morla, A. O.; Lee, W. H.; Wang, J. Y. J., Retinoblastoma cancer suppressor gene product is a substrate of the cell cycle regulator cdc2 kinase. *EMBO J.* **1991**, *10* (4), 857-64.
244. Aleem, E.; Kiyokawa, H.; Kaldis, P., Cdc2-cyclin E complexes regulate the G1/S phase transition. *Nat. Cell Biol.* **2005**, *7* (8), 831-836.
245. Berthet, C.; Aleem, E.; Coppola, V.; Tessarollo, L.; Kaldis, P., Cdk2 Knockout Mice Are Viable. *Curr. Biol.* **2003**, *13* (20), 1775-1785.
246. L'Italien, L.; Tanudji, M.; Russell, L.; Schebye, X. M., Unmasking the redundancy between Cdk1 and Cdk2 at G2 phase in human cancer cell lines. *Cell Cycle* **2006**, *5* (9), 984-993.
247. Satyanarayana, A.; Kaldis, P., A dual role of Cdk2 in DNA damage response. *Cell Div* **2009**, *4*, 9.
248. Du, J.; Widlund, H. R.; Horstmann, M. A.; Ramaswamy, S.; Ross, K.; Huber, W. E.; Nishimura, E. K.; Golub, T. R.; Fisher, D. E., Critical role of CDK2 for melanoma growth linked to its melanocyte-specific transcriptional regulation by MITF. *Cancer Cell* **2004**, *6* (6), 565-576.
249. D'Angiolella, V.; Costanzo, V.; Gottesman, M. E.; Avvedimento, E. V.; Gautier, J.; Grieco, D., Role for cyclin-dependent kinase 2 in mitosis exit. *Curr. Biol.* **2001**, *11* (15), 1221-1226.
250. Zhao, J.; Kennedy, B. K.; Lawrence, B. D.; Barbie, D. A.; Matera, A. G.; Fletcher, J. A.; Harlow, E., NPAT links cyclin E-Cdk2 to the regulation of replication-dependent histone gene transcription. *Genes Dev.* **2000**, *14* (18), 2283-2297.
251. Matsumoto, Y.; Hayashi, K.; Nishida, E., Cyclin-dependent kinase 2 (Cdk2) is required for centrosome duplication in mammalian cells. *Curr. Biol.* **1999**, *9* (8), 429-432.
252. Meraldi, P.; Lukas, J.; Fry, A. M.; Bartek, J.; Nigg, E. A., Centrosome duplication in mammalian somatic cells requires E2F and Cdk2-cyclin A. *Nat. Cell Biol.* **1999**, *1* (2), 88-93.
253. Krasinska, L.; Cot, E.; Fisher, D., Selective chemical inhibition as a tool to study Cdk1 and Cdk2 functions in the cell cycle. *Cell Cycle* **2008**, *7* (12), 1702-1708.
254. Arris, C. E.; Bleasdale, C.; Calvert, A. H.; Curtin, N. J.; Dalby, C.; Golding, B. T.; Griffin, R. J.; Lunn, J. M.; Major, G. N.; Newell, D. R., Probing the Active-Site and Mechanism of Action of O-6-Methylguanine-DNA Methyltransferase with Substrate-Analogs to (O-6-Substituted Guanines). *Anti-Cancer Drug Des.* **1994**, *9* (5), 401-408.
255. Cabiddu, M. G.; Cabiddu, S.; Cadoni, E.; De Montis, S.; Fattuoni, C.; Melis, S., An unusual behaviour of N-(tert-butoxycarbonyl)- and N-pivaloyl(methylthio)anilines in metallation reactions. *Tetrahedron* **2003**, *59* (16), 2893-2897.
256. Kadaba, P. K., New Compounds - Convenient Selective Esterification of Aromatic Carboxylic-Acids Bearing Other Reactive Groups Using a Boron-Trifluoride Etherate-Alcohol Reagent. *J. Pharm. Sci.* **1974**, *63* (8), 1333-1335.
257. Hsu, A. R.; Veeravagu, A.; Cai, W.; Hou, L. C.; Tse, V.; Chen, X. Y., Integrin $\alpha(v)\beta(3)$ antagonists for anti-angiogenic cancer treatment. *Recent Patents on Anti-Cancer Drug Discovery* **2007**, *2* (2), 143-158.
258. Fields, G. B., Integrins: cell adhesion molecules in cancer. *Exp. Opin. Ther. Pat.* **1998**, *8* (6), 633-644.

259. Bedson, P. P., VIII.-On some derivatives of phenylacetic acid. *J. Chem. Soc. Trans.* **1880**, 37, 90-101.
260. Rupe, H.; Messner, W.; Kambli, E., Aldehydes from acetylenecarbinols. I. Cyclohexylideneacetaldehyde. *Helv. Chim. Acta* **1928**, 11, 449-62.
261. Katrak, B. N., Preparation of compounds related to phenacetin. *J. Indian Chem. Soc.* **1936**, 13, 334-6.
262. Breslin, H. J.; Chatterjee, S.; Diebold, J. L.; Dorsey, B. D.; Dunn, D.; Gingrich, D. E.; Hostetler, G. A.; Hudkins, R. L.; Hunter, R.; Josef, K.; Lisko, J.; Mesaros, E. F.; Milkiewicz, K. L.; Ott, G. R.; Sundar, B. G.; Theroff, J. P.; Thieu, T.; Tripathy, R.; Underiner, T. L.; Weinberg, L.; Wells, G. J.; Zificksak, C. A. Preparation of pyrrolotriazines as inhibitors of ALK and JAK2 kinases for treating proliferative diseases.
263. Andrews, C. W.; Chan, J. H.; Freeman, G. A.; Romines, K. R.; Tidwell, J. H. Preparation of benzophenones and phenyl heteroaryl ketones as inhibitors of reverse transcriptase. **2001**.
264. Ulrich, P. C.; Cerami, A.; Wagle, D. R.; Lankin, M. E.; Shih, D. H.; Hwang, S. B. Aminobenzoic acids and derivatives and methods of use for preventing protein aging. **1996**.
265. Sharpe, C. J.; Palmer, P. J.; Evans, D. E.; Brown, G. R.; King, G.; Shadbolt, R. S.; Trigg, R. B.; Ward, R. J.; Ashford, A.; Ross, J. W., Basic ethers of 2-anilinobenzothiazoles and 2-anilinobenzoxazoles as potential antidepressants. *J. Med. Chem.* **1972**, 15 (5), 523-529.
266. Kirchner, F. K. Piperidinecarboxamides and derivatives thereof. 1964.
267. Brain, C. T.; Thoma, G.; Sung, M. J. Preparation of pyrrolopyrimidine compounds as protein kinase inhibitors. 2007.
268. Thyrum, P. T.; Day, A. R., p-Amino-N-[2-(substituted amino)ethyl]benzamides. Potential antifibrillatory drugs. *J. Med. Chem.* **1965**, 8 (1), 107-11.
269. Tran, J. A.; Pontillo, J.; Arellano, M.; Fleck, B. A.; Tucci, F. C.; Marinkovic, D.; Chen, C. W.; Saunders, J.; Foster, A. C.; Chen, C., Structure-activity relationship of a series of cyclohexylpiperazines bearing an amide side chain as antagonists of the human melanocortin-4 receptor. *Bioorg. Med. Chem. Lett.* **2005**, 15 (14), 3434-3438.
270. Reinholz, E.; Becker, A.; Hagenbruch, B.; Schaefer, S.; Schmitt, A., Selectivity in alkylation of phenols with 1-bromo-3-chloropropane using phase-transfer catalysis. *Synthesis* **1990**, (11), 1069-71.
271. Kryczka, K.; Legocki, J., Synthesis of nitrophenyl alkyl ethers. *Organika* **1986**, 9-14.
272. Hooper, M.; Imam, S. H., 11H-isoindolo[2,1-a]indol-11-ones: novel rearrangement products from the attempted preparation of 2-(2-diethylaminomethylphenyl)isatogens. *J. Chem. Soc., Perkin Trans. 1* **1985**, (8), 1583-7.
273. Herbicidal and fungicidal substituted phenylureas. 1980.
274. Lednicer, D.; Heyd, W. E.; Emmert, D. E.; TenBrink, R. E.; Schurr, P. E.; Day, C. E., Hypobetalipoproteinemic agents. 2. Compounds related to 4-(1-adamantyloxy)aniline. *J. Med. Chem.* **1979**, 22 (1), 69-77.
275. Kaye, I. A.; Burlant, W. J.; Price, L., Thiocyanation of p-Dialkylaminoalkoxyanilines. *J. Org. Chem.* **1951**, 16 (9), 1421-1426.
276. Cayon, E.; Marquet, J.; Lluch, J. M.; Martin, X., Use of intramolecular coulombic interactions to achieve impossible reactions. Photochemical

- cleavage of 4-nitrophenyl ethers. *J. Am. Chem. Soc.* **1991**, 113 (23), 8970-8972.
277. Buu-Hoi, N. P.; Hoan, N., Potential Nitrogen-Heterocycle Carcinogens. XII. 9-Ethylcarbazole-3-Aldehyde and its Derivatives. *J. Org. Chem.* **1951**, 16 (8), 1327-1332.
 278. Herbst, R. M.; Simonian, J. V., THE SYNTHESIS OF SOME ACETYLAMINO-PHENOXYETHYLAMINES¹. *J. Org. Chem.* **1952**, 17 (4), 595-599.
 279. Oae, S.; Yano, Y., 3d-orbital resonance in divalent sulphide--XIII : The E2 reaction of p-substituted [beta]-phenylmercapto chlorides and the corresponding oxygen analogues. *Tetrahedron* **1968**, 24 (17), 5721-5729.
 280. Sohda, T.; Mizuno, K.; Imamiya, E.; Sugiyama, Y.; Fujita, T.; Kawamatsu, Y., Studies on Antidiabetic Agents .2. Synthesis of 5-[4-(1-Methylcyclohexylmethoxy)-Benzyl]Thiazolidine-2,4-Dione (Add-3878) and Its Derivatives. *Chem. Pharm. Bull.* **1982**, 30 (10), 3580-3600.
 281. Baraldi, P. G.; Cacciari, B.; Romagnoli, R.; Spalluto, G.; Monopoli, A.; Ongini, E.; Varani, K.; Borea, P. A., 7-Substituted 5-Amino-2-(2-furyl)pyrazolo[4,3-e]-1,2,4-triazolo[1,5-c]pyrimidines as A2A Adenosine Receptor Antagonists: A Study on the Importance of Modifications at the Side Chain on the Activity and Solubility. *J. Med. Chem.* **2002**, 45 (1), 115-126.
 282. Iliceto, A.; Fava, A.; Simeone, A., Nucleophilic direct replacement reactions in homologous series. Transmission of electronic effect along a saturated aliphatic chain. *Gazz. Chim. Ital.* **1960**, 90, 600-70.
 283. Runti, C.; Nisi, C.; Ulian, F., Mannich bases of pharmaceutical interest and their derivatives. II. Pharmacologically active propiophenone derivatives. *Boll. Chim. Farm.* **1964**, 103 (3), 165-70.
 284. Li, R.; Xue, L.; Zhu, T.; Jiang, Q.; Cui, X.; Yan, Z.; McGee, D.; Wang, J.; Gantla, V. R.; Pickens, J. C.; McGrath, D.; Chucholowski, A.; Morris, S. W.; Webb, T. R., Design and Synthesis of 5-Aryl-pyridone-carboxamides as Inhibitors of Anaplastic Lymphoma Kinase. *J. Med. Chem.* **2006**, 49 (3), 1006-1015.
 285. Roth, G. J.; Heckel, A.; Colbatzky, F.; Handschuh, S.; Kley, J.; Lehmann-Lintz, T.; Lotz, R.; Tontsch-Grunt, U.; Walter, R.; Hilberg, F., Design, Synthesis, and Evaluation of Indolinones as Triple Angiokinase Inhibitors and the Discovery of a Highly Specific 6-Methoxycarbonyl-Substituted Indolinone (BIBF 1120). *J. Med. Chem.* **2009**, 52 (14), 4466-4480.
 286. Goldsworthy, L. J.; Harding, G. F.; Norris, W. L.; Plant, S. G. P.; Selton, B., Some sulfides containing the 2-chloroethyl group. *J. Chem. Soc.* **1948**, 2177-9.
 287. Sterk, G. J.; Vandergoot, H.; Timmerman, H., Studies on Histaminergic Compounds .4. Vuf 8405, a Potent and Relatively Easy Accessible Analog of the H-2-Agonist Impromidine. *European J. Med. Chem.* **1986**, 21 (4), 305-309.
 288. Douglass, I. B.; Farah, B. S.; Thomas, E. G., Sulfinyl and Sulfonyl Chlorides by Chlorination^{1,2}. *J. Org. Chem.* **1961**, 26 (6), 1996-1999.
 289. Michel, H. J.; Schwarz, G.; Schuetz, C.; Kleiner, R.; Lang, S.; Jumar, A.; Klepel, M.; Heinze, M., Quantitative structure-activity relations for substituted 2-chloroethyl benzylsulfones with plant growth regulating properties. *Arch. Phytopathol. Pflanzenschutz* **1981**, 17 (5), 341-9.
 290. Montgomery, J. A.; Hewson, K., Synthesis of Potential Anticancer Agents. XX. 2-Fluoropurines². *J. Am. Chem. Soc.* **1960**, 82 (2), 463-468.

291. Pfaltz, A.; Mattenberger, A., Regioselective Opening of Alpha-Alkoxyepoxides and Beta-Alkoxyepoxides with Trimethylaluminum. *Angew. Chem. Int. Ed. Engl.* **1982**, 21 (1), 71-72.
292. Lehmann-Lintz, T.; Lustenberger, P.; Roth, G. J.; Schindler, M.; Thomas, L.; Mueller, S. G.; Stenkamp, D.; Lotz, R. R. H.; Rudolf, K. Preparation of 3-(4-piperidin-1-ylmethylphenyl)propionic acid phenylamides and related compounds used as MCH-1R antagonists (MCH = melanin concentrating hormone) for treating eating disorders. 2005.
293. Heidenbluth, K.; Toenjes, H.; Schmidt, J. 2-Isoindolinoethyl aryl ethers. 1968.
294. Roberts, D. A.; Pearce, R. J.; Bradbury, R. H. Preparation of 4-[(tetrazolylbiphenyl)methoxy]naphthyridines and analogs as angiotensin II antagonists. **1992**.
295. Baldwin, J. J.; Claremon, D. A.; Elliott, J. M.; Ponticello, G. S.; Remy, D. C.; Selnick, H. G. Preparation of arylheterocyclyspiropiperidines as class III antiarrhythmics and cardiotonics. **1991**.
296. Guzi, T. J.; Paruch, K.; Dwyer, M. P.; Labroli, M.; Keertikar, K. M. Preparation of pyrazolopyrimidines as cyclin-dependent kinase inhibitors. 2006.
297. Brown, N. R.; Noble, M. E. M.; Endicott, J. A.; Johnson, L. N., The structural basis for specificity of substrate and recruitment peptides for cyclin-dependent kinases. *Nat. Cell Biol.* **1999**, 1 (7), 438-443.
298. Brown, N. R.; Noble, M. E. M.; Lawrie, A. M.; Morris, M. C.; Tunnah, P.; Divita, G.; Johnson, L. N.; Endicott, J. A., Effects of phosphorylation of threonine 160 on cyclin-dependent kinase 2 structure and activity. *J. Biol. Chem.* **1999**, 274 (13), 8746-8756.